

Abstract

The development of a dendritic cell-based vaccine to enhance CD4⁺ T-cell responses to a breast tumour antigen.

Joanne Louise Carter

With 570,000 new cases in the world every year, breast cancer remains the most common malignancy in women and comprises 16% of all cancer deaths. The use of cytotoxic therapies for the treatment of women with metastatic breast cancer has substantially the emergence of immunotherapy as a potential means of reducing morbidity and improving survival.

The study sought to develop a dendritic cell-based vaccine which was capable of generating CD4⁺ T-cell responses to a breast tumour antigen. The vaccine was composed of T-cells which were transfected with a breast tumour antigen peptide and a peptide from the MHC class II pathway to enhance the presentation of the antigen. Experiments showed that the use of Y27970, a tyrosine kinase inhibitor, to transfect T-cells with a breast tumour antigen peptide and a peptide from the MHC class II pathway to enhance the presentation of the antigen. Experiments showed that the use of Y27970, a tyrosine kinase inhibitor, to transfect T-cells with a breast tumour antigen peptide and a peptide from the MHC class II pathway to enhance the presentation of the antigen.

Experiments showed that the use of Y27970, a tyrosine kinase inhibitor, to transfect T-cells with a breast tumour antigen peptide and a peptide from the MHC class II pathway to enhance the presentation of the antigen. Experiments showed that the use of Y27970, a tyrosine kinase inhibitor, to transfect T-cells with a breast tumour antigen peptide and a peptide from the MHC class II pathway to enhance the presentation of the antigen.

By

Joanne Louise Carter (B.Sc.)

This study has shown that the use of Y27970, a tyrosine kinase inhibitor, to transfect T-cells with a breast tumour antigen peptide and a peptide from the MHC class II pathway to enhance the presentation of the antigen. Experiments showed that the use of Y27970, a tyrosine kinase inhibitor, to transfect T-cells with a breast tumour antigen peptide and a peptide from the MHC class II pathway to enhance the presentation of the antigen.

A thesis submitted in candidature for the degree of

Doctor of Philosophy

University of Leicester

August 2000

UMI Number: U538337

All rights reserved

INFORMATION TO ALL USERS

The quality of this reproduction is dependent upon the quality of the copy submitted.

In the unlikely event that the author did not send a complete manuscript and there are missing pages, these will be noted. Also, if material had to be removed, a note will indicate the deletion.



UMI U538337

Published by ProQuest LLC 2013. Copyright in the Dissertation held by the Author.
Microform Edition © ProQuest LLC.

All rights reserved. This work is protected against
unauthorized copying under Title 17, United States Code.



ProQuest LLC
789 East Eisenhower Parkway
P.O. Box 1346
Ann Arbor, MI 48106-1346

Abstract

Development of a dendritic cell-based vaccine to enhance CD4⁺ T-cell responses to a breast tumour antigen

Joanne Louise Carter

With 570,000 new cases in the world each year, breast cancer remains the commonest malignancy in women and comprises 18% of all female cancer. The failure of current therapies for the treatment of women with metastatic breast cancer has culminated in the emergence of immunotherapy as a potential means of eradicating residual disease following surgery.

The study sought to develop a dendritic cell-based vaccine which was capable of generating CD4⁺ T-cell proliferative responses against a known breast tumour antigen. p53 was selected as the antigen to be manipulated due to increasing evidence of T-cell responses to both mutant and wild type forms in breast cancer patients. As it is favourable to pulse dendritic cells with nucleic acids rather than recombinant protein or peptides it was necessary to target endogenous p53 to the MHC class II pathway to enhance presentation of p53 to CD4⁺ T-cells. cDNA encoding the signal peptide motif, YTPL, present in the cytoplasmic tail of HLA-DM β , known to target HLA-DM to MHC class II compartments, was appended to the 3' terminus of p53. Experiments assessed the ability of YTPL to target p53 to the lysosomal compartment in transfected HeLa cells. Control constructs encoding p53 targeted to other cellular compartments were analysed. In order to transfect DC with nucleic acids, experiments were also performed to establish optimal transfection conditions utilising non-viral methods.

This study has successfully targeted p53 to the lysosomal compartment of HeLa cells by virtue of YTPL and has investigated the use of many non-viral techniques to transfect DC. Further work is necessary to determine which construct encoding p53 provides optimal access to the MHC class II pathway and to improve transfection efficiencies of dendritic cells. Thus, this study has paved the way for a dendritic cell - based vaccine for breast cancer.

Declaration

This thesis, submitted for the degree of Doctor of Philosophy entitled: Development of a dendritic cell-based vaccine to enhance CD4⁺ T-cell responses to a breast tumour antigen, is based upon work conducted by the author in the Department of Surgery between March 1996 and December 1999.

All of the work recorded in this thesis is original except where stated.

None of the work has been submitted for another degree in this or any other University.

Signed:

Date:

Acknowledgements

Firstly I would like to express my gratitude to Dr Roger James and Dr Stephen Thirdborough for all their support and helpful advice throughout this project and also to Professor P.R.F. Bell for creating an excellent working environment. My thanks also extend to Rachel Carter for all her help and technical assistance and for being there as a friend. I would also like to thank all other members of the Department of Surgery (too many to mention) for all their help especially Mike Jackson, Marie Marron, Steve Goodall, Jane Allen and Kay Holmes. Next I would like to thank all those volunteers who donated many pints of blood especially Hash Patel, Christian Kemp and Karen Porter. Many thanks go to Chris d'Lacey for all his patience and technical assistance in the production of all confocal images and also for the many enjoyable conversations which I will miss. I would also like to thank Tracey De Haro for her assistance with flow cytometry.

I would very much like to thank all my friends who have kept me sane throughout the preparation of this Thesis. I am especially grateful to Fee for always being there for me despite living so far away and for being such a special friend. I would not have completed this thesis without the love, support and endless encouragement I have received from Mum, Dad, Russ and Danette. Lastly but not least I would like to thank Craig for all his love and patience and for teaching me all that I need to know about computers.

Abbreviations

APC	Antigen-presenting cell
ATCC	American type culture collection
ATP	Adenosine triphosphate
BiP	Immunoglobulin binding protein
bp	Base pair (DNA)
BSA	Bovine serum albumin
β_2 me	β -mercaptoethanol
β_2 M	β_2 -microglobulin
CAT	Chloramphenicol acetyltransferase
CD	Cluster of differentiation
CD40L	CD40 Ligand
cDNA	Complementary DNA
CEA	Carcinoembryonic antigen
CIAP	Calf intestinal alkaline phosphatase
CIITA	MHC class II transactivator protein
CIIV	Class II vesicles
CITE	<i>Cap</i> -independent translation enhancer
CLIP	Class II-associated invariant chain peptides
CLSM	Confocal laser scanning microscope
CMI	Cellular mediated immunity
CMV	Cytomegalovirus
CTL	Cytotoxic T lymphocyte
CTLA-4	CTL antigen-4
DABCO	Diazabicyclo[2.2.2]octane
DC	Dendritic cell
DEPC	Diethyl pyrocarbonate
DMEM	Dulbecco's Modified Eagle's Medium
DNA	Deoxyribonucleic acid
dNTP	Deoxynucleoside 5'-triphosphates
dsDNA	Double-stranded DNA
DTH	Delayed type hypersensitivity
DTT	Dithiolthreitol

EBV	Epstein-Barr Virus
ECACC	European collection of animal cell cultures
ECL	Enhanced chemiluminescence
EDTA	Ethylenediamine tetraacetic acid
EE	Early endosomes
ELISA	Enzyme-linked immunosorbent assay
ER	Endoplasmic reticulum
FCS	Foetal calf serum
FITC	Fluorescein isothiocyanate
GFP	Green fluorescent protein
GM-CSF	Granulocyte/macrophage colony-stimulating factor
HEL	Hen egg lysozyme
HEPES	N-[2-Hydroxyethyl] piperazine-N'-[2-ethane sulphonic acid]
HLA	Human leukocyte antigen
HPC	Human progenitor cells
HPLC	High pressure liquid chromatography
HPV	Human papillomavirus
HSP	Heat shock protein
ICAM	Intercellular adhesion molecule
IFN	Interferon
Ig	Immunoglobulin
Ii	Invariant chain
IL	Interleukin
IL-2R α	IL-2 receptor alpha
IRES	Internal ribosomal entry site
IVT	<i>In vitro</i> transcription
Kb	Kilobase
kDa	Kilodalton
KLH	Keyhole limpet haemocyanin
LAK	Lymphokine-activated killer (cell)
LAMP-1	Lysosomal-associated membrane protein
LC	Langerhans cells
LB	Luria-Bertoni (media)
L-BCL	Lymphoblastoid B-cell line
LE	Late endosomes

LMP	Low melting point
LPS	Lipopolysaccharide
LS	Leader sequence
LSM	Lymphocyte separation medium
mAb	Monoclonal antibody
MAGE	Melanoma antigen
MCS	Multiple cloning site
MEM	Minimal essential medium
MIIC	MHC class II compartment
MHC	Major histocompatibility complex
MMTV	Mouse mammary tumour virus
M ϕ	Macrophage
mRNA	Messenger RNA
NES	Nuclear export signal
NF	Nuclear factor
NK	Natural killer (cell)
NLS	Nuclear localisation signal
NP	Nucleoprotein
ORF	Open reading frame
PBL	Peripheral blood lymphocytes
PBS	Phosphate buffered saline
PBMC	Peripheral blood mononuclear cell
PCR	Polymerase chain reaction
PE	Phycoerythrin
PEM	Polymorphic epithelial mucin
PFA	Paraformaldehyde
pGL	pGreen Lantern Vector
PI	Phosphatidylinositol
RNA	Ribonucleic acid
rNTP	Ribonucleoside 5'-triphosphates
RPMI	Rosswell Park Memorial Institute (media)
RT-PCR	Reverse transcriptase-PCR
SDS	Sodium dodecyl sulphate
SDS-PAGE	SDS-polyacrylamide gel electrophoresis
SEREX	Serological analysis of recombinant cDNA expression libraries

TAE	Tris-acetate (buffer)
TAP	Transporter of antigenic peptides
TBS	Tris buffered saline
TCR	T-cell antigen receptor
TE	Tris-EDTA
TGF	Transforming growth factor
TGN	Trans-Golgi network
Th	T-helper (cell)
TIL	Tumour-infiltrating lymphocytes
TNE	Tris-Na-EDTA (buffer)
TNF	Tumour necrosis factor
UV	Ultraviolet

Chapter One

1.1 Introduction	1
1.2 Experimental evidence for immunological responses to breast cancer	2
1.3 Experimental approaches to the identification of tumour antigens	4
1.4 Breast tumour associated antigens	6
1.4.1 p53 tumour suppressor protein	6
1.4.2 HER-2/neu protooncogene	8
1.4.3 MAGE-1 and MAGE-2	9
1.4.4 Carcine embryonic antigen	9
1.4.5 Polymorphic epithelial mucin	10
1.4.6 Mouse mammary tumour virus-related peptides	10
1.5 Importance of CD4 ⁺ T-cells in antitumour immunity	11
1.6 Immunological escape mechanisms	14
1.7 Dendritic cells	17
1.8 Dendritic cell-based vaccines	20
1.9 MHC Class I and II pathways	23
1.9.1 MHC Class I pathway	23
1.9.2 Class I MHC presentation of exogenous antigens In Vivo	26
1.9.3 MHC Class II pathway	27
1.9.4 Class II MHC presentation of endogenous antigens	33
1.9.5 Targeting endogenous antigens to the MHC Class II processing pathway	35

1.10 Aims of study	38
Chapter two	
2.1 Materials	39
2.1.1 Standard Reagents	39
2.1.2 Solutions	39
2.1.3 Cell culture media	39
2.1.4 Cytokines	40
2.1.5 Antibodies	40
2.1.6 Molecular biology enzymes and reagents	42
2.1.7 Plasmids	42
2.2 Molecular cloning	44
2.2.1 Isolation of total RNA	44
2.2.2 Spectrophotometric quantification of RNA and DNA	44
2.2.3 RNA reverse transcription	44
2.2.4 Polymerase chain reaction	45
2.2.5 Agarose gel electrophoresis	45
2.2.6 Purification of DNA fragments.	47
2.2.7 TA-cloning of PCR products	48
2.2.8 Ligation of DNA fragments with cohesive ends	48
2.2.9 Transformation of competent cells	48
2.2.10 Small-scale plasmid preparation	49

2.2.11 Digestion of DNA with restriction endonucleases	49
2.2.12 Orientation of inserts	49
2.2.13 Sequence analysis	50
2.2.14 Large-scale Endotoxin-free plasmid preparation	50
2.2.15 Storage of bacterial stock cultures	50
2.2.16 Synthesis of in vitro transcribed RNA	51
2.3 Cell culture	51
2.3.1 Human tumour cell lines	51
2.3.2 Isolation of peripheral blood mononuclear cells	52
2.3.3 Electroporation of HeLa cells with plasmid DNA	52
2.3.4 Detection of apoptosis using Annexin V-FITC	52
2.4 Protein analysis	53
2.4.1 Immunofluorescence microscopy: intra-cellular localisation of proteins	53
2.4.2 Immunofluorescence microscopy: cell surface expression (method I)	54
2.4.3 Immunofluorescence microscopy: cell surface expression (method II)	55
2.4.4 Cytofluorimetric analysis	56
2.4.5 SDS-polyacrylamide gel electrophoresis (SDS-PAGE) of proteins	57
Resolving gel	57
2.4.6 Western Blotting	58
2.4.7 Enhanced chemiluminescence (ECL)	58
2.4.8 Coupled in vitro transcription/translation	59

Chapter Three

3.1 Introduction	61
3.2 Methods	62
3.2.1 Cloning of human p53	62
3.2.2 Construction of pCR3.p53-DM β	62
3.2.3 Construction of pCR3.p53	63
3.2.4 Construction of pSecTagA.p53-DM β	64
3.2.5 Construction of pSecTagA.p53	65
3.2.6 Construction of pSecTagA.p53-TM	65
3.3 Results	69
3.3.1 Cloning of human p53	69
3.3.2 Construction of pCR3.p53-DM β	71
3.3.3 Construction of pCR3.p53	71
3.3.4 Intracellular localisation of p53 and p53-DM β in the absence of an amino terminal signal sequence.	74
3.3.5 Construction of pSecTagA.p53-DM β	83
3.3.6 Construction of pSecTagA.p53	83
3.3.7 Intracellular location of p53 and p53-DM β expressed from the pSecTagA constructs in transfected HeLa cells: utilisation of an amino-terminal signal sequence.	85
3.3.8 Construction of pSecTagA.p53-TM	100
3.3.9 Cell surface expression of p53 in transfected HeLa cells.	100

3.3.10 Secretion of p53 by transfected HeLa Cells.	109
3.3.11 Assessment of apoptosis in HeLa cells following transfection with DNA constructs encoding p53.	115
3.4 Discussion	119
3.5 Future Work	127
Chapter Four	
4.1 Introduction	128
4.2 Methods	130
4.2.1 Generation of DC from peripheral blood	130
4.2.2 IVT of GFP	130
4.2.3 Transfection of DC with GFP RNA transcripts using DOTAP transfection reagent.	130
4.2.4 Transfection of HeLa cells with GFP RNA transcripts using Effectene Transfection Reagent	131
4.2.5 Transfection of HeLa cells with GFP RNA transcripts using DOTAP Liposomal Transfection Reagent	131
4.2.6 Transfection of HeLa cells with GFP RNA transcripts by electroporation	132
4.2.7 Transient transfection of DC by electroporation	133
4.2.8 Transient transfection of DC by lipofection using DMRIE-C	133
4.2.9 Transient transfection of DC using the polycation Superfect	134
4.2.10 Transient transfection of DC using the transfection reagent Effectene	134
4.2.11 Transient transfection of DC using the transfection reagent Fugene- 6	135

4.2.12 Transfection of DC using the cationic amphipathic peptide, KALA	136
4.3 Results	137
4.3.1 Generation of DC from peripheral blood	137
4.3.2 Synthesis of GFP RNA transcripts	141
4.3.3 Optimal transfection conditions of DC with RNA transcripts.	141
4.3.4 Optimal transfection conditions of HeLa cells with GFP transcripts	143
4.3.5 In vitro translation of GFP	143
4.3.6 Optimal conditions of transfection for DC with DNA	145
4.4 Discussion	155
4.5 Future Work	159
Chapter Five	
5.1 Concluding remarks	160
5.2 Future aims and prospects	161
Appendix I	164
Appendix II	166
References	168

Chapter One

Introduction

Chapter One

1.1 Introduction

Breast cancer is the most common malignancy among women (Smith, 1995). In the United Kingdom approximately 24,000 women develop breast cancer annually and 15,000 women die of the condition, representing 20% of all cancer mortality (Yarnold, 1995). Although the management of breast cancer has improved over the past few decades, it remains an important challenge for the clinician. Most women presenting with a malignant breast lump have micrometastatic disease spread outside the breast and regional lymph nodes (Smith, 1995). Local treatment, surgery with or without radiotherapy, is unable to control the micrometastases, and adjuvant systemic treatment with cytotoxic chemotherapy or endocrine therapy can only help to provide substantial palliation of symptoms with a limited impact on survival (de Valeriola, 1997).

The overall failure of current cancer therapies to control metastatic disease reflects their lack of selectivity, the absence of specific target-sites on malignant cells and the consequent inability to discriminate between normal and malignant states. An immunological approach to breast cancer treatment may help to overcome the problem of discrimination by the utilisation and manipulation of the immune system to respond to specific targets on tumour cells which may ultimately result in their eradication.

There are a number of unique clinical and histological features of breast cancer which point to tumour-specific immune responses. Reports have shown that the incidence of non-invasive malignancies determined by mammography is greater than the predicted clinical frequency (Fisher, 1980a). Also it is extremely rare to have two clinical tumours in the same breast, even though there is a significant frequency of additional foci of tumour cells in the presence of a malignancy in a pathological specimen (Baak *et al.*, 1985). Observations at autopsy, have revealed the presence of foci of malignancy that never made clinical disease (Fisher, 1980b). Further clinical reports have shown that monoclonal antibodies (mAb) detect a higher frequency of tumour

cells in regional nodes and bone marrow than would be expected on the basis of recurrence rates (Cote *et al.*, 1991; Osborne *et al.*, 1994). Importantly, numerous studies have noted lymphocytic infiltration in human breast cancers. The most extensive studies carried out by Fisher *et al.* (1974) and Aaltomaa *et al.* (1992) reported that 76% of breast cancers were positive for inflammatory cells. There is, however, much controversy over its significance as a prognostic factor. Yoshimoto *et al.* (1989) demonstrated that the action of this prognostic factor is only apparent 5-10 years of follow up in breast cancer patients.

Despite evidence of an immune response to breast cancer in many patients, it is apparent that these responses are unable to control progression of the disease. Many studies have thus adopted different approaches in an attempt to augment these responses. High dose recombinant interleukin (IL)-2 has been employed alone or in conjunction with doxorubicin in nine patients. Partial responses were found in 1 of 5 and 3 of 4, respectively (Paciucci *et al.*, 1989). High dose IL-2 with infusion of IL-2-expanded lymphokine-activated killer (LAK) cells in two patients with breast cancer yielded one partial response lasting less than one month (Topalian *et al.*, 1992). More recently, Euhus *et al.* (1997) have shown that human breast cancer cells can be effectively transfected with the IL-2 gene and that IL-2 producing autologous tumour cells induce patients CD3⁺, CD56⁺ lymphocytes to bind and kill tumour cells. Tsang *et al.* (1995) have also generated cytotoxic T-cells (CTL) specific for human carcinoembryonic antigen (CEA) derived-epitopes from patients immunised with recombinant vaccinia-CEA vaccine. Although preliminary results obtained from these studies and clinical trials are encouraging, further research is necessary to improve immunological strategies for the treatment of breast cancer.

1.2 Experimental evidence for immunological responses to breast cancer

Breast tumours are almost invariably associated with an inflammatory infiltrate consisting mainly of T lymphocytes with a few B lymphocytes and granulocytic cells including natural killer cells. Some tumour infiltrating lymphocytes (TIL) are positive for both major histocompatibility (MHC) class I and II antigens and the high affinity

IL-2 receptor, indicating activation (Hadden, 1995). The majority of infiltrating T lymphocytes express the $\alpha\beta$ T-cell antigen receptor (TCR), although $\gamma\delta$ TCR- positive T-cells have also been observed (Bank *et al.*, 1993). $\gamma\delta$ T-cells may be cytotoxic, but may also contribute to immune suppression (Seo & Egawa, 1995). Phenotypic analysis of TCR β -chain usage has indicated polyclonal reactivity to multiple antigens (Durie *et al.*, 1992). Analysis of cytokine mRNA expression carried out by Vitolo *et al.* (1992), showed low level expression which increased with the intensity of infiltration. These data indicate that mixed T-cell infiltrates occur in a high percentage of breast tumours and that the T-cells involved show some evidence of activation. Lymphocytic infiltration is possibly due to both a non-specific inflammatory response resulting from tumour-derived cytokines and also a T-cell mediated response involving the recognition of tumour antigens. However, such responses are possibly suppressed by tumour- or T cell-induced suppressor mechanisms (Hadden, 1999).

Many research groups have cloned $CD4^+$ T-cell lines from breast cancer infiltrates with variable reactivity to autologous tumour (reviewed in Hadden, 1999). Other groups have cloned T-cells from peripheral blood, regional lymph nodes or pleural effusions, yielding MHC-restricted CTL specific for autologous targets (reviewed in Hadden, 1999). Dadmarz *et al.* (1995) demonstrated that MHC-class II restricted $CD4^+$ T-cells recognising tumour-associated antigens can be detected in some breast cancer patients. Goedegebuure *et al.* (1997) subsequently demonstrated simultaneous production of T helper-1-like cytokines and cytolytic activity by tumour-specific T-cells in breast cancer and also ovarian cancer.

In addition to the TIL studies, there has been evidence of cellular mediated immunity to breast cancer related antigens using autologous tumour extracts in studies involving more than 350 patients. *In vitro* studies reported that 50% of tests for lymphoproliferative responses of peripheral blood lymphocytes and lymphocytotoxicity were positive. *In vivo* skin tests revealed delayed-type hypersensitivity in 40% of patients (Hadden, 1994; Elliot *et al.*, 1994). Evidence of serological responses to breast cancer extracts were also reported in over 40% of patients.

The experimental and clinical evidence of immune responses to breast cancer outlined above has encouraged immunologists to embark on the identification of breast tumour associated antigens which could lead to the development of effective immunotherapy strategies for breast cancer.

1.3 Experimental approaches to the identification of tumour antigens

Three main approaches to the identification of tumour associated antigens have been used, relying on CTL lines generated predominantly from patients with melanoma to demonstrate tumour-specificity. They have been referred to as the genetic, biochemical or complementary strategy.

The genetic approach, pioneered by Boon and colleagues (van Der Bruggen *et al.*, 1991), involved the transfection of cosmid libraries prepared with DNA from antigenic tumour cells into human leucocyte antigen (HLA)-matched cells. Transfectants expressing the relevant antigen were identified by their ability to stimulate T-cell proliferation or to induce tumour-necrosis factor (TNF)- α production. This approach has been improved by the use of tumour-derived cDNA libraries that are transiently transfected into COS cells to provide very high levels of expression. Once the gene has been identified, the region encoding the antigenic peptide can be isolated by transfecting gene fragments. Synthetic peptides can then be tested for recognition by CTL.

The biochemical approach takes advantage of the observation that acid treatment of MHC class I molecules releases the peptides bound to them. The eluted peptides are fractionated by high pressure liquid chromatography and then tested for their ability to induce CTL-mediated lysis when loaded onto target cells expressing 'empty MHC class I molecules'. Peptides are fractionated further until individual peptides can be tested and identified by mass spectrometry (Cox *et al.*, 1994; Castelli *et al.*, 1995).

The complementary approach involves analysing the coding sequence of proteins known to be over expressed or mutated in tumours to identify potential HLA-binding

peptides. This is based on the observation that peptides binding to a given HLA molecule must have certain amino acids at given positions, which are critical for interacting with the groove of the HLA molecule known as consensus anchor motives (Rammensee *et al.*, 1995a). These peptides are synthesised and tested directly for their ability to bind to the relevant HLA molecule (Cerundolo *et al.*, 1991; Ruppert *et al.*, 1993). Peptides with the highest binding affinities are then used to stimulate T-cells *in vitro* in order to generate CTL that recognise a given peptide-MHC complex (Houbiers *et al.*, 1993; Celis *et al.*, 1994). To ensure that the peptide is a genuine tumour antigen the CTL are tested for their recognition of tumour cells that express the relevant gene.

The strategies described above do not lend themselves to the identification of MHC class II restricted tumour antigens, primarily because of the lack of sensitivity of bulk T-cell activation assays and the size heterogeneity of MHC class II-restricted peptides. A number of different approaches are currently being explored. A recent method, which involves the characterisation of serological responses against autologous tumour cells in cancer patients, has been used to successfully identify antigens recognised by both CD4⁺ and CD8⁺T-cells. This approach, called serological analysis of recombinant cDNA expression libraries (SEREX), employs a serological screening of tumour-derived cDNA libraries expressed in bacteria, to detect tumour antigens specifically bound by low titres of IgG. This approach is based on the assumption that isotype switching from IgM to IgG implies the presence of specific help from CD4⁺ T-cells. Serum from cancer patients can be used to identify tumour antigens recognised by CD4⁺ T-cells using this SEREX technique (Sahin *et al.*, 1995; Chen *et al.*, 1997).

Wang *et al.* (1999a; 1999b) have modified the genetic approach to identify MHC class II restricted tumour antigens instead of those restricted by MHC class I. This involves the generation of a cDNA library from tumour cells that are capable of stimulating proliferation of a MHC class II restricted CD4⁺ T-cell line. To ensure presentation by MHC class II molecules, the cDNA library is cloned downstream of a gene fragment encoding the first 80 amino acids of the invariant chain. The cDNA library is transfected into target cells expressing appropriate MHC class II molecules.

Target cells capable of activating the tumour-specific CD4⁺ T-cell clone are identified followed by the tumour antigen.

Application of the more recent strategies will speed up the identification of new tumour antigens expressed in many cancers including breast, and facilitate the development of cancer vaccines capable of stimulating both CD4⁺ and CD8⁺ T-cell responses.

1.4 Breast tumour associated antigens

The identification of the antigens involved in immune responses to breast cancer has been the focus of intense investigation over the last decade.

1.4.1 p53 tumour suppressor protein

The p53 protooncogene encodes a 53 kDa nuclear phosphoprotein which acts as an important negative regulator of the cell cycle (Hollstein *et al.*, 1991). It is normally expressed at low levels in cells. However, in response to DNA damage, p53 protein levels rise as a result of a posttranslational mechanism that leads to its stabilisation (Maltzman & Czyzyk, 1984). As a consequence, p53 becomes active as a transcription factor, inducing the transcription of genes such as: p21^{waf1}, which mediates G1 arrest by associating with a cyclin/cdk/PCNA complex and causing inhibition of its kinase activity, thus blocking cell cycle progression into S-phase (Waldman *et al.*, 1995); *GADD45*, which functions in DNA repair (Kastan *et al.*, 1992); *Bax*, which induces apoptosis (Miyashita *et al.*, 1995); and *cyclin G*, the function of which is not yet known (Okamoto *et al.*, 1994). These activities prevent the establishment of mutations in future generations of cells. There is evidence that the p53 gene can suppress the growth of both transformed murine (Eliyahu *et al.*, 1989; Finlay *et al.*, 1989) and human cells (Baker *et al.*, 1990; Mercer *et al.*, 1990; Diller *et al.*, 1990). Mutations in the gene results in the oncogenic form and loss of the suppressor function.

Mutations in the p53 gene are the most commonly found genetic alterations in human malignancies (Levine *et al.*, 1991; Hollstein *et al.*, 1991). They are generally diverse, single-base missense mutations (Kovach *et al.*, 1996) which abrogate the function of p53 as a suppressor of cell division. Loss of p53 function in tumour cells occurs in more than half of human malignancies and is associated with high genomic instability, resistance to chemotherapy and radiation therapy and metastasis. p53 protein is normally undetectable in non-malignant tissues (Levine, 1993), however, mutations of p53 induce prolonged stability of the protein and results in higher concentrations of the mutated p53 protein product in the nucleus and cytoplasm (Soong *et al.*, 1996). It is over expressed in 57% of breast cancers and is associated with rapid cell proliferation and poor prognosis in breast cancer patients (Hadden, 1999).

In tumour cells, mutant p53 accumulates to high levels within extranuclear cell compartments, which may influence p53 antigen processing and presentation to T-cells. Therefore, p53 represents an antigen of choice for the study of immune responses to tumour-associated proteins and for the design of vaccines for breast cancer. The majority of the mutant protein overexpressed in tumours resembles wild-type p53 due to mutations resulting in the alteration of a single amino acid (Vogelstein *et al.*, 1992) The spectrum of p53 mutations is very wide and variable (Hollstein *et al.*, 1996), thus making it difficult to conceive targeting a specific mutant p53 epitope for each tumour. Therefore, vaccination against wild-type p53 protein might have much broader applications since it could work against any tumour over expressing p53 without the need to precisely assess the p53 mutation and the HLA-type of a patient.

There is evidence for T-cell responses to both wild type and mutant p53 in breast cancer patients. Houbiers *et al.* (1993) demonstrated *in vitro* induction of human CTL responses against peptides of mutant and wild-type p53. They identified peptides of mutant p53 capable of binding to HLA-A2.1 by using TAP (transporter of antigenic peptides) deficient T2 cells in an *in vitro* peptide binding assay. Tilken *et al.* (1995) reported cell immunity against wild-type p53 in breast cancer patients. Peripheral blood mononuclear cells (PBMC) collected from 6 breast cancer patients were tested

for a lymphoproliferative response to wild-type p53 protein *in vitro*. Significant primary proliferative T-cell responses were detected in 3 out of 6 breast cancer patients whose tumours over expressed p53.

There is additional evidence that accumulation of the p53 protein allows recognition by human CTL of a wild-type p53 epitope presented by breast carcinomas and melanomas. Gnjatic *et al.* (1998) generated a CTL line from PBMC of a healthy donor directed against HLA-A2 restricted peptide 264-272 from wild-type p53. It efficiently lysed breast adenocarcinomas MCF-7, MCF7/RA1 and MDA-MB 231 which all accumulate the p53 protein. Cells with undetectable levels of wild-type p53 and breast tumour cell lines with HLAA2 loss were not recognised. This work illustrates the fact that wild-type p53 epitopes are commonly shared by different breast tumours which raises the possibility of a widely applicable immunotherapeutic approach.

There has been concern that using wild type epitopes of p53 as targets may have adverse autoimmune effects on the patient. However, DeLeo (1998) demonstrated that immunisation of BALB/c mice with bone marrow-derived dendritic cells (DC) prepulsed with the H-2Kd-binding wild-type p53₂₃₂₋₂₄₀ peptide induced anti-peptide CTL responses. These effectors were cross-reactive against sarcomas expressing p53 missense mutations outside of the p53₂₃₂₋₂₄₀ epitope but not within it. The p53 peptide-pulsed DC-based vaccine was shown to be effective in inducing tumour rejection in immunisation and therapy models in the absence of any observable deleterious effect on naïve mice.

1.4.2 *HER-2/neu* protooncogene

HER-2/neu is a type I transmembrane protein consisting of a large cysteine-rich extracellular domain, a short transmembrane domain, and a small cytoplasmic domain with a relative molecular mass of 185 kDa (Coussens *et al.*, 1985). The function of *HER-2/neu* is not well defined but it is associated with increased tyrosine kinase activity (Di Fiore *et al.*, 1990). *HER-2/neu* is amplified and over expressed in many human cancers, largely adenocarcinomas of breast, ovary, colon and lung. In breast cancer, *HER-2/neu* over expression is associated with aggressive disease and poor

prognosis (Paik *et al.*, 1990; Toikkanen *et al.*, 1992). Over expression may also be related to tumour formation with HER-2/*neu* amplification being detectable in 50-60% of *in situ* ductal breast carcinomas. HER-2/*neu* protein has been examined as a possible target for T-cell mediated immunotherapy (Ioannides *et al.*, 1992). Previous studies have shown that some patients with breast tumours have existent CD4⁺ T-cell responses to HER-2/*neu* proteins and peptides. The study carried out by Disis *et al.* (1994) has identified candidate CTL epitopes.

1.4.3 MAGE-1 and MAGE-2

A previously unidentified gene termed MAGE-1 was isolated following the stable transfection of an antigen loss variant with a cosmid library prepared with DNA from the melanoma cell line MZ2-MEL (Van der Bruggen *et al.*, 1991). This gene was found to be expressed in about 37% of melanomas, and in a significant proportion of other tumours, but not in normal tissues except testes. A peptide antigen termed MZ2-E, encoded by MAGE-1 and restricted by HLA-A1, was the first human tumour antigen to be identified (Traversari *et al.*, 1992). MAGE-1 was also found to encode a second peptide antigen that is recognised by melanoma-specific CTL clones in association with HLA-Cw16 (Van der Bruggen *et al.*, 1994). MAGE-1 belongs to family of twelve genes, among which MAGE-3 also encodes a peptide recognized by melanoma-specific CTL on HLA-A1 (Gaugler *et al.*, 1994). MAGE-3 is also silent in normal tissues except testes, but it is expressed in tumours about twice as frequently as MAGE-1. Synthetic peptide epitopes of MAGE-3 are capable of eliciting cytotoxic T cells *in vitro* (Celis *et al.*, 1994). MAGE 1 and 3 have been shown to be expressed in 20% and 26% breast cancer patients respectively (Russo *et al.*, 1995).

1.4.4 Carcinoembryonic antigen

Carcinoembryonic antigen is a 180 kDa glycoprotein and is expressed on most adenocarcinomas of the gastrointestinal tract, on 50% of breast cancers and 70% of non-small-cell lung cancers. Apparently, CEA is not naturally immunogenic, yet possible immunotherapy approaches using peptide epitopes of CEA are underway (Schlom *et al.*, 1996). A CEA-adenovirus construct has been employed in animal studies and has elicited cellular and humoral immune responses and tumour

regression (Kantor *et al.*, 1992; Schlom *et al.*, 1996). Human CTL specific for CEA epitopes have been generated from metastatic carcinoma patients immunised with recombinant vaccinia-CEA vaccine (Tsang *et al.*, 1995). Alters *et al.*, (1997) have shown CEA peptide-pulsed DC to be effective in eliciting specific CTL *in vitro*.

1.4.5 Polymorphic epithelial mucin

Mucins, which are produced by ductal epithelial cells of many tissues are also expressed by tumours originating from these tissues including the breast. The polymorphic epithelial mucin (PEM) produced by breast and pancreatic epithelial cells, is encoded by the gene MUC-1 (Taylor-Papadimitriou *et al.*, 1991; Gendler *et al.*, 1990). It is a transmembrane glycoprotein with an extracellular domain consisting mainly of tandem repeats of 20-amino acids which are highly glycosylated by O-linked carbohydrates (Hareuveni *et al.*, 1990; Lan *et al.*, 1990). Following malignant transformation of ductal epithelial cells, MUC-1 glycoprotein is underglycosylated allowing the exposure of normally cryptic carbohydrates and components of the tandem repeat peptide core segments resulting in CTL recognition (Gendler *et al.*, 1988; Jerome *et al.*, 1993). This recognition which depends on the presence of multiple repeats occurs in the absence of HLA-restriction. These mucin antigens appear to be very specific for tumour cells (Boon & van der Bruggen., 1996). MUC-1 is increased up to 10-fold in breast cancer and is expressed in 90% of breast tumours. High levels are associated with poor prognosis. Studies have demonstrated both cellular and humoral immune responses to MUC-1 peptide antigen in patients with breast cancer (reviewed in Hadden, 1999). Other studies have shown both cellular and humoral immune responses to carbohydrate and core antigens in animal tumour models in association with vaccine immunotherapy-induced tumour regression (Hadden, 1999). Research into the development of vaccines based on MUC-1 is underway (Apostolopoulos *et al.*, 1996).

1.4.6 Mouse mammary tumour virus-related peptides

Mouse mammary tumour virus (MMTV) is a cause of breast cancer in mice. There is genetic evidence that a phylogenetically-altered virus may have entered the human genome long ago and is not expressed as a virus but as related DNA and peptide

sequences (Acha-Orbea & Palmer, 1991). Various studies have detected antibodies and cellular responses to MMTV-related protein sequences in breast cancer patients (De Ricqles *et al.*, 1993). MMTV-related peptides expressed on breast cancer cells have also been used to make immunogens for synthetic vaccines (Dion *et al.*, 1990).

In summary, human breast cancers express a number of defined antigens including p53, HER-2/neu, MAGE-1/3, CEA and mucin repeat sequences. Due to their specific expression in breast tumours, these antigens may be therapeutically useful as targets for vaccine treatment strategies.

1.5 Importance of CD4⁺ T-cells in antitumour immunity

Of the cancer vaccine strategies developed to date, most have focused on the generation of CD8⁺ effector T-cells, primarily because most tumours are positive for MHC class I yet negative for class II. Importantly, numerous studies have demonstrated that CTL can mediate the direct killing of MHC class I⁺ tumour cells. Although these studies emphasise the importance of CD8⁺ T-cells in the antitumour immune response, the involvement of CD4⁺ T-cells should not be overlooked. In antigen-specific immune responses, CD4⁺ T lymphocytes initiate and maintain antigen-specific immunity by providing help in the form of secreted cytokines for both B lymphocyte and CD8⁺ T-cell responses, as well as sustaining immunological memory in the competent host. Recent work carried out using cytokine-secreting tumour cell vaccines has provided evidence of the important role of T helper cells in anti-tumour immunity. Fearon *et al* (1990) performed experiments using the poorly immunogenic CT26 colon carcinoma model in BALB/c mice, in which they were able to bypass the need for a T helper response by inoculating mice with CT26 cells that had been genetically engineered to secrete IL-2. Mice could reject large doses of gene-modified tumours and *in vivo* depletion of T-cell subsets demonstrated that CD4⁺ T-cells were not critical for primary tumour rejection. Bypassing the T helper response in this system, however, resulted in the failure to establish long lasting immunity to a secondary tumour challenge. This was also confirmed by experiments carried out by Karp *et al.* (1993). Furthermore, abrogation of antitumour immunity in

CD4-knockout or mice depleted of CD4⁺ T-cells has been demonstrated in many studies using cell based vaccines, recombinant viral vaccines and recombinant bacterial vaccines (Fearon *et al.*, 1990; Golumbek *et al.*, 1991; Dranoff *et al.*, 1993; Lin *et al.*, 1996; Ostrand-Rosenberg *et al.*, 1994; Pan *et al.*, 1995).

It is well documented that help for CTL is mediated by cytokines produced by T-helper cells activated in proximity to the CTL precursor at the surface of an antigen presenting cell (APC) (Keene *et al.*, 1982). More recent evidence has indicated that a critical pathway for delivery of help for CTL that is dependent on CD4⁺ T-cells, uses the APC as an intermediary. CD40 ligand (CD40L) is expressed on the surface of activated CD4⁺ T helper cells and is involved in their activation and in the development of their effector functions (Grewal *et al.*, 1995; van Essen *et al.*, 1995). Interactions between CD40L on the CD4⁺ T-cell and CD40 on the APC appear critical in activating the APC to present antigens to and costimulate the priming of CD8⁺ CTL precursors (Schoenberger *et al.*, 1998; Bennett *et al.*, 1998; Ridge *et al.*, 1998). The three cells need not meet simultaneously but the CD4⁺ T helper cells can first engage and condition the APC which then becomes able to stimulate CD8⁺ T-cells. There is increasing evidence that the priming of CD8⁺ T-cells to tumour antigens and other antigens occurs predominantly through the cross-priming pathway involving bone-marrow derived APC (Figure 1.1) (Huang *et al.*, 1994). These bone-marrow derived APC represent the critical link between CD4⁺ T-cells and CD8⁺ T-cells that are specific for epitopes restricted by MHC class II and MHC class I respectively.

There is also increasing evidence that tumour-specific CD4⁺ T-cells can mediate other effector functions in antitumour immunity independent of CTL. Recent studies have shown that CD4⁺ T-cells specific for tumour antigens play a critical role in the activation of macrophages to produce nitric oxide and superoxides via the Th1 effector pathway and the activation of eosinophils via the Th2 effector pathway (reviewed in Pardoll & Topalian, 1998).

Pardoll and Topalian (1998) have suggested a model in which CD4⁺ T cells orchestrate multiple effector arms of antitumour immunity (Figure 1.1). The priming phase of tumour-specific T cells is thought to involve uptake into endosomes,

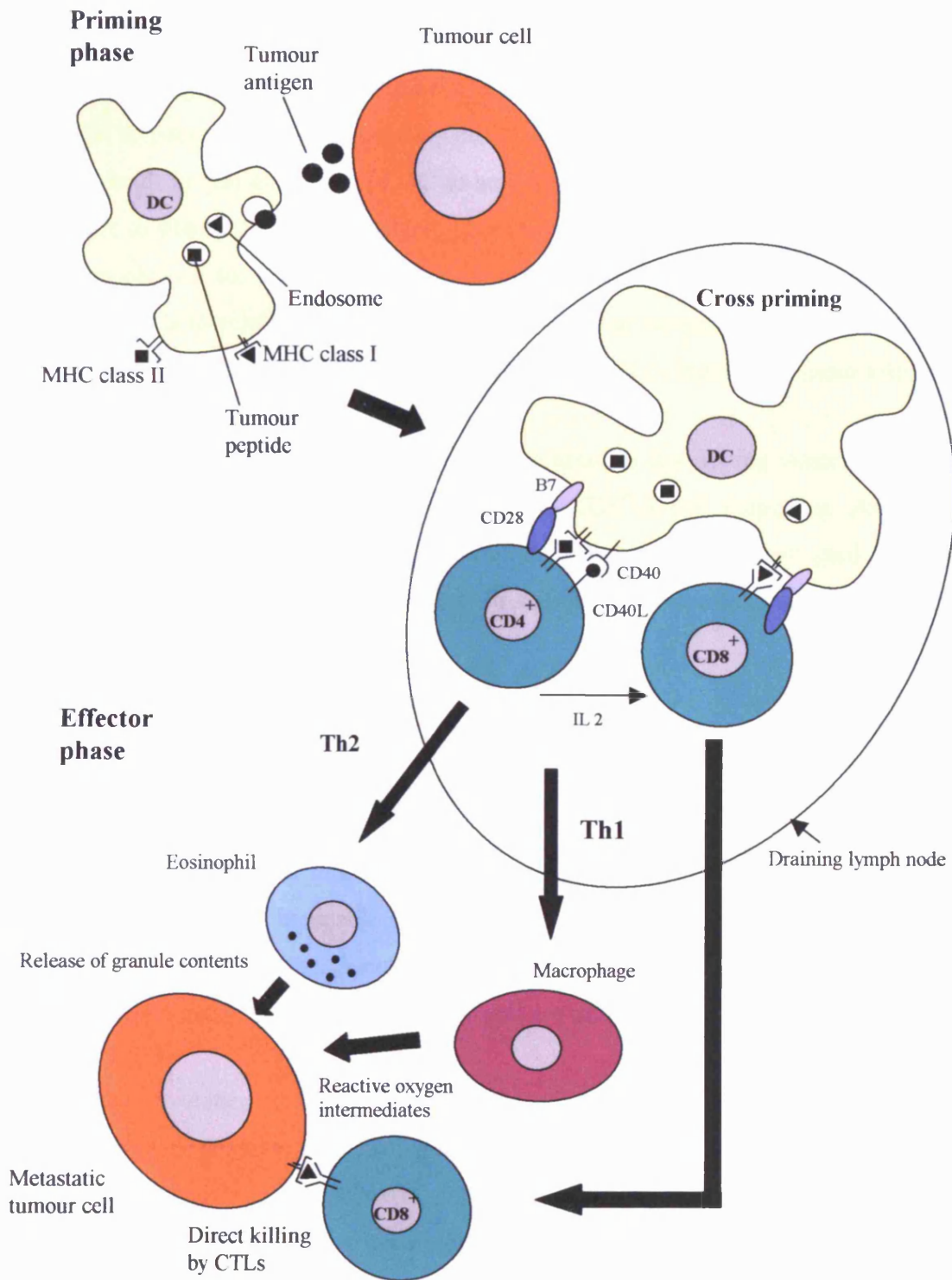


Figure 1.1 Central role of CD4⁺ T-cells in orchestrating multiple effector arms of antitumour immunity. Modified from Pardoll and Topalian (1998)

processing and presentation of tumour antigens by bone-marrow-derived DC. DC, which are potent professional APC, traffic to draining lymph nodes where they present antigens associated with MHC class I and MHC class II to CD8⁺ and CD4⁺ T-cells, respectively. Interactions between CD40L on the CD4⁺ T-cell and CD40 on the DC result in full activation of DC to activate CD8⁺ T-cells. Primed CD4⁺ cells then traffic to sites of tumour metastasis where the effector phase occurs. Th1 cells activate macrophages to produce reactive oxygen intermediates and Th2 cells activate eosinophils to release their granule content. Tumour cells may also be killed directly by CTL. These multiple effectors collaborate to produce maximal tumour killing.

Many tumour immunologists have been interested in developing cancer vaccines, the majority of which are designed to generate CD8⁺ T-cell responses. As it is now evident that CD4⁺ T-cells are a crucial component of potent and longlasting immunity, there is a growing interest in designing anti-tumour vaccines which will enhance the CD4⁺ T-cell response.

1.6 Immunological escape mechanisms

One of the questions that has puzzled immunologists for many years is why the immune system is incapable of eradicating tumours if T-cells have the ability to recognise and lyse them. A number of mechanisms have been proposed which enable tumours to evade the immune response and are outlined below.

There is evidence that some tumours generate antigen-loss variants which results in the failure to develop an effective anti-tumour immune response (Urban *et al.*, 1982; Uyttenhove *et al.*, 1983; Wortzel *et al.*, 1983). Down-regulation of MHC expression by tumour cells of various histological origins is frequently observed (Kageshita *et al.*, 1993; Cordon-Cardo *et al.*, 1991), which represents a major obstacle to successful immunotherapy based on CTL generation. Tumour cells may down-regulate β_2 -microglobulin (β_2 -M), thereby inactivating MHC class I antigen presentation (Restifo *et al.*, 1996). They may also down-regulate specific tumour antigen epitope transport via the TAP-1 protein, resulting in the failure to exhibit potential MHC/peptide

complexes on the tumour-cell surface (Cromme *et al.*, 1994). Tumour cells may express immunosuppressive factors, such as the transforming growth factor (TGF)- β or IL-10 which may down-regulate T-cell activity (Ranges *et al.*, 1987; Torre-Amione *et al.*, 1990) or they may express the Fas ligand which induces the apoptotic death of Fas sensitive, activated T-cells (Strand *et al.*, 1996). In summary, tumours may exhibit one or more of these mechanisms to facilitate immune evasion.

Recent evidence, however, supports a more fundamental mechanism in which in the absence of inflammation or tissue destruction the host becomes tolerant to tumour antigens (Pardoll, 1998). Dying tumour cells preferentially undergo apoptosis and do not release stress proteins and consequently are seen as normal regenerating tissues by the immune system (Matzinger, 1994). This can be explained by the conditions required for T-cell activation. When the immune system encounters a new antigen, it does not necessarily result in the stimulation of T lymphocytes. For stimulation to occur the T cell must receive two signals. The first signal is delivered via the TCR by its recognition of an antigenic peptide presented in the context of MHC. The second signal is provided by costimulatory and adhesion molecules on the cell surface of specialised APC interacting with co-receptors on the T-cells (Croft & Dubey, 1997). TCR engagement in the absence of a costimulatory signal results in T-cells that fail to develop full effector function and are rendered anergic even if both signals are provided in a subsequent encounter with antigen (Schwartz *et al.*, 1990). Experiments have demonstrated that the encounter of antigens by mature T cells often results in the induction of tolerance because of either ignorance, anergy or apoptotic death (Ohashi *et al.*, 1991; Burkley *et al.*, 1989). Therefore, activation of T-cells depends on how the antigen is presented to the immune system. During viral or bacterial infection, or when the antigen is mixed with the appropriate adjuvant, inflammation or tissue destruction occurs which results in the activation of the immune response (Figure 1.2). Conversely, when the antigen is expressed endogenously, there is no tissue destruction or inflammation which results in the development of tolerance (Figure 1.2). In response to certain inflammatory cytokines APC become activated and express costimulatory molecules. The antigen is targeted to these activated APC which results in T-cell activation. If APC are not activated by these inflammatory cytokines the appropriate costimulatory molecules are not expressed which leads to

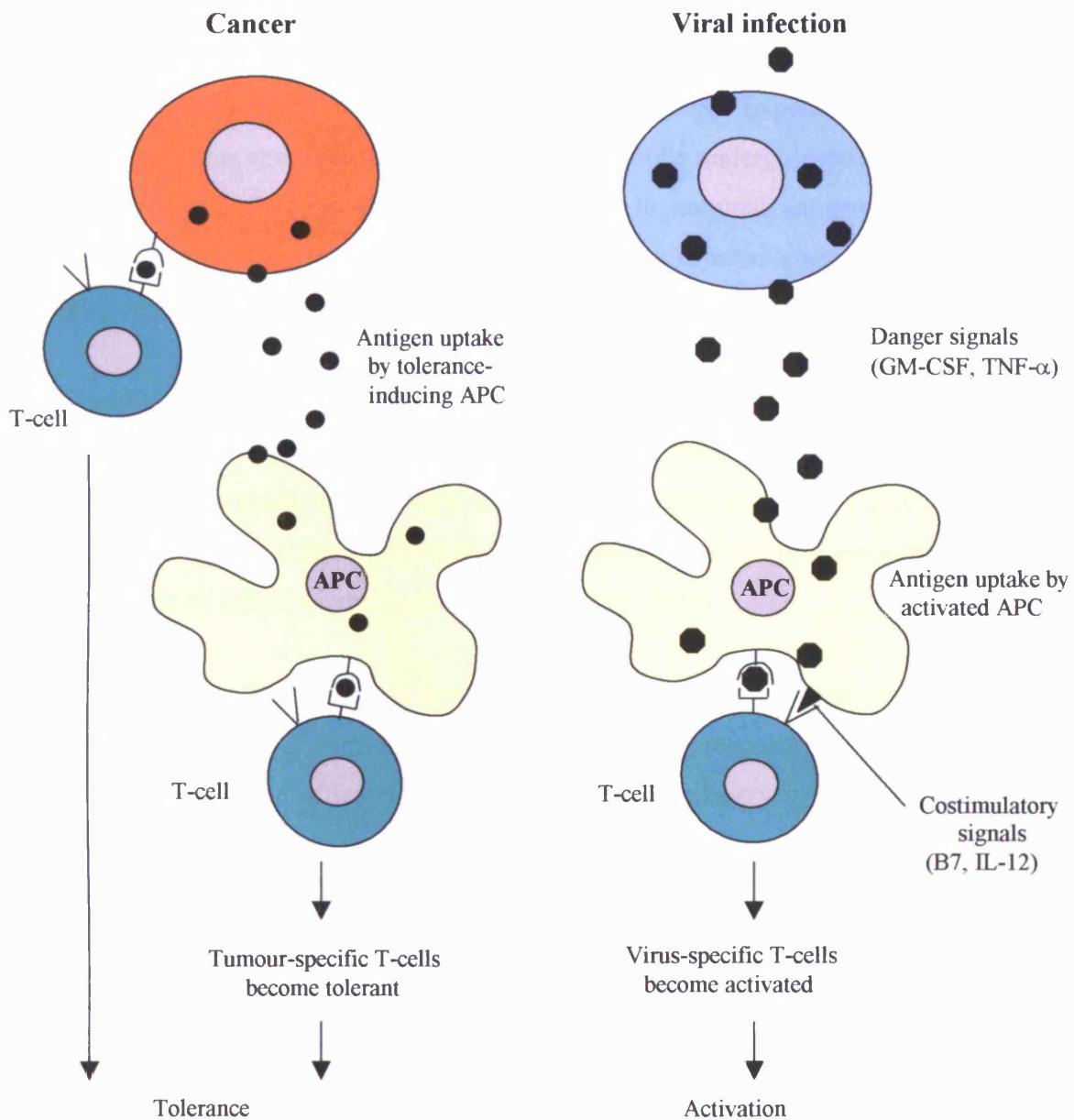


Figure 1.2. Comparison of immune responses to tumour antigens and viral antigens. During the inflammation and tissue destruction associated with a viral infection, antigen is targeted to activated APC that express costimulatory molecules such as B7 resulting in activation. In contrast, tumour cells express endogenous antigens without danger signals. Antigen is either presented directly by the tumour or by APC that do not express costimulatory signals resulting in tolerance. Modified from Pardoll, 1998.

ignorance, anergy or apoptosis of the antigen-specific T-cell when its receptor is bound to the antigen.

The ability of tumours to induce tolerance of T-cells specific to their antigens has been demonstrated by Satveley-O'Carroll *et al.* (1998). Experiments using murine tumour systems revealed that antigen-specific T-cells undergo significant changes in phenotype and function shortly after exposure to nominal antigen in the tumour-bearing host, leading to a state of antigen-specific unresponsiveness. This induction of antigen-specific T cell anergy occurs early during the course of tumour progression.

In addition, Wick *et al.* (1997) and Speiser *et al.* (1997) have shown that in other murine tumour systems, antigenic tumour cells have been found to grow progressively in immunocompetent hosts without inducing either acute or memory T cell responses. These studies prove that tumours are poor stimulators of immune responses and may be capable of actively inducing tolerance (Pardoll, 1998).

In order to be effective, breast cancer vaccines must overcome tolerance and activate both CD4⁺ and CD8⁺ T-cells, generating a long-lasting response. The recent evidence of DC as the most efficient APC for initiation of primary immune responses has encouraged studies to investigate their use to reverse tumour induced anergy through the presentation of tumour antigen in the context of appropriate secondary signals. In this way, immunity directed against these antigens may be amplified and result in tumour rejection.

1.7 Dendritic cells

Dendritic cells, which were first visualised as Langerhans cells (LC) in the skin in 1868, were originally isolated and characterized by Steinman and Cohn in 1973. They are potent APC essential for the initiation and modulation of primary immune responses.

In most tissues, DC are present in an immature state, unable to stimulate T-cells. They lack the requisite accessory signals for T-cell activation such as CD40, CD54 and

CD86 but are extremely well equipped to capture antigens. They are able to take up particles and microbes by phagocytosis (Moll *et al.*, 1993; Svensson *et al.*, 1997) and extracellular fluid and solutes by macropinocytosis (Sallusto *et al.*, 1995). They also express C-type lectin receptors such as macrophage mannose receptor (Sallusto *et al.*, 1995), DEC-205 (Jiang *et al.*, 1995) and Fc γ and FcE receptors (Sallusto *et al.*, 1994), that mediate adsorptive endocytosis. Both macropinocytosis and receptor-mediated endocytosis results in very efficient antigen presentation requiring only picomolar and nanomolar concentrations of antigens compared with the micromolar levels typically needed by other APC.

Exogenous antigens enter the endocytic pathway of the cell. Immature DC possess numerous specialised MHC class II rich compartments (MIIC) which enable them to produce large amounts of MHC class II-peptide complexes. During maturation of DC, MIIC convert to non-lysosomal vesicles that discharge their MHC-peptide complexes to the surface (Pierre *et al.*, 1997; Cella *et al.*, 1997) where they are presented to CD4⁺ T helper cells. Endogenous antigens such as viral proteins are degraded into peptides by the cytosolic proteasome and translocated to the endoplasmic reticulum where they bind to MHC class I molecules. The MHC class I-peptide complexes travel to the cell surface where they are presented to CD8⁺ T-cells. DC also appear to be able to present exogenous peptides from non-replicating microbes (Bender *et al.*, 1995) and dying infected cells (Albert *et al.*, 1998) in the context of MHC class I by a process known as cross priming (Figure 1.1). As mentioned earlier, recent evidence has indicated that class II mediated T helper response via CD40 signalling modulates APC including DC to prime CTL precursors (Toes *et al.*, 1998).

Once DC have been activated by antigen they begin to mature and migrate from peripheral tissues to the lymphoid tissues such as the spleen and lymph nodes, where they complete their maturation. Maturation of DC is crucial for the initiation of immunity and can be influenced by a number of factors such as microbial and inflammatory products. Whole bacteria (Winzler *et al.*, 1997), the microbial cell wall component lipopolysaccharide (LPS) (Sallusto *et al.*, 1995) and cytokines including IL-1, GM-CSF and TNF- α all stimulate DC maturation. Mature DC express high levels of nuclear factor (NF)- κ B family of transcriptional control proteins which

regulate the expression of many genes encoding immune and inflammatory proteins (Granelli-Piperno *et al.*, 1995). Activation of NF- κ B is caused by signalling through the TNF-receptor family e.g. TNF-R, CD40 and TRANCE/RANK. Therefore, an antigen may have to engage these signal transduction pathways in order to activate DCs (Banchereau & Steinman, 1998). IL-10, however, has an opposite effect on DC by preventing maturation. It inhibits differentiation of DC from circulating precursors, downregulates expression of co-stimulatory molecules and blocks IL-12 production and converts DC from an immunogenic to a tolerogenic role (Girolomoni & Ricciardi-Castagnoli, 1997).

Mature DC display many fine dendrites or veils that provide a large surface area for the simultaneous interaction with multiple lymphocytes (Steinman R.M., 1991; Steinman *et al.*, 1973). These dendrites bend, retract and re-extend from the cell body in a non-polarized fashion allowing for motility. Mature DC can readily prime T-cells. Only a few DC are necessary to provoke a strong T-cell response *in vitro* or *in vivo*. *In vitro* a single DC is capable of maximally stimulating 100-30000 T cells. Mature DC derive their stimulatory capacity from the rich expression of MHC, costimulatory and adhesion molecules on their cell surface and from their secretion of IL-12. MHC-peptide complexes are 10-100 times higher on DC than on other APC such as B-cells and monocytes. DC also express many accessory co-stimulatory molecules that interact with receptors on T cells (Caux *et al.*, 1994a; Inaba *et al.*, 1994) to enhance adhesion and signalling. These include CD58 (LFA-3), CD54 (ICAM-1), CD50 (ICAM-3), CD80 (B7-1) and CD86 (B7-2) (Young *et al.*, 1992; Inaba *et al.*, 1994; Caux *et al.*, 1994b). Mature DC are able to resist the suppressive effects of IL-10 and also synthesise high levels of IL-12 (Cella *et al.*, 1996; Koch *et al.*, 1996; Reis e Sousa *et al.*, 1997) that enhance both natural killer cells, B and T-cells. All these properties are upregulated within a day of exposure to many stresses and dangers, including microbial products (Banchereau & Steinman 1998). *In vivo*, immunity develops in lymphoid organs, where DC-T-cell interactions can be seen for all major classes of T-cell ligands (Ingulli *et al.*, 1997; Luther *et al.*, 1997; Kudo *et al.*, 1997).

In summary, immature DC, which are located in most tissues, capture and process antigens and display large amounts of MHC-peptide complexes at their surface. Upon

activation by antigen deposition and inflammation, they begin to mature resulting in the upregulation of their co-stimulatory molecules and loss of their antigen-capture capacity. They migrate to lymphoid tissues where they liaise with a pool of naïve or quiescent T cells and complete their maturation. Mature DC activate antigen-specific T cells which can lead to an effective long-lasting immune response. DC play a crucial role in the immune system and many studies are currently involved in the examination of DC-based vaccines in the generation and regulation of tumour immunity.

1.8 Dendritic cell-based vaccines

Several approaches to investigate DC-based tumour vaccines have been tested in animal models, including dendritic cells loaded *in vitro* with minimal MHC class I restricted peptides (Zitvogel *et al.*, 1996; Mayordomo *et al.*, 1995) or protein (Hsu *et al.*, 1996; Paglia *et al.*, 1996) and DC fused with whole tumour cells (Gong *et al.*, 1997; Celluzzi & Falo, 1998). Other approaches have explored *ex vivo* transduction of DC using either RNA (Boczkowski *et al.*, 1996) or replication-defective recombinant viral vectors (Specht *et al.*, 1997; Song *et al.*, 1997) to introduce genes encoding tumour antigen. Most of these studies have demonstrated rejection of significant tumour burdens.

In vitro studies using human systems have examined DC transfected with DNA and RNA-encoded tumour antigens. Alijagic *et al.* (1995) transfected DC generated from peripheral blood of normal donors with DNA encoding the melanoma antigen tyrosinase using a liposome-based transfection technique. DC transfected with the tyrosinase gene were able to induce specific T-cell activation *in vitro*, indicating appropriate peptide processing and representation in DC after transfection. Nair *et al.* (1998) transfected DC, generated from peripheral blood mononuclear cells of normal donors or cancer patients, with CEA mRNA using a liposome based transfection technique. These DC were able to stimulate a potent CD8⁺ CTL response *in vitro*. Similar results were observed when DC were effectively sensitised with RNA in the absence of liposome based transfection reagents.

DC are beginning to enter the clinical setting. In a recent clinical study, DC were generated in the presence of GM-CSF and IL-4 from 16 melanoma patients and were pulsed with tumour lysate or a cocktail of melanoma peptides known to be recognised by CTL, depending on the HLA haplotype of the patient. Keyhole limpet haemocyanin (KLH) was added as a CD4⁺ helper antigen and an immunological tracer molecule. All 16 patients with advanced melanoma were immunized and all vaccinations were well tolerated with no physical signs of autoimmunity. DC vaccination induced DTH reactivity toward KLH in all patients, as well as a positive DTH reaction to peptide-pulsed DC in 11 patients. Recruitment of peptide-specific CTL to the DTH challenge site was also demonstrated indicating that antigen-specific CTL were induced during DC vaccination. Objective responses were evident in 5 out of 16 patients (2 complete responses, 3 partial responses) with regression of metastases in various organs and one additional minor response. These data indicate that vaccination with autologous DC generated from blood is a safe and promising approach in cancer immunotherapy (Nestle *et al.*, 1998).

In another clinical trial, autologous DC were pulsed *ex vivo* with tumour-specific idiotype protein to stimulate host antitumour immunity when infused as a vaccine. Four patients with follicular B-cell lymphoma received a series of 3 or 4 infusions of antigen-pulsed DC followed, in each instance, by subcutaneous injections of soluble antigen 2 weeks later. All four patients developed a measurable antitumour cellular immune response and one patient experienced tumour regression while another had partial tumour regression. These antigen-pulsed DC, which can be safely infused repeatedly with no significant toxicity, have the ability to stimulate clinically relevant immune responses in humans (Hsu *et al.*, 1996).

A complicating factor in the development of effective DC tumour vaccines is that DC obtained from cancer patients may not express costimulatory molecules and become ineffective APC. This is probably due to the lack of danger signals (inflammatory cytokines) produced by the tumour cells during the cross-priming mechanism resulting in the inactivation of DC. There is evidence that DC isolated from tumour bearing mice were found to be defective with poor stimulatory capacity and impaired function. Also tumour infiltrating DC isolated from a rat colon carcinoma were found

to lack significant expression of costimulatory molecules even after *in vitro* culture with GM-CSF, IL-4 or CD40L (Caux *et al.*, 1997). A recent report showed that DC freshly isolated from cancer patients were found to have weak expression of costimulatory molecules and functioned poorly in T cell stimulation assays. In contrast, DC generated *ex vivo* from progenitor populations derived from cancer patients demonstrated normal phenotype and function (Tarte *et al.*, 1997; Siena *et al.*, 1995). Therefore, it appears favourable to use DC generated *ex-vivo* from either peripheral blood or bone marrow stem cells in tumour vaccinations.

The key to all DC-based approaches is the induction of MHC presentation of peptides derived from the antigenic protein. Such presentation to CD4⁺ and CD8⁺ precursors is required for the generation of antigenic-specific T cells. Pulsing DCs with peptides may not be suitable for clinical application because of the MHC restriction of the immune response. The antigenic peptide sequence would have to be defined and the haplotype of the patient determined to ensure that the appropriate peptides would be presented on the patients MHC molecules. Also the use of unfractionated tumour-derived protein may not be suitable because tumour fragments of sufficient dimension are often not available and because of the possibility of inducing autoimmune responses against self antigens (Girolomoni & Riccardi-Castagnoli, 1997).

An alternative approach is to use nucleic acids (DNA or RNA) delivery to induce expression of antigenic protein and the subsequent MHC presentation of derived proteins. DNA/RNA encodes multiple epitopes for many MHC alleles. Hence RNA/DNA transfected DC can be used to stimulate T cell responses in many patients without prior knowledge of, or need to determine, the haplotype of the patient (Nair *et al.*, 1998).

Many groups have examined the use of DC-based vaccines, which demonstrate the exceptional ability of DC to stimulate T-cell responses both *in vitro* and *in vivo*. However, very few studies have manipulated DC to express breast tumour antigens which result in the enhancement of a CD4⁺ T-cell response. Therefore, an attractive approach may involve the generation of DC *ex-vivo* from peripheral blood or bone marrow stem cells, followed by their transfection with RNA or DNA encoding a

breast tumour antigen, engineered to traffic to the MHC class II pathway. Due to the additional expression of the crucial secondary signals, this may result in the enhancement of a CD4⁺ T-cell response, thus reversing tumour induced anergy.

1.9 MHC Class I and II pathways

In order to design a DC-based tumour vaccine which will enhance the CD4⁺ T helper response it is vital that the tumour antigen of interest has access to the MHC class II pathway. To achieve this, it is important to note the differences between the MHC class I and II antigen-processing pathways and design an appropriate strategy.

1.9.1 MHC Class I pathway

MHC class I molecules are expressed on the surface of virtually all nucleated cells and consist of a transmembrane glycoprotein or class I heavy chain, a small soluble protein known as β_2M and a short peptide usually 8-10 amino acids in length (Pamer & Cresswell, 1998). Many class I-peptide complexes have been crystallised and their 3-dimensional structures determined (Jones, 1997). The peptide binding site consists of two antiparallel α -helices overlaying a platform of antiparallel β -strands. In this binding groove the N- and C-termini of the peptide interacts with invariant residues, while a subset of the peptides amino side chains interacts with pockets lined with polymorphic amino acids which provides specificity. This produces a very stable high affinity interaction. The TCR recognises the complex by binding to the surface formed by exposed residues of the bound peptide and accessible elements of the 2 α -helices.

Peptides associated with MHC class I molecules are generally derived from cytosolic or nuclear proteins (Jardetzky *et al.*, 1991). These endogenous proteins are degraded by large ATP-dependent proteasomes in the cytoplasm. Rock, Goldberg and colleagues have demonstrated, using peptide aldehyde inhibitors, that proteasomes mediated the majority of endogenous cytoplasmic protein degradation (Rock *et al.*, 1994). Recent studies, utilising the more specific proteasome inhibitor, lactocystin (Fenteany *et al.*, 1995), have confirmed their important role in the generation of MHC

class I-associated peptides. The 20S proteasome is a multicatalytic protease with an approximate molecular weight of 700kDa, comprising 28 subunits. These subunits can be classified into α - and β - types and are arranged into 4 heptameric rings which are stacked to enclose three large cavities. The rings of β subunits contain the proteolytically active sites with only three of the seven β subunits possessing activity. This barrel-shaped complex represents the active proteolytic core of larger assemblages, the 26S proteasome and the PA28(11S)-proteasome complex. Interferon (IFN)- γ induces a major structural reorganisation of the 20S proteasome. Coordinative replacement of the 3 active subunits by B2i (MECL1), B1i (LMP2) and B5i (LMP7) results in the formation of 'immunoproteasomes' (reviewed in Tanaka & Kasahara, 1998). Studies have concluded that the formation of immunoproteasomes may alter the substrate specificity in such a way that the peptide repertoire is expanded. In addition, IFN- γ induces the formation of the PA28 activator complex, which replaces the normal 19S (PA700) cap component of the 26S proteasome responsible for ATP-dependent degradation of mostly ubiquitin-conjugated proteins. Recent progress shows that PA28 promotes processing of endogenous antigens (Groettrup *et al.*, 1996; Dick *et al.*, 1996).

It is still unknown how peptides released from proteasomes reach TAP in the ER membrane. Srivastava *et al.* (1994) proposed that heat shock proteins (HSP) may generally serve to carry antigenic peptides to the peptide transporter. Preliminary evidence exists that the blockade of cytoplasmic HSP reduces the amounts of class I binding peptides (Nadeau *et al.*, 1994).

Peptide transporters, which are MHC encoded noncovalent heterodimers, belong to the superfamily of ATP-binding cassette transporters. They are made up of structurally homologous subunits TAP-1 and TAP-2 which both possess an N-terminal hydrophobic region with multiple predicted transmembrane domains and a cytosolic C-terminal ATP-binding domain (reviewed in Heemels *et al.*, 1995; Lehner *et al.*, 1996; Howard, 1995). Numerous *in vitro* studies have demonstrated the ability of TAP to translocate peptides across the ER membrane which is an ATP-dependent process (Shepherd *et al.*, 1993; Androlewicz *et al.*, 1993; Neefjes *et al.*, 1993). Recent studies using photoaffinity labelling with peptides have established that the binding

site is comprised of regions of TAP-1 and TAP-2 at the C-terminal end of the hydrophobic segment, adjacent to the cytosolic hydrophilic domain (Androlewicz *et al.*, 1994; Nijenhuis *et al.*, 1996). The binding of peptides to TAP is ATP-independent (van Endert *et al.*, 1994). TAP molecules preferentially transport peptides of 8-12 amino acids (Androlewicz & Cresswell, 1994; Koopman *et al.*, 1996). Peptide binding to TAP appears to be less stringent than binding of peptide to MHC class I molecules which suggests that the specificity should be more promiscuous in order to supply many allelic class I variants with peptides.

Many chaperones have been proposed to be involved in MHC class I peptide assembly in the ER (reviewed in Pamer & Cresswell, 1998; Cresswell *et al.*, 1999). The ER chaperone, BiP (immunoglobulin binding protein), which is believed to interact with proteins during their translation and insertion to enable their unidirectional movement through the ER membrane, has been shown to bind to free class I heavy chains (Noessner *et al.*, 1995). The dominant chaperone, however, associated with newly synthesised class I heavy chains is calnexin (p88) (Jackson *et al.*, 1994; David *et al.*, 1993; Ortmann *et al.*, 1994; Vassilakos *et al.*, 1996). Calnexin, which is an ER-retained transmembrane protein, facilitates folding and disulfide bridge formation of the nascent heavy chains and promotes assembly of heavy chains with β_2M (Vassilakos *et al.*, 1996). Cresswell and colleagues (Sadasivan *et al.*, 1996) provided evidence that the soluble ER protein, calreticulin, replaces calnexin as chaperone for heavy chain- β_2M heterodimers and remains associated during the transient interaction of class I molecules with TAP. In addition, the soluble ER protein, the thiol oxidoreductase, Erp57 interacts with this multisubunit complex. Recent evidence suggests that disulfide bond formation is initiated when class I heavy chains are associated with calnexin and completed after β_2M binding and calreticulin association, with Erp57 being the thiol oxidoreductase facilitating their formation (Lindquist *et al.*, 1998). Tapasin, which is a proline-rich, type 1 transmembrane glycoprotein of 428 amino acids with a single N-linked glycan (Ortmann *et al.*, 1997) appears to form a bridge between heavy chains and TAP and can independently bind to either TAP or the heavy chain- β_2M -calreticulin complex (Sadasivan *et al.*, 1996). Tapasin may also serve to coordinate peptide translocation as well as MHC class I-TAP association. Peptide translocation by TAP eventually results in the formation of

a class I-peptide complex, which dissociates from tapasin, calreticulin and Erp57. Assembly of MHC I class molecules and peptide to a heterotrimeric complex is essential for efficient release from the ER (Ploegh *et al.*, 1981). After release from ER, this complex is transported through the Golgi apparatus and trans-Golgi network (TGN) to the plasma membrane. For a schematic representation of the MHC class I pathway refer to Figure 1.3.

1.10.2 Class I MHC presentation of exogenous antigens *In Vivo*

Classically, CTL recognise antigens that are localised in the cytoplasm of target cells, processed and presented as peptide complexes with MHC class I molecules (Heemels & Ploegh, 1995). MHC class I molecules are not generally loaded with peptides following processing of exogenous antigens (Townsend & Bodmer, 1989; Morrison *et al.*, 1986.). Numerous studies, however, have provided evidence for an exogenous pathway whereby antigens that are not expected to gain access to the cytoplasm are presented on MHC class I molecules (reviewed in Pamer & Cresswell, 1998; Reimann & Schirmbeck, 1999). This phenomenon is termed cross priming (Figure 1.1). These endocytic pathways are particularly prominent in macrophages and DC, the cells most likely to mediate this unusual mode of loading of class I MHC *in vivo* (Bevan, 1987). Recent studies have shown that APC can acquire antigens from tumours (Huang *et al.*, 1994), transplants (Bevan, 1977) and apoptotic tissues (Albert *et al.*, 1998) by phagocytosis for stimulation or tolerisation of MHC class I restricted CTL.

Recent evidence points to a heterogeneity of processing pathways for exogenous antigens that generate MHC class I binding peptides. These alternative pathways are outlined below (reviewed in Riemann & Schirmbeck, 1999). Endosomal/lysosomal processing of inactivated viruses and virus-like particles result in either their presentation by recycling MHC class I molecules or delivery to the conventional endogenous pathway. Phagocytosed material can be processed by three alternative routes. Firstly, whole microorganism, proteins or peptides can be delivered to the cytosol where they enter the endogenous processing pathway. Secondly, processing in phagosomes may yield peptides that bind to MHC class I molecules recycling through phagolysosomes. However, there is little evidence supporting this. Thirdly, partially

degraded material can be regurgitated and bind to cell surface-associated MHC class I molecules. A direct vesicular route from the cell surface to the ER lumen allows the retrograde transport of peptides or proteins delivering them to the site of peptide loading of nascent MHC class I molecules. Exogenous antigens can also access the endogenous pathway facilitated by stress proteins, adjuvants, toxins, membrane-penetrating microorganisms and intrinsic membrane-translocating properties of antigens. Finally, processing of exogenous antigens at the cell surface may yield MHC class I binding peptides, but there are very few data that support this pathway.

The alternative processing of exogenous antigens for MHC class I restricted peptide presentation may allow additional repertoires of peptides to become visible to CTL precursors and thus increase the presentation of pathogens to the CTL system. Furthermore, pathogen-induced blocking mechanisms of processing or MHC class I display may be circumvented by operating more than one pathway (Reimann & Schirmbeck, 1999).

1.9.3 MHC Class II pathway

In contrast to MHC class I molecules, the constitutive expression of class II molecules is restricted to specialised APC such as macrophages, DC and B-cells (Daar *et al.*, 1984). Expression of class II molecules, however, may be induced in a variety of other cells which are normally class II negative by IFN- γ (Pober *et al.*, 1983). The MHC class II heterodimer consists of two type I transmembrane glycoproteins, an α -chain of 35kDa and a β -chain of 27kDa molecular weight. The highly polymorphic α 1 and β 1 domains of the subunits form the peptide binding site which is situated in the N terminal lumen region. After maturation the binding site is displayed at the plasma membrane (Cresswell *et al.*, 1987). X-ray crystallography studies of HLA-DR1 showed that the MHC class II peptide binding groove is similar to that of class I molecules, with the exception that it is more open at both ends allowing the bound peptide to protrude out of the groove (Stern *et al.* 1994). Class II binding peptides are bound in an extended and non-helical confirmation (Brown *et al.*, 1993). Interactions between the polymorphic amino acids of the MHC molecule that form binding pockets in the binding groove, and side-chains of the anchor-residues in the peptide

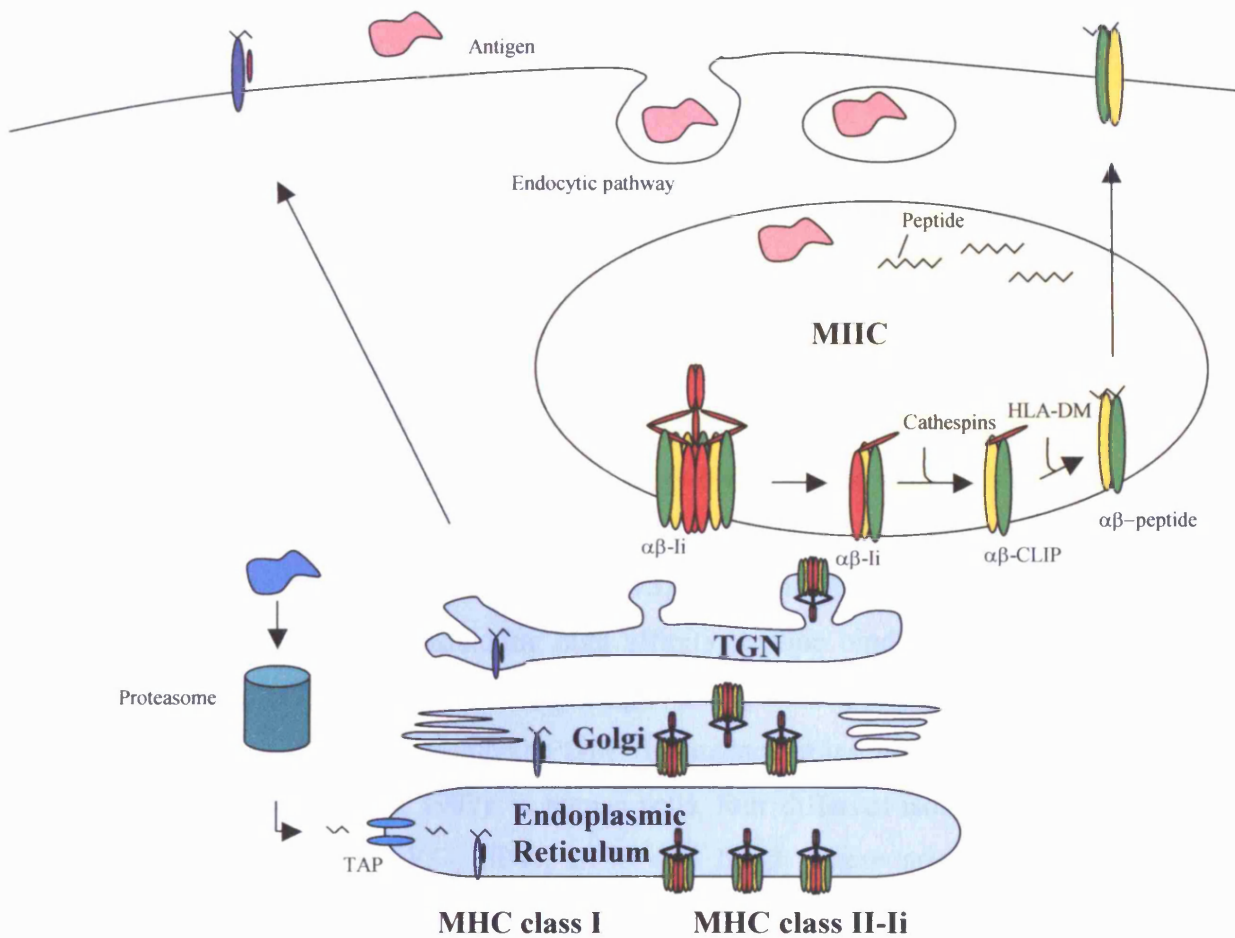


Figure 1.3. Intracellular pathways of MHC class I and MHC class II molecules. MHC class I molecules acquire antigenic peptides, generated by the proteasome, from the cytosol that are translocated into the ER by TAP molecules. MHC class I-peptide complex is transported through the Golgi complex directly to the cell surface for presentation to CD8⁺ T-cells. In contrast, the class II/Ii complex, which is assembled in the ER, is targeted at the TGN network to MIIC by virtue of targeting signals that reside in the Ii cytoplasmic tail. There, the Ii is progressively degraded, at least partially through the action of cathepsins, leaving the CLIP peptide associated with the MHC class II peptide binding groove. CLIP can then be exchanged for antigenic peptides, and this exchange is catalysed by DM molecules. Peptide loaded MHC class II complexes are then transported to the plasma membrane for presentation to CD4⁺ T-cells. Modified from Pieters, 1997.

determine the specificity. Peptides recognised by class II-restricted T cells are usually 10-17 amino acids long (Chicz *et al.* 1993) and are generally derived from exogenous antigens which have been degraded in the endocytic pathway (Yewdell & Bennink, 1990).

After transcription, MHC class II molecules are cotranslationally inserted into the ER where they are assembled. There are reports that MHC class II molecules are retained by the ER resident proteins, calnexin, BiP and GRP94, until they are properly folded. These proteins have promiscuous protein-binding activity and facilitate protein folding. The major chaperone protein that associates with MHC class II molecules in the ER is the invariant chain (Ii). There is evidence that it affects MHC class II conformation (Melnick & Argon, 1995; Peterson & Miller, 1990), assembly (Bikoff *et al.*, 1995;) and transport (Humbert *et al.*, 1993), inhibiting premature peptide binding (Teyton *et al.*, 1990) but promoting high affinity peptide binding (Sherman *et al.*, 1995; Sloan *et al.*, 1995) and affecting antigen presentation (Bodmer *et al.*, 1994). Ii is a non-polymorphic transmembrane type II transmembrane glycoprotein (Koch *et al.*, 1987; Mcknight *et al.*, 1989). In human cells, four different isoforms are usually coexpressed which are IiP33, IiP41, IiP35 and IiP43. These arise as a result of alternative translation sites and alternative splicing (Strubin *et al.*, 1986). Trimers of Ii assemble with class II heterodimers to form a nonameric complex consisting of 3 class II heterodimers with one Ii trimer (Roche *et al.*, 1991; Cresswell, 1996). From biochemical and structural studies a domain has been located within the carboxy-terminal part of Ii responsible for trimerisation (Cresswell, 1996; 1995; Jasanoff *et al.*, 1995; Park *et al.*, 1995). Transmembrane segments of Ii might also contribute to stable trimer formation (Amigorena *et al.*, 1995). CLIP (class II-associated invariant chain peptides) a region of the invariant chain (amino acid residues 81-104) which occupies the peptide binding groove, is thought to mediate the interaction of Ii with MHC molecules and prevent the binding of peptides in the ER (Amigorena *et al.*, 1995; Freisewinkel *et al.*, 1993; Riberdy *et al.*, 1992). Shutze *et al.* (1994) identified an ER retention signal in Ii which is thought to be concealed during the association with MHC class. This results in the release of the nonameric complex from the ER and the subsequent transport along the secretory pathway to the trans-Golgi network. Due to the presence of di-leucine-based targeting signals in the Ii cytoplasmic tail, the

nonameric complexes are diverted from the secretory pathway and targeted to endocytic compartments (Lotteau *et al.*, 1990; Pieters *et al.*, 1993).

There has been much debate over the identification of the endocytic compartments where peptide loading of class II molecules occurs. Since 1990, many studies using immunofluorescence, electron microscopy and subcellular fractionation techniques have denoted various compartments such as early endosomes (EE) (Guagliardi *et al.*, 1990), late endosomes (LE) (Humbert *et al.*, 1993b; Fernandez-Borja *et al.*, 1996), “sac-like” vacuoles (Harding *et al.*, 1991), phagosomes (Harding & Geuze, 1992), lysosomes (Kleijmeer *et al.*, 1994; Lutz *et al.*, 1997; Fernandez-Borja *et al.*, 1996), as the site where class II molecules accumulate. Data also supports the existence of specialized peptide-loading compartments in APC, called MIIC and class II vesicles (CIIV) (Neefjes, 1999).

MIIC consist of vesicles of 200-300nm in diameter which show morphological heterogeneity that varies from multivesicular, multilamellar or tubulovesicular, depending on the cell type (Peters *et al.*, 1991; Harding & Geuze, 1992). Subsequent immunoelectron-microscopic studies have confirmed the presence of MIIC in human B cells (Peters *et al.*, 1995; West *et al.*, 1994), macrophages (Harding & Geuze, 1992), and DC (Kleijmeer *et al.*, 1995; Nijman *et al.*, 1995). MIIC contain the lysosomal enzyme, β -hexosaminidase, the lysosomal-associated membrane proteins lamp-1 and CD63, cathepsin D (Harding & Geuze 1993; Peters *et al.*, 1995), acidic peptidase activity (Fernandez-Borja *et al.*, 1996) and HLA-DM (DM) (Karlsson *et al.*, 1994; Nijman *et al.*, 1995; Sanderson *et al.*, 1994). They lack endosomal markers such as mannose-6-phosphate receptor (LE) and the transferrin receptor (EE). CIIV consist of vesicles, 300-500nm in diameter, with membrane infoldings or internal vesicles (Amigorena *et al.*, 1994 & 1995). CIIV lack lysosomal markers present in MIIC and contain markers of EE. Mellman *et al.* (1995) and Peters *et al.* (1995) proposed that CIIV represent early MIIC that have multivesicular structures containing relatively low amounts of MHC class II molecules and Ii. In contrast, mature multilamellar MIIC are Ii negative and are enriched in MHC class II molecules. Recently, Neefjes *et al.* (1999) proposed that MIIC represent a collection of late endocytic compartments such as late endosomal/early lysosomal structures

which contain DM and proteases, thus providing the optimal environment for efficient peptide loading of MHC class II molecules.

The mode of internalisation of the antigen and the subsequent proteolysis to generate epitopes will also determine the site of MHC class II loading of antigenic peptides. APCs such as DC can internalise antigens in various ways including receptor-mediated uptake (Sallusto *et al.*, 1995; Jiang *et al.*, 1995) and macropinocytosis (Sallusto *et al.*, 1995; Berthiaume *et al.*, 1995). There are three possible mechanisms to generate peptides. Proteins may be degraded by endosomal/lysosomal proteases and the resulting peptides transported into MIIC, possibly with the assistance of a chaperone molecule (Pierce, 1994). Antigens may be internalised in MIIC directly and degraded there. Lastly, antigens may access the MIIC, bind to class II molecules, followed by degradation by exopeptidases generating relatively large polypeptide fragments (Rammensee, 1995b).

After transport of class II-Ii complex to MIICs, Ii is degraded to a nested set of peptides, CLIP, that occupy the binding groove (Avva & Cresswell, 1994; Ghosh *et al.*, 1995). This degradation is most probably mediated by the cysteine proteases cathepsin S and or L (Bevec *et al.*, 1996; Riese *et al.*, 1996). For many class II alleles, efficient exchange of CLIP for antigenic peptide requires DM. DM is expressed in cells that also express MHC class II and Ii and consists of two type I transmembrane glycoproteins, 33-35kDa α and 30-31 kDa β chain, that are homologous to both MHC class I and class II molecules (Kelly *et al.*, 1991). Its crystal structure resembles that of other MHC molecules but the groove is more shallow and unable to fit peptides (Mosyak *et al.*, 1998; Fremont *et al.*, 1998). *In vitro*, DM acts in a catalytic manner to accelerate release of CLIP (Sloan *et al.*, 1995; Denzin & Robbins, 1994, Denzin & Cresswell, 1995; Sherman *et al.*, 1995) and other peptides lacking optimal anchor residues (Weber *et al.*, 1996; Kropshofer *et al.*, 1996). Thus *in vivo*, DM probably favours classII/peptide complexes that will be long-lived at the cell surface. It is also suggested that DM is able to stabilise the class II molecules when they are devoid of peptide (Vogt *et al.*, 1996; Kropshofer *et al.*, 1997) and prone to aggregation (Germain & Hendrix, 1991). Thus, DM could be considered a lysosomal chaperone. DM has been localised in human B lymphoblastoid cells and DC, to the MIIC by

immunoelectron microscopy (Nijman *et al.*, 1995; Sanderson *et al.*, 1994). However, it does not appear to associate stoichiometrically with Ii (Denzin *et al.*, 1994) implying that it possesses a targeting signal of its own. A tyrosine-based motif YTPL present in the cytoplasmic tail of DM β has been shown to direct DM to lysosomal compartments in HeLa cells and reporter molecules to MIIC in B-lymphoblastoid cells (Marks *et al.*, 1995; Lindstedt *et al.*, 1995; Copier *et al.*, 1996). Even though initial studies revealed that there was no association between DM and Ii, further investigations using different detergent systems demonstrated a weak association in the ER and endocytic pathway (Denzin *et al.*, 1994). Recent studies by Copier *et al.* (1998) suggest that although this association is weak, Ii may influence the DM targeting to MIIC in B lymphoblastoid cells, implying that the intracellular trafficking pathways of DM and class II overlap substantially.

DM function seems to be further regulated by the action of HLA-DO (DO) (Liljedahl *et al.*, 1996; Denzin *et al.*, 1997; Jensen, 1998) which also shows homology to MHC class II molecules. DO is expressed in only a subset of APC and mainly in non-activated B cells (Karlsson & Peterson, 1992; Surh *et al.*, 1992). DO is tightly associated with DM which is necessary for the egress of DO from the ER (Van Ham *et al.*, 1997; Liljedahl *et al.*, 1996). It has been shown to inhibit the action of DM in a pH-dependent manner (van Ham *et al.*, 1997; Denzin *et al.*, 1997) being most active in mildly acidic compartments. It is therefore capable of skewing peptide exchange onto class II molecules towards acidic and thus late endosomal compartments. Conversely, DO could allow loading of recycling class II molecules with peptides that would otherwise be removed by the action of DM (Pinet & Long, 1998). Thus, DO appears to be an important modulator of class II-restricted antigen processing in a cell type-specific manner.

Until recently, little was known about the export of class II molecules loaded with peptides to the cell surface. Recent evidence suggests that transport from the perinuclear location does not involve formation of small buds from MIIC (Wubbolts *et al.*, 1996) and appears to be microtubule dependent (reviewed in Wubbolts & Neefjes, 1999). Two possible explanations for the presence of peptide loaded, class II molecules at the cell surface and the absence of the other MIIC components such as

classII/CLIP, lysosomal markers and DM have been proposed. The first possibility may involve the physical separation of the mature class II and other molecules that should be at the cell surface from those that are not found at the cell surface. This process probably requires a budding event from MIIC prior to fusion with the plasma membrane. The second possibility may involve the fusion of an entire MIIC with the plasma membrane which has been observed (Raposo *et al.*, 1996; Wubbolts *et al.*, 1996). This would result in the deposition of both mature class II and other MIIC components on the cell surface followed by rapid internalisation of the surface molecules apart from MHC class II. There is evidence of the retrieval of MIIC components not normally found at the cell surface by clathrin-mediated processes (Liu *et al.*, 1998; van Ham., *et al.*, 1997; Wang *et al.*, 1997). For a schematic representation of the MHC class II pathway refer to Figure 1.3.

1.9.4 Class II MHC presentation of endogenous antigens

It is well established that the predominant pathway of antigen presentation by MHC class II molecules involves endocytosed proteins. Many groups, however, have reported examples of endogenous antigens presented by MHC class II molecules. These include experiments carried out by Long and colleagues which revealed that endogenous measles proteins accessed the class II pathway (Jacobson *et al.*, 1989). Other groups have analysed the presentation of endogenous protein by class II molecules using hen egg lysozyme (HEL) as a model antigen (Humbert *et al.*, 1993; Brooks & McCluskey, 1993; Moreno *et al.*, 1991). Further studies have provided evidence that the TAP complex of the MHC class I pathway may have an influence on the peptide loading of class II molecules (Malnati *et al.* 1993; Carmichael *et al.*, 1996).

There are three mechanisms by which endogenous peptides could bind to class II molecules other than by reaching the cell surface and being endocytosed. The first may involve class II molecules becoming occupied with peptides in the ER which have been referred to as class II molecules “hijacking” the class I pathway (Lechler *et al.* 1996). Evidence supporting this is provided by Bijlmakers *et al.* (1994). They generated microsomes *in vitro* which mimicked physiobiochemical properties found in the ER, and observed the peptide binding of MHC class II molecules. Additional

evidence was provided by the experiments of Malnati *et al.* (1993) with the expression of the influenza nucleoprotein (NP) minigene in B-cell lines with and without TAP expression. The inhibition of NP peptide presentation with DR1 in the TAP-deficient line suggests that ER loading was responsible for the presentation of NP with DR1 in cells with TAP expression. In addition, Urban and colleagues transfected mouse B-cell hybridomas with genetic constructs encoding short polypeptides comprising T-cell-recognised sequences attached to the DR α signal peptide, to transport the peptides into the ER. This led to successful presentation of several different peptides with cell surface class II molecules (see Lechler *et al.*, 1996).

The second possibility is that cytosolic proteins enter MIIC by a process such as microautophagy or as a result of transport by cytosolic heat shock proteins. Microautophagy encompasses the internalisation of small portions of cytoplasm and limiting membrane by LE/MIIC. The integrity of the internal vesicles can be destroyed by proteolysis resulting in cytosolic and membrane derived peptides being bound to class II molecules (Liou *et al.*, 1997). Alternatively, cytosolic proteins can be translocated across the MIIC membrane. Chiang *et al.* (1989) suggested that a 70kDa heat shock protein hsc73 was implicated in the translocation of cytosolic proteins into MIIC. Further evidence has shown that cytosolic proteins can be translocated across the MIIC membrane by a receptor-mediated process requiring ATP and heat shock proteins (Cuervo *et al.*, 1996)

The third possible mechanism, which has received much attention, involves the binding of partially unfolded proteins to nascent MHC class II molecules in the ER. The formation of complexes between class II molecules and proteins has been observed in Ii-negative cells by Anderson *et al.* (1993) and Busch *et al.* (1996). In addition, Lechler *et al.* (1996) carried out extensive studies which involved the expression of HLA-DR molecules in insect cells and a human fibroblast cell line with or without Ii and DM expression. The results revealed that MHC class II molecules are capable of binding to partially folded proteins early in the biosynthetic pathway in the absence of the Ii. Evidence also suggested that MHC class II-protein complexes can exit from the ER, traffic to the cell surface and then be endocytosed. Most

importantly, data obtained using alloreactive T cells as probes of the array of MHC class II-bound peptides suggest that the absence of the Ii leads to the display of a distinct set of DR-bound peptides. Furthermore, the nature of the bound peptides is influenced by the DM molecule, even in the absence of the Ii. Taken together these results suggest that alteration of the ratio of MHC class II, Ii and DM molecules in APCs may result in the display of peptides to which the T-cell repertoire has not previously been exposed.

In conclusion, alternative pathways exist for the presentation of endogenously, cytosolically derived peptides by MHC class II molecules. The characterisation of naturally processed peptides eluted from class II molecules suggests that the presentation of endogenous proteins is a minority event and that class II molecules are primarily devoted to the presentation of endocytic peptides (Lechler *et al.*, 1996).

1.9.5 Targeting endogenous antigens to the MHC Class II processing pathway

To enhance the CD4⁺ T-cell response, it is essential that a vaccine strategy which utilises DC transfected with nucleic acids encoding tumour antigen, results in the presentation of MHC class II restricted peptides. Even though minor alternative pathways exist for MHC class II presentation of endogenous proteins, the endogenously synthesised tumour antigens would be preferentially channelled through the MHC class I processing pathway. Therefore, a strategy which would allow the majority of endogenous antigenic proteins to gain access to the MHC class II pathway would be advantageous.

Recent detailed insight into the molecular mechanisms of the MHC class II pathway has been applied to a variety of methods to optimise class II restricted antigen presentation for the development of vaccines that induce antigen specific CD4⁺ T-cells. A biochemical approach involves the modification of antigenic proteins to target them to receptors that mediate endocytosis on specialised APC (Colomb *et al.*, 1996; Dempsey *et al.*, 1996; Tan *et al.*, 1997; Engering *et al.*, 1997). Also 3 genetic approaches have been developed to target antigenic peptides to MHC class II molecules directly. This has been achieved by replacing the CLIP sequence in the Ii with a sequence encoding an antigenic peptide (van Bergen *et al.*, 1997) and by the

fusion of such sequences via a flexible linker to the N-terminus of the class II β -chain (Ignatowicz *et al.*, 1995) or the C-terminus of Ii (Nakano *et al.*, 1997).

Other strategies have been developed to target endogenous proteins to the MHC class II endocytic compartments by virtue of the signal motifs in MIIC resident proteins such as Lamp-1, Ii and DM. Wu *et al.* (1995) utilised the sorting signal of the lysosomal-associated membrane protein (LAMP-1) to target a model antigen, human papillomavirus (HPV) type 16 E7 oncoprotein, into the endosomal and lysosomal compartments. Initially they placed a signal peptide at the N-terminus of the protein to mediate translocation of this cytoplasmic and nuclear protein into the lumen of the ER. The transmembrane domain and cytoplasmic tail of LAMP-1 were placed at the C-terminus of the E7 protein because these components are known to confer endosomal/lysosomal targeting (Guarnieri *et al.*, 1993). The LAMP-1 sorting signal directed the E7 protein into the MHC class II processing pathway, resulting in enhanced presentation to CD4⁺ T-cells *in vitro*. *In vivo* experiments in mice demonstrated that vaccinia containing the chimeric E7/LAMP-1 gene generated greater E7-specific lymphoproliferative activity, antibody titres and cytotoxic T-lymphocyte activities than vaccinia containing the wild-type HPV-16 E7 gene.

Sanderson *et al.* (1995) demonstrated that endogenously synthesized ovalbumin or HEL can be efficiently presented as peptide-MHC class II complexes when they are expressed as fusion proteins with Ii. Most efficient expression of MHC class II restricted endogenous peptides was obtained with fusion proteins that contained the endosomal di-leucine-based targeting signals within the N-terminal cytoplasmic Ii residues and did not require the luminal residues of Ii that are known to bind MHC molecules.

Marks *et al.* (1995) identified a lysosomal targeting signal in the cytoplasmic tail of the β -chain that directs DM to MIICs. This signal was capable of directing the chimeric protein T-T-Mb in which the cytoplasmic tail of murine DM β was appended to the luminal and transmembrane domains of the α -chain of the IL-2 receptor. Similarly to DM, T-T-Mb was localised by immunofluorescence and immunoelectron microscopy to a lysosomal compartment in HeLa and NRK cells where it was rapidly

degraded by a process that was blocked by inhibitors of lysosomal proteolysis. Deletion of tyrosine-based motif, YTPL, from the DM β cytoplasmic tail, resulted in cell surface expression of T-T-Mb and a loss of both degradation and internalisation. T-T-Mb was localised by immunoelectron microscopy to the MIIC in a human B lymphoblastoid cell line. These results suggest that the signal motif, YTPL, in the cytoplasmic tail of the β chain of DM is sufficient for targeting to MIICs. Copier *et al.* (1996) also demonstrated that the signal motif YTPL was capable of targeting the CD8-DM β hybrid molecules to intracellular compartments situated late in the endocytic pathway.

Nair *et al.* (1998) have utilised the signal motif present in LAMP-1 to redirect the tumour antigen CEA into the class II presentation pathway. They created a chimeric CEA cDNA template by appending a leader sequence to the amino end of CEA and fusing a sequence encoding the lysosomal targeting signal of the human LAMP-1 protein to the C-terminal of CEA (CEA-LAMP-1). RNA encoding CEA-LAMP-1 was transfected into DCs and used to stimulate PBMC which resulted in the enhancement of the induction of CEA-specific CD4⁺ T-cells.

These studies highlight the possibilities of targeting endogenous tumour antigens to the MHC class II pathway. This may lead to the development of effective DC-based vaccines for breast cancer which induce antigen specific CD4⁺ T-cells. The study by Nair *et al.* (1998) is encouraging, but more studies are required to investigate T-helper cell responses to breast tumour antigens targeted to the MHC class II compartment.

1.10 Aims of study

To design a DC-based vaccine strategy for breast cancer with a view to generating a CD4⁺ T-cell proliferation response to p53. Specifically, expression vectors encoding the chimeric protein, p53-DM β , will be assessed for their ability to direct endogenous p53 to the lysosomal compartment of transfected HeLa cells by virtue of the signal peptide motif, YTPL. Control constructs encoding p53, predicted to traffic to other cellular locations, will also be assessed. In addition, optimal transfection conditions for DC with RNA/DNA using non-viral methods will be established. Finally, DC will be transfected with various constructs encoding p53, predicted to traffic to different cellular compartments, followed by comparative analyses of autologous CD4⁺ T-cell proliferative responses to p53.

Chapter Two

Materials and Methods

Chapter Two

2.1 Materials

2.1.1 Standard Reagents

General chemicals were purchased from either Sigma Chemical Company Ltd. (Poole, Dorset) or from Fisher Scientific U.K. (Loughborough, Leicestershire). All solutions required for RNA and DNA work were prepared from molecular biology grade reagents, guaranteed to be RNase/DNase free by the vendor.

2.1.2 Solutions

Solutions were prepared using double-distilled deionised water. The pH of solutions was measured using a Whatman PHA 230 pH meter (Fisher Scientific U.K.), and adjusted with either HCl or NaOH, unless otherwise stated. They were sterilised by either filtration through a 0.22 micron filter or by being autoclaved for 20 minutes at 121°C and 25 lb/in² pressure. Solutions used in the preparation of RNA were treated overnight with 0.1% of the RNase inhibitor Diethyl Pyrocarbonate (DEPC) at 37°C, prior to autoclaving.

For composition of solutions refer to Appendix I.

2.1.3 Cell culture media

All media and additives were purchased from GIBCO BRL (Life Technologies Ltd, Paisley, Renfrewshire) with the exception of sodium pyruvate and β -mercaptoethanol (β_2 me) which were obtained from Sigma. Dulbecco's Modified Eagle's medium (DMEM) and Rosswell Park Memorial Institute (RPMI) 1640 medium were supplemented with 10% foetal calf serum (FCS), 50mM HEPES, 100units/ml penicillin, 100 μ g/ml streptomycin, 2mM L-glutamine, 1mM sodium pyruvate and 0.1mM β_2 me.

2.1.4 Cytokines

Human recombinant IL-4 (4.1×10^7 units/mg) was obtained initially from Genzyme Diagnostics (West Malling, Kent) and subsequently from R&D Systems Europe Ltd (Abingdon, Oxfordshire) at 1×10^6 genzyme units/5 μ g. Human recombinant GM-CSF (5.19×10^7 /mg) was obtained initially from Genzyme Diagnostics (West Malling, Kent) and subsequently from R&D Systems Europe Ltd (Abingdon, Oxfordshire) at 1.685×10^5 genzyme units/5 μ g. TNF- α was obtained from Peprotech EC LTD (London). Cytokines were stored in aliquots at -80°C .

2.1.5 Antibodies

Unless otherwise stated all antibodies were stored at $4-8^\circ\text{C}$

Monoclonal antibodies used in flow cytometric analysis of cell surface markers are shown in Table 2.1. All mAb were directly conjugated to either fluorescein isothiocyanate (FITC) or phycoerythrin (PE). Irrelevant IgG isotype-matched controls were purchased from Dako Ltd (High Wycombe, Buckinghamshire).

For western blot analysis, the secondary antibody Rabbit Ig, horseradish peroxidase-linked whole antibody (from donkey) was purchased from Amersham LIFE SCIENCE (Buckinghamshire, UK).

The following antibodies were used in immunofluorescence procedures and stored in aliquots at -20°C :

Polyclonal rabbit anti human p53 (CM1) was obtained from Novocastra Laboratories. Monoclonal mouse anti human CD63 was obtained from Chemicon International INC Fluorolink Cy3 labelled goat anti mouse IgG (H+L) was obtained from Amersham LIFE SCIENCE

Anti-rabbit IgG FITC conjugate was obtained from Sigma.

Table 2.1 List of the mAb used for flow cytometric analysis

Antigen	Clone	Murine subclass	Source
CD1a	NA1/34-HLK	IgG _{2a}	Serotec
CD14	UCHM1	IgG _{2a}	Serotec
CD40	EA-5	IgG ₁	Serotec
CD80	BB1	IgM	Serotec
CD83	HB15e	IgG ₁	Pharminogen
CD86	BU63	IgG ₁	Serotec
HLA-DR	HK14	IgG _{2a}	Sigma

Serotec Ltd (Kidlington, Oxfordshire)

Pharminogen International (Becton Dickinson Ltd. UK)

2.1.6 Molecular biology enzymes and reagents

Enzymes and reagents were purchased from the following suppliers: Superscript II reverse transcriptase; *Taq* DNA polymerase, T4 DNA ligase; restriction enzymes, deoxynucleoside 5'-triphosphates dATP, dCTP, dGTP, dTTP (dNTPs), Oligo(dT)₁₂₋₁₈, 1Kb and 123bp DNA ladder, ultra pure electrophoresis grade agarose (GIBCO-BRL); RQ1 RNase-free DNase and calf intestine alkaline phosphatase (CIAP) (Promega, Southampton, Hampshire); cloned pfu DNA polymerase (Stratagene Ltd, Cambridge); RNase inhibitor (Amersham International plc, Little Chalfont, Buckinghamshire); Nusieve low-melting temperature (LMP) agarose (Flowgen Instruments Ltd, Lichfield, Staffordshire); Oligonucleotides were synthesised by Oswel DNA service (University of Southampton, Hampshire) or Genosys.

2.1.7 Plasmids

Refer to Appendix II for vector maps.

pCR2.1

The TA-cloning vector pCR2.1 (Invitrogen, NV Leek, The Netherlands) was used for cloning PCR products. The vector is designed for cloning PCR products directly from a PCR reaction without the need for modifying enzymes, purification or restriction digestion. It contains the *lacZ* α complementation fragment for blue-white colour screening, ampicillin and kanamycin resistance genes for selection and a versatile polylinker sequence.

pGreen Lantern-1

The plasmid pGreen Lantern-1 (GIBCO BRL) was used to optimise gene transfection in DC and HeLa cells. The plasmid contains the reporter gene Green Fluorescent Protein (GFP) from *Aequorea Victoria* jellyfish (Prasher *et al.*, 1992; ^hCalfie *et al.*, 1994), which encodes a naturally fluorescent protein requiring no substrates for visualisation. The codon sequence is humanised for efficient translation in mammalian cells and mutated to contain threonine at position 65 to enhance

fluorescence peaking at 510nm with a single excitation peak at 490nm blue light (Heim *et al.*, 1995). The GFP cDNA was cloned as a *NotI* fragment and can be excised from the vector using *NotI*.

pCR3

The eukaryotic expression vector pCR3 (Invitrogen, NV Leek, The Netherlands) was used for gene transfection studies in HeLa cells and DC. pCR3 comprises enhancer-promoter sequences from the immediate early gene of human cytomegalovirus (CMV) for high-level gene transcription, a multiple cloning site (MCS), polyadenylation signal and transcription termination sequences from the bovine growth hormone gene to enhance RNA stability, a separate expression cassette conferring resistance to neomycin, and pBR322 vector sequences for replication and selection in *Escherichia coli*.

A 732 bp *NotI* fragment encoding the entire ORF for GFP was excised from pGreen Lantern and cloned in the sense orientation into the *NotI* site of pCR3. The resulting construct pCR3-GFP was used to optimise gene transfection in DC and HeLa cells and as a template for IVT of GFP .

pCITE-4b

The vector pCITE-4b, containing a *cap*-independent translation enhancer (CITE) sequence, (Novagen, AMS Biotechnology Ltd., Witney, Oxfordshire).was used to synthesise GFP transcripts for subsequent RNA transfection studies in HeLa cells. A 732bp *NotI* fragment encoding the entire ORF for GFP was excised from pGreen Lantern and cloned in the sense orientation into the *NotI* site of pCITE-4b.

pSecTagA

The plasmid pSecTag A (Invitrogen, NV Leek, The Netherlands) is designed for high-level stable transient expression in mammalian hosts. Proteins expressed from pSecTag are fused at the N-terminus to the murine Ig-kappa chain leader sequence for protein secretion and at the C-terminus to a peptide containing the myc epitope and six tandem histidine residues for detection and purification. This vector was used to

ensure proteins expressed were directed into the ER of transfected cells.

2.2 Molecular cloning

2.2.1 Isolation of total RNA

RNA was isolated from cells using the TRIZOL Reagent (GIBCO BRL) according to the manufacturers protocol which is a modification of the method developed by Chomczynski and Sachi (1987). Cells were harvested and resuspended in 1ml of RNA extraction solution per 5×10^6 cells. The lysate was left at room temperature for 5 minutes to ensure complete dissociation of nucleoproteins. Chloroform:isoamyl alcohol (24:1) was added (0.2ml per ml of extraction solution) and the phases mixed by shaking vigorously by hand for 15 seconds. The mixture was left at room temperature for 2-3 minutes and the phases separated by centrifuging at 12,000g for 15 minutes at 4°C. The upper aqueous phase was transferred to a new microfuge tube containing 500µl of isopropyl alcohol, mixed and allowed to precipitate for 10 minutes at room temperature. RNA was collected by centrifugation at 12,000g for 10 minutes at 4°C and washed with 70% ethanol. The RNA pellet was air dried briefly and dissolved in 50µl DEPC treated dH₂O

2.2.2 Spectrophotometric quantification of RNA and DNA

RNA and DNA were quantified by measuring their absorbance in an Ultraviolet (UV)-spectrophotometer (Perkin-Elmer Ltd., Beaconsfield, Buckinghamshire). RNA and DNA absorb in the UV range between 250nm and 270nm. At 260nm an optical density of one is equivalent to 40µg/ml of RNA, 50µg/ml of DNA and 33µg/ml of oligonucleotide. Pure RNA and DNA has an A₂₆₀ / A₂₈₀ ratio absorbance ratio of greater or equal to 2.0 (Sambrook *et al.*, 1989).

2.2.3 RNA reverse transcription

One microgram of total RNA was reverse transcribed by incubation for 50 minutes at 42°C with 200 units of Superscript II reverse transcriptase, 500ng/ml Oligo(dT)₁₂₋₁₈,

1mM each of dNTPs, 10mM DTT, 50mM Tris-HCl (pH 8.3), 75mM KCl, and 3mM MgCl₂, in a total volume of 20μl. Negative control reactions were performed containing all components except the reverse transcriptase. Following reverse transcription the reaction was heat inactivated at 70°C or 15 minutes. 10% of the final reaction volume was used for enzymatic amplification by PCR.

2.2.4 Polymerase chain reaction

Amplification of DNA by PCR was performed essentially as described by Mullis *et al.* (1987). PCR primers were designed to overlap the initiating ATG codon and stop codon of the cDNA to be cloned, and to have a T_m of at least 68°C (> 22 nucleotides in length with a GC content of 45-55%). Amplification reactions were performed in a total volume of 100μl in pfu DNA polymerase reaction buffer (10mM KCl, 10mM (NH₄)₂SO₄, 20mM Tris-HCl (pH 8.8), 2mM MgSO₄, 0.1% Triton X-100, 0.1 mg/1ml nuclease-free BSA), containing template, a high fidelity proofreading cloned pfu polymerase (2.5 units), 0.4μM of each primer and dNTPs at 200μM. Reaction mixtures were overlaid with 50μl of mineral oil to prevent evaporation. Negative controls were included to control for contamination and primer artefacts within the amplification reaction. Reactions were carried out in a Perkin-Elmer Thermal cycler 480 (Perkin-Elmer Ltd). Cycling parameters depended on the T_m of the primers and the nature of the template to be amplified and are indicated with the relevant results. PCR products were extracted with phenol:chloroform:isoamyl alcohol (25:24:1) and precipitated with 0.5 x volume 7.5M ammonium acetate and 2 x volume absolute ethanol for 1-hour at -20 °C.

2.2.5 Agarose gel electrophoresis

DNA was size fractionated on agarose gels between 1 and 2% w/v as appropriate to the size of the fragments being resolved. Nusieve LMP agarose was used for gel purification of PCR products and vector fragments and ultra pure electrophoresis grade agarose was used for size fractionation of DNA fragments. Agarose was heated in 1 x TAE buffer until dissolved, and cooled to approximately 50°C prior to the addition of 0.5μg/ml ethidium bromide. Ethidium bromide allows the observation of DNA fragments under ultra violet illumination. The gel was poured and allowed to set

at room temperature. DNA samples were loaded in 1 x DNA loading buffer and electrophoresed at 50 mA in 1 x TAE buffer until the tracking dye had reached the end of the gel. The size of DNA fragments in base pairs was determined by comparison with either a 123-bp or a 1-Kb dsDNA ladder (GIBCO/BRL) see figure 2.1. The 123-bp DNA ladder consists of a series of fragments ranging in length from 123 to 4182-bp. The 1-Kb ladder contains from 1 to 12 repeats of a 1018-bp DNA fragment. In addition to these 12 bands, the ladder contains vector DNA fragments that range from 75 to 1636-bp. Gels were visualised by transillumination with ultra violet light and photographed using a Polaroid MP-4 land camera and black and white film (iso 3000).

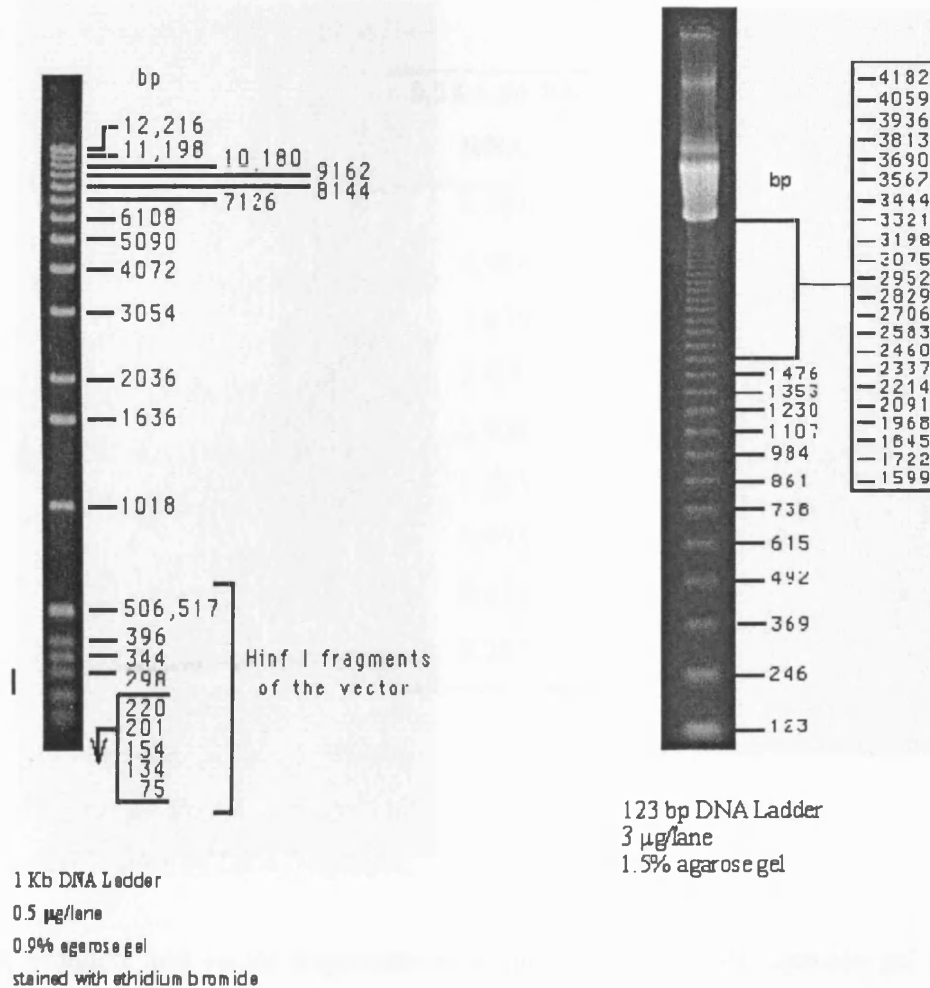


Figure 2.1 DNA Molecular Weight Markers

IVT RNA was size fractionated on 1.5% agarose w/v gels. Prior to electrophoresis the apparatus was soaked in 3% H₂O₂ v/v overnight to remove traces of RNAses. Agarose was heated in 1 x TAE buffer until dissolved, and cooled to approximately 50°C prior to the addition of 0.5µg/ml ethidium bromide. The gel was poured and allowed to set at room temperature. RNA samples were prepared by adding 2µl IVT RNA to 18µl 1 x RNA sample buffer (denaturing) followed by 2µl RNA loading buffer and heated for 5-10 minutes at 65-70°C prior to loading. The samples were electrophoresed at 50 mA in 1 x MOPS buffer until the tracking dye had reached the end of the gel. The size of RNA fragments in base pairs was determined by comparison with the 0.28-6.66 Kb RNA ladder (Sigma) see Table 2.2 for fragment sizes.

Table 2.2. RNA Molecular Weight Marker

0.28-6.66 Kb
RNA
6.583
4.981
3.638
2.604
1.908
1.383
0.955
0.623
0.281

2.2.6 Purification of DNA fragments.

PCR products and vector fragments were purified from LMP agarose gel using the QIAquick gel extraction kit as recommended by the vendor (Qiagen Ltd., Teddington, Middlesex).

2.2.7 TA-cloning of PCR products

PCR products were cloned directly into the eukaryotic expression vector pCR2.1 by TA-cloning (Invitrogen). This approach takes advantage of the terminal transferase activity of non-proofreading polymerases, such as *Taq* DNA polymerase, which add a single 3' deoxyadenosine (A)-overhang to each end of the PCR product. PCR2.1 is supplied linearised with single 5' deoxythymidine (T)-overhangs to enable direct ligation of PCR products at high efficiency. In order to carry out TA-cloning, blunt-ended PCR products generated by *pfu* polymerase were treated with 2 units of non-proofreading *Taq* DNA polymerase in 1 x PCR buffer, containing 200 μ M dATP, for 20 minutes at 72°C.

PCR products were ligated to 60ng of linearised pCR2 (molar ratio of 3:1) (see section 2.2.8) and 1-2 μ l used to transform One Shot competent cells (see section 2.2.9)

2.2.8 Ligation of DNA fragments with cohesive ends

DNA fragments were ligated to 60-100ng of linearised vector (molar ratio of 3:1) by incubation overnight at 15°C with 4 units of T4 DNA ligase in 10 μ l of 1x ligation buffer (6mM Tris-HCl [pH 7.5], 6mM MgCl₂, 5mM NaCl, 7mM β -mercaptoethanol 0.1mg/ml BSA, 0.1mM ATP, 2mM DTT, 1mM spermidine). Ligation reactions were centrifuged briefly and used directly to transform competent bacteria or stored at -20°C.

2.2.9 Transformation of competent cells

Ligation reactions were centrifuged briefly and 1-2 μ l used to transform E.coli One Shot competent cells (TOP10F⁺) according to the protocol provided with the TA-cloning kit (Invitrogen). After transformation, 50 μ l and 200 μ l aliquots of the cells were spread onto LB agar plates containing 50 μ g/ml of ampicillin. The plates were inverted and incubated overnight at 37°C. Individual colonies were picked and placed in LB broth containing 50 μ g/ml of ampicillin and shaken overnight at 37°C.

2.2.10 Small-scale plasmid preparation

Plasmid DNA for restriction analysis was isolated by the method of Serghini *et al.* (1989). Briefly, 1.5ml of an overnight culture was transferred to an eppendorf tube and the cells pelleted by a 1 minute centrifugation at 12,000g. The pellet was resuspended in a 100 μ l of TNE and 100 μ l of phenol:chloroform:isoamyl alcohol (25:24:1) added. The mixture was vigorously vortexed and centrifuged for 5 minutes at 12,000g to yield an almost clear supernatant. The upper aqueous phase was transferred to a new eppendorf tube and the plasmid DNA precipitated with 0.5 x volume 7.5M ammonium acetate and 2 x volume absolute ethanol for 10 minutes on ice. The precipitated DNA was collected by centrifugation for 10 minutes at 12,000g, washed with 75% ethanol, air dried and dissolved in 20 μ l TE.

2.2.11 Digestion of DNA with restriction endonucleases

All restriction digests of DNA were carried out according to the instructions supplied by the vendor. Briefly, 1 unit of enzyme was required to digest 1 μ g of DNA to completion in 1 hour in the recommended buffer at the recommended temperature in a 10-20 μ l reaction. A double digest using two restriction enzymes with similar requirements was performed simultaneously. Alternatively, if the enzymes had different requirements a sequential digest was performed which involved incubation with the first enzyme in the appropriate conditions, followed by phenol extraction of the enzyme, ethanol precipitation of the DNA and incubation with the second enzyme.

In order to prevent cohesive ends of digested vector DNA annealing on themselves, the DNA was dephosphorylated with calf intestinal alkaline phosphatase (CIAP) according to the manufacturer's instructions (Promega).

2.2.12 Orientation of inserts

The orientation of inserts cloned into, pCR2, pCR3, pCITE-4a, and pSecTagA were analysed using restriction analysis (Sambrook *et al.*, 1989). Plasmid DNA (2 μ l) containing 0.2-0.3 μ g of DNA prepared from the small scale procedure was incubated with the appropriate restriction enzyme according to the instructions recommended by

the vendor. The quantity of DNA to be cleaved was adjusted accordingly. Heat-treated RNase A solution (1µl of 20µg/ml) was also added to the mixture to remove any contaminating RNA.

2.2.13 Sequence analysis

The sense and anti-sense strands of cloned cDNAs were sequenced using the ABI PRISM™ dRhodamine terminator cycle sequencing ready reaction kit, marketed by Perkin-Elmer Ltd. High-quality double-stranded DNA was prepared by alkaline lysis/Qiagen® anion-exchange chromatography using P20 columns (Qiagen Ltd). 500ng of plasmid DNA template was sequenced using the protocol supplied with the ABI PRISM™ kit, employing the relevant primers which bind to complementary sites within the MCS flanking regions of pCR3, pSecTagA and pCITE-4b. Sample electrophoresis was performed by the MRC sequencing service (University of Leicester), excess dye terminators having been removed by ethanol precipitation. The resulting sequence data was analysed using Gene Jockey II (Biosoft, Cambridge) and Sequence Navigator software (Perkin-Elmer Ltd). Internal primers enabling full-length sequencing were designed as required.

2.2.14 Large-scale Endotoxin-free plasmid preparation

High-quality endotoxin-free plasmid DNA for gene transfection was prepared by alkaline lysis/Qiagen® anion-exchange chromatography (100ml maxi-prep yielding up to 500µg of DNA) as recommended by the supplier (Qiagen Ltd.). The “EndoFree Plasmid Procedure” filters the neutralized bacterial lysate through a QIAfilter cartridge and subsequent incubation on ice with the endotoxin removal buffer prevents lipopolysaccharide (LPS) molecules from binding to the resin in the QIAGEN-tips allowing purification of DNA containing less than 0.1 endotoxin units per µg plasmid DNA.

2.2.15 Storage of bacterial stock cultures

Aliquots of bacterial culture (850µl) were mixed with sterile glycerol (150µl) in a sterile 1.5ml freezing vial (Sarstedt Ltd., Leicester) and snap-frozen in liquid nitrogen.

For long-term storage the vials were transferred to a -80°C freezer.

2.2.16 Synthesis of *in vitro* transcribed RNA

In vitro transcribed RNA was synthesised using the RiboMAX™ Large Scale RNA Production System-T7 as recommended by the supplier Promega. Briefly, template DNA was linearised with the appropriate enzyme downstream of the polyadenylation sequence and the BGH polyadenylation signal in pCITE-4b and pCR3 vectors respectively, followed by phenol extraction and ethanol precipitation. Linearised DNA was dissolved in nuclease-free water and approximately 4µg was incubated for 4 hours at 37°C in a 40µl reaction volume containing T7 transcription 5 x buffer (8µl), rNTPs (100mM), T7 enzyme mix (4µl) and nuclease free water. To remove the DNA template, RQ1 RNase-Free DNase was added at a concentration of 1U/µg of template DNA and incubated for 15 minutes at 37°C. The samples were extracted with 1 volume of TE-saturated (pH 4.5) phenol:chloroform:isoamyl alcohol (25:24:1) followed by 1 volume of chloroform:isoamyl alcohol (24:1) and precipitated with 0.1 x volume 3M sodium acetate and 1 x volume of isopropanol for 2-5 minutes on ice. The precipitated RNA was collected by centrifugation for 10 minutes at 12,000g, washed with 1ml of 70% ethanol, air dried for 5 minutes and dissolved in 40µl of nuclease free water. Aliquots were stored at -70°C.

2.3 Cell culture

2.3.1 Human tumour cell lines

HeLa cells (epithelial cells from the adenocarcinoma of the cervix) and the breast tumour cell lines MDA-MB⁻²³¹ and MCF-7 were all purchased from the American Type Culture Collection (ATCC, Rockville, MD U.S.A.) These cell lines were cultured in 80cm² flasks (Life Technologies Ltd) at 37°C in complete DMEM supplemented with 10% FCS in a humidified atmosphere of 5%CO₂/95% air. Cell lines were maintained as monolayer cultures and passaged by trypsinisation with trypsin-EDTA as required. All cell lines were monitored routinely for Mycoplasma infection using a PCR-based kit supplied by Stratagene Ltd. (Cambridge).

2.3.2 Isolation of peripheral blood mononuclear cells

Peripheral blood from normal healthy volunteers was collected into heparinised 7.5ml monovettes (Sarstedt Ltd.), diluted 1:2 with minimal essential medium (MEM), layered over lymphocyte separation medium (LSM, 1.077 g/ml, 280 mOsm; Robbins Scientific Ltd, Knowle, West Midlands) and then centrifuged at 680g (no brake) for 20 minutes at room temperature. Peripheral blood mononuclear cells (PBMC) were aspirated from the interface and washed extensively with MEM-2% FCS + 4mM EDTA.

2.3.3 Electroporation of HeLa cells with plasmid DNA

HeLa cells were transiently transfected with plasmid DNA by electroporation using the Bio-Rad Gene Pulser (Bio-Rad Laboratories Ltd., Hemel Hempstead, Hertfordshire). Exponentially growing HeLa cells were harvested using Trypsin-EDTA, washed twice with serum-free DMEM, and resuspended in the same medium at 5.0×10^6 cells/ml. Plasmid DNA (2 μ g) was added to a 4 mm cuvette, 400 μ l of the cell suspension added and the cuvette immediately subjected to a single voltage pulse. Electroporation was performed at 960 μ F, 0.30 kV and the cells were transferred immediately to either petri dishes containing 1% gelatin coated coverslips, 6-well plates or 80cm² flasks. Up to 48-hours after electroporation the cells were analysed for protein expression by immunofluorescence microscopy, Western blotting or cytofluorimetry.

2.3.4 Detection of apoptosis using Annexin V-FITC

Assessment of apoptosis was performed using the Annexin V-FITC Apoptosis Detection Kit as recommended by the supplier Oncogene Research Products (Cambridge, MA, USA). Briefly, 48-hours after transfection of HeLa cells, media was transferred from the T-80 flask to a 15ml conical flask and placed on ice. The adherent cells were washed with 10ml PBS, removed with trypsin-EDTA and resuspended in the media, previously removed from the flask, at a concentration of 1×10^6 cells/ml. The cell suspension (0.5ml) was transferred to a microfuge tube and 10ml of Media Binding Reagent was added followed by 1.25ml Annexin V-FITC.

The cell suspension was incubated at room temperature in the dark for 15 minutes and centrifuged at 1000 x g for 5 minutes at room temperature. The media was removed and cells were resuspended in 0.5ml cold 1X Binding Buffer followed by the addition of 10ml of propidium iodide. Samples were placed on ice away from light and were analysed immediately by cytofluorimetry.

2.4 Protein analysis

2.4.1 Immunofluorescence microscopy: intra-cellular localisation of proteins

To examine the intra-cellular localisation of the p53 protein in HeLa cells transfected with plasmids encoding p53, and also the endogenous lysosomal membrane protein, CD63, immunofluorescence microscopy was employed. Zero grade coverslips (18 x 18mm) suitable for subsequent confocal microscopy were sterilised with 70% ethanol and treated with 1% Gelatin (Sigma) in PBS. Transfected cells were grown on coverslips in petri dishes containing 2mls DMEM + 10% FCS for up to 48 hours at 37°C. HeLa cells were either left untreated or treated with a protease inhibitor Leupeptin at 1mg/ml (Sigma) for 4-hours at 37°C prior to the fixation stage. HeLa cells were fixed by washing twice in serum-free medium and placing in ice-cold 4% paraformaldehyde (PFA) in PBS (4% PFA-PBS) for 15 minutes. PFA-PBS (4%) was removed and the cells were permeabilised by incubation with 0.5% Triton X-100 in TBS for 5 minutes at room temperature. After rinsing the cells in 0.1% Triton X-100 in TBS (TBS-T), blocking buffer (TBS-T + 10% BSA w/v) was added for 10 minutes at room temperature to reduce non-specific staining.

Proteins were visualised by indirect dual staining using two specific primary antibodies followed by two species specific secondary antibodies conjugated to CY3 or Fluorescein isothiocyanate (FITC). Primary antibodies were diluted in blocking buffer at the optimum dilution and 39µl was placed onto clean nesco film in a box containing moist blotting paper. The coverslips were lowered carefully onto the antibody droplets cell-side down and incubated in the humidified chamber for 1 hour at 37°C. Coverslips were removed and placed cell side up in petri dishes and washed three times with TBS-T + 10% BSA for 5 minutes on a rocker at room temperature.

The cells were incubated with the secondary antibodies (anti-rabbit FITC + anti-mouse CY3) as for the primary antibodies in a humidified chamber for 1 hour at 37°C. The coverslips were placed cell side up in petri dishes and washed four times with TBS-T + 10% BSA for five minutes on a rocker at room temperature followed by one final wash in double distilled water. Coverslips were mounted in Diazabicyclo[2.2.2]octane (DABCO) on microslides 76 x 26mm and 0.8/1.0mm thick.

Cells were visualised by epifluorescence using an Olympus microscope and were examined by a confocal laser scanning microscope (CLSM) (MRC-600 BioRad Laboratories, Herts, UK) equipped with an Argon ion laser (BioRad Laboratories, Herts, UK). The green fluorochrome, FITC, was excited at $\lambda=488\text{nm}$ and emitted at $\lambda=520\text{nm}$. The red fluorochrome, CY3, was excited at $\lambda=514\text{nm}$ and emitted at $\lambda=556$. The digital confocal images which were obtained are monochromatic, and where appropriate, images were pseudocoloured to reproduce as accurately as possible, the original image. The Confocal Assistant software program (Biorad Laboratories, Herts, UK) was used to produce superimposed images in dual labelling experiments. Multiple images of a specimen were also acquired at regular increments from the apex through to the base of the cell which is called a z-series. All sections in a z-series are the same size and in perfect registration in the XZ plane. These images were subsequently projected into a single picture which contains the brightest pixel in the XZ plane at each of the full screen coordinates. The projected images of cells which had been processed for dual staining with FITC and CY3 were subsequently superimposed.

2.4.2 Immunofluorescence microscopy: cell surface expression (method I)

To examine surface expression of p53 in HeLa cells, the electroporated cells were plated onto sterile zero grade coverslips coated with 1% gelatin and grown for up to 48 hours in the appropriate media containing 10% FCS. HeLa cells were fixed by washing twice in serum-free medium and placing in ice-cold 4% paraformaldehyde (PFA) in PBS (4% PFA-PBS) for 15 minutes. TBS + 10% BSA w/v was added for 10 minutes at room temperature to reduce non-specific staining.

Proteins were visualised by indirect staining using a specific primary antibody followed by a species specific secondary antibody conjugated to Fluorescein isothiocyanate (FITC). The primary antibody was diluted in blocking buffer at the optimum dilution and 39µl was placed onto clean nesco film in a box containing moist blotting paper. The coverslips were lowered carefully onto the antibody droplets cell-side down and incubated in the humidified chamber for 1 hour at 37°C. Coverslips were removed and placed cell side up in petri dishes and washed three times with TBS + 10% BSA for five minutes on a rocker at room temperature. The cells were incubated with the secondary antibody as for the primary antibody in a humidified chamber for 1 hour at 37°C. The coverslips were placed cell side up in petri dishes and washed four times with TBS + 10% BSA for 5 minutes on a rocker at room temperature followed by one final wash in double distilled water. Coverslips were mounted in DABCO on microslides 76 x 26mm and 0.8/1.0mm thick. Cells were visualised by epifluorescence using an Olympus microscope and were subsequently examined by CSLM to produce monochromatic digital confocal images. In some cases multiple images of a specimen were acquired at regular increments from the apex through to the base of the cell which is called a z-series. All sections in a z-series are the same size and in perfect registration in the XZ plane. These images were subsequently projected into a single picture which contained the brightest pixel in the XZ plane at each of the full screen coordinates.

2.4.3 Immunofluorescence microscopy: cell surface expression (method II)

To examine surface expression of p53 in transfected HeLa cells, the cells were plated onto sterile zero grade coverslips coated with 1% gelatin and grown for up to 48 hours in the appropriate media containing 10% FCS. The media was carefully removed and the cells were washed with PBS. Proteins were visualised by indirect staining using a specific primary antibody followed by a species specific secondary antibody conjugated to Fluorescein isothiocyanate (FITC). Primary antibody (anti-p53) was diluted in PBS + 0.2% FCS at varying dilutions and 39µl was placed onto clean nesco film in a box already containing moist blotting paper. The coverslips were lowered carefully onto the antibody droplets cell-side down and incubated in the humidified chamber for 30 minutes at 37°C. Coverslips were removed and placed cell side up in

petri dishes and washed four times with PBS + 10% FCS for 2 minutes on a rocker at room temperature. The cells were incubated with the secondary antibody (anti-rabbit FITC) as for the primary antibody at varying dilutions in a humidified chamber for 1 hour at 37°C. The coverslips were placed cell side up in petri dishes and washed three times with PBS + 10% FCS for 2 minutes on a rocker at room temperature. Ice-cold PFA (3%) containing 5% sucrose was used to fix the cells for 15 minutes at room temperature before the coverslips were mounted in DABCO on microslides 76 x 26mm and 0.8/1.0mm thick. Cells were visualised by epifluorescence using an Olympus microscope and were photographed on Kodak ASA 400 colour film.

2.4.4 Cytofluorimetric analysis

For indirect antibody labelling, adherent HeLa cells were removed from tissue culture flasks by treatment with 0.04% EDTA/PBS, washed twice in PBS containing 2% FCS + 0.02% sodium azide, and 2×10^5 cells were incubated with the primary antibody diluted in PBS + 2% FCS for 40 minutes on ice. After washing three times with PBS + 2% FCS (4mls), the cells were incubated with the secondary antibody conjugated with FITC diluted in PBS + 2% FCS for 40 minutes on ice. The cells were washed as before and fixed in 1% PFA-PBS.

For direct antibody labelling, adherent cells were removed from tissue culture flasks by treatment with 0.04% EDTA/PBS, washed twice in PBS containing 2% FCS + 0.02% sodium azide, and 2×10^5 cells stained with saturating amounts of FITC- or PE- directly conjugated mAb in PBS + 2% FCS for 40 min on ice. After washing three times with PBS + 2% FCS, the cells were fixed in 1% PFA-PBS.

Cells transfected with GFP were harvested up to 48 hours post transfection and washed twice in PBS + 2% FCS. Cells (5×10^5) were resuspended in either 1ml of PBS containing propidium iodide and incubated for 10 minutes at room temperature or in 1ml of 1% PFA-PBS.

In all cases, fluorescence was measured using a Becton-Dickinson FACStar® (Becton-Dickinson, Cowley, Oxford) and the data analysed using WinMDI software (www.bio.unmass.edu/mcbfacs/). 5000-10,000 cells were analysed per sample.

2.4.5 SDS-polyacrylamide gel electrophoresis (SDS-PAGE) of proteins

Separations of proteins was performed under denaturing conditions using the discontinuous method of Laemmli (1970). Discontinuous SDS-PAGE systems use a stacking gel with a lower percentage of polyacrylamide than the resolving gel. This allows better separation of proteins, with an increased resolution over continuous systems which use one polyacrylamide concentration. The denaturing conditions split proteins into their component subunits and the addition of SDS ensures that all proteins carry the same overall charge to mass ratio so that separation is purely on the basis of molecular mass (Laemmli, 1970).

Table 2.3. Composition of SDS-PAGE gels

	Resolving gel 10% acrylamide	Stacking gel 5% acrylamide
d.H₂O	9.6 ml	13.7 ml
2M TrisCl pH 8.8	3.7 ml	----
1M TrisCl pH 6.8	----	2.5 ml
10% SDS	200 µl	200 µl
30% Acrylamide/bisacrylamide (Amersham)	6.7 ml	3.3 ml
10%(NH₄)₂S₂O₈	134 µl	200 µl
Tetramethyl-ethylenediamine (TEMED) (Amersham)	14 µl	20 µl

Protein samples were prepared from HeLa cells and corresponding supernatants 48-hours after transfection. Briefly, HeLa cells were transiently transfected by electroporation with various constructs encoding p53 and 6-well plates were seeded with 3×10^5 cells/well in 2mls of serum-free OPTI-MEM. After 48-hours the supernatants were carefully aspirated, filtered with 0.22µM filters to remove contaminating non-adherent cells and concentrated using microcon centrifugal devices containing 30 kDa filters as recommended by the supplier Amicon.

Concentrated supernatants (approximately 10 μ l-30 μ l) were mixed with protein loading buffer (3x) containing 100mM DTT in the ratio of 2 parts sample and 1 part sample buffer, boiled for 5 minutes and allowed to cool on ice before application to the gel. After careful removal of the supernatants, HeLa cells were washed once with PBS and lysed by the addition of 50 μ l of protein loading buffer (2x) containing 100mM DTT. Samples were sonicated ($\lambda = 10$ microns) for 20 seconds, boiled for 5 minutes and allowed to cool on ice before application to the gel.

SDS-PAGE was performed using the Mini Protean II Electrophoresis System according to the manufacturer's instructions (Bio-Rad, Hemel Hempstead, Herts, UK). The tank was filled with running buffer, the samples loaded onto the gel and a voltage of 150 V was applied until the dye front had moved into the resolving gel. The voltage was subsequently increased to 180 V and the gel was run until optimum separation was achieved as judged by the position of the prestained molecular weight markers (refer to Table 2.4 for description of marker).

2.4.6 Western Blotting

Proteins separated on SDS-PAGE gels were electrophoretically transferred to a membrane by a process commonly termed Western blotting. The polyacrylamide gel was positioned cathode side of a membrane (Hybond C nitrocellulose membranes, Amersham International, Amersham, UK), and sandwiched between Whatman 3MM filter paper (membrane and filter paper had been presoaked in transfer buffer). These were inserted into a Mini Trans-Blot apparatus (Biorad, Hemel Hempstead, Herts, UK) and a tank was filled with transfer buffer. Proteins were transferred overnight by applying a current of 120 mA at room temperature. Blots were used directly or blocked and stored wet at 4°C.

2.4.7 Enhanced chemiluminescence (ECL)

Detection of immobilised proteins conjugated indirectly with horseradish peroxidase-labelled antibodies was carried out using the technique of Enhanced Chemiluminescence and detection of light emission on X-ray film.

After electroblotting, the free protein binding sites on the membrane were blocked by incubating the membrane in a blocking agent (TBS-T + 5% BSA) for 1 hour. Primary antibodies were diluted at the appropriate dilution in blocking buffer and incubated for 1 hour. The membrane was washed three times for 15 minutes using TBS-T followed by an hour incubation with HRP conjugated secondary antibody specifically reacting against the primary antibody optimally diluted in blocking buffer. The membrane was washed as before to remove unbound antibody.

Visualisation of bound antibody was performed by carefully immersing the membrane in 10mls detection reagent (Sigma) for 1 minute. The membrane was removed, drained of excess reagent before covering with Saran WrapTM ensuring the elimination of bubbles. To minimise decay of the detection reagent the membrane was placed immediately in a light tight cassette, proteins side up and light emission visualised on Kodak XAR5 film (Sigma) for the optimum period.

N.B. All incubations and washing steps were carried out at room temperature on a rocker.

For determination of relative molecular weight on western blots, the Coloured Standard Molecular Weight Marker (Sigma) was used. Refer to Table 2.4 for distribution of proteins.

2.4.8 Coupled *in vitro* transcription/translation

Protein translation *in vitro* was performed using the TNT Coupled Reticulocyte Lysate System as recommended by the supplier Promega. Briefly, the following reaction components were assembled in a 1.5ml microcentrifuge tube:

TNT rabbit reticulocyte lysates	12.5 μ l
TNT reaction buffer	1.0 μ l
TNT RNA T7 polymerase	0.5 μ l
Amino acid mixture minus methionine	0.5 μ l
[³⁵ S]methionine (1,000Ci/mmol, at 10mCi/ml)	2.0 μ l
Rnasin ribonuclease inhibitor, 40u/ μ l	0.5 μ l
DNA template	0.5 μ g
Nuclease-free water to final volume	25.0 μ l

For the positive control reaction 0.5 μ l of the luciferase control DNA was used whereas the negative control reaction did not contain a DNA template. The reactions were incubated at 30°C for 60-120 minutes. Once the 25 μ l reaction was complete, 5 μ l was removed for analysis. The remainder of the sample was stored at -20°C. The sample was separated by SDS-PAGE then visualised by autoradiography.

Table 2.4 Colour Molecular Weight Marker for Proteins

Proteins	Native Molecular Weight of Subunit (Daltons)	Colour of Conjugate
Myosin, Rabbit muscle	205,000	Blue
β -Galactosidase, E.coli	116,000	Turquoise
Albumin, Bovine Serum	66,000	Pink
Ovalbumin, chicken egg	45,000	Yellow
Carbonic Anhydrase, Bovine erythrocytes	29,000	Orange
Trypsin Inhibitor, Soybean	20,000	Green
α -Lactalbumin	14,200	Purple
Aprotinin, Bovine milk	6,500	Blue

Chapter Three

Targeting of p53 to the lysosomal compartment

Chapter Three

3.1 Introduction

The overall aim of this study is to design a DC-based vaccine system for breast cancer which is capable of inducing an enhanced CD4⁺ T-cell response. As the strategy involves the transfection of DC with cDNA encoding a known tumour antigen, the endogenously synthesised protein must be effectively trafficked to the MHC class II pathway in order to induce such a CD4⁺ T-cell proliferative response. Initially, this study sought to design an expression vector which was capable of targeting a known breast tumour antigen to the lysosomal compartment. As mentioned in chapter one, the tumour suppressor protein p53 is over expressed in 57% of breast tumours and there is evidence of CTL responses against both wild-type and mutant forms in breast cancer patients (Hadden, 1999). As the majority of mutations documented for p53 result in the alteration of a single amino acid (Vogelstein *et al.*, 1992), mutant p53 over expressed in tumours resembles the wild-type form (McCarty *et al.*, 1998). Therefore, wild-type p53 was selected as the breast tumour antigen to be manipulated in this DC-based vaccine strategy as it represents an attractive target for immunotherapy without the need to assess the p53 mutation and the HLA type of a patient.

Many groups have successfully targeted endogenous antigens to MHC by utilising signal peptide motifs present in LAMP-1, Ii chain and DM (Wu *et al.*, 1995; Nair *et al.*, 1998; Sanderson *et al.*, 1995; Marks *et al.*, 1995). In this study the YTPL signal motif was utilised in order to target p53 to the lysosomal compartment. This tyrosine based signal peptide which is located in the cytoplasmic tail of HLA-DM β has been shown to direct DM to lysosomal compartments in HeLa cells (Marks *et al.*, 1995).

Experiments described in this chapter sought to engineer a chimeric p53-DM β cDNA template by fusing a sequence, encoding the YTPL signal peptide motif of DM, to the C-terminus of p53. Comparative analyses would assess the ability of the targeting signal, YTPL, to direct endogenous p53 to the lysosomal compartments of HeLa cells in the presence and absence of a leader sequence (LS) fused at the N-terminus.

3.2 Methods

3.2.1 Cloning of human p53

To clone p53, total RNA from the MCF-7 breast tumour cell line was reverse-transcribed into cDNA and amplified by PCR using specific-oligonucleotides encompassing the entire p53 ORF. The following primers were used, the design of which was based on the sequence reported in GenBank under the accession number M14694.

Forward primer: 5'-CTCGAGATTGGCAGCCAGACTGCCTT-3'

Reverse primer: 5'-AGAATTCGAGTCTGAGTCAGGCCCTTCTGT-3'

Polymerase chain reaction was performed under the following conditions: 45 seconds at 94°C, 45 seconds at 60°C, 72°C at 2 minutes and 26 seconds for 20 cycles, followed by 10 minutes at 72°C. After electrophoresis on a 1.5% LMP agarose gel, the PCR product was excised, purified using the QIAquick gel extraction kit, and cloned into the TA-site of pCR2.1. Recombinant clones in the correct orientation were sequenced across the pCR2.1 polylinker by cycle sequencing using dye-labelled terminators.

3.2.2 Construction of pCR3.p53-DM β

A vector, pCDM8 containing the RING-7 gene which encodes HLA-DM β , was kindly donated by Dr Trowsdale. Specific-oligonucleotides encompassing the transmembrane region and the cytoplasmic tail containing the YTPL signal motif were used to amplify this region of HLA-DM β by PCR. The design of the following primers was based on the published sequence for HLA-DM β (Kelly *et al.*, 1991) and contained restriction sites (highlighted blue and yellow) for the generation of compatible ends for subsequent sub-cloning .

Forward primer: 5'-AATC**GGATCC**GAGTTTCTGTGTCTGCAGTG-3'

Reverse primer: 5'-CCGC**GAATTC**TAGGAAATGTGCCATCCTTC-3'

BamHI

EcoRI

Stop codon

Polymerase chain reaction was performed under the following conditions: 45 seconds at 94°C, 45 seconds at 60°C and 30 seconds at 72°C for 20 cycles, followed by 10 minutes at 72°C. After electrophoresis on a 1.5% LMP agarose gel, the resulting (139bp) PCR product, shown in Figure 3.2, was excised, purified using the QIAquick gel extraction kit, and cloned into the *Bam*HI and *Eco*RI site of the pCR3 vector. Restriction analysis identified recombinant clones in the correct orientation and the resulting construct was designated pCR3.DMβ

A *Kpn*I fragment from the vector pCR2.1.p53 encompassing the entire ORF of p53 was subcloned into the *Kpn*I site situated approximately 15bp upstream of the DMβ insert present in the construct pCR3.DMβ. Recombinant clones in the correct orientation were sequenced across the pCR3 polylinker by cycle sequencing using dye-labelled terminators.

For a schematic representation of the construct and the predicted location of p53 expressed in transfected cells refer to Figure 3.2.

3.2.3 Construction of pCR3.p53

A *Kpn*I fragment, released from pCR2.1.p53 encompassing the entire ORF of p53 was subcloned into the *Kpn*I site of pCR3. Recombinant clones in the correct orientation were sequenced across the pCR3 polylinker by cycle sequencing using dye-labelled terminators.

For a schematic representation of the construct and the predicted location of p53 expressed in transfected cells refer to Figure 3.2.

3.2.4 Construction of pSecTagA.p53-DM β

An *EcoRI* fragment containing the p53-DM β was released from pCR3.p53-DM β and amplified by PCR using specific-oligonucleotides encompassing the entire p53-DM β cDNA insert. The design of the forward and reverse primers was based on the p53 sequence reported in GenBank under the accession number M14694 and the published sequence for HLA-DM β (Kelly *et al.*, 1991), respectively and contained restriction sites (highlighted blue and yellow) for the generation of compatible ends for sub-cloning into the vector pSecTagA.

Forward primer: 5'-GGCCCAGCTGGCCATGGAGGAGCCGCAGTCAG-3'

Reverse primer: 5'-CCGCGAATTCATAGGAAATGTGCCATCCTTC-3'

*Sfi*I

EcoRI

Start codon

Stop codon

Polymerase chain reaction amplification was performed under the following conditions: 45 seconds at 94°C, 45 seconds at 60°C, 72°C at 2 minutes and 42 seconds for 20 cycles, followed by 10 minutes at 72°C. After electrophoresis on a 1.5% LMP agarose gel, the resulting (1350bp) PCR product was excised, purified using the QIAquick gel extraction kit, and cloned into the TA-site of pCR2.1. The insert, p53-DM β , was subsequently released from pCR2.1 by sequential restriction endonuclease digestion with the enzymes *Sfi*I and *EcoRI* and subcloned into the equally cut pSecTagA downstream of the leader sequence. The *Sfi*I site is situated 10bp downstream of the LS and the *EcoRI* site is situated further downstream in the polylinker sequence. Recombinant clones in the correct orientation were sequenced across the pSecTagA polylinker by cycle sequencing using dye-labelled terminators.

For a schematic representation of the construct and the predicted location of p53 in expressed in transfected cells refer to Figure 3.2.

3.2.5 Construction of *pSecTagA.p53*

An expression vector was constructed which was identical to the construct *pSecTagA.p53-DM β* but lacked the DM β region fused at the carboxyl terminus of the p53. The approach used is summarised in Figure 3.1 and described below. All DNA manipulations were performed using techniques as described in chapter two. A *Eco81I-PstI* fragment from *pCR3.p53* encompassing 683bp-1179bp of the p53 cDNA insert plus a small region of the polylinker sequence were removed. This fragment was subcloned into *pSecTagA.p53-DM β* , in which the fragments *Eco81I-PstI* and *PstI-PstI* encompassing 683bp-1350bp of the p53-DM β insert plus a small downstream region of the polylinker sequence, were removed. Recombinant clones in the correct orientation were sequenced across the *pSecTagA* polylinker by cycle sequencing using dye-labelled terminators. The resulting construct, designated *pSecTagA.p53*, contained the p53 insert in frame with the leader sequence, which is situated 10bp upstream from p53.

For a schematic representation of the construct and the predicted location of p53 expressed in transfected cells refer to Figure 3.2.

3.2.6 Construction of *pSecTagA.p53-TM*

An *EcoRI* fragment containing the p53-DM β insert, was released from *pCR3.p53-DM β* and amplified by PCR using specific-oligonucleotides encompassing the entire p53 cDNA sequence, the transmembrane region of the DM β cDNA sequence plus a small region of the cytoplasmic tail immediately upstream of the signal motif. The design of the forward and reverse primers was based on the p53 sequence reported in GenBank under the accession number M14694 and the published sequence for HLA-DM β (Kelly *et al.*, 1991) respectively and contained restriction sites (highlighted blue and yellow) for the generation of compatible ends for sub-cloning into the vector *pSecTagA*.

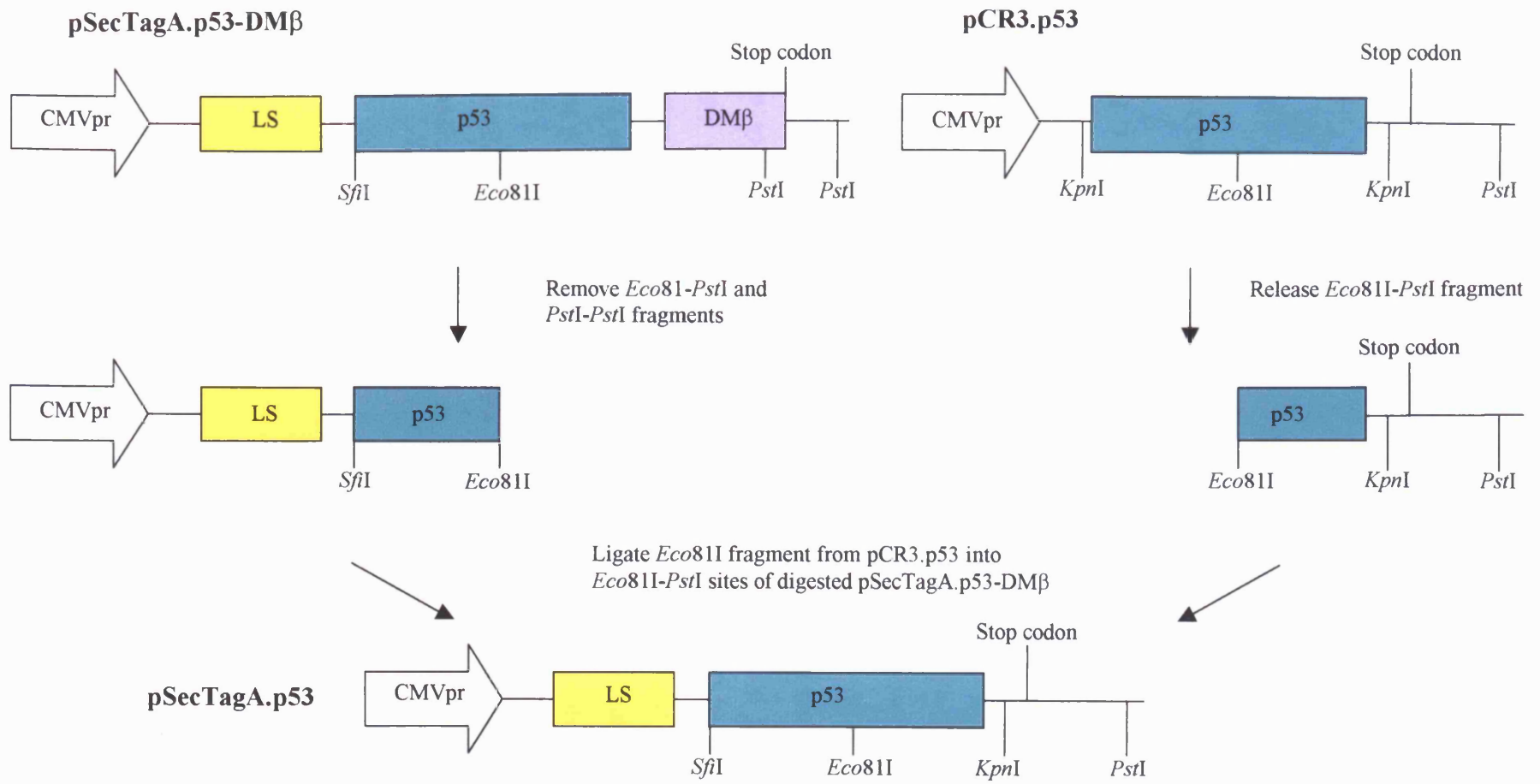


Figure 3.1 Construction of pSecTagA.p53

Forward primer; 5'-GGCCCAGCTGGCCATGGAGGAGCCGCAGTCAG-3'

Reverse primer, 5'-CCGGAATTC~~TA~~ACTAGAGTGGCCAGCTCT-3'

*Sfi*I

*Eco*RI

Start codon

Stop codon

Polymerase chain reaction amplification was performed under the following conditions: 45 seconds at 94°C, 45 seconds at 60°C, 72°C at 2 minutes and 42 seconds for 20 cycles, followed by 10 minutes at 72°C. After electrophoresis on a 1.5% LMP agarose gel, the resulting (1293bp) PCR product was excised, purified using the QIAquick gel extraction kit, and cloned into the TA-site of pCR2.1. The insert, designated p53-TM, was released from pCR2.1 by sequential restriction endonuclease digestion using the enzymes *Sfi*I and *Eco*RI and subcloned into the equally cut pSecTagA downstream of the leader sequence. The *Sfi*I site is situated 10bp downstream of the LS and the *Eco*RI site is situated further downstream in the polylinker sequence. Recombinant clones in the correct orientation were sequenced across the pSecTagA polylinker by cycle sequencing using dye-labelled terminators.

For a schematic representation of the construct and the predicted location of p53 in transfected cells refer to Figure 3.2.

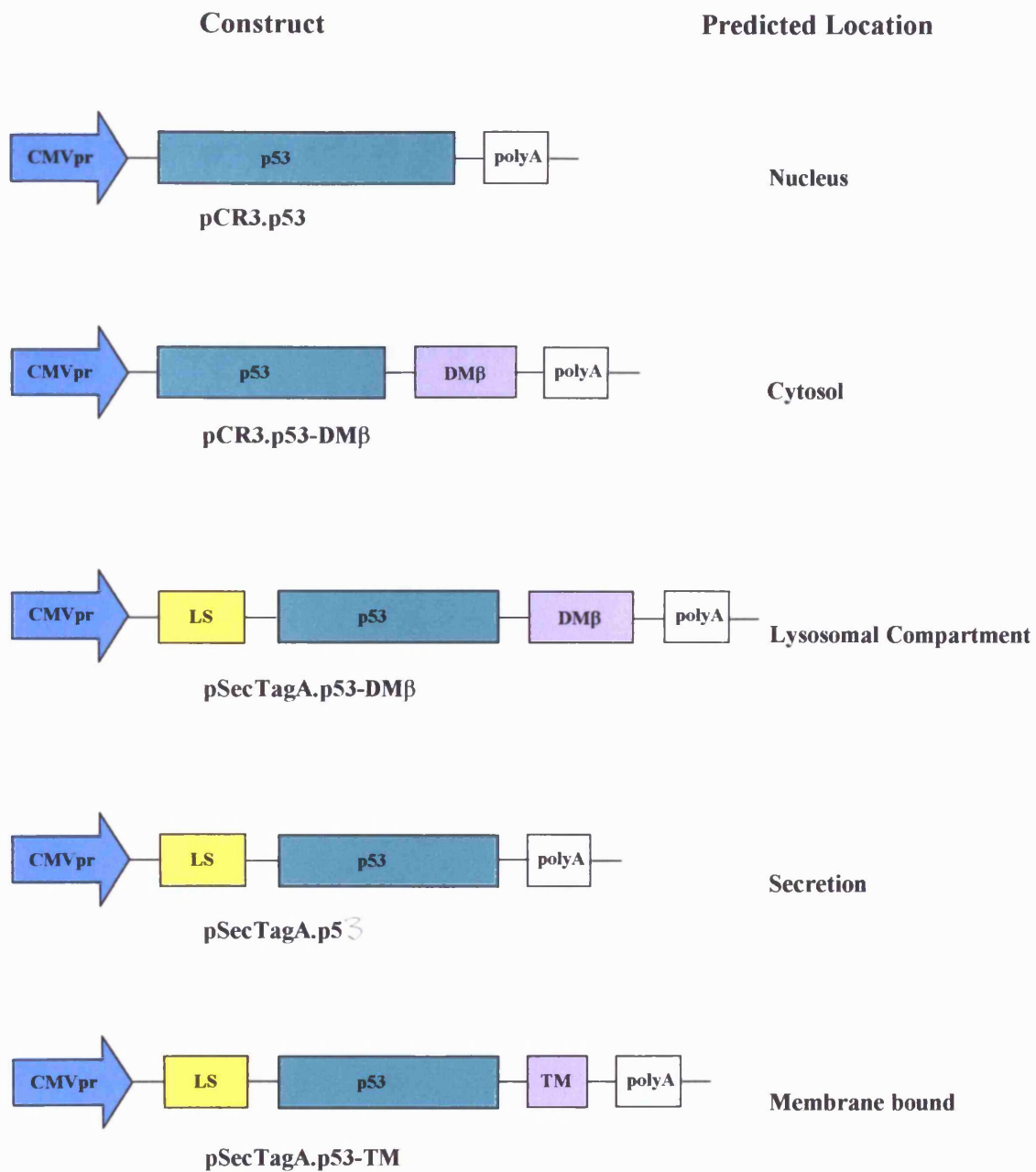


Figure 3.2 Mammalian expression constructs encoding p53 engineered to traffic to predicted locations as indicated.

3.3 Results

3.3.1 Cloning of human p53

The open reading frame of human p53 was generated by RT-PCR from MCF-7 total RNA, using the primers and conditions described. The resulting 1216bp PCR product, shown in Figure 3.3, was cloned directly into the TA-site of the TA-cloning vector pCR2.1. Cycle sequencing confirmed the cloned p53 cDNA sequence to be identical to that reported in GenBank under accession number M14694. Sequencing also revealed that the stop codon was not present and a *Kpn*I site had been generated 12bp downstream of the insert. A *Kpn*I site was also situated 54bp upstream of p53 in the polylinker sequence of pCR2.1. This enabled p53 to be subcloned as a *Kpn*I fragment in subsequent DNA manipulations.

3.3.4 Characterization of pCR3-p53-DMB

The region of HLA-DNA encompassing the transmembrane region and cytoplasmic tail including the YXX ϕ signal motif was amplified by PCR using the primers and conditions described. The resulting PCR product (139bp), shown in Figure 3.4, was

cloned into the TA-cloning vector pCR3 using a BamHI and EcoRI

digested pCR3 and the PCR product of pCR3 and

in the correct orientation. The

product was further to undergo a

restriction enzyme digestion with

ApaI to generate fragments of p53 without a

signal sequence. The resulting fragments were

ligated into the pCR3-DMB vector. The resulting construct

was designated pCR3-p53-DMB(1).

The resulting construct, designated pCR3-p53-DMB(1),

was used to transfect HeLa cells to determine the localization of p53-DMB by

immunofluorescence microscopy. The analysis of the localization of the DMB

region of p53 was in the correct reading frame with the stop codon located within

the polyoma sequence of pCR3, 27bp downstream of p53. The resulting construct

was designated pCR3-p53-DMB(2) and served as a control vector in the localization studies of

p53-DMB in transfected HeLa cells.

The resulting construct, designated pCR3-p53-DMB(2),

was used to transfect HeLa cells to determine the localization of p53-DMB by

immunofluorescence microscopy. The analysis of the localization of the DMB

region of p53 was in the correct reading frame with the stop codon located within

the polyoma sequence of pCR3, 27bp downstream of p53. The resulting construct

was designated pCR3-p53-DMB(3) and served as a control vector in the localization studies of

p53-DMB in transfected HeLa cells.

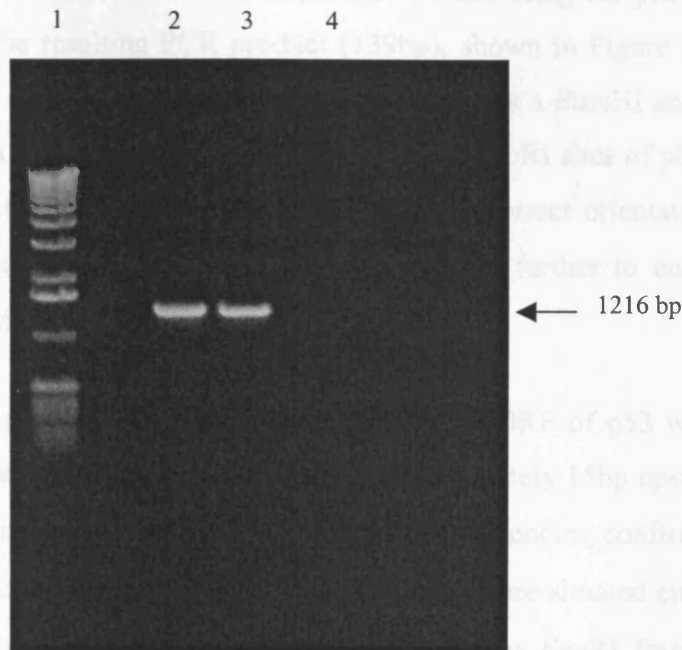


Figure 3.3 Agarose gel (1.5%) stained with ethidium bromide showing RT-PCR of human p53 cDNA for insertion into a TA-cloning vector. Lane (1) 1Kb DNA Marker. Lane (2) PCR amplification product of p53 using 10ng of reverse transcribed MCF-7 breast tumour cell line total RNA. Lane (3) PCR amplification product of p53 using 100ng of reverse transcribed MCF-7 breast tumour cell line total RNA. Lane (4) Negative control using mRNA demonstrating that the amplification did not originate from contaminating chromosomal DNA.

3.3.2 Construction of pCR3.p53-DM β

The region of HLA-DM β encompassing the transmembrane region and cytoplasmic tail containing the YTPL signal motif was amplified by PCR using the primers and conditions described. The resulting PCR product (139bp), shown in Figure 3.4, was cloned into the TA-site of pCR2.1 and subsequently released as a *Bam*HI and *Eco*RI fragment. This fragment was subcloned into the *Bam*HI and *Eco*RI sites of pCR3 and restriction analysis identified the recombinant clones in the correct orientation. The resulting construct, designated pCR3.DM β , was manipulated further to engineer a chimeric cDNA p53-DM β template.

A *Kpn*I fragment from pCR2.1.p53 encompassing the entire ORF of p53 without a stop codon was subcloned into the *Kpn*I site situated approximately 15bp upstream of the DM β insert present in the construct pCR3.DM β . Cycle sequencing confirmed that p53 was in the correct reading frame with DM β . *Eco*RI sites were situated either side of the insert which enabled p53-DM β to be subcloned as an *Eco*RI fragment in subsequent DNA manipulations. The resulting construct, designated pCR3.p53-DM β , encoded a chimeric protein p53-DM β , illustrated in Figure 3.5, and was used to transfect HeLa cells to determine the localisation of p53-DM β by immunofluorescence microscopy studies. The amino acid sequence of the DM β region appended to the C-terminus of p53 is illustrated in Figure 3.6.

3.3.3 Construction of pCR3.p53

A *Kpn*I fragment, released from pCR2.1.p53 encompassing the entire ORF of p53 without a stop codon, was subcloned into the *Kpn*I site of pCR3. Sequencing analysis confirmed that p53 was in the correct reading frame with a stop codon located within the polylinker sequence of pCR3, 27bp downstream of p53. The resulting construct was designated pCR3.p53 and served as a control vector in the localisation studies of p53-DM β in transfected HeLa cells.

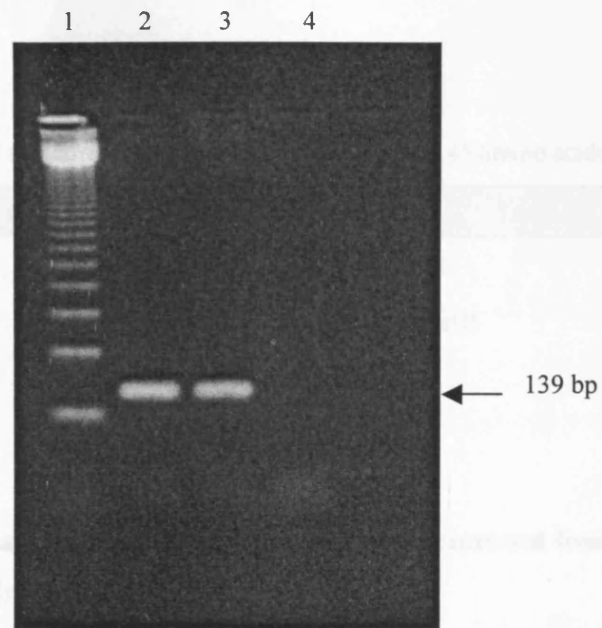


Figure 3.4 Agarose gel (1.5%) stained with ethidium bromide showing PCR of human DM β cDNA encoding the transmembrane region and YTPL peptide motif of the cytoplasmic region. Lane(1) 123bp repeat DNA ladder. Lane(2) PCR amplification product of DM β using 10ng of pCDM8.RING-7 vector DNA. Lane(3) PCR amplification product of DM β using 100ng of pCDM8.RING-7 vector DNA. Lane (4) Negative control.

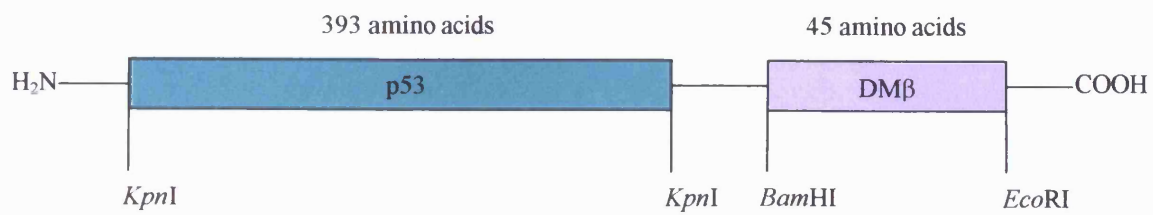


Figure 3.5 Schematic diagram of the chimeric protein p53-DM β expressed from the construct pCR3.p53-DM β in transiently transfected HeLa cells

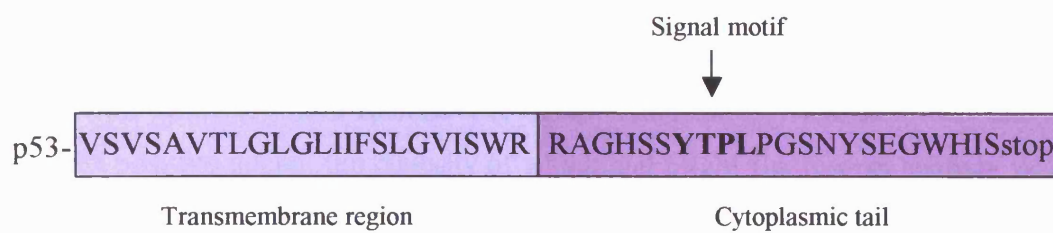


Figure 3.6 Structure of the transmembrane region and cytoplasmic tail of the hybrid p53-DM β molecule containing the wild-type DM β sequence.

3.3.4 Intracellular localisation of p53 and p53-DM β in the absence of an amino terminal signal sequence.

In the absence of an amino terminal signal sequence, it was predicted that p53 and p53-DM β would localise to the nucleus and cytosol, respectively. To confirm this the epithelial cell line HeLa was transfected with the constructs pCR3.p53 or pCR3.p53-DM β . Intracellular immunofluorescence staining using antibodies to p53 and CD63 followed by CLSM was employed to determine whether p53-DM β co-localised with an endogenous lysosomal marker, CD63.

Prior to the localisation studies of p53, HeLa cells were utilised in preliminary experiments to determine the optimal dilutions of the primary anti human monoclonal CD63 antibody and the secondary anti-mouse antibody conjugated with CY3 (Table 3.1). The staining pattern obtained for CD63 is illustrated and described below in the localisation studies of p53 in transfected HeLa cells.

The breast tumour-cell lines MCF-7 and MDA-MB-231, which express wild-type p53 at low levels and mutant p53 at high levels, respectively, were utilised to establish optimal dilutions for the primary rabbit anti-human p53 antibody and the secondary anti rabbit-FITC antibody (Table 3.1). They also served as positive controls for p53 expression in subsequent p53 localisation experiments. The immunofluorescence pattern obtained for p53 in both cell lines, revealed that p53 was localised to the nuclei with relatively little fluorescence in the cytoplasm. The MCF-7 cell line had scattered positive nuclei, the majority of which had bright fluorescent staining with a few cells showing moderate staining (Figure 3.7). Conversely, virtually all the nuclei from the MDA-MB-231 cell line showed bright fluorescent staining for p53 (Figure 3.7). These results are consistent with published data. Although wild-type p53 in normal cells is kept at low levels by its relatively short-half-life of 15-30 minutes (Oren *et al.*, 1981) and is usually undetectable by standard immunocytochemical techniques (Lane & Benchimol, 1990), some sublines of MCF-7 cells, show strong nuclear staining in a small number of cells (Vojtesek & Lane, 1993). This may be due to the cells exhibiting elevated p53 levels in response to normal growth conditions such as damage induced by aberrant DNA replication. Occasionally p53 positive cells

are seen in sections of normal tissues and might reflect events which occur rather more frequently in rapidly dividing immortal cell lines like MCF-7. Interestingly other sublines of MCF-7 cells show a mixture of diffuse cytoplasmic p53 and nuclear overexpression in exponentially growing cultures (Segrini *et al.*, 1994). In contrast, MDA-MB 231 cells which harbour a p53 missense mutation at codon 280 express transcriptionally inactive mutant p53 which accumulates to high levels in the nuclei (Moll *et al.*, 1996).

Table 3.1. Optimal dilutions of antibodies used in intracellular immunofluorescence microscopy.

Antibodies	Optimal Dilutions
Primary polyclonal anti-human p53	
(raised in rabbit)	1:1000
Primary monoclonal anti-human CD63	
(raised in mouse)	1:100
Secondary monoclonal anti-rabbit conjugated with FITC	
(raised in goat)	1:200
Secondary monoclonal anti-mouse conjugated with CY3	
(raised in goat)	1:250

Further preliminary experiments were performed using HeLa cells transfected with p53 constructs to determine whether cross reactivity existed between the primary polyclonal p53 antibody raised in rabbit and the secondary anti-mouse antibody conjugated with CY3 and also between the primary monoclonal CD63 antibody raised in mouse and the secondary rabbit antibody conjugated with FITC. The data, which

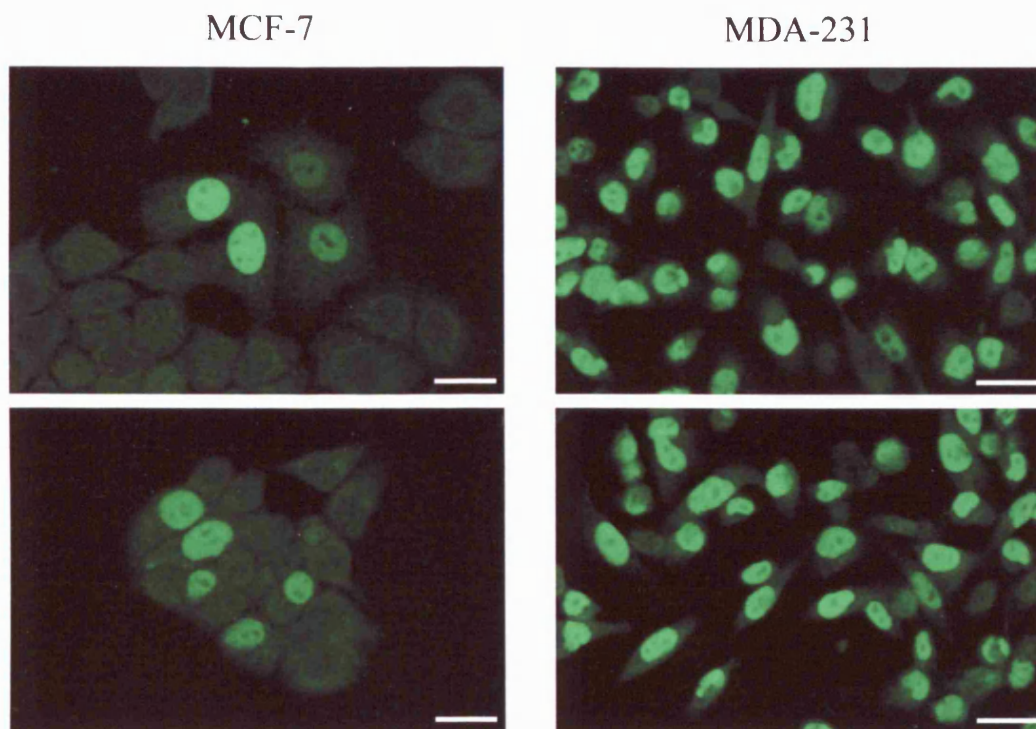


Figure 3.7 Immunofluorescence analysis of the intracellular localisation of endogenous p53 in MCF-7 and MDA-MB 231 cells. Cells were grown on coverslips for 48h and were fixed, permeabilised and labelled with a rabbit anti-human p53 polyclonal Ab. p53 was detected by secondary incubation with an anti-rabbit FITC conjugated mAb (green label). Cells were examined by CLSM and digital images were recorded. Both cell lines acted as positive controls for intracellular staining of p53. Scale bars, 25 μ m.

are not shown, confirmed that there were no cross reactions with these antibodies and consequently could be used in the following dual staining experiments.

HeLa cells were transiently transfected with the constructs pCR3.p53 and pCR3.p53-DM β by electroporation, the conditions having been optimised using pCR3.GFP (data not shown). A mock transfection was also performed using the vector pCR3 alone which served as a negative control in these localisation studies. Electroporated cells were transferred to petri dishes containing 2mls of DMEM + 10% FCS and 1% gelatin-treated coverslips. At 24 and 48-hours, cells were either left untreated or were treated with leupeptin, subsequently fixed, permeabilised and labelled with antibodies to detect p53 and CD63, as described in chapter two. HeLa cells were examined by conventional fluorescence microscopy and CLSM. Digital confocal images were obtained. It is important to note that all experiments described below included negative controls for p53 and CD63 labelling in which cells were also labelled with secondary antibodies alone to ensure that non-specific binding of these antibodies had not occurred and the background levels of fluorescence were low.

The intensity of immunofluorescence staining for p53 and p53-DM β was similar in HeLa cells at 24 and 48-hours which suggests that expression levels at these time points were similar. Only confocal images of HeLa cells at 48-hours are shown (Figures 3.8-3.10). A low transfection efficiency of approximately 1-3% was obtained in HeLa cells electroporated with the constructs pCR3.p53 and pCR3.p53-DM β compared with HeLa cells electroporated with the GFP construct pCR3.GFP which had an efficiency of 40% (data not shown).

HeLa cells were transfected with the construct pCR3.p53 encoding p53 alone in the absence of the DM β signal peptide. This construct served as a control in the localisation studies of p53. The results showed that bright fluorescent labelling for p53, in positively transfected HeLa cells at 48-hours, was localised to the nuclei without any cytoplasmic staining (Figure 3.8, Panel B). Identical staining was observed in cells treated with leupeptin, an inhibitor of a subset of lysosomal proteases (Figure 3.8, Panel E). The immunofluorescence pattern for antibodies directed to the endogenous lysosomal marker, CD63, revealed perinuclear structures

and sporadic vesicles in the cell periphery (Figure 3.8, Panel A). This pattern of staining is indicative of the distribution of lysosomes. The composite images did not reveal any areas of co-localisation of p53 and CD63. The pattern of staining for p53 was consistent with the nuclear localisation of endogenous wild-type p53 in MCF-7 cells from which cDNA p53 was cloned (Figure 3.7). To ensure that these results were not due to endogenous expression of wild-type p53 in HeLa cells in response to their rapid division, untransfected cells and those transfected with empty vector (pCR3) were also dual stained for p53 and CD63. Fluorescent labelling for p53 was not observed in both untreated and leupeptin-treated untransfected HeLa cells (data not shown). However, the distinct punctate vesicular staining for CD63 was present (data not shown). Similarly, HeLa cells transfected with pCR3 alone, treated with (data not shown) or without leupeptin, showed distinct punctate vesicular staining for CD63 (Figure 3.22, Panel A) and no fluorescence for p53 (Figure 3.22, Panel B). The composite image (Figure 3.22, Panel C), therefore, did not reveal any areas of co-localisation. The results demonstrated that HeLa cells do not normally express p53 at detectable levels and p53 expression driven by the CMV promoter resulted in localisation to the nucleus in transiently transfected HeLa cells.

In HeLa cells transfected with pCR3.p53-DM β , the levels of p53-DM β detected by immunofluorescence appeared to be very high. This was illustrated by intense immunofluorescence for p53 distributed internally throughout the cell apart from the nucleus which was completely devoid of fluorescence, thus making it very difficult to detect the exact localisation of p53 (Figure 3.9, Panel B). In contrast, the immunofluorescence pattern for antibodies directed to the endogenous lysosomal marker, CD63, revealed perinuclear structures and sporadic vesicles in the cell periphery (Figure 3.9, Panel A). Panel C in Figure 3.9 represents the composite image of the two labels p53 and CD63. However, this composite image revealed areas in the perinuclear region where p53 had possibly co-localised with CD63. These areas appeared yellow caused by the combination of the green (FITC) and red signal (CY3).

To test whether p53-DM β was being degraded by proteases present in the lysosomes, transfected cells were treated with leupeptin prior to the indirect dual immunofluorescence analysis with antibodies to p53 and CD63. The staining pattern

for p53 in leupeptin-treated cells (Figure 3.9, Panel E) was similar to the pattern in untreated cells and did not illustrate the punctate staining of lysosomes. p53 appeared to be distributed internally throughout the cytosol, apart from the nucleus with little evidence of localisation to the lysosomes. In contrast, the immunofluorescence pattern for antibodies directed to the endogenous lysosomal marker, CD63, revealed perinuclear structures and sporadic vesicles in the cell periphery (Figure 3.9, Panel D) which was also observed in untreated cells. Whereas the fluorescent pattern for p53 did not reveal conspicuous localisation to the lysosomes, the composite image revealed a few yellow areas in the perinuclear region due to the combination of the green (FITC) and red signal (CY3), which may indicate areas in which p53 has co-localised with CD63 (Figure 3.9, Panel F).

In order to examine the location of p53-DM β and CD63 in more detail a z-series of confocal images was collected at 0.7 μ m intervals through a HeLa cell expressing p53-DM β (Figure 3.10). All the panels labelled A and B show fluorescence using the FITC and CY3 filter respectively. Panels 1A and 1B represent a confocal image in the horizontal plane near the apex of the cell and the subsequent panels (2A+B – 11A+B) represent images in the horizontal plane at every 0.7 μ m through the cell approaching the base (12A and 12B). Panel 13 represents a composite image of the projected images acquired in the z-series. As before, it was difficult to ascertain from these images whether co-localisation of the chimeric protein p53-DM β with the lysosomal marker CD63 had occurred. p53-DM β may have accumulated at steady state in the cytosol with some localisation to the lysosomes. In summary the results revealed that p53-DM β expressed from pCR3 in transiently transfected cells, was not localised to the nucleus but instead to undetermined locations in the cytoplasm due to the YTPL signal peptide appended to its C-terminus.

All immunofluorescence experiments described in this section were performed at least three times and the observations found to be reproducible.

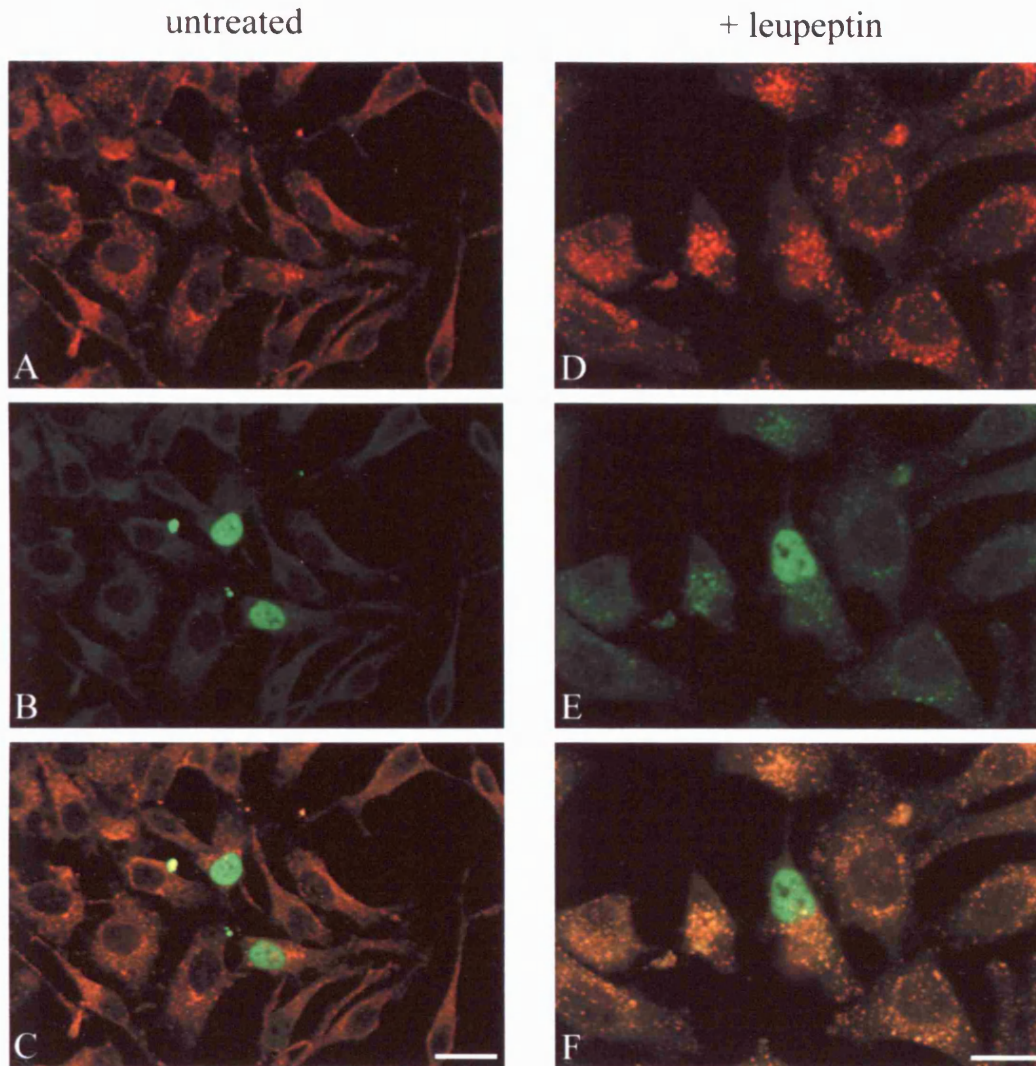


Figure 3.8 Immunofluorescence analysis of the intracellular localisation of p53 and CD63 in HeLa cells 48h after transient transfection with the construct pCR3.p53. Cells were transiently transfected and were treated with 1mg/ml leupeptin for the final 4h (D,E,F) or left untreated (A,B,C). Cells were fixed, permeabilised and co-labelled with a rabbit anti-human p53 polyclonal Ab and a mouse anti-human CD63 mAb. p53 and CD63 were detected by secondary incubation with an anti-rabbit-FITC conjugated mAb (green label) and an anti-mouse-CY3 conjugated mAb (red label), respectively. Cells were examined by CLSM and digital images of identical fields were obtained using filters for both CY3 (A, D) and FITC (B, E). The lower panels C and F represent composite images of A and B, and D and E, respectively. Scale bars, 25 μ m.

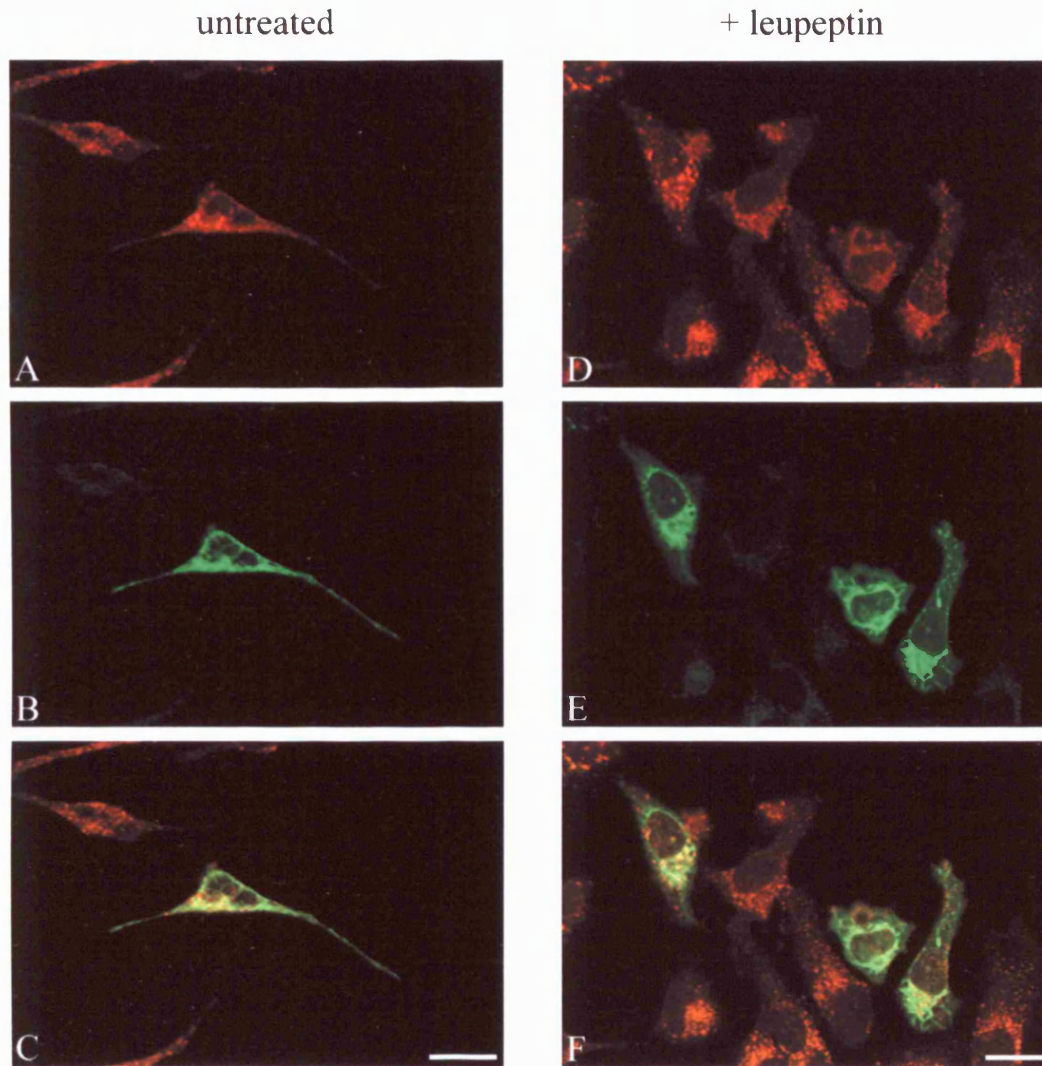


Figure 3.9 Immunofluorescence analysis of the intracellular localisation of p53 and CD63 in HeLa cells 48h after transient transfection with the construct pCR3.p53-DM β . Cells were transiently transfected and were treated with 1mg/ml leupeptin for the final 4h (D,E,F) or left untreated (A,B,C). Cells were fixed, permeabilised and co-labelled with a rabbit anti-human p53 polyclonal Ab and a mouse anti-human CD63 mAb. p53 and CD63 were detected by secondary incubation with an anti-rabbit-FITC conjugated mAb (green label) and an anti-mouse-CY3 conjugated mAb (red label), respectively. Cells were examined by CLSM and digital images of identical fields were obtained using filters for both CY3 (A and D) and FITC (B and E). The lower panels C and F represent composite images of A and B, and D and E, respectively. Scale bars, 25 μ m.

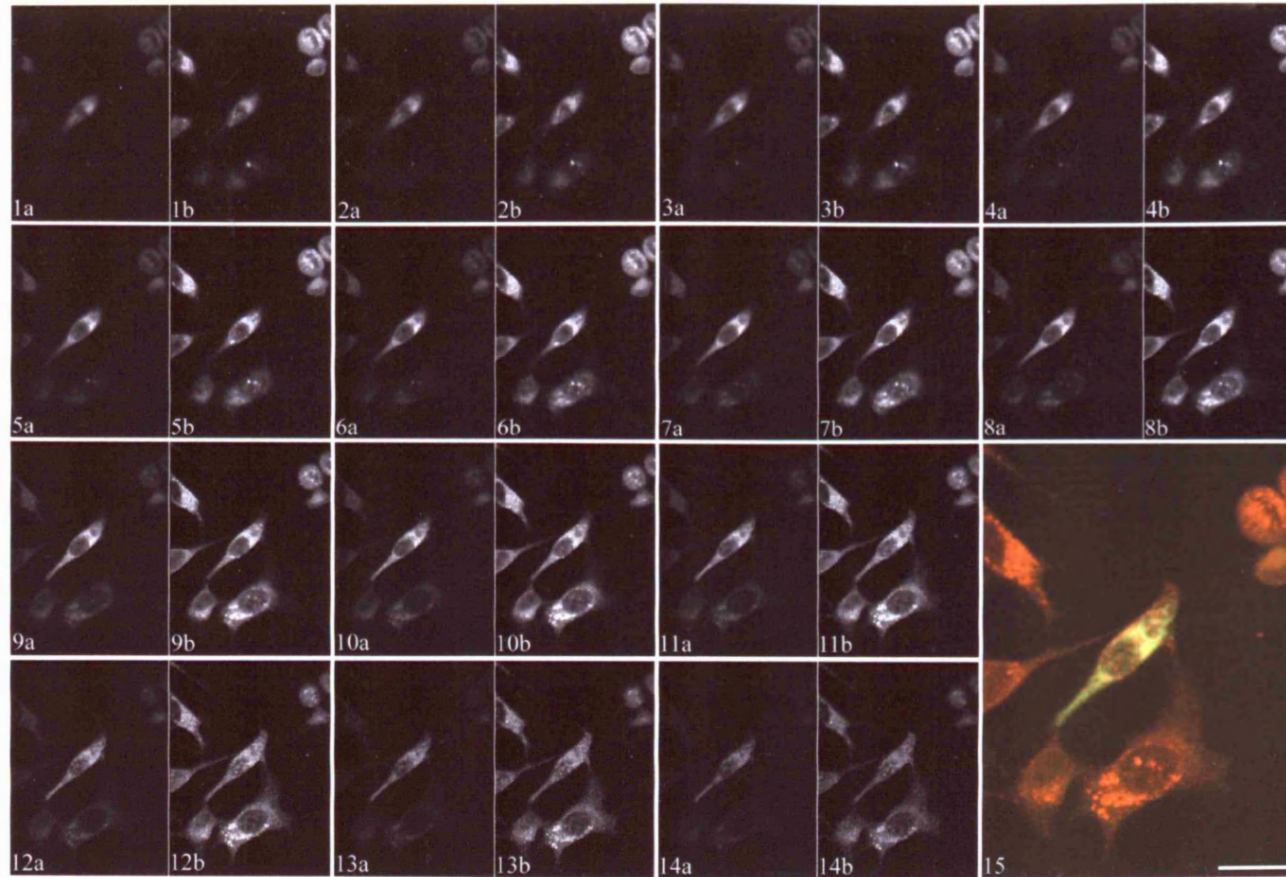


Figure 3.10 Immunofluorescence analysis of the intracellular localisation of p53 and CD63 in HeLa cells 48h after transient transfection with the construct pCR3.p53-DM β . Transfected cells were fixed, permeabilised and co-labelled with a rabbit anti-human p53 polyclonal Ab and a mouse anti-human CD63 mAb. p53 and CD63 were detected by secondary incubation with an anti-rabbit-FITC conjugated mAb (green label) and an anti-mouse-CY3-conjugated mAb (red label), respectively. Cells were examined by CLSM. Panels 1-14 represent a series of optical sections (z-series) of an identical field collected using filters for both FITC (A) and CY3 (B), at 0.7 μ m intervals from the apex of the cell (1) through to the base (14). Panel 15 represents a projection of the images obtained in the z-series which have been superimposed to detect co-localisation of p53 (FITC) and CD63 (CY3). Scale bar, 25 μ m.

3.3.5 Construction of *pSecTagA.p53-DM β*

The insert p53-DM β was released as an *EcoRI* fragment from the construct pCR3.p53-DM β and amplified by PCR using the primers and conditions described. The resulting 1350bp PCR product was cloned directly into the TA-site of the TA-cloning vector pCR2.1 and subsequently released by sequential digestion with *SfiI* and *EcoRI*. This fragment was subcloned into the *SfiI* and *EcoRI* site of the previously digested eukaryotic expression vector pSecTagA. This vector contains a strong CMV-derived promoter, upstream of the leader sequence (LS) and MCS, which drives the constitutive expression of the inserted gene product in eukaryotic cells. Restriction analysis identified positive clones and cycle sequencing confirmed that the cloned p53-DM β cDNA sequence was identical to that of the insert, p53-DM β , present in the construct pCR3.p53-DM β . Sequencing analysis also confirmed that p53-DM β was in frame with the LS which was located 15bp upstream of the insert. This construct which was designated pSecTagA.p53-DM β encoded a chimeric protein LS-p53-DM β , illustrated in Figure 3.11, and was used to transfect HeLa cells to determine the localisation of p53-DM β by immunofluorescence microscopy studies. The amino acid sequence of the DM β region appended to the carboxyl terminus of p53 is illustrated in Figure 3.12.

3.3.6 Construction of *pSecTagA.p53*

pSecTagA.p53 was constructed as described in section 3.2.5. Restriction analysis identified positive clones and cycle sequencing confirmed that the cloned p53 cDNA was in frame with the leader sequence which was situated 15bp upstream. A stop codon was located 27bp downstream of p53 in the polylinker sequence. This pSecTagA-p53 construct served as a control in localisation studies of p53-DM β expressed from the construct pSecTagA-p53-DM β in transfected HeLa cells.

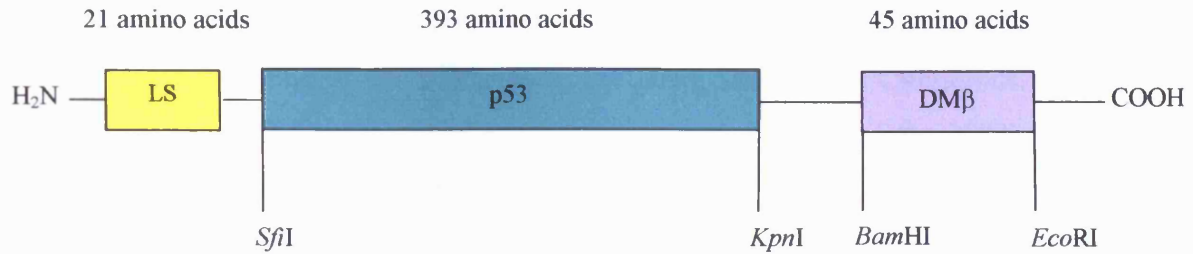


Figure 3.11 Schematic diagram of the chimeric protein LS-p53-DM β expressed from the construct pSecTagA.p53-DM β in transiently transfected HeLa cells.



Figure 3.12 Amino-acid sequence of the transmembrane region and cytoplasmic tail of DM β present in the hybrid LS-p53-DM β molecule.

3.3.7 Intracellular location of p53 and p53-DM β expressed from the pSecTagA constructs in transfected HeLa cells: utilisation of an amino-terminal signal sequence.

In the presence of an amino-terminal signal sequence, it was predicted that p53-DM β would translocate across the ER membrane and then traffic to the lysosomal compartment by virtue of the YTPL signal motif appended to its C-terminus. It was also envisaged that the LS would enable p53, in the absence of the YTPL signal motif, to traffic through the secretory pathway resulting in its secretion. To confirm this the HeLa cell line was transfected with the constructs pSecTagA.p53-DM β and pSecTagA.p53. Intracellular immunofluorescence staining using antibodies to p53 and CD63 followed by CLSM analyses was employed to determine the exact locations of p53 and p53-DM β .

HeLa cells were transiently transfected with the constructs pSecTagA.p53-DM β and pSecTagA.p53 by electroporation, the conditions having been optimised using pCR3.GFP (data not shown). A mock transfection was also performed using the vector pSecTagA alone which acted as a negative control in the localisation studies. Electroporated cells were transferred to petri dishes containing 2mls of DMEM + 10% FCS and 1% gelatin treated coverslips. At 48 hours, cells were fixed, permeabilised and co-labelled with antibodies to detect p53 and CD63 as described in chapter two. For optimal dilutions of antibodies used in these experiments refer to Table 3.1. All experiments described below included negative controls for p53 and CD63 labelling in which the cells were also labelled with the secondary antibodies alone to ensure that non-specific binding of these antibodies had not occurred.

Interestingly, the transfection efficiency of approximately 40-60% obtained in HeLa cells electroporated with the constructs pSecTagA.p53-DM β and pSecTagA.p53 was considerably higher than the transfection efficiency of 1-3% achieved in HeLa cells electroporated with the constructs pCR3.p53-DM β and pCR3.p53.

As in the case of HeLa cells transfected with the construct pCR3.p53-DM β , it was very difficult to determine the exact location of p53 at 48 hours after transfection with

the construct pSecTagA.p53-DM β . The levels of p53-DM β expressed in positively transfected cells appeared to be very high as illustrated by the intense immunofluorescence pattern. Immunofluorescence for p53 was distributed internally throughout the cell apart from the nucleus which was completely devoid of fluorescence thus making it difficult to detect localisation of p53 to lysosomal structures (Figure 3.13, Panel B). Fluorescent labelling for p53 was particularly prominent around the perinuclear region of each cell suggesting that p53 was present in the ER and possibly the nuclear envelope. In contrast, the immunofluorescence pattern for antibodies directed to the endogenous lysosomal marker, CD63, revealed perinuclear structures and sporadic vesicles in the cell periphery indicative of lysosomal staining (Figure 3.13, Panel A). The composite image, however, revealed a few yellow areas in the perinuclear region due to the combination of the green (FITC) and the red signal (CY3), which may indicate areas in which p53 has co-localised with CD63 (Figure 3.13, Panel C).

To find out if p53 was being degraded by proteases present in lysosomes, transfected cells were treated with leupeptin prior to the indirect dual immunofluorescence analysis with the antibodies to p53 and CD63. However, the staining pattern for p53 in leupeptin-treated cells was similar to that observed in untreated cells and did not reveal the punctate staining obtained with the antibody directed to CD63 (Figure 3.13, Panel D). As seen in untreated cells, fluorescence of p53 was observed in a prominent perinuclear ring suggesting that it is present in the ER and possibly the nuclear envelope (Figure 3.13, Panel E), and the nucleus was completely devoid of fluorescence. The composite image also revealed areas in the perinuclear region which appeared yellow and thus, indicated possible co-localisation of p53 with CD63 in the lysosomes (Figure 3.13, Panel F).

In order to examine the location of p53-DM β and CD63 in more detail a z-series of confocal images was collected at 0.7 μ m intervals through a HeLa cell expressing p53-DM β (Figure 3.14). All the panels labelled A and B show fluorescence using the FITC and CY3 filter, respectively. Panels 1A and 1B represent a confocal image in the horizontal plane near the apex of the cell and the subsequent panels (2A+B–11A+B) represent images in the horizontal plane at every 0.7 μ m through the cell

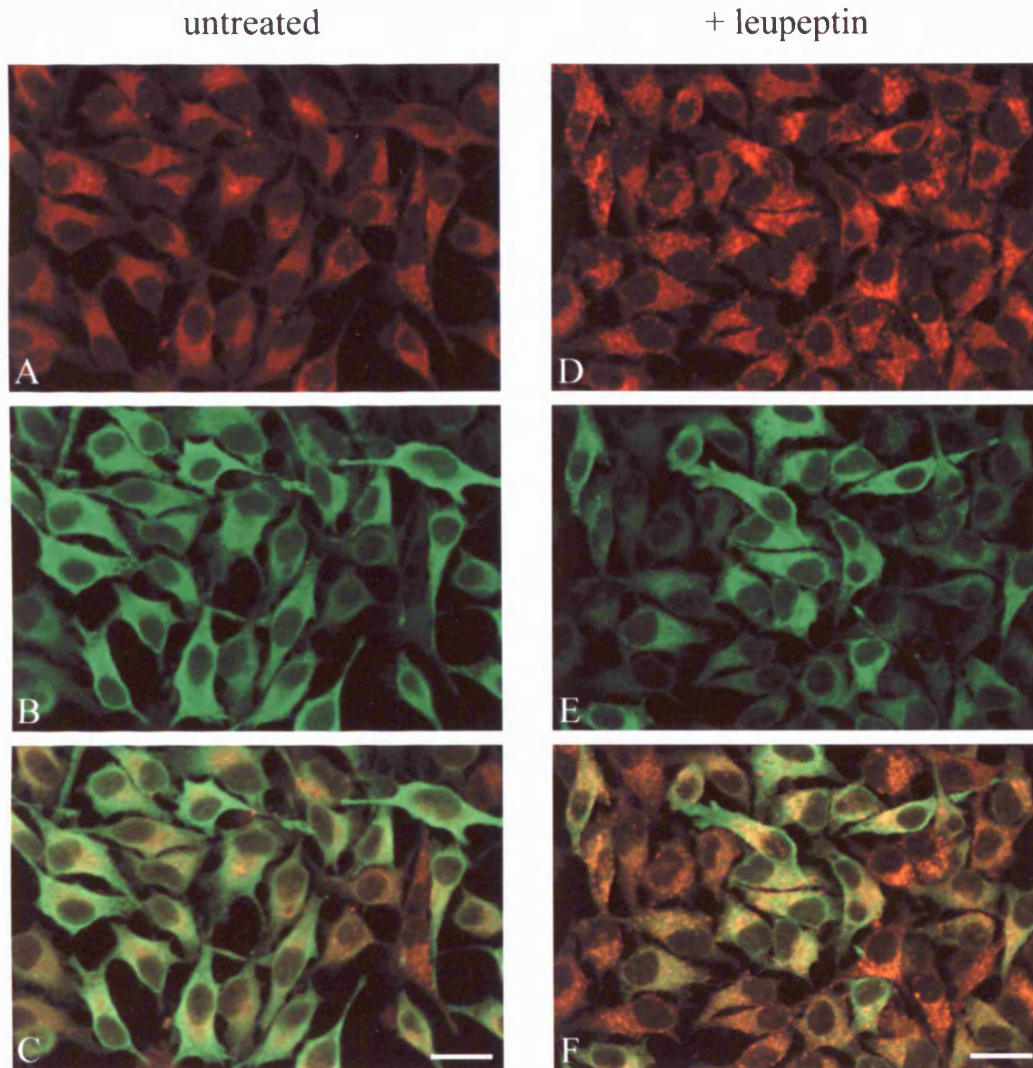


Figure 3.13 Immunofluorescence analysis of the intracellular localisation of p53 and CD63 in HeLa cells 48h after transient transfection with the construct pSecTagA.p53-DM β . Cells were transiently transfected and were treated with 1mg/ml leupeptin for the final 4h (D,E,F) or left untreated (A,B,C). Cells were fixed, permeabilised and co-labelled with a rabbit anti-human p53 polyclonal Ab and a mouse anti-human CD63 mAb. p53 and CD63 were detected by secondary incubation with an anti-rabbit-FITC conjugated mAb (green label) and an anti-mouse-CY3 conjugated mAb (red label), respectively. Cells were examined by CLSM and digital images of identical fields were obtained using filters for both CY3 (A and D) and FITC (B and E). The lower panels C and F represent composite images of A and B, and D and E, respectively. Scale bars, 25 μ m.

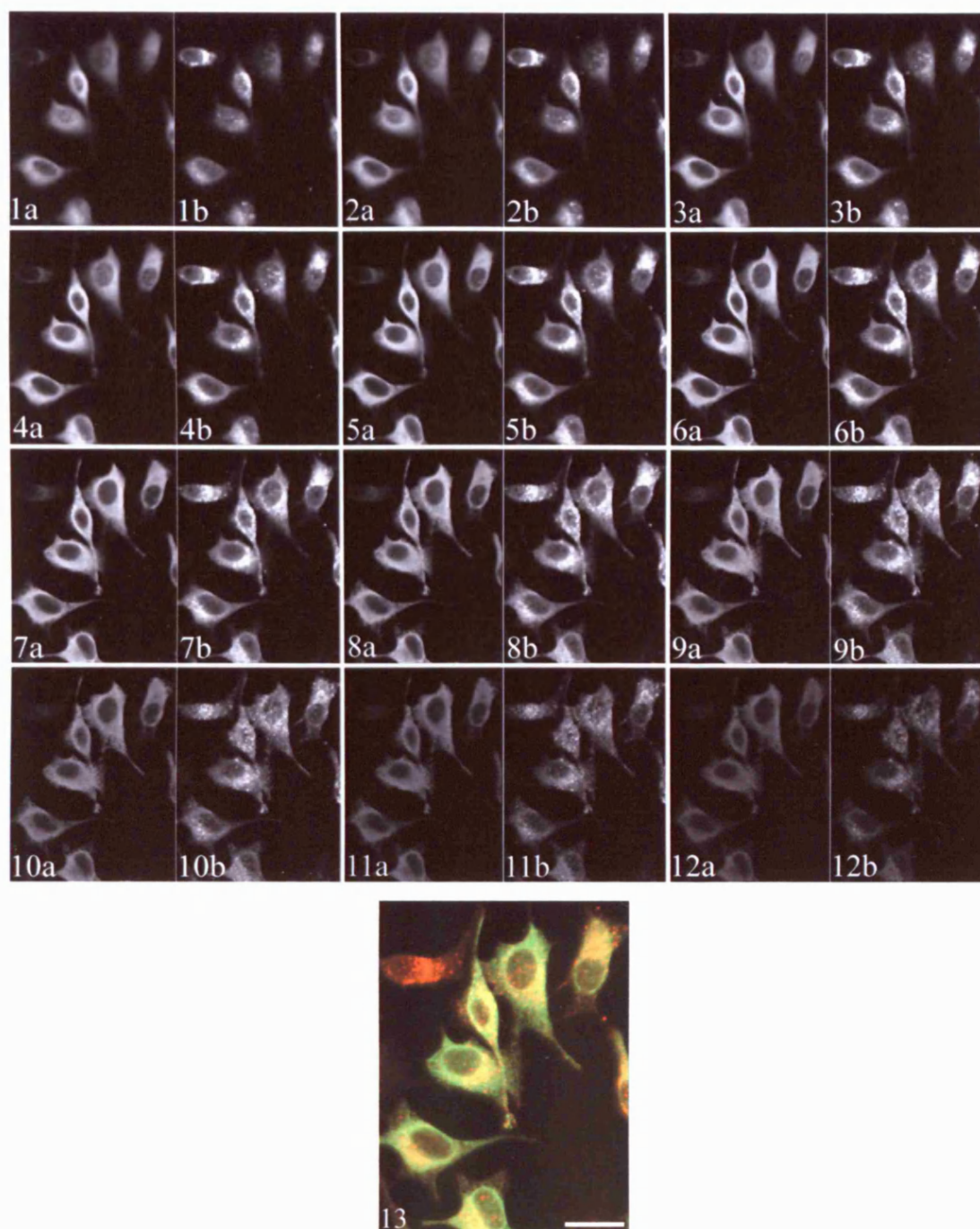


Figure 3.14 Immunofluorescence analysis of the intracellular localisation of p53 and CD63 in HeLa cells 48h after transient transfection with the construct pSecTagA.p53-DM β . Transfected cells were fixed, permeabilised and co-labelled with a rabbit anti-human p53 polyclonal Ab and a mouse anti-human CD63 mAb. p53 and CD63 were detected by secondary incubation with an anti-rabbit-FITC conjugated mAb (green label) and an anti-mouse-CY3-conjugated mAb (red label), respectively. Cells were examined by CLSM and digital images were recorded. Panels 1-12 represent a series of optical sections (z-series) of an identical field collected using filters for both FITC (A) and CY3 (B), at 0.7 μ m intervals from the apex of the cell (1) through to the base (12). Panel 13 represents a projection of the images obtained in the z-series which have been superimposed to detect co-localisation of p53 (FITC) and CD63 (CY3). Scale bar, 25 μ m.

approaching the base (12A and 12B). Panel 13 represents a composite image of the projected images acquired in the z-series. These images revealed that there were areas of co-localisation of the chimeric protein, p53-DM β , with the lysosomal marker, CD63, which were represented by yellow areas in the perinuclear region. These results suggested that p53-DM β had accumulated in the ER with some possible localisation in the lysosomes.

p53-DM β is constitutively expressed up to 72h after transient transfection due to the potent CMV enhancer-promoter sequence present in pSecTagA which results in its high level expression. The overexpression of p53-DM β may lead to steady state accumulation of p53-DM β in the ER and also at the cell surface caused by saturation of intracellular binding sites within the pathway involved in directing proteins to lysosomes. To find out if lysosomal targeting of p53-DM β was more conspicuous prior to the accumulation of protein within the cells, a time course experiment was performed over 48 hours. HeLa cells transfected with the construct pSecTagA.p53-DM β and grown on coverslips, were removed from the medium at 6, 12, 24 and 48-hour time points. They were subsequently treated with leupeptin for 4-hours or left untreated, fixed, permeabilised and co-labelled with antibodies to detect p53 and CD63 as described in chapter two. For optimal dilutions of antibodies refer to Table 3.1.

At 6-hours, the fluorescent labelling of p53 was similar in untreated and leupeptin-treated cells (Figure 3.15). Observations revealed that fluorescent staining had accumulated in the perinuclear region with diffuse staining present in the cell periphery. Punctate vesicular staining was observed for antibodies directed to CD63. The composite images revealed possible areas of co-localisation, which were particularly prominent in the perinuclear ring. These regions appeared yellow as a result of the combination of the green (FITC) and red signal (CY3). Fluorescent patterns of p53 and CD63 observed in cells, treated and untreated with leupeptin, at 12 (Figure 3.16) and 24-hours (Figure 3.17) were similar to those observed in cells at 48-hours (Figure 3.13). Disappointingly, the results obtained at each time point were unable to provide convincing evidence of conspicuous staining of p53 localised to the

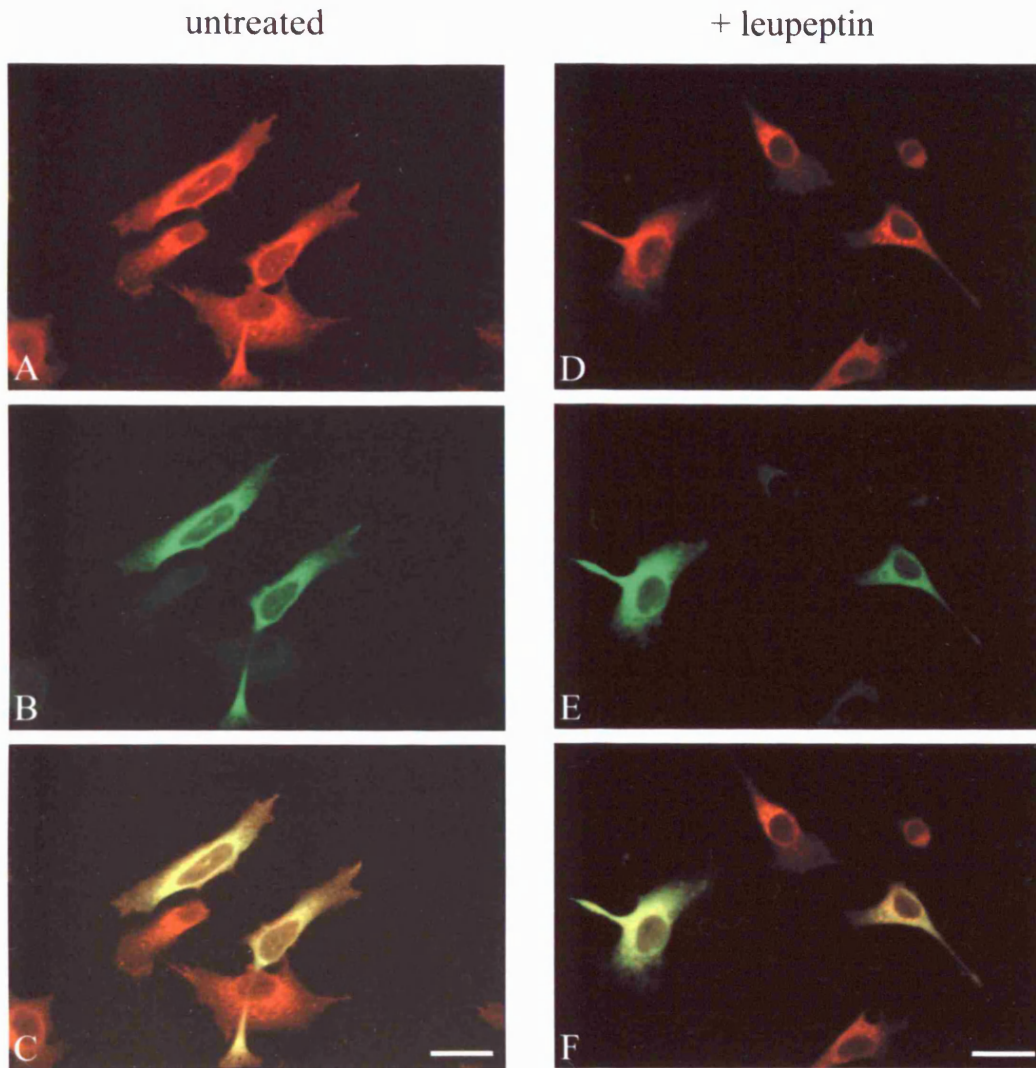


Figure 3.15 Immunofluorescence analysis of the intracellular localisation of p53 and CD63 in HeLa cells 6h after transient transfection with the construct pSecTagA.p53-DM β . Cells were transiently transfected and were treated with 1mg/ml leupeptin for the final 4h (D,E,F) or left untreated (A,B,C). Cells were fixed, permeabilised and co-labelled with a rabbit anti-human p53 polyclonal Ab and a mouse anti-human CD63 mAb. p53 and CD63 were detected by secondary incubation with an anti-rabbit-FITC conjugated mAb (green label) and an anti-mouse-CY3 conjugated mAb (red label), respectively. Cells were examined by CLSM and digital images of identical fields were obtained using filters for both CY3 (A and D) and FITC (B and E). The lower panels C and F represent composite images of A and B, and D and E, respectively. Scale bars, 25 μ m.

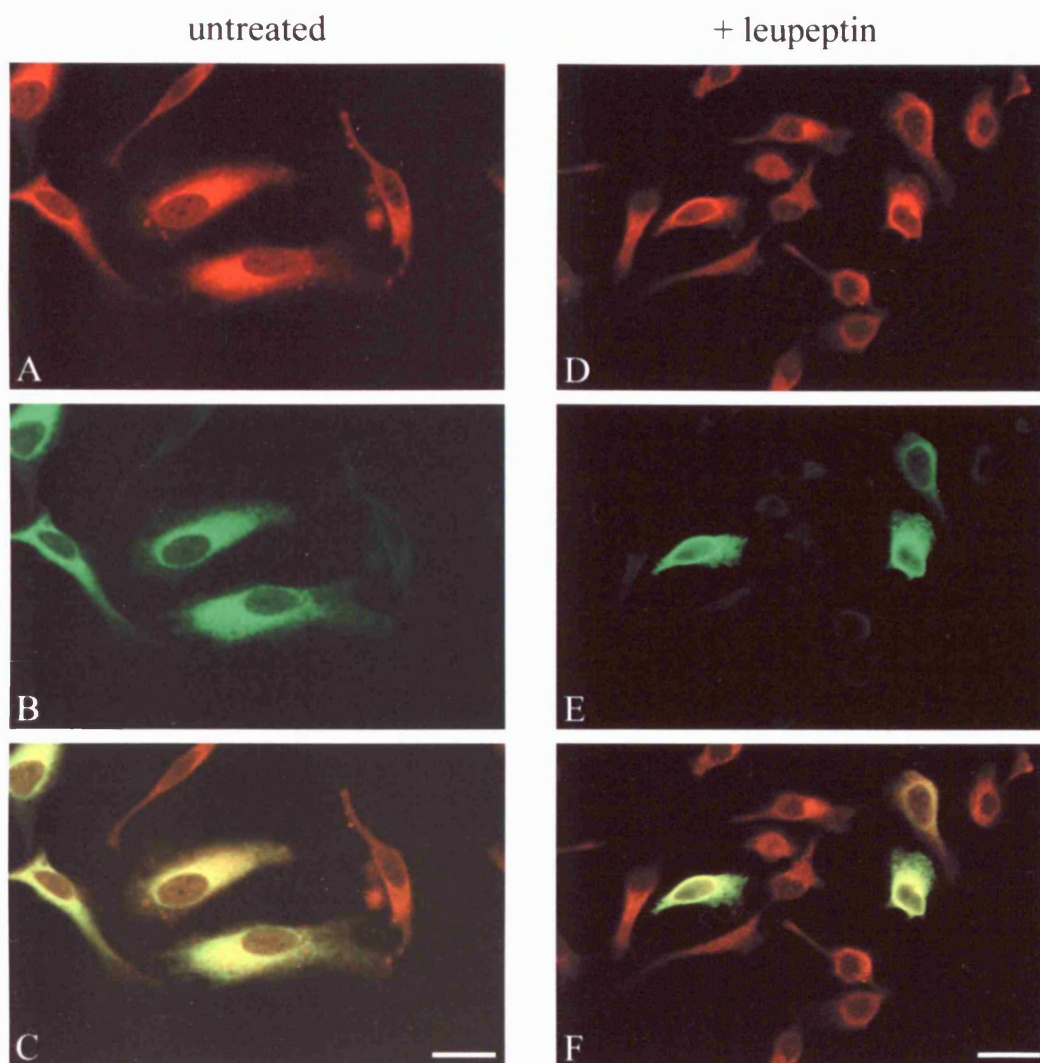


Figure 3.16 Immunofluorescence analysis of the intracellular localisation of p53 and CD63 in HeLa cells 12h after transient transfection with the construct pSecTagA.p53-DM β . Cells were transiently transfected and were treated with 1mg/ml leupeptin for the final 4h (D,E,F) or left untreated (A,B,C). Cells were fixed, permeabilised and co-labelled with a rabbit anti-human p53 polyclonal Ab and a mouse anti-human CD63 mAb. p53 and CD63 were detected by secondary incubation with an anti-rabbit-FITC conjugated mAb (green label) and an anti-mouse-CY3 conjugated mAb (red label), respectively. Cells were examined by CLSM and digital images of identical fields were obtained using filters for both CY3 (A and D) and FITC (B and E). The lower panels C and F represent composite images of A and B, and D and E, respectively. Scale bars, 25 μ m.

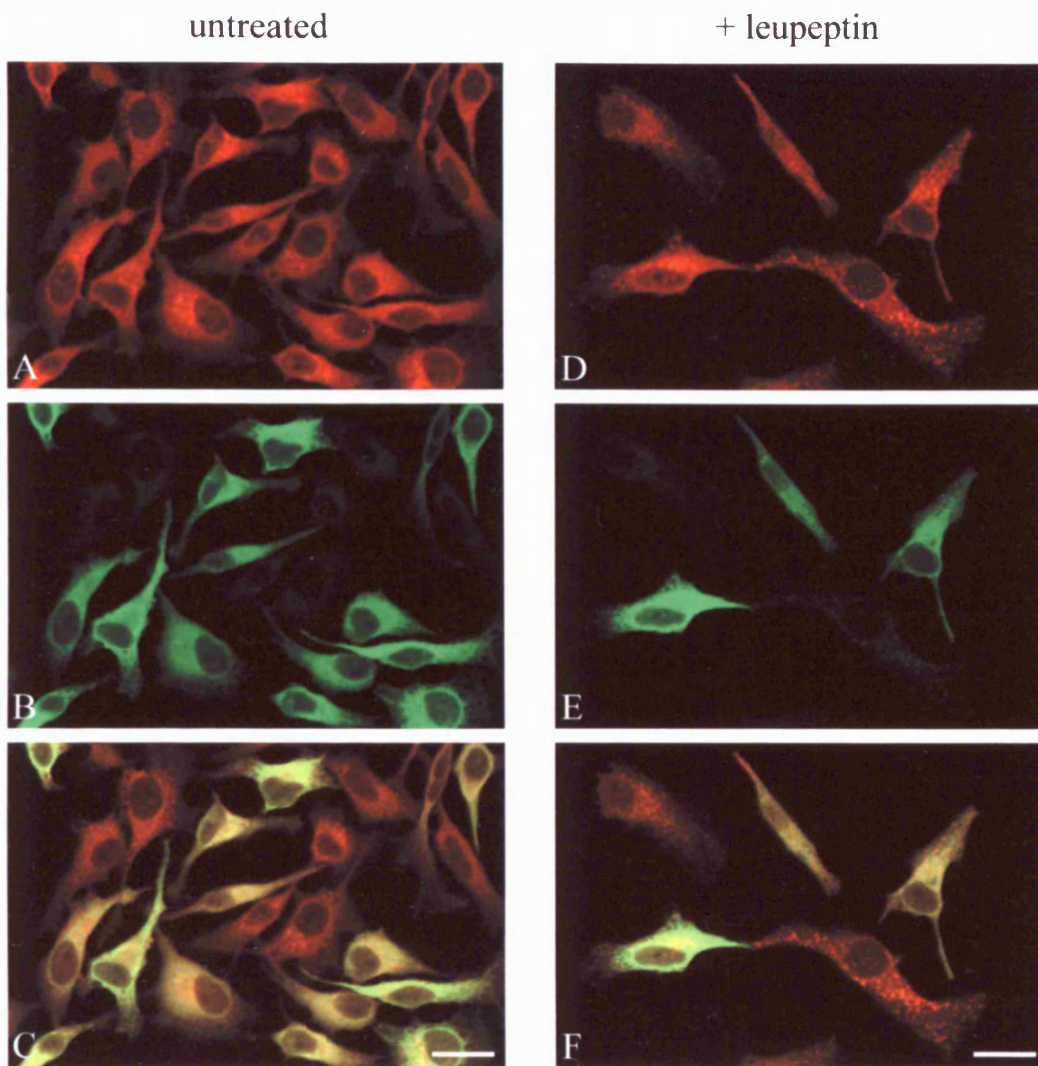


Figure 3.17 Immunofluorescence analysis of the intracellular localisation of p53 and CD63 in HeLa cells 24h after transient transfection with the construct pSecTagA.p53-DM β . Cells were transiently transfected and were treated with 1mg/ml leupeptin for the final 4h (D,E,F) or left untreated (A,B,C). Cells were fixed, permeabilised and co-labelled with a rabbit anti-human p53 polyclonal Ab and a mouse anti-human CD63 mAb. p53 and CD63 were detected by secondary incubation with an anti-rabbit-FITC conjugated mAb (green label) and an anti-mouse-CY3 conjugated mAb (red label,) respectively. Cells were examined by CLSM and digital images of identical fields were obtained using filters for both CY3 (A and D) and FITC (B and E). The lower panels C and F represent composite images of A and B, and D and E, respectively. Scale bars, 25 μ m.

lysosomes. It is important to note that the cells became more confluent over the 48-hour period which was associated with a proportional increase in numbers of positive transfectants. Also the cells did not appear as spread out at 6-hours compared with their appearance at 48-hours. However, this did not have any affect on the localisation results of p53 and CD63.

In addition, HeLa cells were transfected with the construct pSecTagA.p53 encoding p53 alone in the absence of the DM β signal peptide. This construct served as a control in the localisation studies of p53-DM β . p53, expressed from pSecTagA in positively transfected HeLa cells, was expected to be secreted from the cells by virtue of the LS appended to its N-terminus. The fluorescence pattern of p53, 48-hours after transfection (Figure 3.18 Panel B), was located prominently in the perinuclear region but became more punctate in the cell periphery unlike the more diffuse pattern observed in cells transfected with pSecTagA.p53-DM β . Punctate vesicular staining was observed for antibodies directed to CD63 (Figure 3.18, Panel A). The composite images (Figure 3.18, Panel C) were remarkably similar to those obtained of cells transfected with pSecTagA.p53-DM β . Co-localisation areas which appeared yellow were located in the perinuclear ring. However, this was an unusual observation as p53 alone does not contain the YTPL residue and thus p53 in theory should not be located to the lysosomes. A similar pattern of staining for p53 and CD63 was also observed in cells treated with leupeptin (Figure 3.18, Panels D,E and F).

A time course experiment was performed, as before, to determine the exact location of p53 prior to its steady state accumulation within the cell at 48-hours. HeLa cells transfected with the construct pSecTagA.p53 and grown on coverslips, were removed from the medium at 6, 12, 24 and 48-hour time points. They were subsequently treated with leupeptin for 4-hours or left untreated, fixed, permeabilised and co-labelled with antibodies to detect p53 and CD63 as described in chapter two. For optimal dilutions of antibodies refer to Table 3.1.

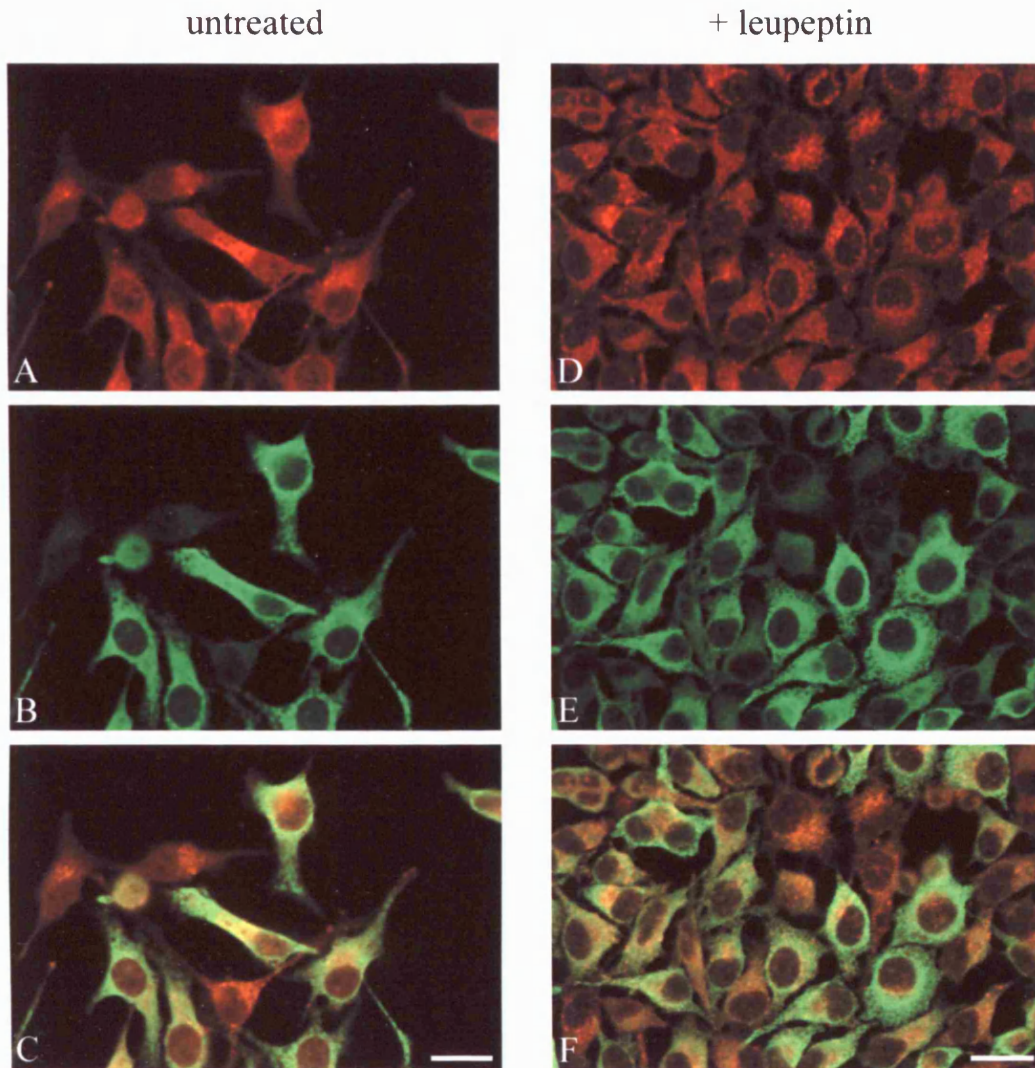


Figure 3.18 Immunofluorescence analysis of the intracellular localisation of p53 and CD63 in HeLa cells 48h after transient transfection with the construct pSecTagA.p53. Cells were transiently transfected and were treated with 1mg/ml leupeptin for the final 4h (D,E,F) or left untreated (A,B,C). Cells were fixed, permeabilised and co-labelled with a rabbit anti-human p53 polyclonal Ab and a mouse anti-human CD63 mAb. p53 and CD63 were detected by secondary incubation with an anti-rabbit-FITC conjugated mAb (green label) and an anti-mouse-CY3 conjugated mAb (red label), respectively. Cells were examined by CLSM and digital images of identical fields were obtained using filters for both CY3 (A and D) and FITC (B and E). The lower panels C and F represent composite images of A and B, and D and E, respectively. Scale bars, 25 μ m.

At 6-hours, the fluorescent pattern was similar to the pattern observed in cells, positively transfected with pSecTagA.p53-DM β . The fluorescent labelling for p53 was located prominently in the perinuclear region with additional diffuse fluorescence located in the cell periphery (Figure 3.19, Panel B). This was also observed in cells at 12-hours (Figure 3.20, Panel B). However, at 24-hours (Figure 3.21, Panel B) the fluorescent staining in the cell periphery appeared to be more punctate which is similar to the observations made in cells at 48-hours (Figure 3.18, Panel B). The fluorescence also remained more prominent in the perinuclear region. The fluorescent patterns for p53 observed at each time point were similar in leupeptin-treated cells (Panels E in Figures 3.18, 3.19, 3.20 and 3.21). The fluorescent patterns of CD63 obtained at each time point in both untreated and leupeptin-treated cells revealed distinct punctate vesicular staining (Panels A and D in Figures 3.18, 3.19, 3.20 and 3.21). Composite images obtained at 24 and 48-hours only revealed areas of co-localisation of p53 with CD63 in the perinuclear region (Panels C and F in Figures 3.21 and 3.18). The punctate staining for p53 observed in the cell periphery did not co-localise with punctate staining for CD63.

HeLa cells transfected with pSecTagA alone, treated with (data not shown) or without leupeptin, showed distinct punctate vesicular staining for CD63 (Figure 3.22, Panel D) and no fluorescence for p53 (Figure 3.22, Panel E). The composite image (Figure 3.22, Panel F), therefore, did not reveal any areas of co-localisation. Similarly, fluorescence for p53 was not observed in untransfected HeLa cells (data not shown), which had been untreated or treated with leupeptin. However, the distinct punctate vesicular staining for CD63 was present (data not shown).

All immunofluorescence experiments described in this section were performed at least three times and the observations found to be reproducible.

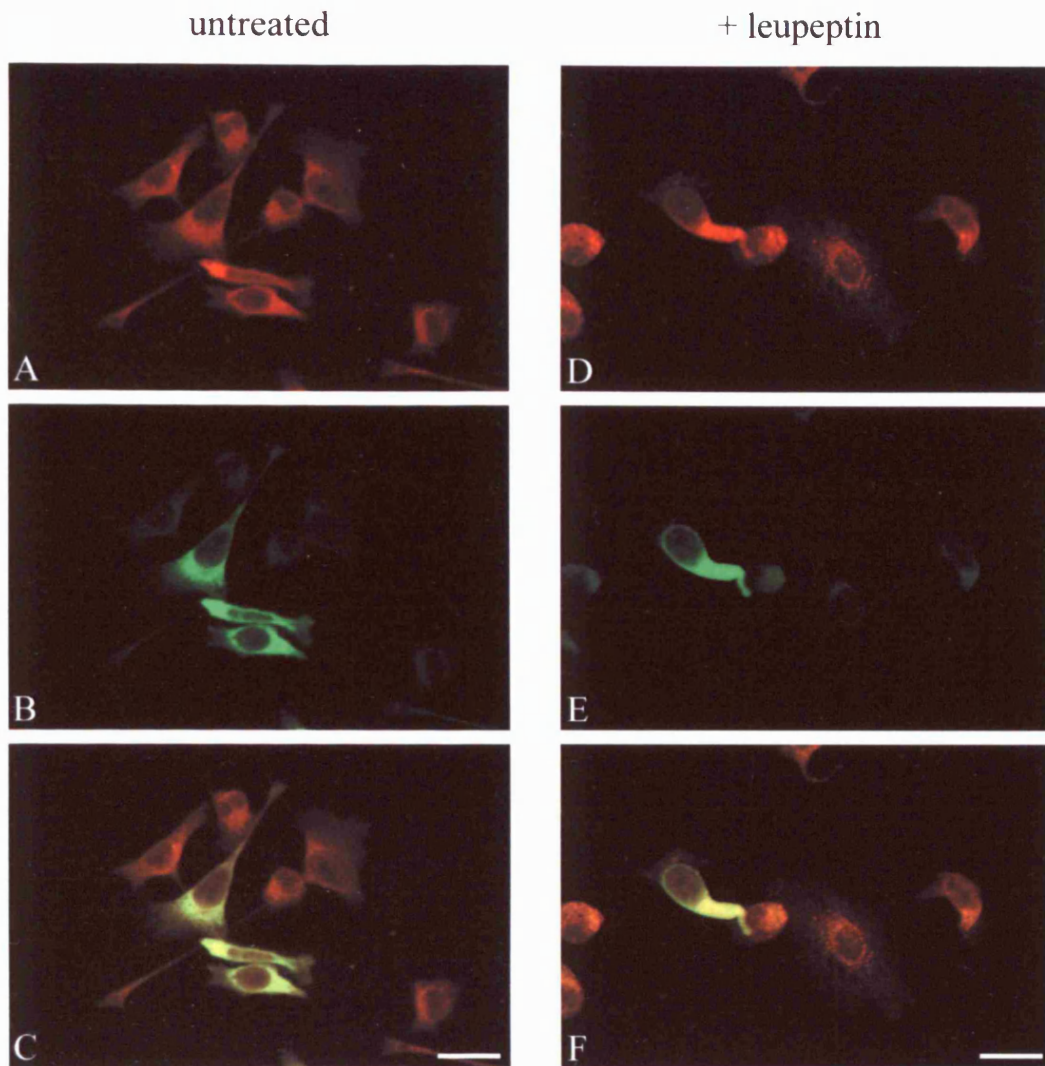


Figure 3.19 Immunofluorescence analysis of the intracellular localisation of p53 and CD63 in HeLa cells 6h after transient transfection with the construct pSecTagA.p53. Cells were transiently transfected and were treated with 1mg/ml leupeptin for the final 4h (D,E,F) or left untreated (A,B,C). Cells were fixed, permeabilised and co-labelled with a rabbit anti-human p53 polyclonal Ab and a mouse anti-human CD63 mAb. p53 and CD63 were detected by secondary incubation with an anti-rabbit-FITC conjugated mAb (green label) and an anti-mouse-CY3 conjugated mAb (red label), respectively. Cells were examined by CLSM and digital images of identical fields were obtained using filters for both CY3 (A and D) and FITC (B and E). The lower panels C and F represent composite images of A and B, and D and E, respectively. Scale bars, 25µm.

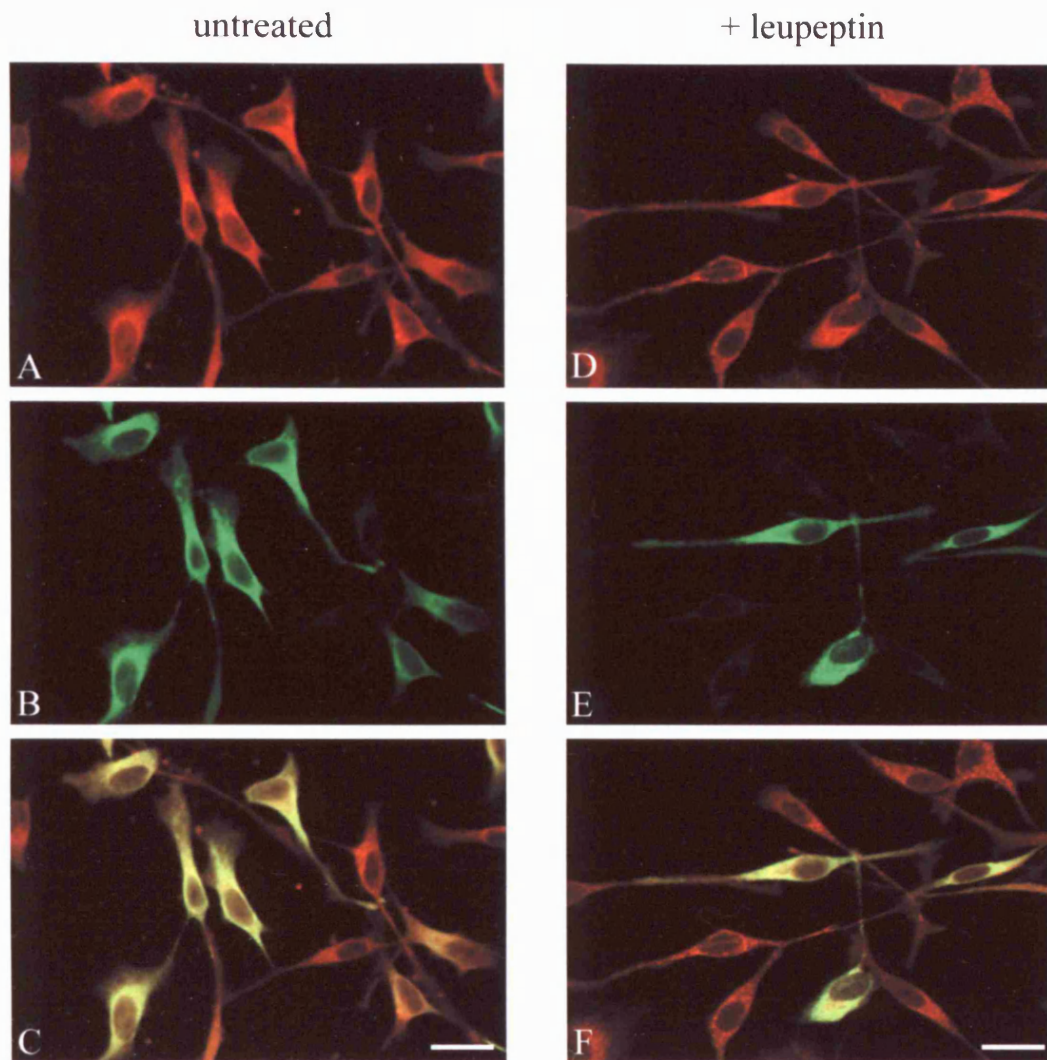


Figure 3.20 Immunofluorescence analysis of the intracellular localisation of p53 and CD63 in HeLa cells 12h after transient transfection with the construct pSecTagA.p53. Cells were transiently transfected and were treated with 1mg/ml leupeptin for the final 4h (D,E,F) or left untreated (A,B,C). Cells were fixed, permeabilised and co-labelled with a rabbit anti-human p53 polyclonal Ab and a mouse anti-human CD63 mAb. p53 and CD63 were detected by secondary incubation with an anti-rabbit-FITC conjugated mAb (green label) and an anti-mouse-CY3 conjugated mAb (red label), respectively. Cells were examined by CLSM and digital images of identical fields were obtained using filters for both CY3 (A and D) and FITC (B and E). The lower panels C and F represent composite images of A and B, and D and E, respectively. Scale bars, 25 μ m.

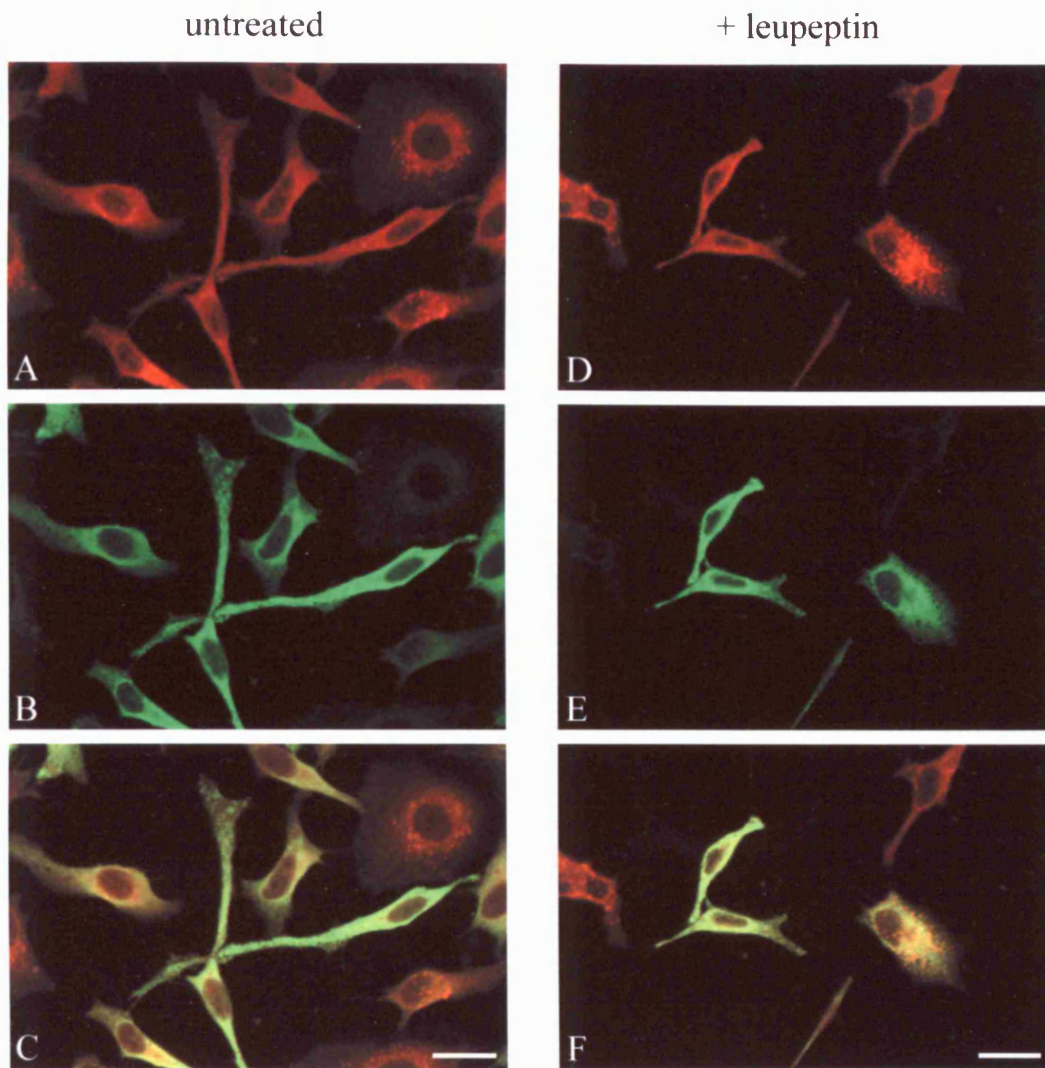


Figure 3.21 Immunofluorescence analysis of the intracellular localisation of p53 and CD63 in HeLa cells 24h after transient transfection with the construct pSecTagA.p53. Cells were transiently transfected and were treated with 1mg/ml leupeptin for the final 4h (D,E,F) or left untreated (A,B,C). Cells were fixed, permeabilised and co-labelled with a rabbit anti-human p53 polyclonal Ab and a mouse anti-human CD63 mAb. p53 and CD63 were detected by secondary incubation with an anti-rabbit-FITC conjugated mAb (green label) and an anti-mouse-CY3 conjugated mAb (red label), respectively. Cells were examined by CLSM and digital images of identical fields were obtained using filters for both CY3 (A and D) and FITC (B and E). The lower panels C and F represent composite images of A and B, and D and E, respectively. Scale bars, 25 μ m.

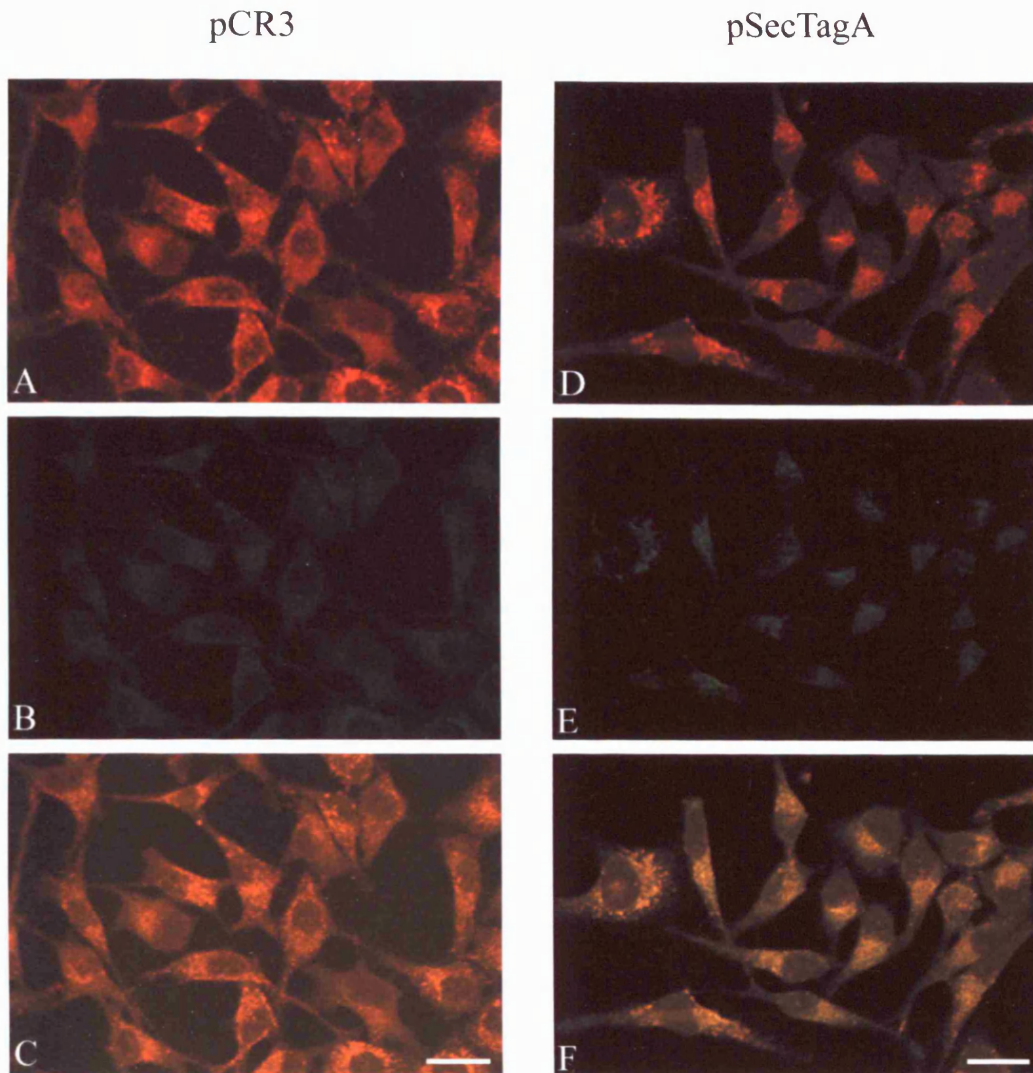


Figure 3.22 Immunofluorescence analysis of the intracellular localisation of p53 and CD63 in HeLa cells transiently transfected with the vectors pCR3 and pSecTagA. Transfected cells were processed for immunofluorescence microscopy using the primary antibodies rabbit anti-human p53 and mouse anti-human CD63 and the secondary antibodies anti-rabbit-FITC (green label) and anti-mouse-CY3 (red label), respectively. The cells were examined by CLSM and digital images of identical fields were obtained using filters for both CY3 (A and D) and FITC (B and E). The lower panels C and F represent composite images of A and B, and D and E, respectively. These transfectants served as negative controls for p53 expression in HeLa cells transfected with constructs encoding p53. Scale bars, 25 μ m.

3.3.8 Construction of pSecTagA.p53-TM

The entire cDNA p53 sequence and the cDNA sequence of the DM β transmembrane region plus a small region of the cytoplasmic tail upstream of the signal motif was amplified by PCR using the primers and conditions described. The resulting 1293bp PCR product was cloned into the TA-site of pCR2.1 and subsequently released by sequential restriction digestion using the enzymes *Sfi*I and *Eco*RI. This fragment was subcloned into the *Sfi*I and *Eco*RI site of the previously digested eukaryotic expression vector pSecTagA. Restriction analysis identified positive clones and cycle sequencing confirmed that the cloned p53 cDNA possessed three base mutations as before which were located in the 5' terminus region of p53. The remaining sequence was identical to that of the p53-DM β insert present in pCR3.p53-DM β apart from the absence of the signal motif sequence and the 3' terminus cytoplasmic tail sequence which had been omitted. Sequencing analysis also confirmed that the insert was in frame with the LS which was located 15bp upstream. The resulting construct designated pSecTagA.p53-TM, encoded a chimeric protein LS-p53-TM, illustrated in Figure 3.23, and was used to transfect HeLa cells to determine the localisation of p53-TM by cytofluorimetry and immunofluorescence microscopy. The amino acid sequence of the truncated DM β region appended to the carboxyl terminus of p53 is illustrated in Figure 3.24.

3.3.9 Cell surface expression of p53 in transfected HeLa cells.

It is evident from the results obtained in the intracellular localisation studies of p53-DM β and p53 expressed from the constructs, pCR3 and pSecTagA, that there is great difficulty in determining whether p53-DM β has been targeted to the lysosomes due to the accumulation of the overexpressed proteins in HeLa cells. Marks *et al.* (1995) have shown that accumulation at the cell surface of a chimeric protein termed T-T-Mb in which the cytoplasmic tail of murine DM β was appended to the luminal and transmembrane domains of a cell surface protein, Tac, was exacerbated by overexpression in transiently HeLa and COS-1 cells. To find out if similar missorting of the protein p53-DM β had occurred in HeLa cells transiently transfected with pSecTagA.p53-DM β , experiments were performed which analysed cell surface

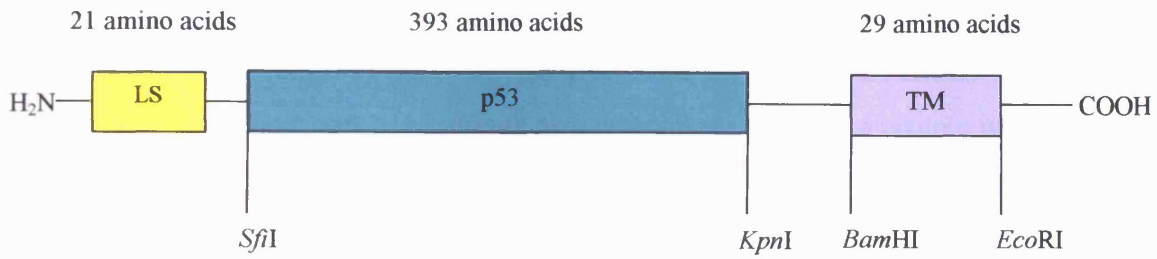


Figure 3.23 Schematic diagram of the chimeric protein LS-p53-TM expressed from the construct pSecTAGA.p53-TM in transiently transfected HeLa cells.

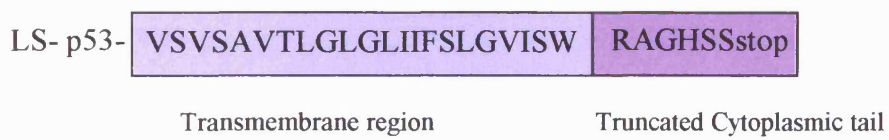


Figure 3.24 Amino-acid sequence of the transmembrane region and truncated cytoplasmic tail of DMβ present in the hybrid LS-p53-TM molecule

expression of p53, 48-hours after transfection. As p53 is not normally expressed at the cell surface as a membrane protein it was necessary to design a construct which enabled p53 when expressed to be associated with the plasma membrane, thus acting as a positive control in these experiments. A construct, termed pSecTagA.p53-TM was engineered (see section 3.3.8 and Figures 3.22 and 3.23) which contained the chimeric DNA template encoding the transmembrane region plus the truncated cytoplasmic tail of the HLA-DM β protein fused to p53 at the carboxyl-terminus. Importantly this construct lacked the YTPL signal motif thus allowing p53 to follow the constitutive secretory pathway by virtue of its LS fused at its amino-terminus and associate with the plasma membrane as a type I transmembrane protein with the short cytoplasmic tail orientated within the cytosol and p53 situated at the cell surface.

HeLa cells were transiently transfected with the constructs pSecTagA.p53-TM, pSecTagA.p53-DM β and pSecTagA.p53 by electroporation. A mock transfection was also performed using the vector pSecTagA alone which acted as a negative control in the analysis of cell surface expression of p53. Electroporated cells were transferred to either T-80 flasks or petri dishes containing DMEM + 10% FCS and 1% gelatin treated coverslips. After 48-hours, the cells were examined for cell surface expression of p53 either by cytofluorimetry or immunofluorescence microscopy. All experiments described below included negative controls for p53 labelling in which the cells were also labelled with the secondary antibody alone to ensure that non-specific binding of this antibody had not occurred.

For cytofluorimetric analysis, cells were processed for indirect labelling with antibodies to detect p53 as described in chapter two. Initially the rabbit anti-human p53 primary polyclonal antibody was diluted 1:200 and 1:500 and the anti-rabbit secondary antibody conjugated with FITC was diluted 1:200. The results revealed that surface expression of p53 could not be detected on cells transfected with the pSecTagA.p53-TM and pSecTagA.p53DM β constructs (data not shown). The results were similar for cells transfected with pSecTagA.p53. Also there was no detectable p53 found on the negative controls of cells transfected with pSecTagA alone and untransfected cells (data not shown). The experiment was repeated using increased concentrations of the primary (1:50 dilution) and secondary antibodies (1:20 dilution).

Again the results revealed that there was no detectable p53 found on any of the transfectants and negative controls (data not shown). This may be attributed to ineffective labelling by the primary and secondary antibodies which have not been validated for cytofluorimetry and therefore may not function efficiently in this procedure. This phenomenon implies that if there are cells expressing p53 at the cell surface they have not been detected successfully.

To further analyse surface expression of p53, immunofluorescence microscopy (method I) was adopted as an alternative method of analysis (refer to section 2.4.2). The primary and secondary antibodies used for p53 detection have been validated for this application and have been shown to work efficiently in earlier intra-cellular localisation studies of p53 described in this chapter. After 48-hours, the transfected cells were fixed followed by indirect labelling with antibodies to detect p53 and analysed by CLSM as described in section 2.4.2. The primary and secondary antibody were diluted 1:1000 and 1:200, respectively. The confocal images of HeLa cells transfected with pSecTagA.p53-TM revealed that there was some evidence of cell surface staining of p53 in 10-20% of the transfectants. A z-series was also collected at 1.0 μ m intervals through fluorescent cells to ensure the staining pattern was indicative of surface staining in which fluorescence is located at the apex of the cells above the nuclei in the uppermost planes and at the cell surface in the periphery in the lower planes. This was confirmed by the confocal images obtained in the z-series (see Figure 3.25). Panels 1-3, which represent planes at the apex of the cells above the nuclei, show fluorescence in this region. Panels 4-6 indicate that the fluorescence forms a ring in the perinuclear regions 4-6 μ m beneath the apex. Panels 7-10, which represent planes near the surface of the cells in the periphery, indicate that the fluorescence becomes more punctate in this region with the fluorescence fading rapidly above the nuclei, whereas there is no fluorescence observed at the base of the cells in the lower planes (panels 11+12). In addition panels 4-9 reveal possible internal vesicular structures situated in the perinuclear region which may represent secretory vesicles in transit from the ER to the plasma membrane. The projected confocal image (panel 13) illustrates that p53 cell surface staining was evident in these cells. The presence of a prominent fluorescent ring in the perinuclear region

may be due to the accumulation of p53 in the ER and implies that the cells have become slightly permeabilised allowing the occurrence of some intra-cellular staining.

The confocal images of HeLa cells transfected with pSecTagA.p53-DM β were remarkably different and did not reveal a typical staining pattern indicative of surface staining. The fluorescence appeared to be situated in a prominent area above the nucleus with the remainder of the cell completely devoid of fluorescence. A z series was collected at 1 μ m intervals through fluorescent cells to determine whether the fluorescence of p53 was located at the surface of the cell (see Figure 3.25). Panels 1-3 which represent horizontal planes near the apex of the cell above the nuclei, illustrated that fluorescence was located above the nuclei which may be surface staining. Panels 4-6, which represent horizontal planes approximately 4-6 μ m beneath the cell surface at the apex, illustrated that the fluorescence is located in the perinuclear region as a distinct ring, which may indicate ER and nuclear envelope staining, with the staining above the nuclei becoming more diffuse. Surprisingly, panels 7-8, which represent planes approximately 7-8 μ m beneath the surface at the apex of the cell, revealed possible fluorescent nuclear staining which appeared patchy. Finally, panels 9-12 showed the fluorescence becoming increasingly faint towards the base of the cells. Although p53 may be located at the cell surface and also in the nuclear envelope, the unusual pattern of staining observed in the plane 7-8 μ m beneath the surface of the cell, possibly within the nuclei (Panels 7 and 8) was not indicative of surface staining and was not consistent with the results obtained in previous intra-cellular localisation studies of p53 in which nuclei were devoid of fluorescence. This staining pattern was only observed in 10% of the cells whereas the remaining cells showed very low levels of background fluorescence comparable with the levels observed in negative controls in which the cells were incubated with the secondary antibody only. There is a possibility that this unusual nuclear staining pattern may be caused by an artefact. The experiment was repeated and similar observations were obtained.

HeLa cells transfected with pSecTagA.p53 were also examined for cell surface p53 expression. The confocal images revealed that p53 was located in numerous internal structures in the perinuclear region which may represent secretory vesicles in transit from the ER and Golgi body to the plasma membrane and into the cell exterior(Figure

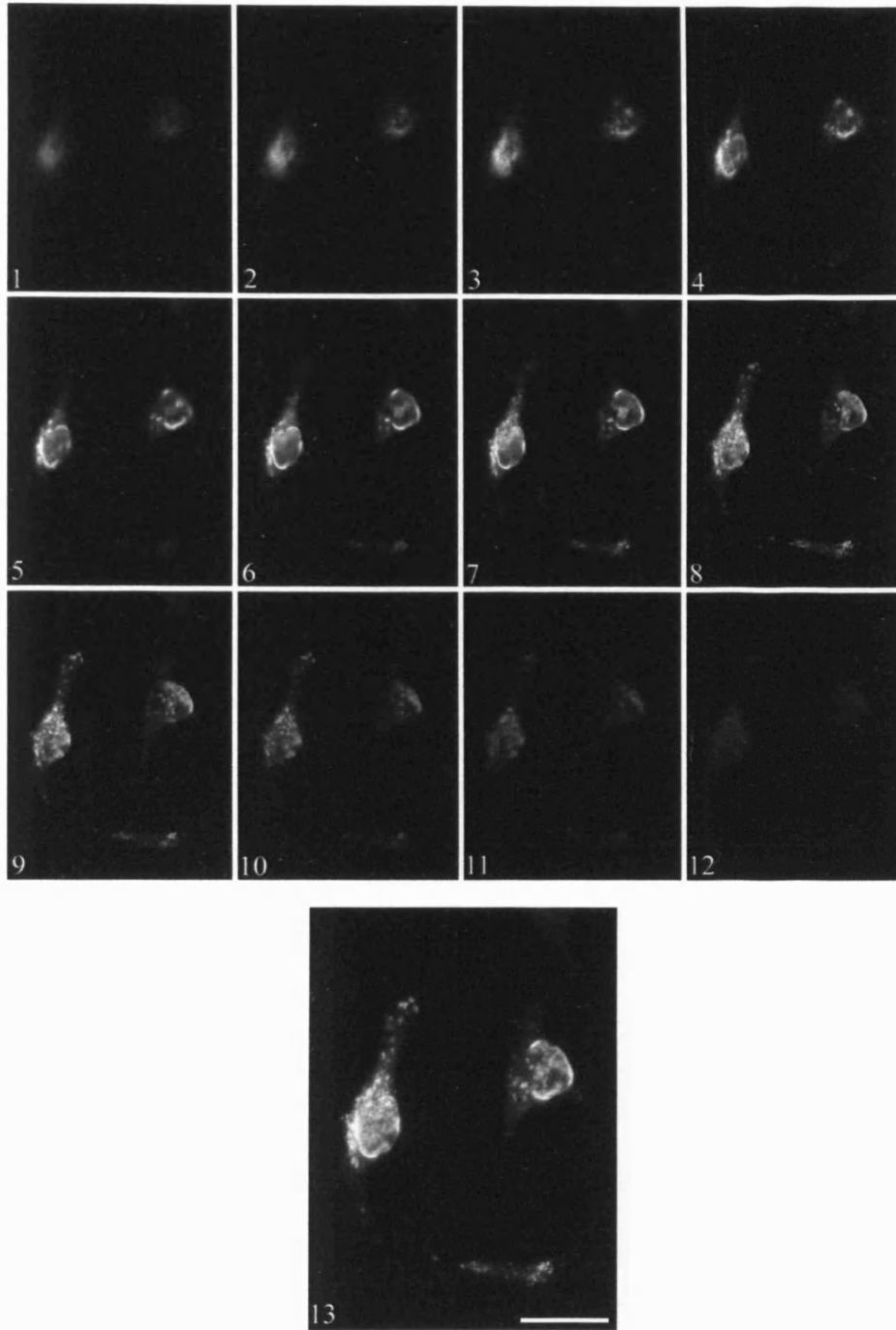


Figure 3.25 Immunofluorescence analysis of the cell surface expression of p53 in HeLa cells 48h after transient transfection with the construct pSecTagA.p53-TM. Transfected cells were fixed and labelled with a rabbit anti-human p53 polyclonal Ab. p53 was detected by secondary incubation with an anti-rabbit-FITC conjugated mAb. Cells were examined by CLSM and the digital confocal images recorded. Panels 1-12 represent a series of optical sections (z-series) of an identical field collected using the filter for FITC, at $1.0\mu\text{M}$ intervals from the apex of the cell (1) through to the base (12). Panel 13 represents a projection of the images obtained in the z-series. Scale bar, $25\mu\text{m}$.

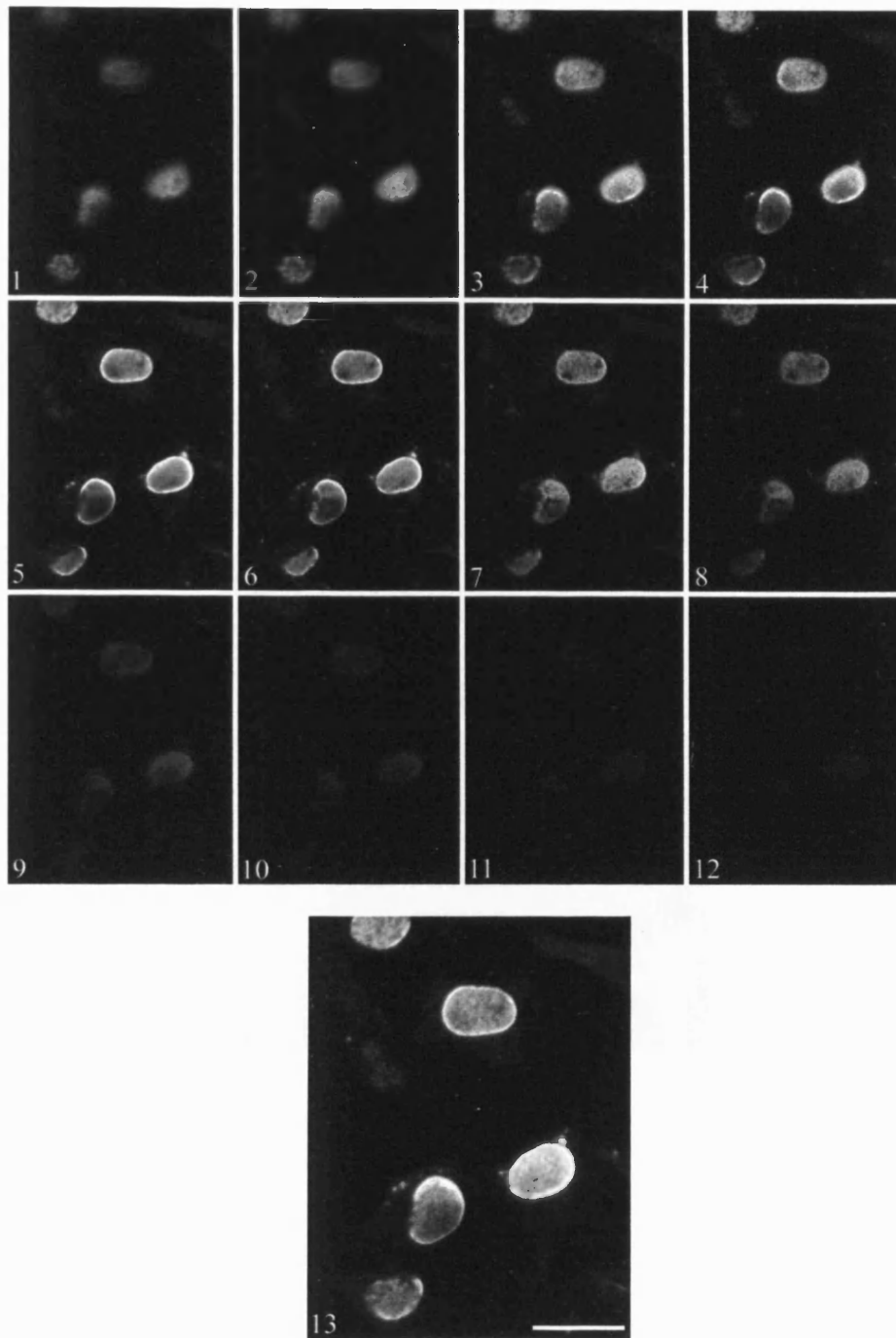


Figure 3.26 Immunofluorescence analysis of the cell surface expression of p53 in HeLa cells 48h after transient transfection with the construct pSecTagA.p53-DM β . Transfected cells were fixed and labelled with a rabbit anti-human p53 polyclonal Ab. p53 was detected by secondary incubation with an anti-rabbit-FITC conjugated mAb. Cells were examined by CLSM and digital confocal images recorded. Panels 1-12 represent a series of optical sections (z-series) of an identical field collected using the filter for FITC, at 1.0 μ M intervals from the apex of the cell (1) through to the base (12). Panel 13 represents a projection of the images obtained in the z-series. Scale bar, 25 μ m.

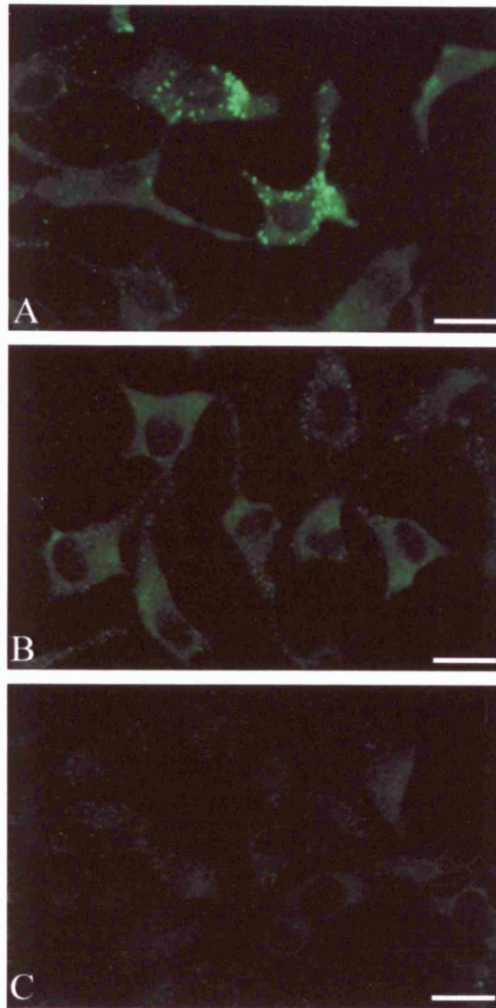


Figure 3.27 Immunofluorescence analysis of cell surface expression of p53 in HeLa cells 48h after transient transfection with the vectors pSecTagA.p53 (A) and pSecTagA (B) and also untransfected cells (C). Transfected and untransfected cells were grown on coverslips for 48h and were subsequently fixed and labelled with a rabbit anti-human p53 polyclonal Ab. p53 was detected by secondary incubation with an anti-rabbit-FITC conjugated mAb (green label). Cells were examined by CLSM and digital confocal images were recorded. Scale bar, 25 μ m.

3.27, Panel A). However, there was no prominent fluorescent ring present in the perinuclear region in comparison with cells transfected with pSecTagA.p53-TM and pSecTagA.p53-DM β . HeLa cells transfected with pSecTagA alone (Figure 3.27, Panel B) and untransfected cells (Figure 3.27, Panel C) were also analysed for the cell surface expression of p53. The confocal images of these negative controls revealed that there was no fluorescent staining of p53 at the cell surface or internally. The background staining in cells transfected with vector alone appeared to be higher compared with untransfected cells but was comparable with the negative controls in which cells were labelled with the secondary antibody only (data not shown).

Although the results obtained using immunofluorescence microscopy illustrated possible surface staining of p53 in cells expressing p53-TM and p53-DM β , they also illustrated possible intracellular staining just beneath the surface of these positive transfectants which was also observed in cells transfected with pSecTagA.p53, suggesting that the cells have become osmotically stressed thus causing slight permeabilisation and allowing antibody entry. Additional intracellular staining may lead to the inaccurate interpretation of data for cell surface analysis. To avoid the possibility of slight permeabilisation of the cells, a gentler approach to analyse cell surface expression of p53 by immunofluorescence microscopy (method II) was adopted (see section 2.4.3.). This method aimed to reduce the osmotic stresses of cells by the use of a less stringent buffer and indirectly labelling cells with antibodies to detect p53 prior to their fixation. After 48-hours, the cells were labelled with the primary rabbit anti-human p53 antibody (diluted either 1:500 or 1:1000) followed by the secondary anti-rabbit antibody conjugated with FITC (diluted 1:200). The fluorescent secondary antibody was visualised using immunofluorescence microscopy and the cells were viewed and photographed at x 40 magnification. The photomicrographs revealed that the cells transfected with pSecTagA.p53-TM, pSecTagA.p53-DM β and pSecTagA.p53 did not show any fluorescence for p53 at the cell surface or internally (data not shown). The photomicrographs of cells transfected with pSecTagA alone and untransfected cells showed similar results. This experiment was repeated and the observations found to be reproducible.

In addition HeLa cells transfected with pSecTagA.p53-TM were analysed by intracellular immunofluorescence microscopy to determine the intracellular location of p53-TM. The cells were transfected and 48-hours later were processed for intracellular immunofluorescence microscopy as before and examined by CLSM. The confocal images revealed that the fluorescent labelling for p53 in positive transfectants was particularly prominent in the perinuclear region, becoming more diffuse in the cell periphery (Figure 3.28, Panel B). The nucleus, however, was completely devoid of fluorescence. The distinct punctate vesicular staining for CD63 was present (Figure 3.28, Panel A). Surprisingly the composite image revealed a few yellow areas in the perinuclear region due to the combination of the green (FITC) and the red signal (CY3), which possibly indicate areas in which p53 has co-localised with CD63 (Figure 3.27, Panel C). These intracellular fluorescent patterns suggested that p53 was located in the ER and were similar to those obtained for HeLa cells transfected with pSecTagA.p53-DM β and pSecTagA.p53.

3.3.10 Secretion of p53 by transfected HeLa Cells.

In earlier localisation experiments of p53-DM β , p53 and p53-TM expressed from pSecTagA in transfected HeLa cells (see sections 3.3.7 and 3.3.9), similar intracellular staining patterns of p53 were observed with high levels of fluorescent staining. Thus, it was necessary to find out if p53 was secreted from cells transfected with pSecTagA.p53, as expected, in comparison with p53-DM β and p53-TM expressed from pSecTagA, which in theory should be targeted to the lysosomes and membrane respectively, and not secreted from the cell. In order to detect the presence of p53 in cell secretions, a Western blot analysis of p53 in supernatants and corresponding lysates of HeLa cells transiently transfected with pSecTagB.p53-HisTag, pSecTagA.p53, pSecTagA.p53-DM β , pSecTagA.p53-TM and pSecTagA was carried out. The construct pSecTagB.p53-HisTag had previously been made (data not shown) with a view to synthesising recombinant p53 in preparation for future experiments related to this study. This construct was similar to pSecTagA.p53 as it also expressed p53 fused to the murine Ig k-chain leader sequence at the amino-terminus to allow for secretion and lacked the DM β signal peptide at the carboxyl-terminus. However, it differed slightly, as p53 was subcloned 52bp further

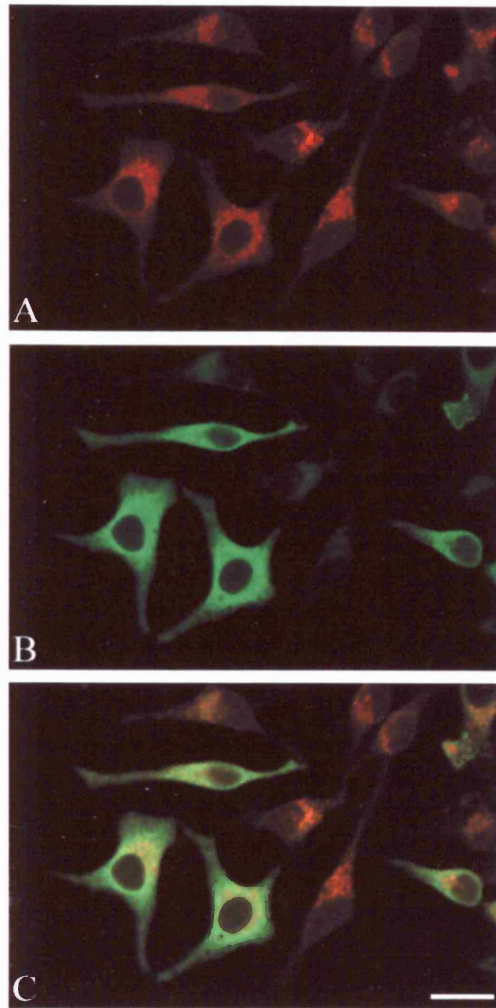


Figure 3.28 Immunofluorescence analysis of the intracellular localisation of p53 and CD63 in HeLa cells 48h after transient transfection with the construct pSecTagA.p53-TM. After 48h transfectants were fixed, permeabilised and co-labelled with a rabbit anti-human p53 polyclonal Ab and a mouse anti-human CD63 mAb. p53 and CD63 were detected by secondary incubation with an anti-rabbit-FITC conjugated mAb (green label) and an anti-mouse-CY3 conjugated mAb (red label), respectively. Cells were examined by CLSM and digital images of identical fields were obtained using filters for both CY3 (A) and FITC (B). The lower panel C represents a composite image of A and B. Scale bar, 25 μ m.

downstream from LS in the *Bam*HI-*Xba*I site and the stop codon was situated immediately after the polyhistidine tag sequence. Consequently p53 expressed from this vector was fused at the C-terminus to a peptide containing the *myc* epitope and six tandem histidine residues for detection and purification. This vector acted as a positive control in the detection of p53 in secretions from HeLa cells 48-hours after transfection with p53 constructs. In addition, Western blot analysis of p53 was performed on supernatants and corresponding lysates of HeLa cells previously transfected with pCR3.p53-DM β , pCR3.p53 and pCR3.

HeLa cells (2×10^6) were transiently transfected with the pSecTagA and pCR3 constructs encoding p53 mentioned above, and 6-well plates were seeded with 3×10^5 transfectants/well in 2mls of OPTI-MEM media. After 48-hours, supernatants were carefully removed from the wells, filtered with a 0.22 μ M filter and concentrated. The monolayer cells in each well were subsequently lysed by the addition of the sample buffer. Total supernatant concentrates were loaded onto the gel (10-30 μ l) whereas 0.25 (15 μ l) and 0.5 (30 μ L) of the whole cell lysates for pSecTagA and pCR3 transfectants, respectively, were loaded. The proteins were fractionated on a 10% polyacrylamide-SDS gel under reducing conditions, transferred to a nitrocellulose membrane and probed with the polyclonal p53 antibody diluted 1:1000. Proteins were detected by incubating with a horse radish peroxidase secondary antibody diluted 1:2000 and visualised by chemiluminescence (Figures 3.29 and 3.30).

The immunoblot of p53 in supernatants collected from transfected HeLa cells (Figure 3.29) indicated that p53 was only present in cell secretions from HeLa cells transfected with the constructs pSecTagA.p53 (Lane 3) and pSecTagB.p53-HisTag (Lane 2) as expected. p53 secreted from HeLa cells transfected with pSecTagB.p53-HisTag had a higher MW (61 kDa) than p53 secreted from cells transfected with pSecTagA.p53, which had MW of 54 kDa. This was due to the *myc* epitope and polyhistidine sequence fused at the carboxyl terminus of p53 in pSecTagB.p53-HisTag. Interestingly higher levels of p53 were secreted from cells transfected with pSecTagA.p53-HisTag compared with cells transfected with pSecTagA.p53. In contrast, p53 was not detected in supernatants collected from HeLa cells transfected with the remaining pSecTagA and pCR3 constructs encoding p53 (lanes 4,5,7 and 8)

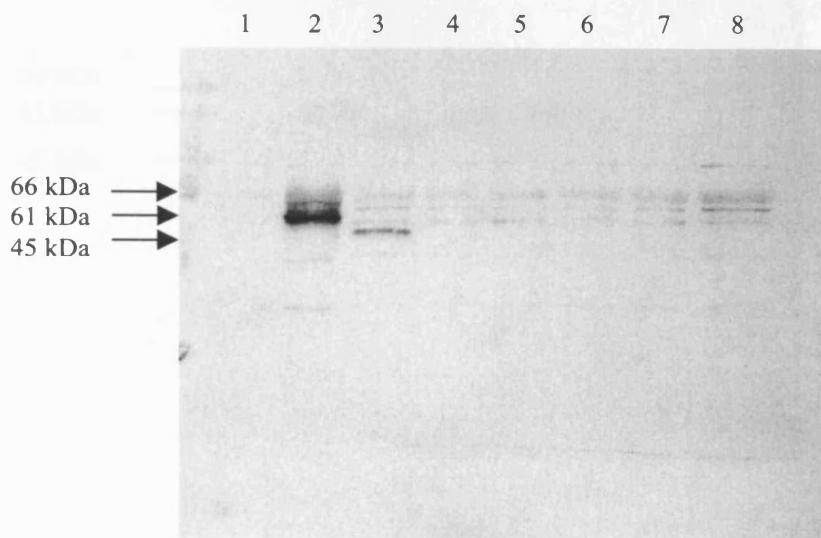


Figure 3.29 Western Blot analysis of p53 in supernatants from HeLa cells transfected with constructs encoding p53. Supernatants were concentrated and proteins were analysed on a 10% polyacrylamide-SDS gel under reducing conditions and transferred to a nitrocellulose membrane. The membrane was incubated with 1:1000 dilution of rabbit anti-human p53 polyclonal antibody followed by incubation with 1:2000 anti-rabbit horseradish peroxidase secondary antibody. Proteins were visualised by chemiluminescence. Lane (1) Control: Supernatant from cells transfected with pSecTagA. Lane (2) Supernatant from cells transfected with pSecTagB.p53-HisTag. Lane (3) Supernatant from cells transfected with pSecTagA.p53. Lane (4) Supernatant from cells transfected with pSecTagA.p53-TM. Lane (5) Supernatant from cells transfected with pSecTagA.p53-DM β . Lane (6) Control: Supernatant from cells transfected with pCR3. Lane (7) Supernatant from cells transfected with pCR3.p53. Lane (8) Supernatant from cells transfected with pCR3.p53-DM β .

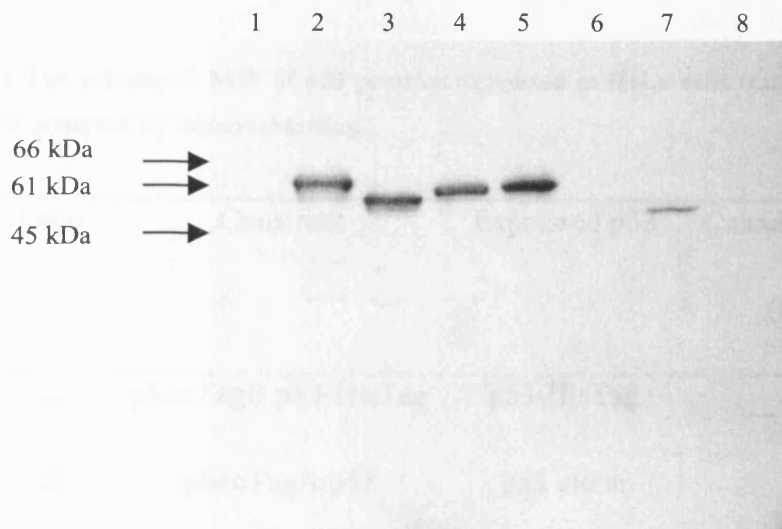


Figure 3.30 Western blot analysis of p53 expression in HeLa cells transfected with constructs encoding p53. HeLa cells were lysed, 48-hours after transient transfection, and proteins were analysed on a 10% polyacrylamide-SDS gel under reducing conditions and transferred to a nitrocellulose membrane. The membrane was incubated with 1:1000 dilution of rabbit anti-human p53 polyclonal antibody followed by incubation with 1:2000 anti-rabbit horseradish peroxidase secondary antibody. Proteins were visualised by chemiluminescence. Lane (1) Control: lysates of cells transfected with pSecTagA.neo. Lane (2) Lysates of cells transfected with pSecTagB.p53-HisTag. Lane (3) Lysates of cells transfected with pSecTagA.p53. Lane (4) Lysates of cells transfected with pSecTagA.p53-TM. Lane (5) Lysates of cells transfected with pSecTagA.p53-DM β . Lane (6) Lysates of cells transfected with pCR3.neo. Lane (7) Lysates of cells transfected with pCR3.p53. Lane (8) Lysates of cells transfected with pCR3.p53-DM β .

suggesting that p53 was not secreted from these cells and thus may have reached its expected intracellular destination. p53 was not detected in the negative controls (lanes 1 and 6), which were supernatants collected from HeLa cells transfected with pSecTagA and pCR3 alone. Cell secretions from untransfected HeLa cells were also analysed and did not contain p53 (data not shown).

Table 3.2 The calculated MW of p53 proteins expressed in HeLa cells transfected with various constructs analysed by immunoblotting.

Lane	Construct	Expressed p53	Calculated MW (kDa)
2	pSecTagB.p53-HisTag	p53-HisTag	61
3	pSecTagA.p53	p53 alone	54
4	pSecTagA.p53-TM	p53-TM	58
5	pSecTagA.p53-DM β	p53-DM β	60
7	pCR3.p53	p53 alone	51
8	pCR3.p53-DM β	p53-DM β	Non-detectable

The corresponding cell lysates were also analysed for p53 by immunoblotting. The immunoblot (Figure 3.30) showed that p53 was expressed at high levels by cells transfected with pSecTagA constructs encoding p53. The different MW of p53 proteins expressed by the cells due to the presence or absence of various amino-acids fused at the C-terminus of p53 are displayed in Table 3.2 and correspond to the MW of proteins detected on the immunoblot. Interestingly, the MW of p53 (54 kDa) expressed from pSecTagA was slightly higher than the MW of p53 (51 kDa)

expressed by pCR3. This may reflect possible glycosylation of p53 expressed from pSecTagA which has traversed the ER and Golgi body in contrast to p53 expressed from pCR3 which is located in the nuclei. However, the immunoblot revealed that the levels of p53 and p53-DM β expression from pCR3 constructs in transfected cells were low (Lane 7) and non-detectable (Lane 8), respectively. This is consistent with the very low transfection efficiencies of HeLa cells obtained previously with these constructs. Together these results confirmed that only a very small proportion of HeLa cells transfected with the pCR3 constructs express p53 and p53-DM β . p53 was not detected in the negative controls which were lysates of cells transfected with pSecTagA and pCR3 alone (Lanes 1 and 6). In addition, p53 was not present in lysates of untransfected HeLa cells (data not shown).

3.3.11 Assessment of apoptosis in HeLa cells following transfection with DNA constructs encoding p53.

Stabilisation and transient accumulation of wild-type transcriptionally active p53 in the nucleus leads to cell cycle arrest or apoptosis (reviewed in Levine, 1997). Thus, additional experiments were performed to assess apoptosis in HeLa cells 48-hours after transfection with the aforementioned constructs. The cells were stained with Annexin V-FITC and propidium iodide and analysed by cytofluorimetry as described in chapter two. Data are shown as cytograms with the log of Annexin V-FITC fluorescence displayed on the x-axis and the log of PI fluorescence on the y axis. Five thousand cells are displayed on each cytogram. Viable cells do not bind Annexin V-FITC and exclude propidium iodide and will be found in the lower left quadrant of the dot plot. Early apoptotic cells bind Annexin V-FITC but exclude propidium iodide and would be found in the lower right quadrant and finally necrotic or apoptotic cells in terminal stages would be found in the upper right quadrant.

The results demonstrated that none of the transfectants were exhibiting apoptosis above spontaneous levels (Figures 3.31 and 3.32). Although p53 encoded by the constructs, originally cloned from MCF-7 cells, is wild-type and transcriptionally active, none of the transfectants exhibited levels of apoptosis higher than spontaneous levels. However, the constructs have been designed to redirect p53 from the nuclei to

the lysosomal compartment, the membrane or allow p53 to be secreted from the cell and thus the transfectants would not exhibit p53-induced apoptosis. Surprisingly the cells transfected with pCR3.p53 also exhibited low levels of apoptosis. Cells transfected with this control construct were expected to express p53 at high levels in the nuclei which in theory would result in p53-induced apoptosis. However, the unexpected low levels are possibly a reflection of the low transfection efficiency of only 1-3% achieved in these cells as illustrated previously by intracellular immunofluorescence analysis of p53 expression and also by Western blot analysis of the cell lysates which showed low detectable levels of p53. Therefore, the low number of positive transfectants would not have caused a significant increase in the number of apoptotic cells which has been demonstrated in this experiment.

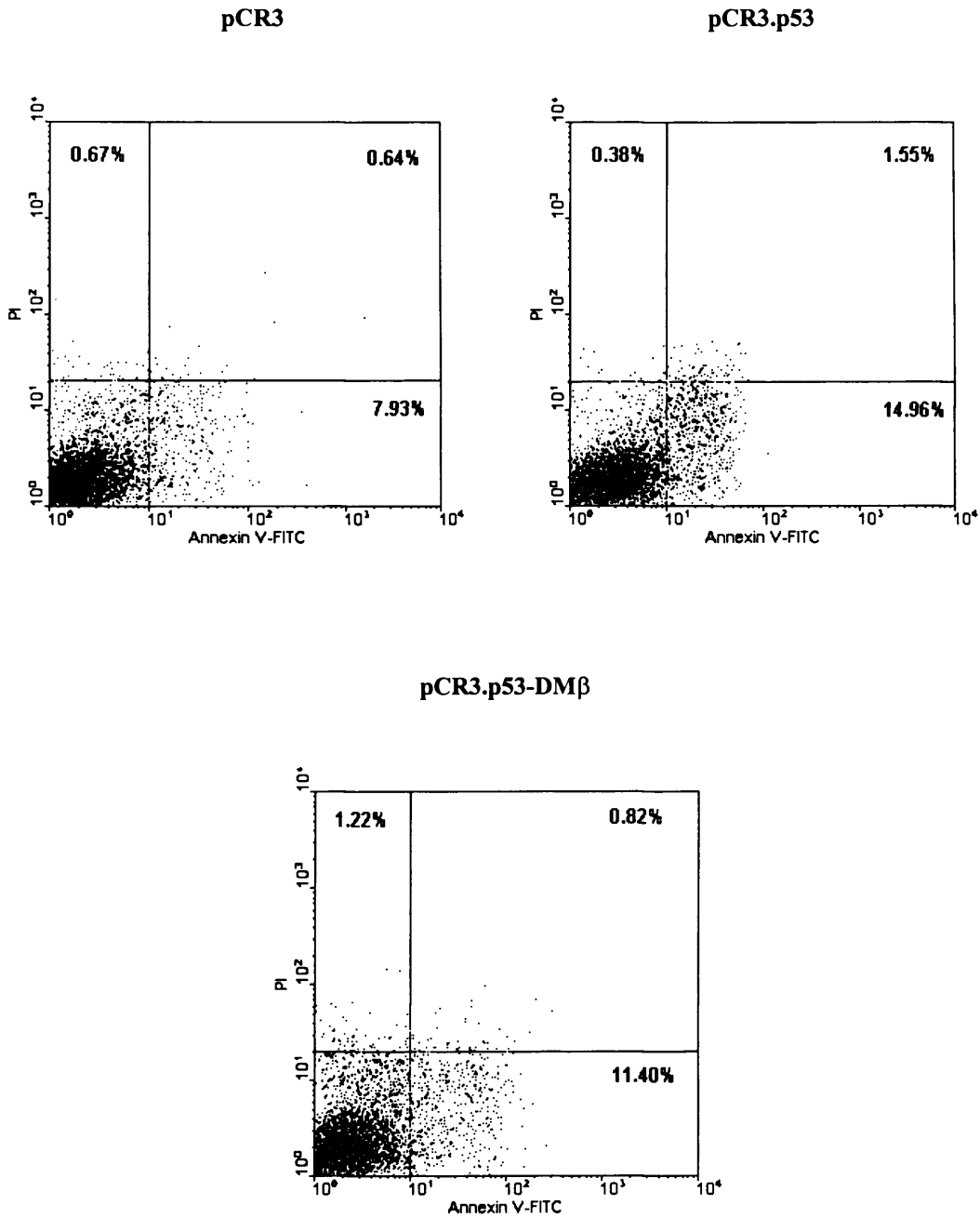


Figure 3.31 Assessment of apoptosis in HeLa cells transfected with pCR3, pCR3.p53 and pCR3.p53-DMβ after 48-hours. Cells were stained with annexin V-FITC and propidium iodide (PI) and analysed by cytofluorimetry.

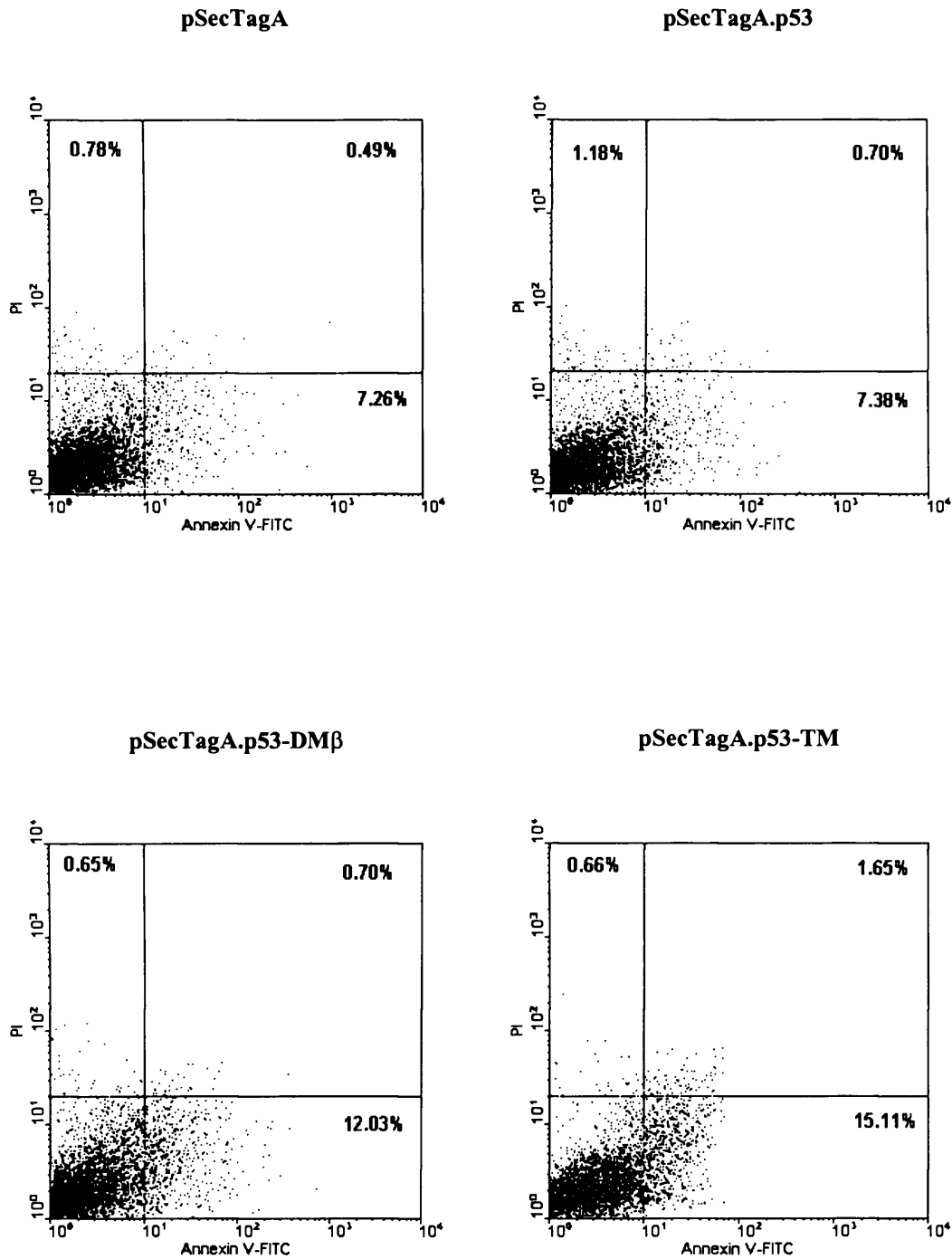


Figure 3.32 Assessment of apoptosis in HeLa cells transfected with pSecTagA, pSecTagA.p53, pSecTagA.p53-DMβ and pSecTagA.p53-TM after 48-hours. Cells were stained with annexin V-FITC and propidium iodide (PI) and analysed by cytofluorimetry.

3.4 Discussion

Initial experiments described in this chapter utilised the mammalian expression vector pCR3 to determine the location of p53-DM β in the absence of an amino-terminal signal sequence. Immunofluorescence analysis, however, revealed that only 1-3% of HeLa cells were positively transfected. Similarly, a low transfection efficiency was observed in HeLa cells transfected with the construct pCR3.p53. p53-DM β and p53 were located in the cytosol and nuclei, respectively, with the remaining cells completely devoid of fluorescence. The low number of cells expressing p53-DM β and p53 may reflect the fact that the human cervical carcinoma cell line, HeLa, contains viral genes from the oncogenic HPV type 18 which encodes the oncoproteins E6 and E7 (Yee *et al.*, 1985). There is evidence that the E6 proteins from this viral isotype bind p53 and stimulate its degradation. The E6-promoted degradation of p53 is ATP dependent and involves the ubiquitin-dependent protease system (Scheffner *et al.*, 1990; Werness *et al.*, 1990). Consequently, wild-type p53 normally expressed by HeLa cells is unable to stabilise and function as a tumour suppressor protein due to its inactivation by E6 which contributes to the immortalisation of these cells. This was confirmed by intracellular immunofluorescence and Western Blot analyses described in this chapter which were unable to detect p53 in untransfected HeLa cells and HeLa cells transfected with vector alone. Furthermore, assessment of apoptosis in cells transfected with pCR3.p53 in which p53 was expected to be expressed at high levels in the nuclei resulting in apoptosis, revealed that apoptosis was not induced in these cells suggesting that p53 had been inactivated or degraded. Although some cells were expressing p53 in the nuclei as indicated by immunofluorescence analysis, the levels of apoptosis were not detected due to such low numbers of positive cells. Thus, it can be concluded that p53-DM β and p53 expressed from the constructs pCR3.p53-DM β and pCR3.p53, respectively, in transfected HeLa cells have probably been degraded due to the presence of the viral oncoprotein E6. This was also confirmed by Western Blot analyses which revealed very low or non-detectable levels of p53-DM β and p53 in transfected cells. The small percentage of cells that are expressing p53-DM β and p53 have possibly escaped degradation due to their overexpression. Interestingly, Hamada *et al* (1996) demonstrated that the wild-type p53 gene transfected into HeLa cells via the recombinant adenoviral vector, AdCMV-p53, resulted in a high

proportion of the cells expressing high levels of p53 together with a significant decrease in the growth rate as detected by both cell count and [³H]thymidine incorporation assay. Thus, the adenoviral vector which contained the CMV promoter was capable of mediating high levels of p53 expression which apparently were sufficient to overcome the capabilities of the endogenous E6 to bind the protein. In this study, however, electroporation of cells with the pCR3 constructs, which also contained the potent CMV promoter, was incapable of overcoming the inactivation of E6 and consequently failed to yield high proportions of cells overexpressing p53.

More importantly, these initial experiments did not reveal co-localisation of p53-DM β with the endogenous lysosomal protein CD63, but instead revealed a possible cytosolic staining pattern in the small numbers of HeLa cells positively transfected with pCR3.p53-DM β , at 24 and 48-hours post transfection. The steady state accumulation of this chimeric protein in the cytosol is a reflection of the inability of p53-DM β to gain access to the ER and hence the lysosomal compartments due to the absence of an amino-terminus signal sequence. Lysosomal proteins, such as HLA-DM, CD63, and also ER, Golgi, membrane and secretory proteins, must first enter the ER via an ER-translocation process before they traffic to their respective destinations. The translation of these proteins is initiated on cytosolic ribosomes and the first protein sequence to emerge from the ribosome contains a short hydrophobic amino-terminal signal sequence (Rapaport *et al.* 1996). The nascent polypeptide chain is then recognised by a 54kDa protein complex called the signal recognition particle (SRP). The binding of cytosolic SRP to the ribosome-bound polypeptide targets the complex to the ER membrane, where the signal sequence is inserted into an aqueous translocation pore, or translocan. Protein synthesis on membrane-bound ribosomes continues and once completed the ribosome and SRP dissociate from the ER membrane. For soluble proteins and type I transmembrane proteins (which possess a C-terminal transmembrane domain), the signal sequence is cleaved off by a luminal signal peptidase (reviewed in Roche, 1999). In contrast, p53, is a nuclear protein and like cytosolic and mitochondrial proteins does not contain an amino-terminal signal sequence. These proteins are translated in the cytosol bound to free ribosomes and consequently do not translocate the ER. Therefore, the absence of the amino-terminal signal sequence in the chimeric protein p53-DM β expressed from the pCR3 construct

has prevented translocation across the ER membrane and subsequent trafficking to the lysosomal compartment via its YTPL peptide motif.

However, there is evidence that endogenous proteins can access the MHC class II pathway in APCs by three other mechanisms which are described in chapter one. The first mechanism may involve class II molecules becoming occupied with peptides in the ER which is referred to as class II molecules hijacking the class I pathway (Lechler *et al.* 1996). The second mechanism involves the binding of partially unfolded proteins to nascent MHC class II molecules in the ER (Anderson *et al.* 1993; Busch *et al.* 1996; Lechler *et al.* 1996). HeLa cells, however, do not normally express MHC class II molecules and thus the uncharacteristic binding of p53-DM β and MHC class II molecules in the ER would not have occurred in this system. Finally, a third mechanism which is more feasible involves cytosolic proteins entering lysosomes/MIICs by a process such as microautophagy or as a result of transport by cytosolic heat shock proteins. Microautophagy encompasses the internalisation of small portions of cytoplasm and limiting membrane by these compartments. In APCs the integrity of the internal vesicles can be destroyed by proteolysis resulting in cytosolic and membrane derived peptides being bound to class II molecules (Liou *et al.*, 1997). Thus, there is a possibility that p53-DM β which has accumulated to high levels in the cytosol, has entered the lysosomes via microautophagy or cytosolic heat shock proteins. This phenomenon may provide an explanation for the very few areas of co-localisation of p53-DM β with CD63. However, this is not a suitable mechanism of ensuring that the majority of p53-DM β expressed enters the lysosomal compartment. Alternatively, the areas where the green label has overlapped with the red label may not represent areas of co-localisation, but instead may represent areas where intense cytosolic staining of p53-DM β has overlapped with lysosomal staining.

Although the signal motif YTPL has not targeted p53-DM β to the lysosomes due to the absence of an amino-terminal signal sequence, it has prevented the expression of p53 in the nuclei as demonstrated by its accumulation in the cytosol with concomitant nuclear exclusion. Before the possibilities for this subcellular location are discussed, it is important to note that p53 is spatially regulated during the cell cycle and contains signal sequences for nuclear import and export which may contribute to the

subcellular localisation of p53 (Middeler *et al.*, 1997). Three nuclear localisation signals (NLS), which mediate nuclear import, are clustered at the C-terminus (Shaulsky *et al.*, 1990a) and there is recent evidence of a highly conserved leucine-rich nuclear export signal (NES) located in the tetramerisation domain (Stommel *et al.*, 1999). In normal unstressed cells p53 is predominantly nuclear in G1 and is largely cytoplasmic during S and G2 (Shaulsky *et al.*, 1990b; David-Pfeuty *et al.*, 1996) consistent with its role as a mediator of G1 checkpoints. In response to stress, however, p53 is stabilised and retained in the nucleus where it induces an expression of genes involved in cell cycle arrest or apoptosis. In addition, the protein, MDM2, is transcriptionally induced (Barak *et al.*, 1993) which is capable of blocking the activity of p53 as a transcription factor and also targeting it for ubiquitinylation and subsequent degradation in the cytoplasmic proteasome. Therefore, MDM2 and p53 are predicted to form an autoregulatory feedback loop in which p53 limits its own activity through the production of MDM2 (Wu *et al.*, 1993). This autoregulatory feedback loop, however, can be modulated to allow p53 to become stabilised and active as a transcription factor following DNA damage (Shieh *et al.*, 1997). MDM2 also contains a NES which may be responsible for the nuclear export of p53. Stommel *et al.* (1999), however, have postulated that p53 is capable of nuclear export via its own NES situated in the tetramerisation domain independently of MDM2 and also the attenuation of p53 function involves the conversion of tetramers into monomers or dimers, in which the NES is exposed to the proteins which mediate their export to the cytoplasm.

Due to these complex mechanisms involved in the regulation of the levels and subcellular location of p53, it is difficult to predict how the YTPL signal motif has affected the location of p53-DM β expressed from pCR3 in transfected HeLa cells. However, a few possibilities are now discussed. The presence of YTPL may abrogate the effect of the NLS and prevent translocation of p53 into the nucleus or it may enhance nuclear export via the NES. Alternatively, the C-terminal attachment of the DM β transmembrane region and cytoplasmic tail may cause nonconformational changes in the quaternary structure of the p53 which interfere with its translocation to the nucleus. Furthermore, these additional amino acids may inhibit or hinder tetramer formation which is essential for DNA binding and transactivation of p53 (Hupp and

Lane, 1994; McLure and Lee, 1998) resulting in monomeric p53 with an exposed NES and subsequent enhanced exportation to the cytoplasm (Stommel *et al.*, 1999). However, Norris and Haas (1997) demonstrated that normal p53 functions and conformation are unaffected by the C-terminal attachment of GFP. Finally, the DM β region appended to p53 contains a hydrophobic transmembrane region situated at the carboxyl terminus which may cause an abnormal association with membranes of organelles such as the ER, Golgi. The insertion of transmembrane regions of proteins into membranes, however, normally occurs during ER translocation of nascent polypeptide chains containing an amino-terminus signal sequence as mentioned above and thus the anchorage of p53-DM β to internal membranes via its transmembrane region without this translocation process seems an unlikely occurrence. Unfortunately, these hypotheses have not shed any light on how the presence of DM β fused at the C-terminus of p53 causes abnormal sequestration of p53-DM β with concomitant nuclear exclusion.

In contrast, p53 in the absence of the YTPL sequence, was located in the nuclei as detected by immunofluorescence analysis of HeLa cells transfected with the control construct pCR3p53. In a small number of transfectants, p53, which had overcome the degradation effects of E6, became stabilised and was located in the nuclei probably in response to the aberrant replication of DNA exhibited by the rapidly proliferating HeLa cells.

From these experiments which utilised the pCR3 vector, it was concluded that p53-DM β had accumulated in the cytosol by virtue of the YTPL sequence in the absence of an amino-terminal signal sequence. A second series of experiments was performed to determine whether p53-DM β had been targeted to the lysosomal compartment in the presence of an amino-terminal signal sequence. The vector pSecTagA was utilised which contains such a sequence termed the leader sequence (LS). Control pSecTagA constructs were also designed for use in these experiments which were predicted to guide p53 to the membrane or to result in its secretion.

In theory, the presence of the LS and the hydrophobic transmembrane region of DM β at the C-terminus will enable p53-DM β , expressed from pSecTagA, to translocate the

ER and anchor itself to the membrane causing the protein to assume an orientation with p53 facing the lumen and the cytoplasmic tail of DM β containing YTPL facing the cytosol. The high levels of protein indicated by the intense immunofluorescent staining and Western blot analysis suggest that p53-DM β is not present in the cytosol where it would be degraded, mediated by the E6 oncoprotein and thus has translocated the ER successfully and anchored itself to the membrane. In addition immunofluorescence and Western blot analysis of HeLa cells transfected with pSecTagA.p53-DM β revealed that the transfection efficiency was 40%, considerably higher than the efficiencies achieved using the pCR3 constructs. These data confirm that p53-DM β has not been degraded and, therefore, is not situated in the cytosol. However, it is difficult to determine the exact location of p53-DM β which appears to be located in the ER and Golgi body. Although the fluorescent labelling of p53 is not indicative of punctate lysosomal staining there are some areas of co-localisation with the lysosomal marker, CD63, in the perinuclear region.

For proteins to traverse the biosynthetic pathway, it is essential that they undergo correct folding and in some cases oligomerisation. As already mentioned, tetramer formation is essential for DNA binding and transactivation of p53. The tetramerisation domain which is situated at the C-terminus of p53, would be situated near the transmembrane region of p53-DM β at the lumen side of the membrane in the ER. Normally p53 is soluble in the nuclei and cytoplasm where it assembles as a tetramer. However, p53-DM β expressed from pSecTagA will be anchored to the ER membrane following translocation and the formation of the tetramer may cause unfavourable steric effects which may hinder its transport to the lysosomes. In addition p53-DM β may be misfolded or misassembled. Both events would result in the retention of this chimeric protein in the ER and ultimately its degradation (Hurtley & Helenius, 1989). However, from the high levels of p53-DM β detected by immunofluorescence and Western blot analyses in this study there is no indication that p53-DM β expressed from pSecTagA has been degraded. Alternatively, p53-DM β may not oligomerise in the ER in which case it would be targeted to the lysosomes as a monomer. Therefore, it is probable that p53-DM β has trafficked through the biosynthetic pathway either as a monomer or tetramer.

p53-DM β is constitutively expressed up to 72h after transient transfection due to the potent CMV enhancer-promoter sequence present in pSecTagA which results in its high level expression. There is evidence that proteins containing tyrosine- and dileucine-based signal which are overexpressed, accumulate at the cell surface owing to increased movement to the surface through the constitutive secretory pathway (“default” pathway) by virtue of saturation of intracellular binding sites (Uthayakumar & Granger, 1995; Warren *et al.*, 1997). In addition Copier *et al.* (1996) have proposed that HLA-DM could access the endocytic pathway via internalisation from the cell surface. However, due to the possible saturation of intracellular binding sites p53-DM β may not internalise and remain at the cell surface. Therefore, it was necessary to investigate cell surface expression of p53. The construct, pSecTagA.p53-TM was engineered to guide p53 to the plasma membrane and served as positive control in the following experiments for cell surface analysis. There was some evidence of surface staining observed in cells transfected with pSecTagA.p53-TM using immunofluorescence microscopy (method I). In contrast, cells transfected with pSecTagA.p53-DM β showed very little evidence of cell surface staining of p53. Some intracellular staining observed in both transfectants suggested these results may be obscured because of partial permeabilisation of the cells due to osmotic stress. However, further analyses of cells transfected with pSecTagA.p53-TM and pSecTagA.p53-DM β using the gentler approaches, cytofluorimetry and immunofluorescence microscopy (method II), revealed that staining for p53 was not evident at the cell surface. Failure to detect p53 may have been due to the lack of sensitivity of these procedures. Alternatively, p53-DM β or p53-TM may not be expressed at the cell surface due to the retention of these proteins in the ER which may have misfolded or assembled incorrectly as oligomers. A more sensitive application which will not subject the cells to osmotic stresses may provide more convincing evidence of p53 expression at the cell surface. Furthermore subcellular fractionation may determine whether cell surface expression of p53 has occurred. Interestingly, pSecTagA.p53-TM could potentially gain access to the MHC class II pathway via internalisation following surface expression and subsequent association with MHC class II molecules. Thus, future experiments could analyse CD4⁺ T-cell proliferative response to autologous DC transfected with this construct.

Finally to ensure that p53 is capable of traversing the biosynthetic pathway, control constructs, pSecTagA.p53 and pSecTagB.p53-His, were designed to allow p53 to follow the constitutive secretory pathway resulting in its secretion. Western blot analysis revealed that p53 was present in the supernatants collected from cells transfected with these constructs and but was not detected in supernatants from HeLa cells transfected with pSecTagA.p53-DM β , pSecTagA.p53-TM and pSecTagA. This confirmed that p53 was capable of traversing the ER and Golgi body and had not been degraded. As in the case of pSecTagA.p53-TM, pSecTagA.p53 could also potentially gain access to the MHC class II pathway via secretion and subsequent endocytosis by DC. To investigate this, future studies could analyse CD4⁺ T-cell proliferative responses to autologous DC transfected with this construct.

In summary, the results described in this chapter highlight the difficulty in targeting the nuclear protein, p53, to the lysosomal compartment. However, it can be concluded that p53-DM β has probably trafficked to the lysosomes via the YTPL signal motif in the presence of the LS but due to the overexpression of the protein, the intense staining of p53-DM β in the biosynthetic pathway has masked lysosomal staining. Comparative analysis with control constructs has also provided evidence that localisation to the lysosomes has probably occurred. Subcellular fractionation could provide further evidence but time constraints prevented this strategy being pursued.

3.5 Future Work

- Perform subcellular fractionation of HeLa cells transfected with pSecTagA.p53-DM β , pSecTagA.p53, pSecTagp53-TM, pSecTagA, followed by Western blot analysis of cell fractions, to confirm that p53-DM β and p53-TM have been targeted to the lysosomal compartment and plasma membrane, respectively.
- Determine whether p53-DM β has been transported as a tetramer or monomer by Western blot analysis using non-reducing conditions.
- Repeat intracellular immunofluorescence analyses of p53-DM β and p53 using an alternative cell-line, which is easily transfected with plasmid DNA, only expresses p53 at low non-detectable levels and does not contain proteins that affect the expression of p53.
- Select a more sensitive method for the detection of p53 at the cell surface and repeat cell surface analysis of p53 expression.
- Select another tumour antigen known to be over expressed in breast cancer, preferably one that normally traverses the biosynthetic pathway as a membrane protein such as the proto-oncogene HER-2/*neu*, and target it to the lysosomes utilising the signal motif YTPL from DM.
- Transfect DC with pSecTagA.p53-DM β , pSecTagA.p53-TM and pSecTag.A.p53 and subsequently compare CD4⁺ T-cell proliferative responses to p53, targeted to the different compartments of the cell, in order to establish which construct provides optimal access to the MHC class II pathway.

Chapter Four

Non-viral transfection of human monocyte-derived DC

Chapter Four

4.1 Introduction

As discussed in chapter one, DC are the most potent professional APC of the immune system with the capacity to acquire and process antigen, migrate to lymphoid organs and stimulate antigen-specific T cells to proliferate (reviewed in Steinman 1991; Banchereau & Steinman 1998). Recent identification of *in vitro* conditions in which DC can be generated from PBMC by culturing progenitor cells in the presence of GM-CSF and IL-4 (Sallusto *et al.*, 1994; Romani *et al.*, 1994) has led to the potential use of DC therapeutically as adjuvants for immunisation. Evidence has shown that tumours in murine models are reduced in size following immunisation with DC genetically modified with tumour antigens (Song *et al.*, 1997; Specht *et al.*, 1997). More importantly, immunisation with antigen-pulsed DC has been reported in melanoma, cervical cancer and lymphoma patients (Nestle *et al.*, 1998; De Bruijn *et al.*, 1998; Hsu *et al.*, 1996). Due to the ready availability of cultured DC and the growing evidence of their capacity to stimulate potent and antigen-specific antitumour immunity, DC will be utilised in this vaccine strategy to express a known breast tumour antigen, the tumour suppressor protein p53 to enhance CD4⁺ T-cell responses.

DC pulsed with recombinant protein or peptides may not be ideal in the clinical setting due to the difficulty in producing large quantities of protein. The use of nucleic acids as the form of antigen loaded onto DC would overcome these practical limitations as the technology exists to synthesise sufficient quantities of DNA/RNA encoding defined tumour antigens at ease. In addition, this approach does not require definition of antigenic peptides sequences and avoids the complication of HLA haplotype preferences for antigen presentation. Thus, the ultimate aim of this strategy is to transfect DC with cDNA encoding p53, engineered to traffic to the MHC class II antigen processing pathway. It is necessary, however, to establish the optimal DNA transfection conditions of DC prior to these experiments. Although the use of viral vectors may be more efficient for gene transfer into DC (Brossart *et al.*, 1997; Reeves *et al.*, 1996) their therapeutic use entails many problems (Felgner *et al.*, 1997). Patients generate an immune response to the viral proteins leading to neutralising

antibodies that limit effective repeated application of recombinant viruses. Some viral vectors may disrupt the DNA of the cells they infect with potentially harmful results. Also insertion of foreign DNA into the genome may occur, raising the risk of integration into a critical cellular gene. Furthermore, weakened viruses can conceivably change inside the body and regain their pathogenic activity. None of these potential drawbacks, however, are associated with non-viral techniques making them a suitable choice for the transfection of DC with subsequent therapeutic applications. Thus, experiments performed in this chapter sought to establish optimal conditions, for the transfer of DNA into DC using a variety of nonviral methods which are currently available.

An alternative to DC vaccines loaded with DNA-based antigens are RNA-transfected DC. A potentially significant advantage of using RNA-encoded antigens is safety. The half-life of stable mRNA species in the mammalian cell is less than 24-hours, whereas unintegrated DNA can persist and function in non-dividing cells for extended periods of time (Gilboa., 1998). Thus, a safer approach would be to transfect DC with RNA transcripts encoding the chimeric protein p53-DM β . Experiments in this chapter also sought to synthesise GFP RNA transcripts by IVT, followed by transfection experiments of DC and HeLa cells with such transcripts.

4.2 Methods

4.2.1 Generation of DC from peripheral blood

Dendritic cells were generated as described by Romani *et al.* (1994). Briefly PBMC from healthy donors (see section 2.3.2) were resuspended in serum-free complete RPMI 1640 and allowed to adhere to 6-well plates (1×10^7 /3ml per well). After 2-hours at 37°C, non-adherent cells were gently removed and the adherent cells cultured in complete RPMI + 5% FCS supplemented with recombinant human GM-CSF (800 U/ml) and IL-4 (500 U/ml) (DC complete medium). Every 2 days, 1ml of spent medium was replaced by 1.5ml of fresh medium containing 1600U/ml GM-CSF and 1000U/ml IL-4 to give final concentrations of 800U/ml and 500U/ml, respectively.

4.2.2 IVT of GFP

A 732bp *NotI* fragment encoding the entire ORF for GFP was excised from pGL and cloned in the sense orientation into the *NotI* site of pCR3. Similarly, a 732bp *NotI* fragment encoding the entire ORF for GFP was excised from pGL and cloned in the sense orientation into the *NotI* site of pCITE-4b. The resulting constructs were designated pCR3.GFP and pCITE.GFP, respectively and were utilised as templates for the synthesis of GFP transcripts. Prior to IVT, pCR3.GFP was linearised downstream of the BGH polyadenylation signal using the restriction endonuclease *SpeI* whereas pCITE.GFP was linearised downstream of poly A sequence using the restriction endonuclease *AflIII*. Refer to section 2.2.16 for details of IVT.

4.2.3 Transfection of DC with GFP RNA transcripts using DOTAP transfection reagent.

DC were transfected with GFP RNA transcripts using the cationic lipid, DOTAP (Roche Ltd.), according to the protocol described by Boczkowski *et al.* (1996). Briefly, immature DC were harvested on day-7 of culture, resuspended in OPTI-MEM medium at 2×10^6 cells/ml and added to polypropylene tubes (Falcon). RNA (5µg in 500µl OPTI-MEM medium) and DOTAP (0, 10µg DOTAP in 500µl) were mixed in tubes at room temperature for 20 minutes. The complex was added to the

DC in a total volume of 2ml and incubated at 37°C with occasional agitation for 3-hours. The cells were washed and after 48-hours of incubation at 37°C, GFP expression was examined by epifluorescence using the Nikon diaphot microscope and photographed on Kodak ASA 400 colour film.

4.2.4 Transfection of HeLa cells with GFP RNA transcripts using Effectene Transfection Reagent

Transfection of *in vitro* transcribed GFP into HeLa cells using Effectene Reagent (Qiagen Ltd.) was performed according to the protocol described by Sugie *et al.* (1999). Briefly, the day before transfection, 24-well plates were seeded with 7×10^4 cells/well in 1ml of DMEM + 10% FCS to provide a confluence of 40-80% on the day of transfection. The following day GFP RNA (1.0µg), which had been previously *in vitro* transcribed from the linear DNA templates pCR3.GFP and pCITE.GFP, was diluted with Buffer EC to a total volume of 100µl in polypropylene tubes. Diluted RNA was mixed with 0-4µl Enhancer and incubated at room temperature for 3 minutes. Effectene Reagent (0-4µl) was added to the RNA solutions, incubated for 10 minutes to allow Effectene-RNA formation. After removing the medium, the complexes were added to the HeLa cells. Fresh complete medium (200µl) was immediately added to the cells, and a further 1ml complete was added to the cells 2-hours after transfection. After 48-hours of incubation at 37°C, GFP expression was examined by epifluorescence using the Nikon diaphot microscope and photographed on Kodak ASA 400 colour film.

HeLa cells were also transfected with 0.4µg pGL using 10µl Effectene and 3.2µl Enhancer and served as positive controls in the RNA transfection experiments. The protocol was identical to that of the RNA transfection of HeLa cells outlined above.

4.2.5 Transfection of HeLa cells with GFP RNA transcripts using DOTAP Liposomal Transfection Reagent

Transfection of *in vitro* transcribed GFP into HeLa cells using DOTAP Reagent was performed according to the manufacturer's instructions (Roche Ltd). Briefly, the day before transfection, 6-well plates were seeded with 1×10^5 cells/well in 2ml of

complete medium to provide a confluence of 40-80% on the day of transfection. GFP RNA (2.5µg), which had been previously *in vitro* transcribed from the linear DNA templates pCR3.GFP and pCITE.GFP, was diluted to a final volume of 25µl with 20mM Hepes buffer (pH 7.4) in polypropylene tubes. In separate tubes 0, 5, 10, 15, 20, 25µl DOTAP was diluted to final volumes of 50µl. Diluted RNA was transferred to diluted DOTAP solutions, mixed by gentle pipetting and incubated at room temperature for 10-15min. The DOTAP/RNA mixtures were added directly to the cultures and gently mixed by rocking the plates. DC were incubated for 6-hours at 37°C, followed by the replacement of medium with fresh culture medium. After 48-hours of incubation at 37°C, GFP expression was examined by epifluorescence using the Nikon diaphot microscope and photographed on Kodak ASA 400 colour film.

HeLa cells were also transfected with pGL using DOTAP and served as positive controls for the RNA transfection experiments. The DNA transfection protocol was identical to that of the RNA transfection outlined above. The only difference being *in vitro* transcribed RNA was replaced with plasmid DNA.

4.2.6 Transfection of HeLa cells with GFP RNA transcripts by electroporation

HeLa cells were transiently transfected with *in vitro* transcribed GFP RNA by electroporation using the Bio-Rad Gene Pulser. Exponentially growing HeLa cells were harvested using Trypsin-EDTA, washed twice with serum-free DMEM, and resuspended in the same medium at 5.0×10^6 cells/ml. GFP RNA (5µg) was added to a 4 mm cuvette, 400µl of the cell suspension added and the cuvette immediately subjected to a single voltage pulse. Electroporation was performed at 960µF, 0.30kV and the cells were transferred immediately to 80cm² flasks. After 48-hours of incubation at 37°C, GFP expression was examined by epifluorescence using the Nikon diaphot microscope and photographed on Kodak ASA 400 colour film.

HeLa cells were also transfected by electroporation with pGL and served as positive controls for the DC transfection experiments. Refer to section 2.3.3 for details.

4.2.7 Transient transfection of DC by electroporation

DC were transiently transfected with pGL by electroporation using the Bio-Rad Gene Pulser. Immature DC, generated as described above, were harvested on day-7 of culture, washed twice with serum-free RPMI, and resuspended in the same medium at 1.25×10^6 cells/ml. Plasmid DNA (10 μ g) was added to a 4mm cuvette, 400 μ l of the cell suspension added (5×10^5 cells in total) and the cuvette immediately subjected to a single voltage pulse. Electroporation volume and DNA quantity was kept constant at 400 μ l and 10 μ g throughout the experiments. Following transfection, cells were immediately resuspended in 1.5ml of media and transferred to 24-well plates. In addition, transfections were also performed in the presence of 40 μ M chloroquine (Sigma). After 24- and 48-hours incubation at 37°C, GFP expression was examined by epifluorescence using the Nikon diaphot microscope and photographed on Kodak ASA 400 colour film.

HeLa cells were also transfected by electroporation with pGL and served as positive controls. Refer to section 2.3.3 for details.

4.2.8 Transient transfection of DC by lipofection using DMRIE-C

Transfection of DC by the DMRIE-C reagent (GIBCO BRL) was performed according to Ciccarone *et al.* (1996). Briefly, varying amounts of DMRIE-C (0, 2, 4, 6, 10 μ g) in 0.25ml OPTI-MEM were added to each well of a 24-well plate. After 30 minutes at room temperature, 0.25ml of OPTI-MEM containing 1 μ g of DNA (pGL) was added to the wells containing lipid reagent and incubated 15 minutes at room temperature to allow formation of lipid-DNA complexes. On day-7 of culture, immature DC were harvested and 0.1ml of a cell suspension containing 1×10^6 cells in OPTI-MEM was added to each well. Cells were incubated for 4-hours at 37°C, followed by the addition of 1ml of DC complete media. In addition, transfections were also performed in the presence of 40 μ M chloroquine. After 24- and 48-hours incubation at 37°C, reporter GFP expression was examined by epifluorescence using the Nikon diaphot microscope and photographed on Kodak ASA 400 colour film.

HeLa cells were also transfected with pGL using DMRIE-C reagent according to the manufacturer's instructions and served as positive controls.

4.2.9 Transient transfection of DC using the polycation Superfect

Transfection of DC using Superfect (Qiagen Ltd.) was performed according to Dr Carstens (personal communication, 1999). Immature DC were harvested on day-7 of culture and 24-well plates were seeded with 5×10^5 cells/well in 50 μ l of serum-free RPMI. Serum and antibiotic-free RPMI (50 μ l) containing Superfect (5 μ g or 8 μ g) was added to 50 μ l of serum and antibiotic-free RPMI containing 1 μ g of DNA (pGL) and mixed by pipetting up and down 5 times. The samples were incubated for 5-10 minutes at room temperature to allow complex formation. The transfection complexes were added to the cells in 24-well plate, the samples were gently swirled and incubated for 30 minutes at 37°C. DC complete media (1ml) was added and DC were incubated for 6-hours. The media was removed and replaced with 1.5ml of complete DC media. In addition, transfections were also performed in the presence of 40 μ M chloroquine. After 24- and 48-hours of incubation at 37°C, GFP expression was examined by epifluorescence using the Nikon diaphot microscope and photographed on Kodak ASA 400 colour film.

HeLa cells were also transfected with pGL (2 μ g) using Superfect (0, 4, 10, 20 μ l) and served as positive controls in the DC transfection experiment. Briefly, the day before transfection, 6-well plates were seeded with 1.5×10^5 cells/well in 2ml of complete DMEM + 10% FCS. The transfection was performed according to the manufacturer's instructions.

4.2.10 Transient transfection of DC using the transfection reagent Effectene

Transfection of DC with pGL using Effectene was performed according to the manufacturer's protocol (Qiagen Ltd.). Immature DC were harvested on day-7 of culture and 6-well plates were seeded with 6.75×10^5 cells/well in 1.6ml of DC complete media. DNA (0.4 μ g) was diluted in 96 μ l buffer EC, followed by the addition of 3.2 μ l Enhancer. After mixing, the samples were incubated for 2-5 minutes at room temperature, followed by the addition of varying amounts of Effectene

reagent: 0, 4, 10, 20 μ l. After mixing, the samples were incubated for 5-10 minutes at room temperature to allow complex formation. Complete DC media (600 μ l) was added to each tube, the contents were mixed carefully and transferred to the appropriate wells. The plates were gently swirled to ensure uniform distribution of the complexes. In addition, transfections were also performed in the presence of 40 μ M chloroquine. After 24- and 48-hours of incubation at 37°C, GFP expression was examined by epifluorescence using the Nikon diaphot microscope and photographed on Kodak ASA 400 colour film.

HeLa cells were also transfected with pGL using Effectene and served as positive controls in the DC transfection experiments. Briefly, the day before transfection, 6-well plates were seeded with 1.5×10^5 cells/well in 1.6ml of complete DMEM + 10% FCS. The following day HeLa cells were transfected with identical amounts of DNA and Effectene with Enhancer according to the protocol for DC transfection outlined above.

4.2.11 Transient transfection of DC using the transfection reagent Fugene- 6

Transfection of DC using FuGENE-6 was performed according to the manufacturer's protocol (Roche Ltd.). Briefly, immature DC were harvested on day-6 of culture and 6-well plates and 24-well plates were seeded with 3×10^5 cells/well in 2ml of DC complete media and 3×10^5 cells/well in 1ml of DC complete media, respectively. The following day a sufficient amount of serum-free RPMI was added to a polypropylene tube to dilute Fugene-6 to 100 μ l, followed by varying amounts of Fugene-6 (0, 3, 6, 9, 12 μ l) which were added directly to the medium. Diluted Fugene-6 was incubated for 5 minutes at room temperature and then added dropwise to tubes containing 2 μ g of DNA (pGL). The tubes were gently mixed and incubated for 15 minutes at room temperature. Transfection mixtures were added dropwise to each well and the plates were swirled to ensure even dispersal. In addition, transfections were also performed in the presence of 40 μ M chloroquine. After 24- and 48-hours of incubation at 37°C, GFP expression was examined by epifluorescence using the Nikon diaphot microscope and photographed on Kodak ASA 400 colour film.

HeLa cells were also transfected with pGL using the Fugene-6 reagent and served as positive controls in the DC transfection experiments. Briefly, the day before transfection 6-well plates were seeded with 1.5×10^5 cells/well in 2ml complete DMEM + 10% FCS. The following day HeLa cells were transfected with 2 μ g DNA using Fugene-6 (0, 3, 6, 9, 12 μ l) according to the protocol for DC transfection outlined above.

4.2.12 Transfection of DC using the cationic amphipathic peptide, KALA

A cationic peptide, KALA, kindly donated by Dr S. Thirdborough (University of Southampton) was used to transfect DC. Briefly, on day-7 of culture, DC were harvested and 24-well plates were seeded with 3×10^5 cells/ well in 0.9ml. DNA (2 μ g) and peptide were diluted in 2 x HEPES buffer (total volume 0.1ml) to give the following DNA:peptide ratios: 5:1, 10:1 and 20:1 as described by Felgner *et al.* (1997). The DNA and peptide complexes were incubated for 15mins at room temperature. The transfection mixtures were then added dropwise to each well and incubated at 37°C for 2-hours. DC were washed and resuspended in 1ml DC complete media. In addition, transfections were also performed in the presence of 40 μ M chloroquine. After 24- and 48-hours of incubation at 37°C, GFP expression was examined by epifluorescence using the Nikon diaphot microscope and photographed on Kodak ASA 400 colour film.

4.3 Results

4.3.1 Generation of DC from peripheral blood

It was necessary to determine whether immature DC were generated from monocyte precursors in the presence of GM-CSF and IL-4 and also were capable of differentiating into mature DC in the presence of TNF- α . Thus, experiments were performed comparing the phenotype of DC from GM-CSF and IL-4 cultures with that of DC cultured with additional TNF- α .

Preparation of immature DC were obtained from adherent PBMC that were differentiated for 7-days in IL-4 and GM-CSF cultures as previously described. By day-7 the vast majority of the cells appeared as loosely adherent clusters or isolated free floating cells with characteristic DC veiled morphology as assessed by phase contrast microscopy (Figure 4.1). Analysis of cell surface markers revealed that DC expressed high levels of CD1a but no CD14 or CD83 (Figure 4.2). These large cells also expressed low levels of CD80 and higher levels of HLA-DR, CD40 and CD86 (Figure 4.3). Thus, HPC cultured with GM-CSF and IL-4 present morphological and phenotypic characteristics consistent with immature DC.

Research performed by Romani *et al.*, (1994) has shown that CD14⁺ blood monocytes cultured in the presence of GM-CSF and IL-4 need an additional stimulation with TNF- α to induce DC maturation. This correlates with the upregulation of class II and many co-stimulatory molecules (reviewed in Banchereau & Steinman 1998). Also the cells become CD83⁺ which has been characterized as a unique cell surface marker of mature dendritic cells (Zhou *et al.*, 1993; Zhou *et al.*, 1995). Therefore, experiments were performed to assess the ability of immature DC to differentiate into mature DC in the presence of TNF- α . On day-6 of culture immature DC were incubated with TNF- α (25ng/ml) together with the medium containing IL-4 and GM-CSF, for an additional 48-hours. On day-8 analysis of cell surface markers revealed that DC in the presence of TNF- α , expressed higher levels of, HLA-DR, CD40, CD80, CD86 compared with immature ones (Figure 4.3). These cells also expressed CD83 which is a typical characteristic of mature DC (Figure 4.2). The overall increase in expression

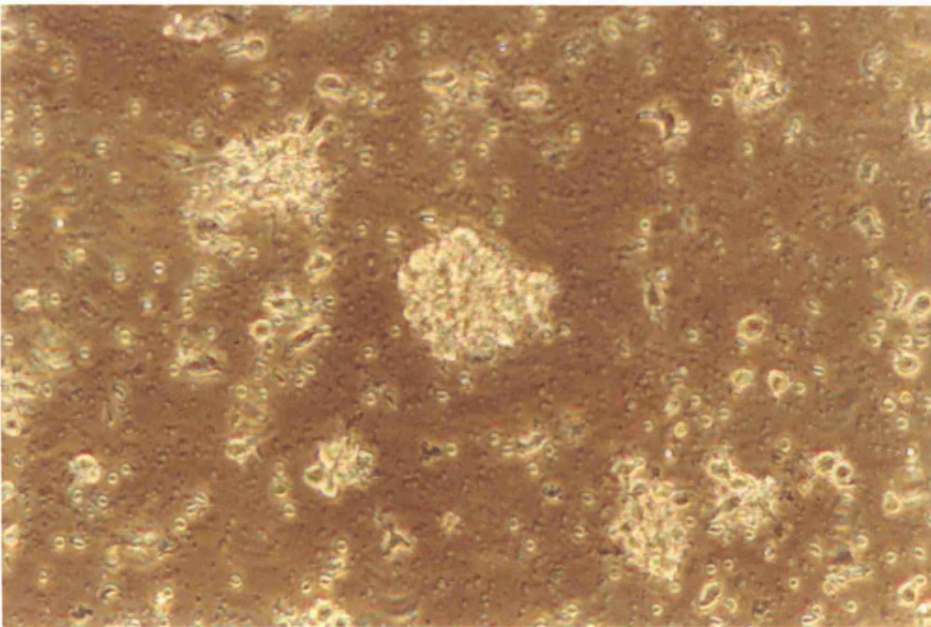
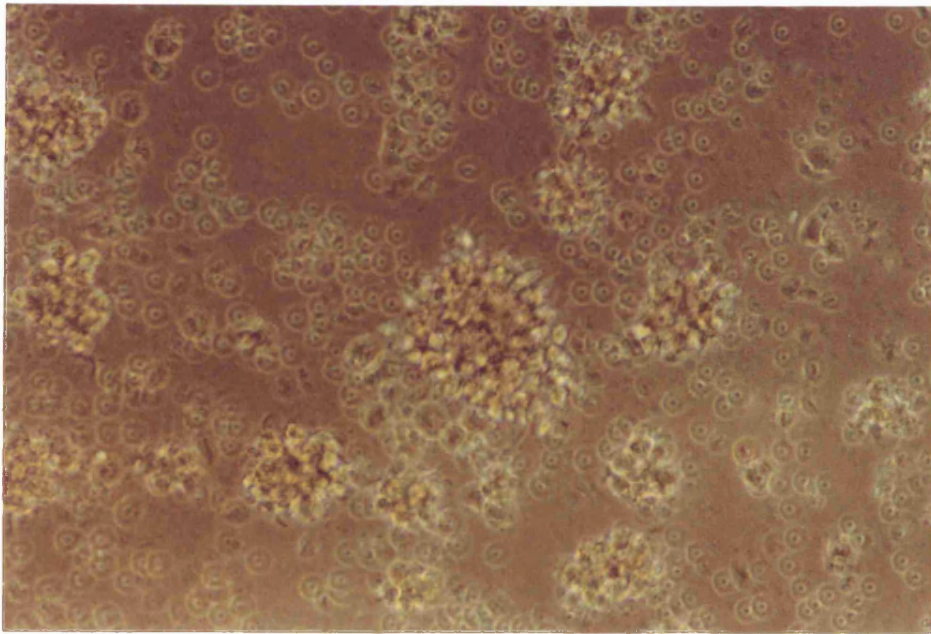


Figure 4.1 Development of immature DC from peripheral blood by culturing HPC in media supplemented with GM-CSF and IL-4. After 7 days, large aggregates are visible by phase-contrast microscopy, with individual cells displaying veiled morphology.

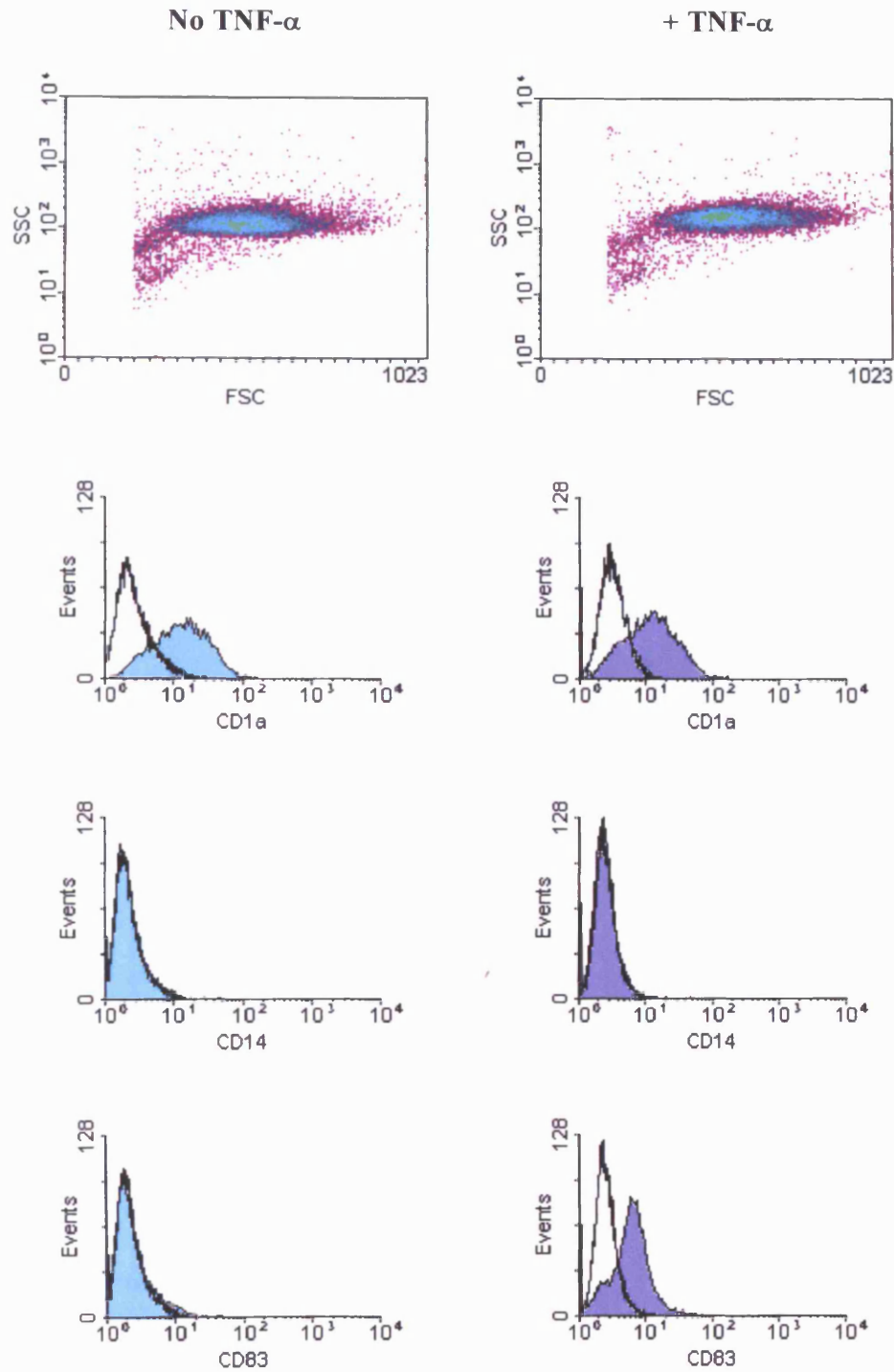


Figure 4.2. Phenotypic analysis of DC in the presence and absence of TNF- α . The upper panels (cytograms) illustrate a population of large cells which are DC. The histograms show fluorescence values on un-gated cells. Open histograms represent labelling with control irrelevant Ab and solid histograms represent staining by FITC- or PE-labelled relevant mAb as indicated.

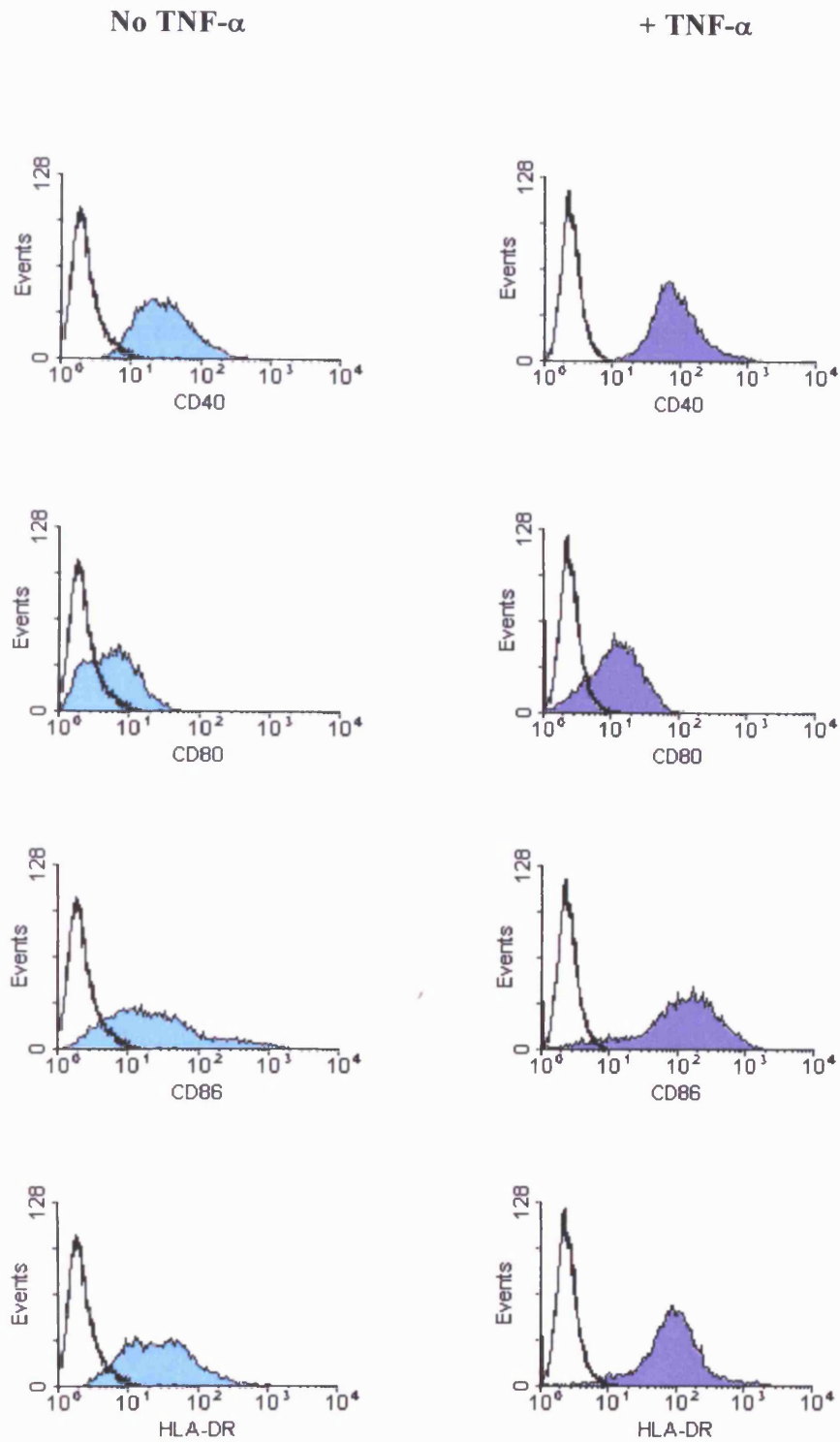


Figure 4.3. Phenotypic analysis of DC in the presence and absence of TNF- α . The histograms show fluorescence values on un-gated cells. Open histograms represent labelling with control irrelevant Ab and solid histograms represent staining by FITC- or PE-labelled relevant mAb as indicated.

of the surface markers, HLA-DR, CD40, CD80, CD86 and CD83, reflects the maturity of DC. The levels of CD1a and CD14 were comparable with that of immature DC (Figure 4.2). Thus, immature DC cultured with GM-CSF and IL-4 and the additional cytokine, TNF- α , present phenotypic characteristics consistent with mature DC.

These results confirmed that immature monocyte-derived DC were generated successfully from GM-CSF and IL-4 cultures with the capacity to differentiate into mature DC following TNF- α treatment. Due to the effectiveness of culturing immature DC in the presence of GM-CSF and IL-4, this method was adopted for the generation of DC for subsequent transfection experiments.

4.3.2 Synthesis of GFP RNA transcripts

GFP transcripts generated by IVT were analysed by gel electrophoresis (Figure 4.4). GFP transcripts generated from pCITE.GFP are represented by a single band (lanes 4 and 5) at approximately 1.47Kb, which is of the correct MW and indicates successful IVT. However, GFP transcripts generated from pCR3.GFP are represented by 2 bands of equal intensity (lanes 2 and 3) at approximately 1.2Kb and 0.8Kb in size. This may have been caused by secondary structure of the RNA. In addition, the positive control produced a band of 1.8Kb which corresponds to the correct MW weight of the luciferase transcript (lane 6) whereas there was no transcript generated by the negative control (lane 7).

4.3.3 Optimal transfection conditions of DC with RNA transcripts.

DOTAP Liposomal Transfection Reagent, which is a liposome formulation of the cationic lipid DOTAP, is suitable for the transfer of RNA into eukaryotic cells in the presence and absence of serum. DC were transfected with RNA transcripts using the transfection reagent DOTAP according to the protocol described by Boczkowski *et al.* (1996) (see section 4.2.3). Initially the GFP transcript was utilised which had been generated by IVT from the DNA template pCR3.GFP. Unfortunately this method did not yield positive transfectants (data not shown). The negative results may be due to absence of the poly A sequence in the DNA template resulting in unstable transcripts.

In order to overcome this problem a GFP insert was sub-cloned into the pCITE-48 vector which contains a polyA sequence at the 3' terminus of the MCS to ensure stability of the transcript. GFP transcripts were generated and used to transfect DC using DOTAP as before. Again most of the DC were expressing GFP (data not shown). In order to test the effectiveness of these transcripts the epithelial cell line, HeLa, which is readily transfected with DNA, was transfected with these transcripts (see section 4.2.4 below).

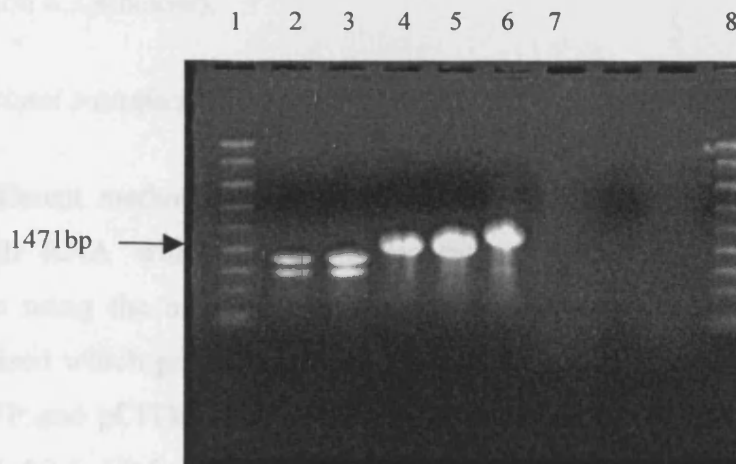


Figure 4.4 Agarose gel (1.5%) stained with ethidium bromide showing GFP transcripts generated by IVT from the DNA templates pCR3.GFP and pCITE.GFP. Lane (1) RNA ladder. Lane (2) GFP transcript (1.98 μg) generated from pCR3.GFP. Lane (3) GFP transcript (3.955 μg) generated from pCR3.GFP. Lane (4) GFP transcript (4.36 μg) generated from pCITE.GFP. Lane (5) GFP transcript (8.725 μg) generated from pCITE.GFP. Lane (6) Positive control: luciferase transcript (6.32 μg). Lane (7) Negative control: no template. Lane (8) RNA ladder.

Figure 4.5) revealed a relatively intense signal at approximately 27 kDa in lane 3, which corresponds to the correct MW of GFP protein generated from pCITE.GFP. In contrast, a very weak signal also at 27 kDa was observed in lane 2 which corresponds to GFP protein generated from pCR3.GFP. However this signal was much weaker than background signals and thus was not significant. In addition, the positive control produced an intense signal at 59 kDa (lane 6) which corresponds to the correct MW of luciferase protein whereas a signal was not observed for the negative control (lane 7). These

In order to overcome this problem a GFP insert was sub-cloned into the pCITE-4b vector which contains a polyA sequence at the 3' terminus of the MCS to ensure stability of the transcript. GFP transcripts were generated and used to transfect DC using DOTAP as before. Again none of the DC were expressing GFP (data not shown). In order to test the effectiveness of these transcripts the epithelial cell line, HeLa, which is readily transfected with DNA, was transfected with these transcripts (see section 4.3.4 below).

4.3.4 Optimal transfection conditions of HeLa cells with GFP transcripts

Three different methods were adopted to optimise transfection conditions of HeLa cells with RNA which were electroporation, lipofection using DOTAP and a technique using the non-liposomal reagent, Effectene. In all cases GFP transcripts were utilised which previously had been generated by IVT from the DNA templates pCR3.GFP and pCITE.GFP. Details of the methods are described in sections 4.2.4, 4.2.5 and 4.2.6. Unfortunately none of the techniques yielded positive transfectants. However, transfections using the positive controls in which GFP transcripts were replaced with pGL produced positive transfectants and thus provided evidence that all three transfection techniques were functioning effectively. The negative results may reflect the quality of the RNA or the abundance of RNAses present in the transfection systems.

4.3.5 In vitro translation of GFP

In order to assess the ability of the DNA templates pCR3.GFP and pCITE.GFP to produce protein products of GFP *in vitro*, coupled *in vitro* transcription/translation was performed as described in section 2.4.8. The autoradiograph (Figure 4.5) revealed a relatively intense signal at approximately 27 kDa in lane 3, which corresponds to the correct MW of GFP protein generated from pCITE.GFP. In contrast, a very weak signal also at 27 kDa was observed in lane 2 which corresponds to GFP protein generated from pCR3.GFP. However this signal was much weaker than background signals and thus was not significant. In addition, the positive control produced an intense signal at 60 kDa (lane 1) which corresponds to the correct MW of luciferase protein whereas a signal was not observed for the negative control (lane 4). These

results suggest that pCITE.GFP was capable of generating GFP transcripts followed by the protein products of the correct MW in vitro. In contrast the control pCR3.GFP was not as effective and produced levels of protein which were hardly detectable.

4.3.0 Optimal conditions of transfection for DC with DNA

Various non-viral transfection methods were studied to optimize transfection conditions for DC. DC were transfected with plasmid DNA as demonstrated by electroporation (see section 4.2.1) and were analysed as demonstrated by SDS-PAGE analysis and autoradiography (see section 3.1). For details of the transfection methods refer to section 4.2.1. In the transfection experiments the vector pCR3.GFP was used as a positive control. The GFP reporter gene that can be measured was expressed in DC by electroporation and flow cytometry resulting in antibodies for measuring GFP levels, which are readily transfected by all methods tested, served as a positive control. The transfection efficiency was estimated 24- and 48 hours post-transfection.

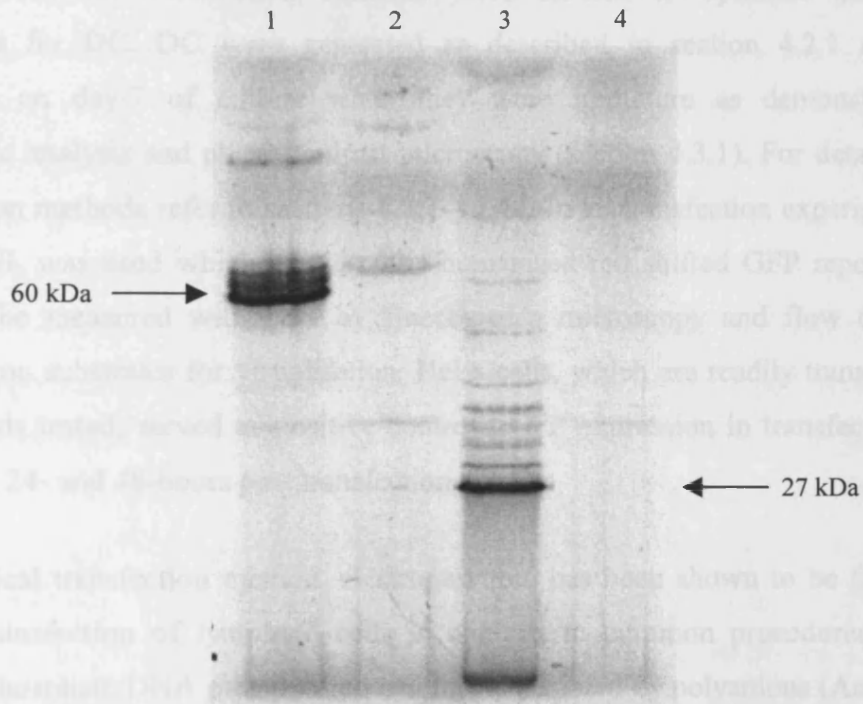


Figure 4.5 Autoradiograph showing GFP products generated by coupled *in vitro* transcription/translation from the DNA templates pCR3.GFP and pCITE.GFP and resolved by SDS-PAGE analysis. Lane (1) Positive control: luciferase product. Lane (2) GFP product generated from pCR3.GFP. Lane (3) GFP product generated from pCITE.GFP. Lane (4) Negative control: no template.

transfected that autocrine-derived DC were successfully transfected by electroporation with plasmid DNA (Zhang *et al.*, 1999; Van Tendeloo *et al.*, 1998; Artalejo *et al.*, 1997).

The cationic lipid DMR18-C (DMR18-BR1) is a cationic liposome suitable for the transfection of non-adherent normal leukemia cell lines RL6 (Jacks, MOLT4, KG-1) and K562 (Civra *et al.*, 1996). The ability of DMR18-C to transfect cells in

results suggest that pCITE.GFP was capable of generating GFP transcripts followed by the protein products of the correct MW *in vitro*. In contrast the construct pCR3.GFP was not as effective and produced levels of protein which were barely detectable.

4.3.6 Optimal conditions of transfection for DC with DNA

Various non-viral transfection methods were studied to optimise transfection conditions for DC. DC were generated as described in section 4.2.1 and were harvested on day-7 of culture when they were immature as demonstrated by phenotypic analysis and phase-contrast microscopy (section 4.3.1). For details of the transfection methods refer to sections 4.2.7-4.2.12. In all transfection experiments the vector pGL was used which contains the humanised red shifted GFP reporter gene that can be measured with ease by fluorescence microscopy and flow cytometry requiring no substrates for visualisation. HeLa cells, which are readily transfected by all methods tested, served as positive controls. GFP expression in transfectants was examined 24- and 48-hours post transfection.

The physical transfection method, electroporation, has been shown to be favourable for the transfection of lymphoid cells in contrast to common procedures such as calcium phosphate/DNA precipitation and those mediated by polyanions (Anderson *et al.*, 1991). Thus, electroporation of DC with plasmid DNA was assessed. Examination by fluorescence microscopy revealed that none of the cells were positive for GFP expression (data not shown). Similar results were also obtained in the presence of chloroquine (data not shown). However, transfection was observed in control HeLa cells run in parallel with 30-40% of the cells on average exhibiting GFP expression (data not shown). These results are consistent with recent published data which demonstrated that monocyte-derived DC were unsuccessfully transfected by electroporation with plasmid DNA (Zhong *et al.*, 1999; Van Tendeloo *et al.*, 1998; Arthur *et al.*, 1997).

The transfection reagent, DMRIE-C (GIBCO-BRL), is a cationic liposome suitable for the transfection of non-adherent human leukemia cell lines like Jurkat, MOLT4, KG-1 and K562 (Ciccarone *et al.*, 1996). The ability of DMRIE-C to transfect cells in

suspension prompted experiments to assess the transfection of DC using DMRIE-C. DC were transfected using several different amounts of the liposome to establish optimal conditions. Similar results were also obtained in the presence of chloroquine (data not shown). However, fluorescence microscopy revealed that none of the cells were positive for GFP expression (data not shown) whereas approximately 30% of the HeLa cells expressed GFP (data not shown).

Superfect Transfection Reagent is an activated-dendrimer designed for effective transfection results in many cell lines including suspension cells and primary cells (Tang *et al.*, 1996). The ability of Superfect to transfect primary cells makes this reagent an attractive candidate for the successful transfection of DC. Thus, experiments were performed to determine whether this polycation was capable of successful transfection of DC with plasmid DNA. DC were transfected using several different amounts of Superfect in an attempt to determine optimal conditions. Fluorescence microscopy revealed that none of the cells were positive for GFP expression whereas 30% of the HeLa cells expressed GFP (data not shown). These experiments adopted a method recommended by Dr Carstens (person^anel communication, 1999) but the efficiencies of 0.1-1% allegedly obtained by Dr Carstens were not reproduced. Similar results were also obtained in the presence of chloroquine (data not shown). The positive controls, which exhibited up to 30% of HeLa cells expressing GFP, confirmed that the DNA and Superfect were both functional.

The cationic peptide, KALA, which binds to DNA, destabilizes membranes and mediates DNA transfection (Wyman *et al.*, 1997) was also utilised to transfect DC with DNA in the presence and absence of chloroquine. Unfortunately, these transfection experiments were also unable to produce any positive transfectants as assessed by fluorescence microscopy.

In summary the results from the transfection experiments of DC with plasmid DNA using electroporation and the transfection reagents DMRIE-C, Superfect and KALA revealed that these methods were unable to yield positive transfectants. However, the results obtained in experiments which utilised the recent commercially available

transfection reagents, Effectene and Fugene-6, to transfer plasmid DNA into DC were more encouraging.

Fugene-6 Transfection Reagent is a unique blend of lipids (non-liposomal formulation) and other compounds which is capable of transfection of mammalian and other cell types with high efficiency and minimal damage to cells (Roche Ltd.). The fact that this reagent is able to transfect many cell types successfully, prompted further transfection experiments of DC using this reagent. DC were transfected using a range of different amounts of Fugene-6 to determine optimal conditions. Examination by fluorescence microscopy revealed that a very small percentage of DC (<0.1%) were positive for GFP expression after 24- and 48-hours. This extremely low transfection efficiency was observed in DC transfected with pGL using 6, 9 and 12 μ l of Fugene-6, 24 and 48-hours post transfection (Figures 4.6, 4.7, 4.8; Panels B). In all cases the morphology of GFP-expressing cells was typical of DC with many cell processes as assessed by phase contrast microscopy (Figures 4.6, 4.7, 4.8; Panels A). Similar results were also obtained in the presence of chloroquine (data not shown). These results were not consistent with data obtained by the company Cobra Therapeutics which achieved higher transfection efficiencies of 0.1-1.0% in DC (Peter Trinder, personal communication, 1999). In addition GFP expression was observed in approximately 30-40% of control cells run in parallel (Figure 4.9; Panel B). Additional transfection experiments of DC, using identical conditions as above apart from using less media per well to increase the density of cells/ml, resulted in none of the DC expressing GFP.

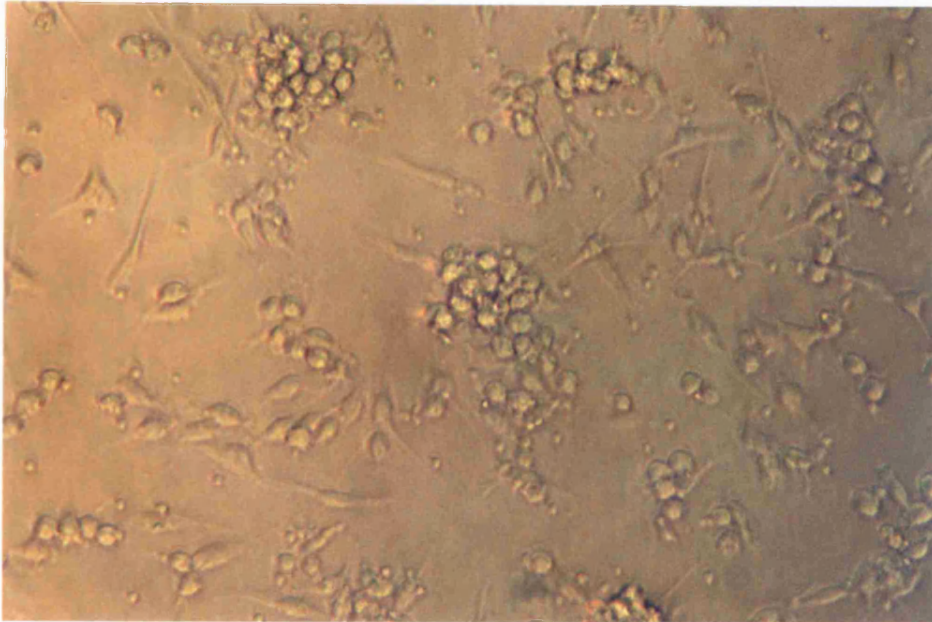
Effectene Transfection Reagent is based on a unique non-liposomal lipid formulation combined with a specific DNA-condensing Enhancer. Effectene Reagent has been shown to produce higher transfection efficiencies in many cell lines including suspension cells and primary cells than many widely used liposomal reagents (Sugie *et al.*, 1999). Effectene also allows transfection in the presence of serum to ensure healthy cells and low cytotoxicity without lowering transfection efficiencies. Thus, the ability of this reagent to transfect suspension cells and primary cells prompted additional transfection experiments of DC using Effectene. DC were transfected using a range of different amounts of Effectene, as recommended by the manufacturer, to

determine optimal conditions. Examination by fluorescence microscopy revealed that a low percentage of cells (<0.1%), transfected with pGL using 4µl of Effectene, were positive for GFP expression (Figure 4.10, Panel B). DC transfected with pGL using other amounts of Effectene did not express GFP. The morphology of GFP-expressing cells was typical of DC with many cell processes as assessed by phase contrast microscopy (Figure 4.10, Panel A). Similar results were also obtained in the presence of chloroquine (data not shown). In addition, GFP expression was observed in approximately 60% of control cells run in parallel (Figure 4.11, Panel B).

N.B. The transfection efficiencies of HeLa cells were calculated by counting the number of positive cells in the field of view and converting this to a percentage of the total number of cells in the identical area.

Overall the majority of the transfection methods described above were unable to successfully transfect DC with plasmid DNA. However, Fugene-6 and Effectene did achieve very low transfection efficiencies of <0.1%. These low and null transfection efficiencies highlight the difficulties encountered in the successful transfection of DC using a range of different non-viral methods including those which have been reported to be successful in the transfection of primary cell lines. Further experiments are required using more effective non-viral transfection methods to increase the transfection efficiencies of DC to at least 5-10% in order to guarantee a detectable level of gene expression.

A

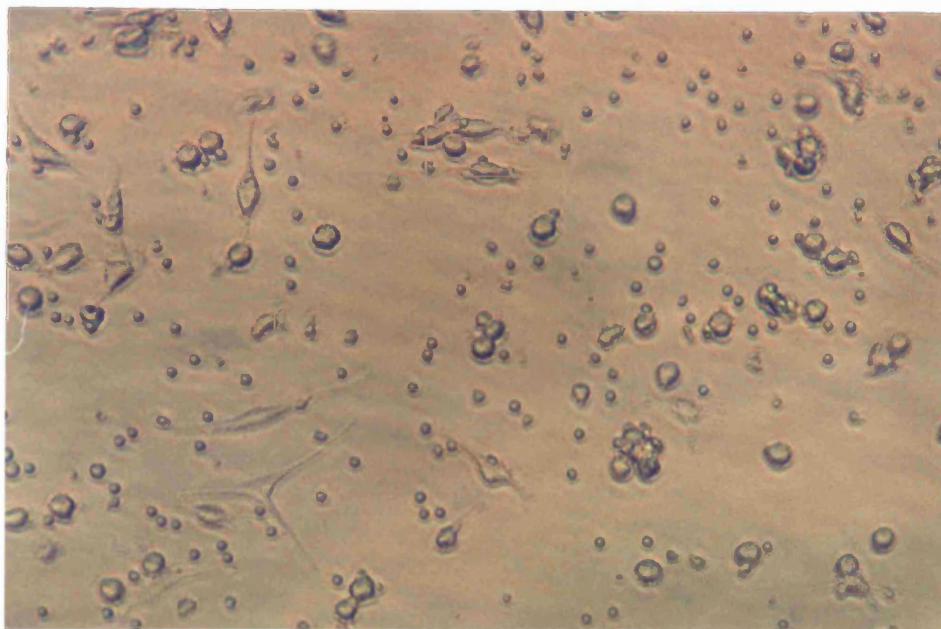


B



Figure 4.6 Photomicrographs taken of an identical area of DC transfected with pGL using 6 μ l of Fugene-6 24-hours after transfection. (A) Total number of cells under phase contrast microscopy. (B) Immunofluorescence microscopy showing the number of cells which have been transfected with pGL.

A



B

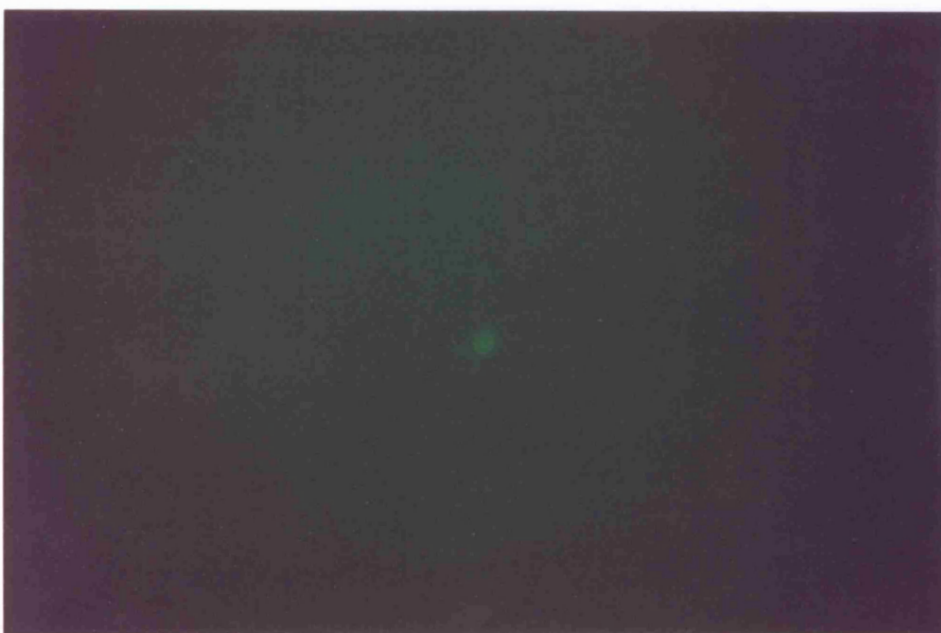
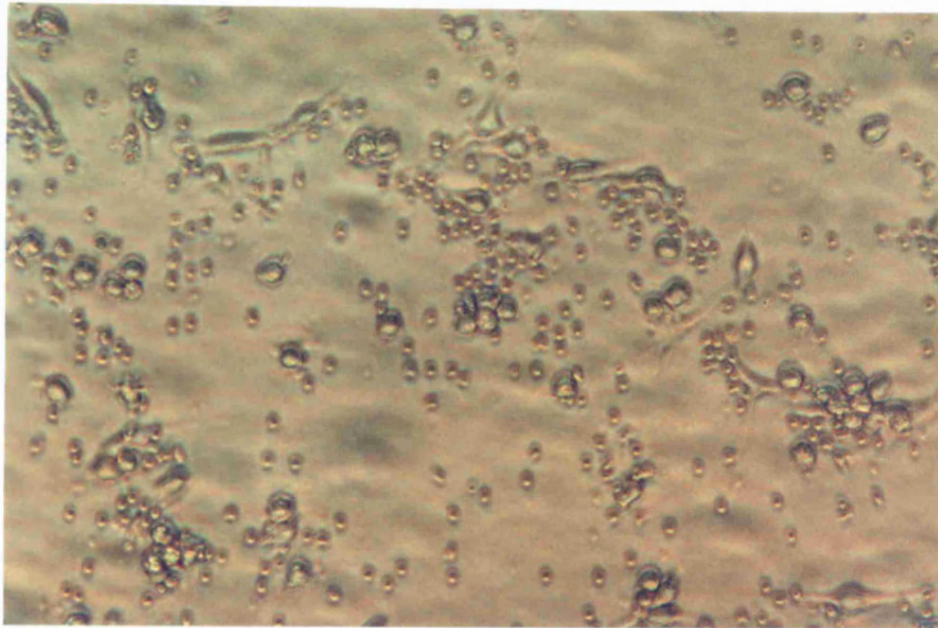


Figure 4.7 Photomicrographs taken of an identical area of DC transfected with pGL using 9 μ l of Fugene-6 48-hours after transfection. (A) Total number of cells under phase contrast microscopy. (B) Immunofluorescence microscopy showing the number of cells which have been transfected with pGL.

A



B

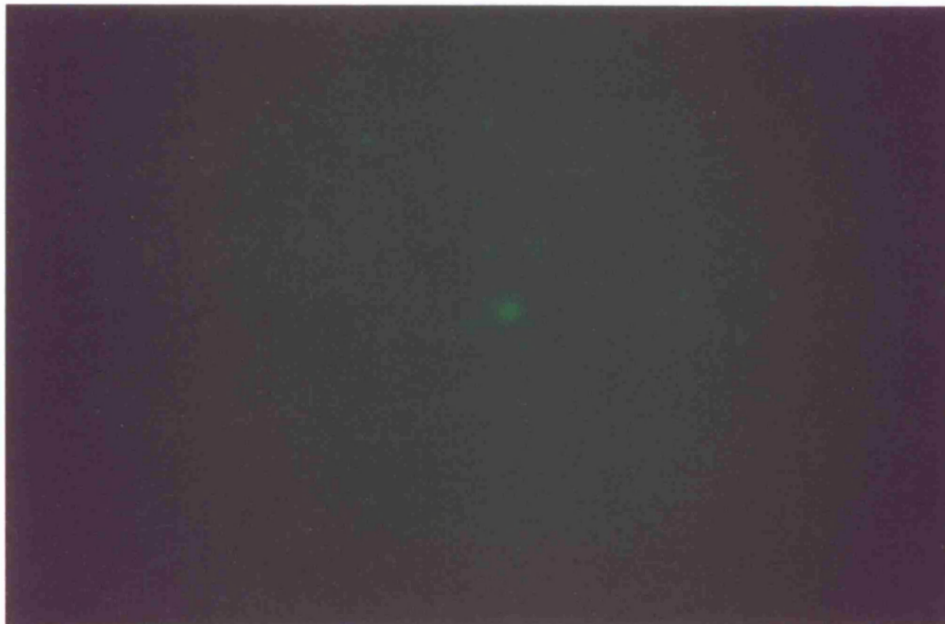
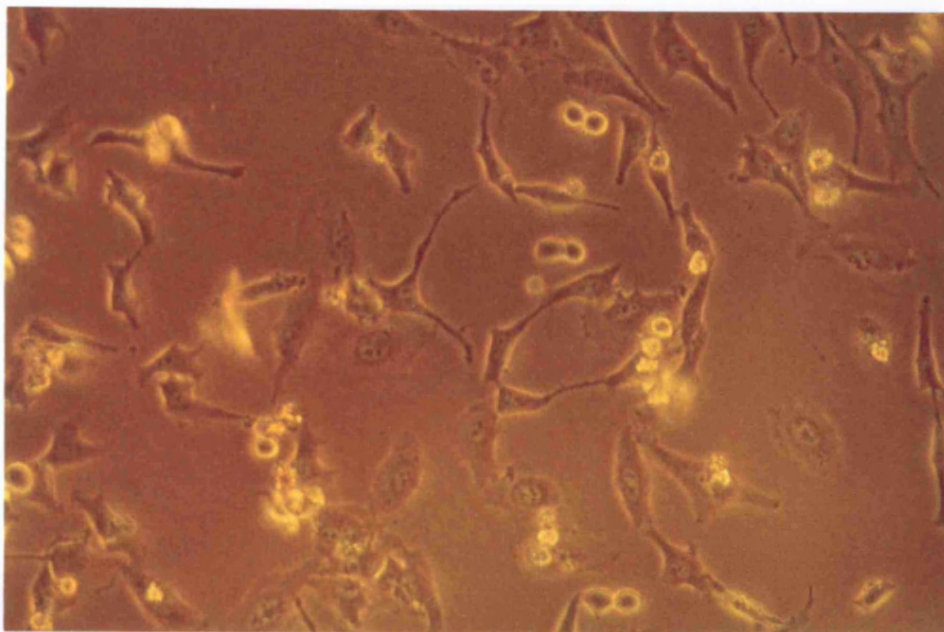


Figure 4.8 Photomicrographs taken of an identical area of DC transfected with pGL using 12 μ l of Fugene-6 48-hours after transfection. (A) Total number of cells under phase contrast microscopy. (B) Immunofluorescence microscopy showing the number of cells which have been transfected with pGL.

A



B

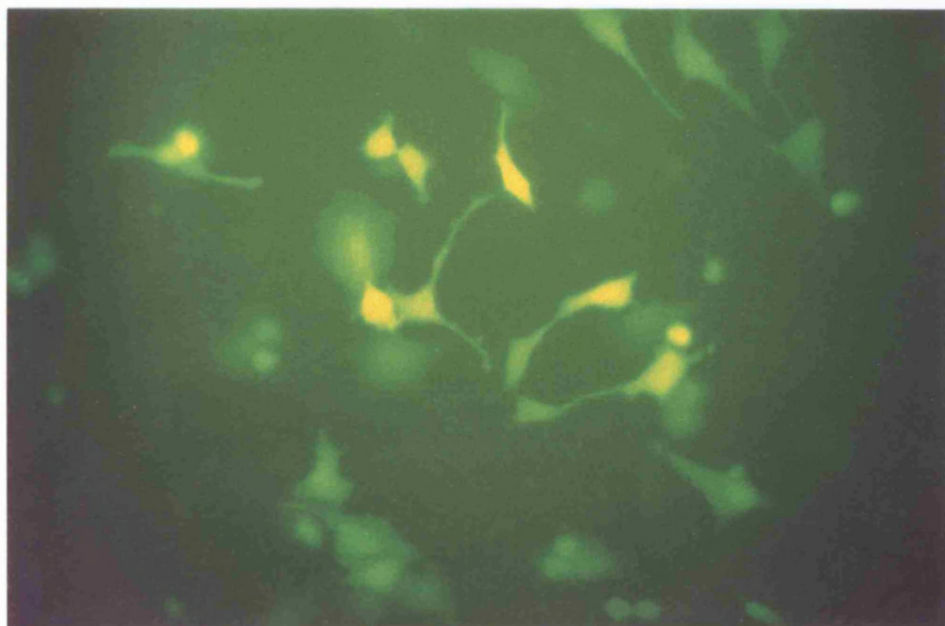
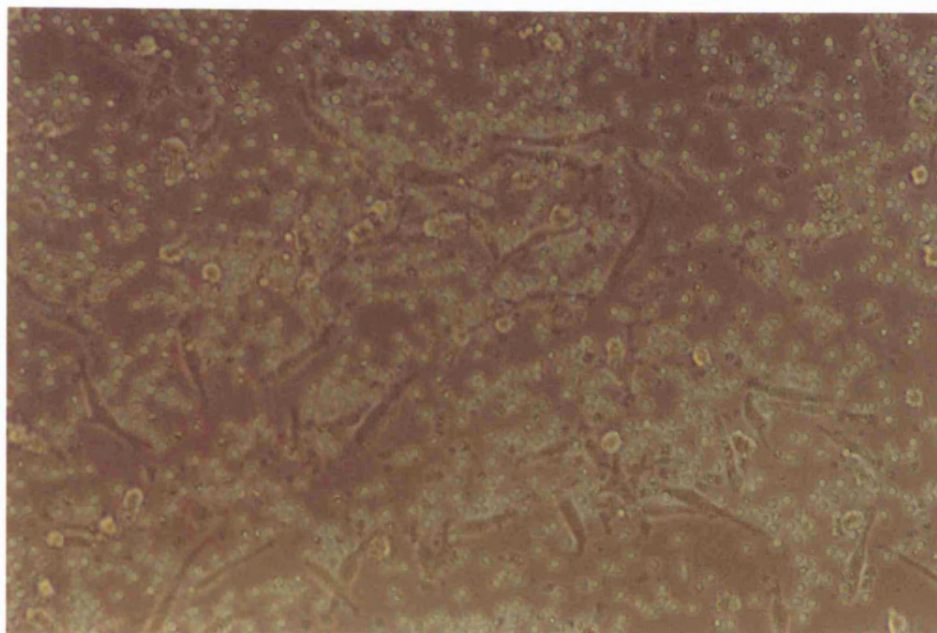


Figure 4.9 Photomicrographs taken of an identical area of HeLa cells transfected with pGL using 3 μ l of Fugene-6 48-hours after transfection. (A) Total number of cells under phase contrast microscopy. (B) Immunofluorescence microscopy showing the number of cells which have been transfected with pGL.

A



B

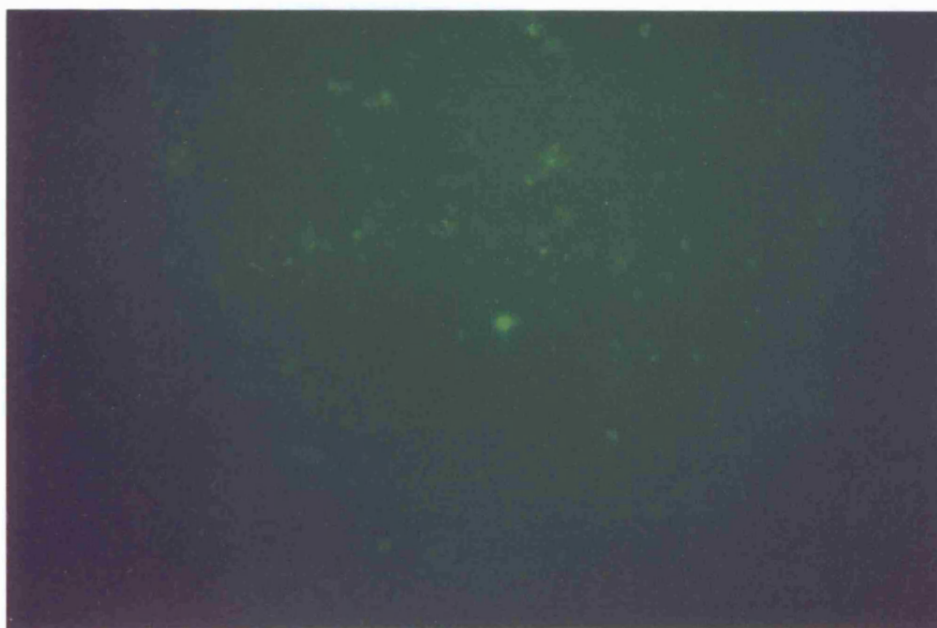
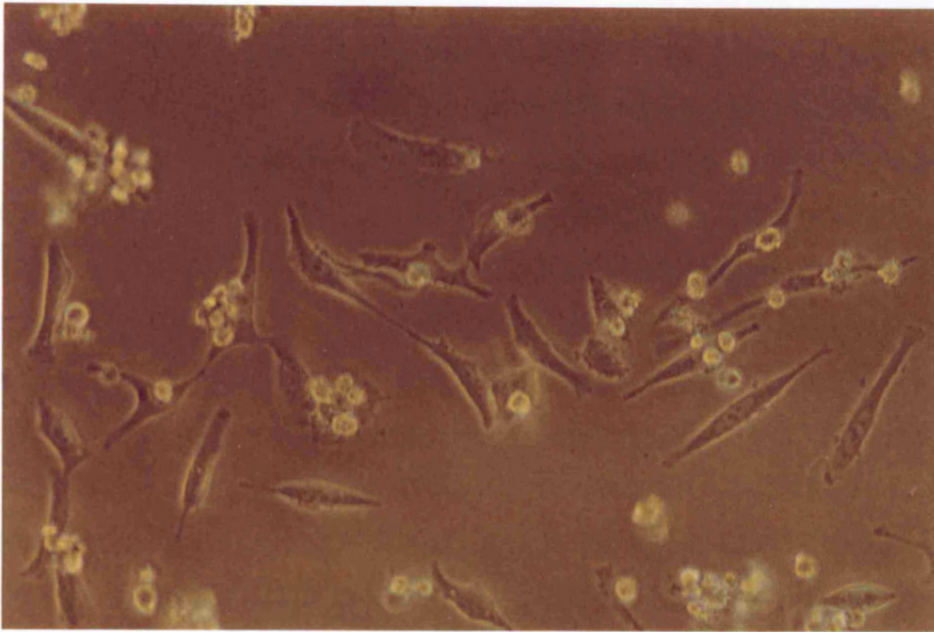


Figure 4.10 Photomicrographs taken of an identical area of DC transfected with pGL using 4 μ l of Effectene 48-hours after transfection. (A) Total number of cells under phase contrast microscopy. (B) Immunofluorescence microscopy showing the number of cells which have been transfected with pGL.

A



B

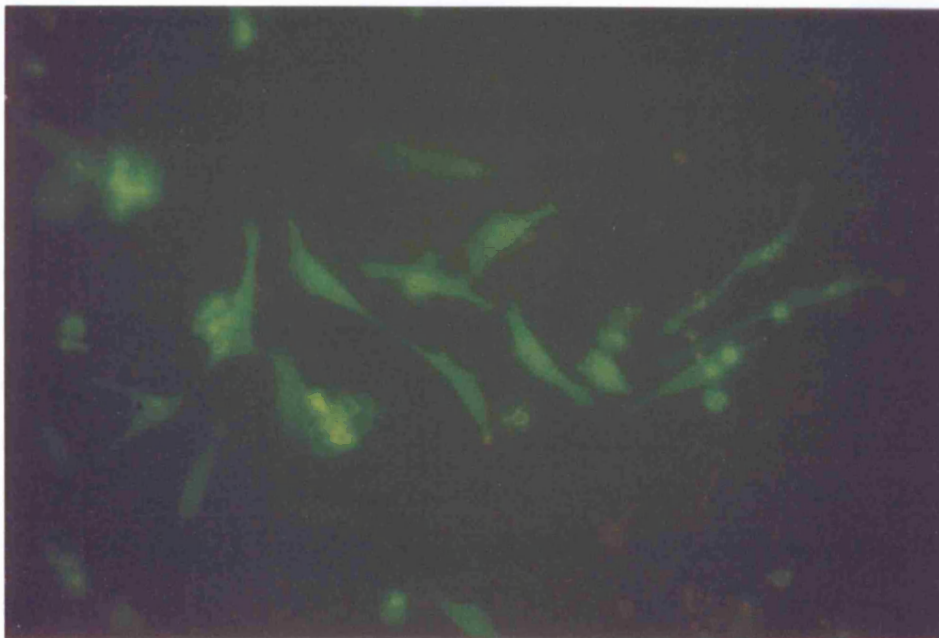


Figure 4.11 Photomicrographs taken of an identical area of HeLa cells transfected with pGL using 10 μ l of Effectene 48-hours after transfection. (A) Total number of cells under phase contrast microscopy. (B) Immunofluorescence microscopy showing the number of cells which have been transfected with pGL.

4.4 Discussion

A safer alternative to transfecting DC with plasmid DNA is to use transcripts of RNA which have a shorter half life and therefore reduce the potential risk of tumour antigens remaining in the system for prolonged periods (Gilboa., 1998). Boczkowski *et al.* (1996) have successfully transfected DC with RNA using the transfection reagent, DOTAP, along with others such as Nair *et al.* (1998) who used the transfection reagent, DMRIE-C. Thus, in this chapter attempts were made to transfect DC with RNA transcripts encoding GFP using DOTAP. Results revealed that none of the cells were expressing GFP and consequently optimal conditions were not established. In order to assess the effectiveness of these transcripts, HeLa cells, which are readily transfected with DNA, were transfected with RNA using three different methods: DOTAP, Effectene and electroporation. However, none of these approaches resulted in positive transfectants. In contrast, Sugie *et al.* (1999) achieved transfection efficiencies of up to 58.6% in 293 cells transfected with *in vitro* transcribed RNA using the reagent Effectene.

The unsuccessful transfections in this study may have been caused by the poor quality of the RNA transcript and its inability to produce detectable levels of the functional protein product, GFP. In order to investigate this possible cause, *in vitro* coupled transcription/translation was performed using the DNA templates, pCR3.GFP and pCITE.GFP. The results revealed that protein products of the correct MW were synthesised using pCITE.GFP in comparison with extremely low levels of protein product produced by pCR3.GFP. These low levels of GFP may reflect the inability of pCR3.GFP to synthesise RNA effectively *in vitro* due to the absence of a poly A sequence which confers stability. In contrast pCITE.GFP contains such a sequence which is situated at the 3' terminus of the MCS. Although pCITE.GFP was capable of the transcription and translation of GFP *in vitro*, transfections of HeLa cells with the corresponding transcripts were also unsuccessful. Despite vigorous attempts to minimise RNase contamination, RNases present in the system may have rapidly degraded the transcripts before translation took place. Also transfection reagents may not have formed complexes with RNA and consequently did not allow RNA transfer. Control cells, which were HeLa cells transfected with GFP cDNA using identical

transfection reagents, yielded a high percentage of positive transfectants and therefore demonstrated that all the reagents were functional.

Also in this chapter, several different approaches for non-viral transfer of DNA into DC were investigated which included electroporation, lipofection, and techniques utilising a cationic peptide or non-liposomal reagents. Of the approaches used the non-liposomal reagents, Fugene-6 and Effectene, were the most effective whereas the remaining techniques induced levels of gene expression that were barely detectable above background. However, as stated, GFP expression was still minimal using Fugene-6 and Effectene compared with the expression achieved when control HeLa cells were transfected.

Due to the high endosomal or lysosomal activities of DC, transfections were also performed in the presence of chloroquine which raises the pH of lysosomal compartments thereby reducing the degradative enzymatic activity. Despite treatment with chloroquine, there were no differences in GFP expression. These results imply that low or null transfection efficiencies of DC using the non-viral methods described in this chapter have not been caused by rapid degradation in the lysosomal and endosomal compartments. Alternatively, the results may reflect the ineffective transfection methods for DNA transfer into DC.

The difficulty of measuring protein expression in transfected DC has been demonstrated by Philip *et al.* (1998). They performed experiments in which they transfected DC using an adeno-associated virus plasmid DNA complexed to cationic liposomes. Although they were able to show transgene expression of several genes as measured by mRNA levels using RT-PCR, the only protein levels detected were of an enzymatic protein, CAT. The protein expression of non-enzyme molecules (MART-1, CEA) was undetectable by methods such as flow cytometry or Western blot analysis whereas CAT was detected by very sensitive enzymatic assays. Similarly, other Research Groups have successfully detected transgene protein products in transfected DC which are enzymatic proteins such as CAT, β -galactosidase, luciferase and tyrosinase as assessed by enzyme activity despite low transfection efficiencies (Alijagic *et al.*, 1995; Arthur *et al.*, 1997). Therefore, alternative reporter genes which

code for enzymes such as CAT may be more efficient at measuring transfection efficiencies as opposed to GFP due to the more sensitive detection methods used.

The extremely low levels of transgene expression in DC, which have been detected in this study, may not be as disappointing as originally thought. As mentioned in chapter one, DC are the most potent stimulatory APC. Only a few DC are necessary to provoke a strong T-cell response *in vitro* or *in vivo* with a single DC maximally stimulating 100-30000 T cells *in vitro*. This immunostimulatory capacity of DC has been confirmed by recent transfection experiments. Alijagic *et al* (1995) performed experiments in which monocyte-derived GM-CSF- and IL-4-cultured DC were transfected with the tyrosinase gene using the lipofection reagent, Lipofectin, (GIBCO BRL). Although only low levels of transgene expression were observed, as in this study, tyrosinase-transfected DC were able to cluster and activate T cells. Also experiments performed by Nair *et al.* (1998) have shown that DC transfected with RNA transcripts of GFP and CEA were capable of inducing CTL, which recognised and lysed only the antigen specific target, despite the fact that the GFP protein product could not be detected in transfected DC by fluorescence microscopy or flow cytometry (Gilboa., personal communication, 1999). Therefore, further experiments will need to investigate whether GFP expression produced by any of the transfection techniques in this study will be sufficient to allow DC to stimulate antigen-specific T-cells. This would confirm the potent immunostimulatory capacity of DC and the fact that a only small proportion of the DC have to be positively transfected in order to generate such a response.

Interestingly, Cobra therapeutics have developed a novel non-viral system for the efficient *ex vivo* transfection of human DC with plasmid DNA. The proprietary formulation system, consisting of a cationic peptide, CL22, generates self-assembling complexes containing plasmid DNA which can transfect approximately 17% of DC. DC transfected with a model antigen, tyrosinase related protein-2, result in the stimulation of autologous antigen-specific T-cells. Unfortunately, this gene delivery system is not currently available. However, it holds promise for an effective non-viral method of transfection for human DC which is capable of achieving higher

transfection efficiencies than those obtained using the non-viral reagents and systems currently available.

In summary, these experiments illustrate the difficulty of achieving high efficiency RNA/DNA transfer in DC using non-viral methods. Although results of DC transfected with DNA, which reveal a small proportion of DC expressing GFP, are encouraging, further experiments are necessary to establish optimal transfection conditions using more effective methods such as the recent non-viral system pioneered by Cobra therapeutics. This will enable progress towards an effective vaccine for breast cancer.

4.5 Future Work

- Identify optimal transfection conditions of DC with Fugene-6 and Effectene, using the reporter gene, CAT, in order to increase the sensitivity of detection by using a sensitive ELISA detection method.
- Assess transfections by determining whether positively transfected DC can induce autologous T-cell responses *in vitro* utilising the reporter genes, GFP and CAT. This approach could be adopted as an alternative method for the establishment of optimal conditions instead of gene expression analysis.
- Repeat transfection experiments of HeLa cells with RNA using fresh reagents and RNA transcripts in order to minimise possible contamination with RNAses. Also perform identical experiments replacing HeLa cells with 293 cells.
- Establish optimal transfection conditions of DC with DNA using the cationic peptide produced by Cobra Therapeutics. (Details of peptide sequence and transfection protocol currently in press).
- Transfect DC using an optimal non-viral method, with constructs encoding p53 and analyse CD4⁺ T-cell proliferative responses.

Chapter Five

Concluding Remarks

Chapter Five

5.1 Concluding remarks

The aim of this study was to design a DC-based vaccine for breast cancer which would elicit an antitumour CD4⁺ T-cell response. The tumour suppressor protein, p53, was selected as the antigen for manipulation in this strategy due to the increasing evidence of immune responses to both wild type and mutant p53 in breast cancer patients. As the delivery of nucleic acids is preferable to using recombinant protein or peptide, DC would be genetically modified to express MHC class II restricted p53 epitopes, thus, leading to the induction of antigen-specific CD4⁺ T-cells.

There were two major goals to attain during the initial preparation of this vaccine. Firstly, to enhance the CD4⁺ T-cell response, it was necessary to target endogenous p53 to the MHC class II pathway for presentation to CD4⁺ T-cells. A signal peptide, YTPL, present in the cytoplasmic tail of DM was fused at the C-terminus of p53 to allow trafficking of this chimeric protein to the lysosomal compartment. In addition, an amino signal sequence, LS, was appended to the N-terminus to allow p53 to translocate the ER membrane prior to lysosomal sorting. Intracellular immunofluorescence staining using antibodies to p53 and CD63 followed by CLSM were employed to determine whether p53-DM β co-localised with an endogenous lysosomal marker, CD63. The results revealed that p53-DM β , in the absence of the LS, had accumulated in the cytosol whereas p53 alone localised to the nucleus as expected. More importantly in the presence of LS, p53-DM β trafficked to the lysosomal compartment but due to over expression of the protein, intense staining of p53-DM β in the biosynthetic pathway had masked lysosomal staining. Comparative analysis with control constructs, which targeted p53 to the membrane and also allowed secretion of p53, provided further evidence that localisation to the lysosomes had probably occurred. Further subcellular fractionation experiments are necessary to confirm these results.

The second objective involved the establishment of optimal transfection conditions of DC with nucleic acids using non-viral methods. Although viral gene transfer methods

are currently the most successful in the genetic modification of DC, they are associated with many risks as discussed in chapter four. Therefore, non-viral methods of transfection are favourable eliminating many of the patient and environmental safety considerations. Initially, DC were transfected with RNA transcripts encoding GFP. Unfortunately, these experiments did not produce positive transfectants. Further experiments are required to test the effectiveness of these transcripts using HeLa cells and 293 cells. Transfection experiments of DC with DNA were also performed using variety of transfection methods. DC were transfected with the reporter gene, GFP, and expression was assessed by fluorescence microscopy at various time points post transfection. However, the majority of these transfection techniques did not result in DC which were positive for GFP expression. Only, the transfection reagents, Fugene-6 and Effectene yielded positive transfectants, albeit efficiencies were very low. However, these results were not discouraging as very low numbers of DC are capable of provoking strong T-cell responses *in vitro* and *in vivo*. Further experiments are necessary to analyse T-cell responses to DC transfected with GFP followed by the comparative analyses of T-cell responses to DC transfected with constructs encoding p53.

In summary, this study has successfully targeted p53-DM β to lysosomal compartments of HeLa cells and has investigated the use of many non-viral techniques to transfect DC. Further work is necessary to confirm localisation of p53-DM β and to further optimise transfections conditions for DC. Therefore, this study has paved the way for the design of a DC-based vaccine strategy for breast cancer with a view to inducing a MHC class II restricted CD4⁺ T-cell response to p53 and conferring long-term and effective antitumour immunity.

5.2 Future aims and prospects

Once experiments have confirmed that p53-DM β has been targeted to the lysosomal compartments of HeLa cells and optimal conditions of DC have been established, further experiments are necessary to determine whether DC transfected with p53,

targeted to the MHC class II pathway, can activate and prime antigen-specific CD4⁺ T-cell proliferative responses.

If preclinical studies provide evidence that this vaccination strategy is capable of generating potent anti-p53 CD4⁺ and CD8⁺ T-cell responses and reducing tumour load *in vivo* using animal models, there is a possibility that the DC-based vaccine could enter clinical trials in the foreseeable future. Briefly, this would involve the generation of DC from breast cancer patients PBMC *ex vivo*, followed by subsequent transfection of DC with p53 engineered to traffic to the MHC class II pathway. The use of an efficient non-viral system for genetic modification of DC would eliminate potential risks posed by viral methods. Subsequent administration of these antigen expressing DC to the patients may result in a potent antitumour immune response involving both the CD4⁺ and CD8⁺ T-cell cells. This form of adjuvant therapy would lead to the eradication of residual tumour cells, following surgical removal of the primary tumour, and would prevent recurrence of secondary tumours.

An additional aspect which could be addressed in future stages of this project is whether the immunostimulatory capacity of DC could be enhanced by the presence of cytokines such as GM-CSF, TNF- α or ligation of CD40 with soluble CD40L. As discussed in chapter one, DC up-regulate costimulatory molecules in response to certain inflammatory cytokines which in turn promote T-cell activation. GM-CSF has been identified as an important growth factor for DC (Inaba *et al.*, 1992) and maintains the efficient presentation of soluble antigen (Sallusto *et al.* 1994). TNF- α is known to contribute to both DC maturation (Sallusto *et al.*, 1995) and activation (Rieser *et al.*, 1997). Also cross-linking CD40 on DC by cell-bound CD40L has been shown to promote DC maturation (Caux *et al.*, 1994a; Flores-Romo *et al.*, 1997; Brossart *et al.*, 1998), upregulate expression of costimulatory molecules (Caux *et al.*, 1994a; Cella *et al.*, 1996) and enable DC to stimulate CTL (Ridge *et al.*, 1998; Bennett *et al.*, 1998; Schoenberger *et al.*, 1998). Recent evidence suggests that incorporation of such molecules in DC-based vaccine strategies improves the immunogenicity of DC resulting in optimal induction of tumour-specific T-cell responses. Klein *et al.* (2000) engineered bone-marrow derived DC to express MAGE-1 and also either GM-CSF, TNF- α or CD40L. Their findings revealed that

coexpression of either GM-CSF, TNF- α or CD40L with MAGE-1 led to a significantly increased therapeutic effect in tumour bearing mice compared with DC expressing MAGE-1 alone. The immunological mechanism as shown for GM-CSF-transduced DC, involved MAGE-1 specific CD4⁺ and CD8⁺ T-cells. Expression of GM-CSF by DC led to enhanced CTL activity, potentially mediated by increased numbers of DC in draining lymph nodes as detected by dye tracking experiments. In addition, Morse *et al.* (1998) demonstrated that optimal stimulation of CEA-specific CTL *in vitro* by RNA-transfected DC occurred when the DC, from cancer patients, were loaded with CEA RNA, followed by maturation with CD40L. The results from these studies imply that the immunostimulatory capacity of DC, to be utilised in this p53-based vaccination strategy, could be improved by the incorporation of either GM-CSF, TNF- α or CD40L. Future experiments could investigate this possibility.

Thus, immunotherapy using autologous DC, loaded with nucleic acids encoding p53 engineered to enhance the CD4⁺ T-cell response, in the presence or absence of accessory molecules, emerges as a potentially powerful vaccination strategy for the treatment of breast cancer patients. Furthermore, the model breast tumour antigen, p53, utilised in this strategy is shared with many other tumour types such as ovarian, lung and stomach, which could lead to the widespread clinical application of this approach.

Appendix One

Composition of solutions

Agarose gel loading buffer (6x)

0.25% bromophenol blue, 0.25% xylene cyanol FF, 30% glycerol in water

Detection reagent for ECL

0.2mM p-coumaric acid, 1.25mM luminol, 5-amino-2,3-dihydro-1,2-phthalazinedione, 0.009% H₂O₂, 0.1M Tris-HCL pH 8.5.

Luria-Bertoni (LB) media

1% tryptone, 0.5% yeast extract, 1% NaCl

Phosphate-buffered saline (PBS)

80mM Na₂HPO₄, 20mM NaH₂PO₄.2H₂O, 100mM NaCl (pH 7.4)

Protein electrophoresis buffer (Lammeli et al., 1970)

250mM glycine, 25mM tris base, 0.1% SDS

Protein loading buffer (3x)

187.5mM Tris-HCL pH 6.8, 6% SDS, 30% glycerol, 15mM EDTA pH6.8, 0.1% bromophenol blue, 100mM DTT (DTT is added to 3x or 2x buffer just before use and stored at -20°C).

Protein transfer buffer (Towbin et al., 1979)

0.025M Tris-HCL pH8.3, 0.15 glycine, 20% methanol

MOPS (10x)

0.2M sodium MOPS (3-[Morpholino]-propane-sulphonic acid), 0.08M sodium acetate, 0.01M disodium EDTA pH 7.0

RNA extraction solution

4M guanidinium thiocyanate, 25mM sodium citrate, combined with phenol and 2M sodium acetate in a ratio of 1:1:0.1, with 0.1M β-mercaptoethanol

SOC media

2% tryptone, 0.5% yeast extract, 10mM NaCl, 2.5mM KCl, 10mM MgCl₂, 10mM MgSO₄, 20mM glucose

Tris-acetate (TAE)

40 mM Tris-base, 40 mM glacial acetic acid, 1 mM EDTA (pH 8.0)

Tris-buffered saline (TBS)

20mM Tris base, 137mM NaCl (pH 7.6)

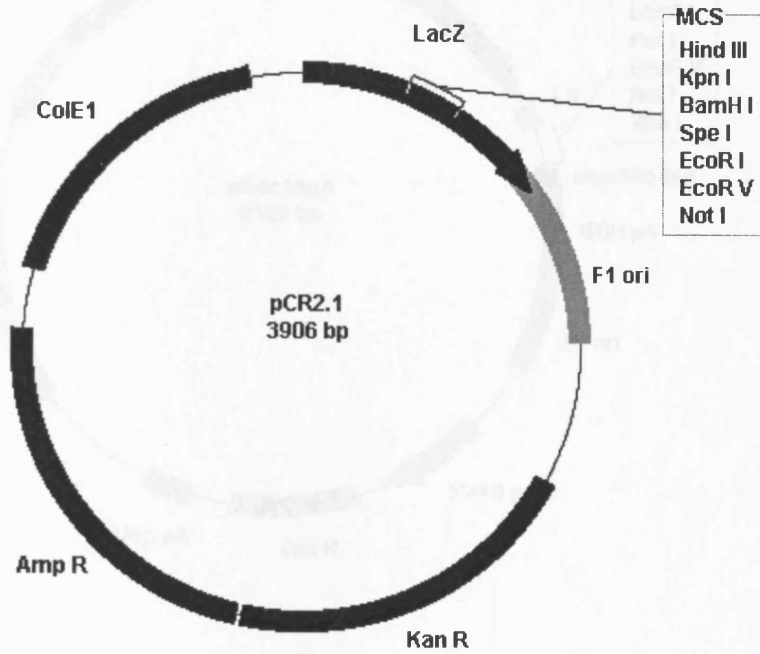
Tris-EDTA (TE)

10mM Tris-HCl, 1mM EDTA (pH 7.5)

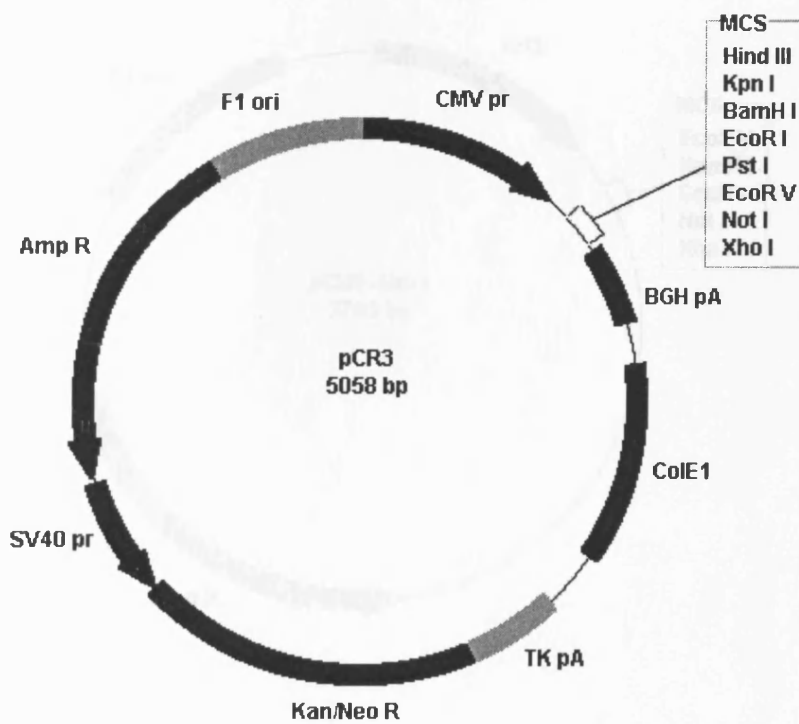
TNE

10mM Tris-HCl, 100mM NaCl, 1mM EDTA (pH 8.0)

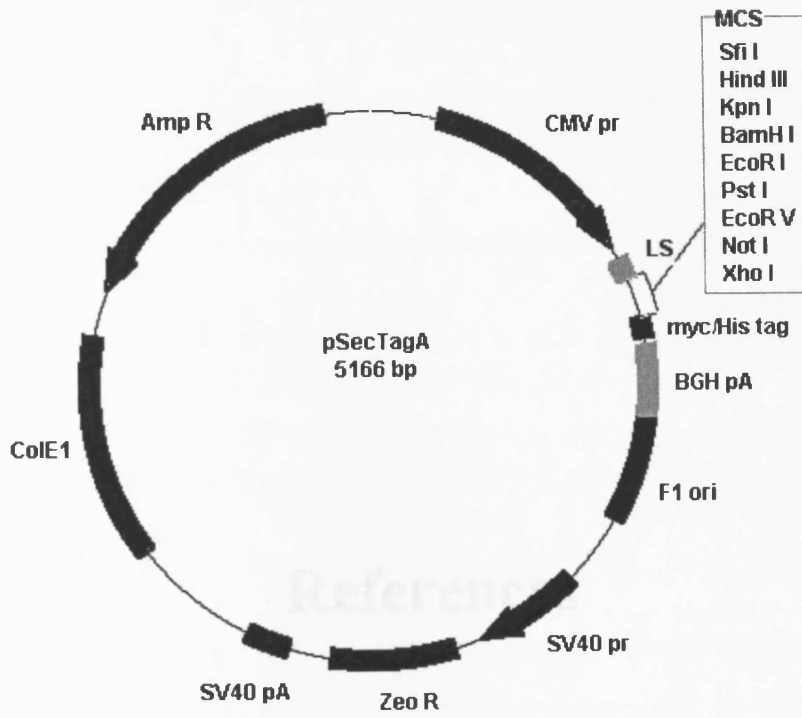
Appendix Two



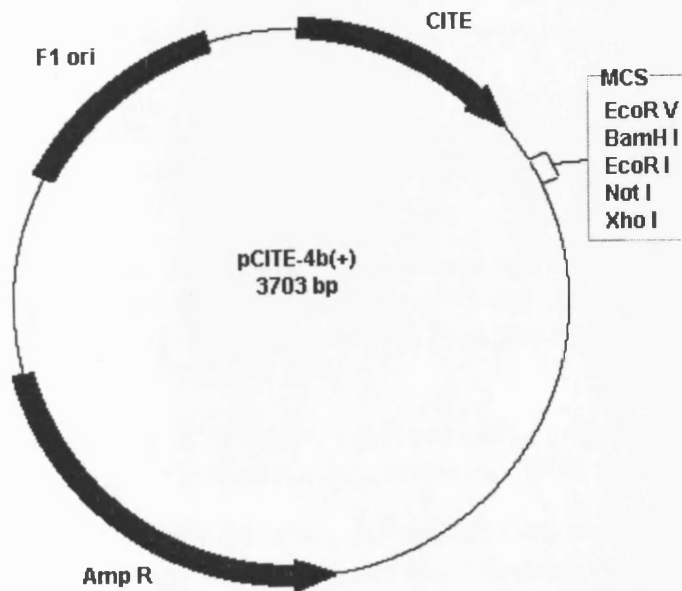
pCR2.1 Vector Map



pCR3 Vector Map



pSecTagA Vector Map



pCITE-4b(+) Vector Map

References

References

- Aaltomaa S., Lipponen P., Eskelinen M., Kosma V-M., Marin S., Alhava E., & Syranen K. Lymphocyte infiltrates as a prognostic variable in female breast cancer. *Eur. J. Cancer*. 1992, 28A:859-864.
- Acha-Orbea H., & Palmer E. Mls-a retrovirus exploits the immune system. *Immunol. Today*. 1991, 12:356-361.
- Albert M.L., Sauter B., & Bhardwaj N. Dendritic cells acquire antigen from apoptotic cells and induce class-I restricted CTLs. *Nature*. 1998, 182:86-89.
- Alijagic S., Moller P., Artuc M., *et al.* Dendritic cells generated from peripheral blood transfected with human tyrosinase induces specific T cell activation. *Eur. J. Immunol.* 1995, 25:3100-3107.
- Alters S.E., Gadea J.R., & Philip R. Immunotherapy of cancer, generation of CEA specific CTL using CEA peptide pulsed dendritic cells. In R. Castagnoli (Ed.), *Dendritic cells in fundamental and clinical immunology*. 1997, pp.519-514. NY: Plenum Press.
- Amigorena S., Drake J., Webster P., & Mellman I. Transient accumulation of new class II MHC molecules in a novel endocytic compartment in B lymphocytes. *Nature*. 1994, 369:113-120.
- Amigorena S., Webster P., Drake J., Newcomb J., Cresswell P., & Mellman I. Invariant chain cleavage and peptide loading in major histocompatibility complex class II vesicles. *J. Exp. Med.* 1995, 181:1729-1741.
- Anderson M.L.M, Spandidos D.A., & Coggins J.R. Electroporation of lymphoid cells – factors affecting the efficiency of transfections. *J. Biochem & Biophysical Methods*. 1991, 22:207-222.
- Anderson M.S., Swier K., Arneson L., & Miller J. Enhanced antigen presentation in the absence of the invariant chain endosomal localisation signal. *J. Exp. Med.* 1993, 178:1959-1969.
- Androlewicz M.J., Anderson K.S., & Cresswell P. Evidence that transporters associated with antigen processing translocate a major histocompatibility complex class I-binding complex into the endoplasmic reticulum in an ATP-dependent manner. *Proc. Natl. Acad. Sci. USA*. 1993, 90:30-34.
- Androlewicz M.J. & Cresswell P. Human transporters associated with antigen processing possess a promiscuous peptide-binding site. *Immunity*. 1994, 1:7-14.
- Androlewicz M.J., Ortmann B., van Endert P.M., Spies T., & Cresswell P. Characteristics of peptide and major histocompatibility complex class I/ β_2 -microglobulin binding to the transporter associated with antigen processing (TAP1 and TAP2). *Proc. Natl. Acad. Sci. USA*. 1994, 91:12716-12720.
- Apostolopoulos V., McKenzie I.F.C., & Pietersz G.A. Breast cancer immunotherapy, Current status and future prospect. *Immunol. Cell Biol.* 1996, 74:457-464.

- Arthur J.F., Butterfield L.H., Roth M.D., *et al.* A comparison of gene transfer methods in human dendritic cells. *Cancer Gene Therapy*. 1997, 4:17-25.
- Avva R.R. & Cresswell P. *In vivo* and *in vitro* formation and dissociation of HLA-DR complexes with invariant chain-derived peptides. *Immunity*. 1994, 1:763.
- Baak J.P.A., Van Dop H., Kurver P.H.J., & Hermans J. The value of morphometry to classic prognosticators in breast cancer. *Cancer*. 1985, 56:374-382.
- Baker S.J., Markowitz E.R., Fearon E.R. *et al.* Suppression of human colorectal carcinoma cell growth by wild type p53. *Science*. 1990, 249:912-915.
- Banchereau J., Steinman R.M. Dendritic cells and the control of immunity. *Nature*. 1998, 392:245-252.
- Bank I., Book M., Huszar M., Baram Y., Schnirer I., & Brenner H. V2+ and γ T lymphocytes are cytotoxic to the MCF 7 breast carcinoma cell line and can be detected among the T cells that infiltrate breast tumours. *Clin. Immunol. Immunopathol.* 1993, 67:17-24.
- Barak Y., Juven T., Haffner R., & Oren M. mdm2 expression is induced by wild type p53 activity. *EMBO J.* 1993, 12:461-468.
- Bender A., Bui L.K., Feldman M.A.V., Larsson M., & Bhardwaj N. Inactivated influenza virus, when presented on dendritic cells, elicits human CD8⁺ cytolytic T cell responses. *J. Exp. Med.* 1995, 182:1663-1671.
- Bennett S., Carbone F., Karamalis F., Flavell R., Miller J., & Heath W. Help for cytotoxic-T-cell responses is mediated by CD40 signalling. *Nature*. 1998, 393:478-480.
- Berthiaume E.P., Medina C., & Swanson J.A. Molecular size-fractionation during endocytosis in macrophages. *J. Cell. Biol.* 1995, 129:989-998.
- Bevan M.J., 1977. Priming for a cytotoxic response to minor histocompatibility antigens: antigen specificity and failure to demonstrate a carrier effect. *J. Immunol.* 1977, 118:1370-1374.
- Bevan M.J., 1987. Class discrimination in the world of immunology. *Nature*. 1987, 325:192-194.
- Bevec T., Stoka V., Pungercic G., Dolenc I., & Turk V. Major histocompatibility complex class II –associated p41 invariant chain fragment is a strong inhibitor of lysosomal cathepsin. *L.J. Exp. Med.* 1996, 183:1331-1338.
- Bikoff E.K., Germain R.N., & Robertson E.J. Allelic differences affecting invariant chain dependency of MHC class II subunit assembly. *Immunity*. 1995, 2:301-310.
- Bijlmakers M., Benaroch P., & Ploegh H.L. Assembly of HLA-DR1 molecules translated *in vitro*: binding of peptide in the endoplasmic reticulum precludes association with invariant chain. *EMBO J.* 1994, 13:2699-2707.
- Boczkowski D., Nair S.K., Snyder D., Gilboa E. Dendritic cells pulsed with RNA are potent antigen-presenting cells *in vitro* and *in vivo*. *J. Exp. Med.* 1996, 184:465-472.

- Bodmer H., ViVille S., Benoist C., Mathis D. Diversity of endogenous epitopes bound to MHC class II molecules limited by invariant chain. *Science*. 1994, 263:1284-1286.
- Boon T., & van der Bruggen P. Human tumour antigens recognised by T lymphocytes. *J.Exp.Med.* 1996, 183:725-729.
- Brooks A.G., & McCluskey J. Class II-restricted presentation of a hen egg lysozyme determinant derived from endogenous antigen sequestered in the cytoplasm or endoplasmic reticulum of the antigen presenting cells. *J. Immunol.* 1993, 150:3690-3697.
- Brossart P., Goldrath A.W., Butz E.A., Martin S., & Bevan M.J. Virus-mediated delivery of antigenic epitopes into dendritic cells as a means to induce CTL. *J. Immunol.* 1997, 158:3270
- Brossart P., Grunebach F., Stuhler G., Reichardt V.L., Mohle R., Kanz L., Brugger W. Generation of functional human dendritic cells from adherent peripheral blood monocytes by CD40 ligation in the absence of granulocyte-macrophage colony-stimulating factor. *Blood*. 1998, 92:4238-4247.
- Brown J.H., Jardetzky T.S., Gorga J.C., Stern L.J., Urban R.G., Strominger J.L. & Wiley D.C. 3-dimensional structure of the human class-II histocompatibility antigen HLA-DR1. *Nature*. 1993, 364:33-39.
- Burkly L.C., Lo D., Kanagawa O., Brinster R.L. & Flavell R.A. T-cell tolerance of clonal anergy in transgenic mice with nonlymphoid expression of MHC class I-E. *Nature*. 1989, 342:564-566.
- Busch R., Cloutier I., Sekaly R.-P., & Hammerling G.J. Invariant chain protects class II histocompatibility antigens from binding intact polypeptides in the endoplasmic reticulum. *EMBO. J.* 1996, 15:418-428.
- Carmichael P., Kerr L.-A., Kelly A., et al., The TAP complex influences allorecognition of class II MHC molecules. *Hum. Immunol.* 1996, 50:70-77.
- Castelli C., Storkus W.J., Maeurer M.J., *et al.* Mass spectrometric identification of a naturally processed melanoma peptide recognised by CD8⁺ cytotoxic T lymphocytes. *J. Exp. Med.* 1995, 181:363-368.
- Caux C., Massacrier C., Vanbervliet B., Dubois B., Van Kooten C., Durand I., & Banchereau J. Activation of human dendritic cells through CD40 cross-linking. *J.Exp.Med.* 1994a, 180:1263-1272.
- Caux C., Vanbervliet B., Massacrier C. *et al.* B70/B7-2 is identical to CD86 and is the major functional ligand for CD28 expressed on human dendritic cells. *J. Exp. Med.* 1994b, 180:1841-1847.
- Caux P., Favre N., Martin M., & Martin F. Tumour-infiltrating dendritic cells are defective in their antigen-presenting function and inducible B7 expression in rats. *Int. J. Cancer*. 1997, 72:619-624.

- Celis E., Tsai V., Crimi C., *et al.* Induction of anti-tumour cytotoxic T lymphocytes in normal humans using primary cultures and synthetic peptide epitopes. *Proc. Natl. Acad. Sci. U.S.A.* 1994, 91:2105-2109.
- Cella M., Scheidegger D., Palmer-Lehmann K., Lane P., Lanzavecchia A., & Albert G. Ligation of CD40 on dendritic cells triggers production of high levels of interleukin-12 and enhances T cell stimulatory capacity: T-T help via APC activation. *J.Exp.Med.* 1996, 184:747-752.
- Cella M., Engering A., Pinet V., Pieters J., & Lanzavecchia A. Inflammatory stimuli induce accumulation of MHC class II complexes on dendritic cells. *Nature* 1997, 388: 782-787.
- Celluzzi C.M. & Falo L.D. Cutting edge: Physical interaction between dendritic cells and tumour cells result in an immunogen that protective and therapeutic tumour rejection. *J. Immunol.* 1998, 160:3081-3085.
- Cerundolo V., Elliot T., Elvin J., Bastin J., Rammensee H.G., & Townsend A. The binding affinity and dissociation rates of peptides for class I major histocompatibility complex molecules. *Eur. J. Immunol.* 1991, 21:2069-2075.
- Chalfie M., Tu Y., Euskuchen G., Ward W.W. & Prasher D.C. Green fluorescent protein as a marker for gene expression. *Science.* 1994, 263:802-805.
- Chen Y.T., Scanlan M.J. & Sahin U. A testicular antigen aberrantly expressed in human cancers detected by autologous antibody screening. *Proc. Natl. Acad. Sci. USA.* 1997, 94: 1914-1918.
- Chiang H.-L. Terlecky S.R., Plant C.P., & Dice J.F., A role for a 70-kilodalton heat shock protein in lysosomal degradation of intracellular proteins. *Science.* 1989, 246:382-385.
- Chicz R.M., Urban R.G., Gorga J.C., Vignali D.A.A., Lane W.S., & Strominger J.L. Specificity and promiscuity among naturally processed peptides bound to HLA-DR alleles. *J. Exp. Med.* 1993, 178:27-47.
- Ciccarone V., Anderson D., Lan J., Schifferli K., & Jesse J. DMRIE-C reagent for transfection of suspension cells and for RNA transfections. *Focus* 17 1996, No. 3:84-87.
- Colomb M.G., Villiers C.L., Villiers M.-B., Gabert F.M., Santoro L., & Rey-Millet C.A. The role of antigen bound C3b in antigen processing. *Res. Immunol.* 1996, 147:75-82.
- Chomczynski P., & Sachi N. Single-step method of RNA isolation by acid guanidium thiocyanate-phenol-chloroform extraction. *Anal. Biochem.* 1987, 162:156-159.
- Copier J., Kleijmeer M.J., Ponnambalam S., Oorschot V., Potter P., Trowsdale J., & Kelly A. Targeting signal and subcellular compartments involved in the intracellular trafficking of HLA-DM β . *J. Immunol.* 1996, 157:1017-1027.
- Copier J., Potter P., Sacks S.H., & Kelly A.P. Multiple signals regulate the intracellular trafficking of HLA-DM in B-lymphoblastoid cells. *Immunology.* 1998, 93:505-510.

- Cordon-Grado C., Fuks Z., Drobnyak ., Moreno C., Eisenbach L., & Feldman M. Expression of HLA-A,B,C antigens on primary and metastatic tumour cell populations of human carcinomas. *Cancer Res.* 1991, 51:6372-6380.
- Cote R.J., Rosen P.P., Lesser M.L., Old L.J., & Osborne M.P. Prediction of early relapse in patients with operable breast cancer by detection of occult bone marrow micrometastases. *J.Clin.Oncol.* 1991, 9:1749-1756.
- Coussens L., Yang-Feng T.L., Chen Y.L.E., Gray A., McGrath J., Seeburg P.H., Liberman T.A., Schlessinger J., Francke U., Levinson A., & Ullrich A. Tyrosine kinase receptor with extensive homology to EGF receptor shares chromosomal location with *neu* oncogene. *Science.* 1985, 230:1132-1139.
- Cox A.L., Skipper J., Chen Y., *et al.* Identification of a peptide recognised by five melanoma-specific human cytotoxic T-cell lines. *Science* 1994, 264:716-719.
- Cresswell P., Blum J.S., Kelner D.N., & Marks M.S. Biosynthesis and processing of class II histocompatibility antigens. *Crit. Rev. Immunol.* 1987, 7:31-35.
- Cresswell P. Invariant chain structure and MHC class II function. *Cell.* 1996, 84:505-507.
- Cresswell P., Bangia N., Dick T., & Diedrich G. The nature of the MHC class I peptide loading complex. *Immunol. Rev.* 1999, 172:21-28.
- Croft M. & Dubey C. Accessory molecule and costimulation requirements for CD4 T-cell response. *Crit. Rev. Immunol.* 1997, 17:89-118.
- Cromme F.V., Airey J., Heemels M.-T., Ploegh H.L., Keating P.J., Sterns P.L., Meijer C..J.L.M, & Walboomers J.M.M. Loss of transporter protein encoded by the TAP-1 gene, is highly correlated with loss of HLA expression in cervical carcinomas. *J. Exp. Med.* 1994, 179:335-340.
- Cuervo A.M. & Dice J.F. A receptor for the selective uptake and degradation of proteins by lysosomes. *Science.* 1996, 273:501-503.
- Daar A.S., Fuggle S.V., Fabre J.W., Ting A., & Morris P.J. The detailed distribution of MHC class II antigens in normal human organs. *Transplantation.* 1984, 38:293-298.
- Dadmarz R., Sgagias M.K., Rosenberg S.A., & Schwartzentruber D.J. CD4⁺ T lymphocytes infiltrating human breast cancer recognise autologous tumour in an MHC-class-II restricted fashion. *Cancer. Immunol. Immunother.* 1995, 40:1-9.
- David V., Hochstenbach F., Rajagopalan S., & Brenner M.B. Interaction with newly synthesised and retained proteins in the endoplasmic reticulum suggests a chaperone function for human integral membrane protein IP90 (calnexin). *J. Biol. Chem.* 1993, 268:9585-9592.
- David-Pfeuty T., chakrani F., Ory K., & Nouvian-Dooghe Y. Cell cycle-dependent regulation of nuclear p53 traffic occurs in one subclass of human tumour cells and in untransformed cells. *Cell Growth Differ.* 1996, 7:1211-1225.
- De Bruijn M.L., Schuurhuis D.H., Vierboom M.P., *et al.* Immunisation with human papillomavirus type 16 (HPV 16) oncoprotein-loaded dendritic cells as well as protein

- in adjuvant induces MHC class I-restricted protection to HPV-16 induced tumour cells. *Cancer Res.* 1998, 58:724-731.
- DeLeo A.B. p53-based immunotherapy of cancer. *Crit. Rev. Immunol.* 1998, 18:29-35.
- Dempsey P.W., Allisson M.E.D., Akkaraju S., Goodnew C.C., & Fearon D. C3d of complement as a molecular adjuvant: bridging innate and acquired immunity. *Science.* 1996, 271:348-350.
- Denzin L.K., Robbins N.F., Carboy-Newcomb C., & Cresswell P. Assembly and intracellular transport of HLA-DM and correction of the class II antigen-processing defect in T2 cells. *Immunity.* 1994, 1:595.
- Denzin L.K., & Cresswell P. HLA-DM induces CLIP dissociation from MHC class II alpha/beta dimmers and facilitates peptide loading. *Cell.* 1995, 82:155.
- Denzin L.K., Sant' Angelo D.B., Hammond C., Surman M.J., & Cresswell P. Negative regulation by HLA-DO of MHC class II-restricted antigen processing. *Science.* 1997, 278:106-109.
- De Ricqles D., Olomucki A., Gosselin F., & Lideraeau R. Breast cancer and T-cell mediated immunity to proteins of the mouse mammary tumour virus (MMTV). *Eur. Cytokine Netw.* 1993, 4:153-160.
- Dick T.P., Ruppert T., Groettrup M., Kloetzel P.M., Kuehn L., Koszinowski U.H., Stevanovic S., Schild H., & Rammensee H.-G. Coordinated dual cleavages induced by the proteasome regulator PA28 lead to dominant MHC ligands. *Cell.* 1996, 86:253-262.
- Di Fiore P., Segatto O., Lonardo F., Fazioli F., Pierce J., & Aaronson S. The carboxy-terminal domains of erbB-2 and epidermal growth factor receptor exert different regulatory effects on intrinsic receptor tyrosine kinase function and transforming. *Mol.Cell.Biol.* 1990, 10:2749-2756.
- Diller L., Kassel J., Nelson C.E., *et al.* p53 functions as a cell cycle control protein in osteosarcomas. *Mol. Cell. Biol.* 1990, 10: 5772-5781.
- Dion A.S., Knittel J.J., & Morneweck S.T. Virus envelope-based peptide vaccines against virus-induced mammary tumours. *Virology.* 1990: 179:474-477.
- Disis M.L., Smith J.W., Murphy A.E., Chen W., & Cheever M.A. *In vitro* generation of human cytolytic T-cells specific for peptides derived from HER-2/neu protooncogene protein. *Cancer Res.* 1994, 54:1071-1076.
- Dranoff G., Jaffee E., Lazenby A., Golumbek P., Levitsky H., Brose K., Jackson V., Hamada H., Pardoll D.M. & Mulligan R.C. Vaccination with irradiated tumour cells engineered to secrete murine granulocyte-macrophage colony-stimulating factor stimulates potent, specific, long anti-tumour immunity. *Proc. Natl. Acad. Sci. USA.* 1993, 90:3539-3543.
- Durie F.H., George W.D., Campbell A.M. & Damato B.E. Analysis of clonality of tumour infiltrating lymphocytes in breast cancer and uveal melanoma. *Immunol. Letters.* 1992, 33:263-270.

- de Valeriola D., Awada A., Roy J-A., Di Leo A., Biganzoli L., & Piccart M. Breast cancer therapies in development. *Drugs*. 1997, 3:385-413.
- Eliyahu D., Michalovitz S., Eliahu O., *et al.* Wild type p53 can inhibit oncogene-mediated focus formation. *Proc. Natl. Acad. Sci. USA*. 1989, 86: 8763-8767.
- Elliot R.L., Head J.F., & McCoy J.L. Comparison of estrogen and progesterone receptor status to lymphocyte immunity against tumour antigens in breast cancer patients. *Breast Cancer Res. Treatment*. 1994, 30:299-304.
- Engering A.J., *et al.* The mannose receptor functions as a high capacity and broad specificity antigen receptor in human dendritic cells. *Eur. J. Immunol.* 1997, 27:2417-2425.
- Euhus D.M., Kimura L., & Arnold B. Expansion of CD3⁺ CD56⁺ lymphocytes correlates with induction of cytotoxicity by interleukin 2 gene transfer in human breast tumour cultures. *Ann. Surg.Oncol.* 1997, 4:432-439.
- Fearon E.R., Pardoll D.M., Itaya T., Golumbek P., Levitsky H.I., Simons J.W., Karasuyama H., Vogelstein B., & Frost P. Interleukin-2 production by tumour cells bypasses T helper function in the generation of an antitumour response. *Cell*. 1990, 60:397-403.
- Fenteany G., Standaert R.F., Lane W.S., Choi S., Corey E.J., Schreiber S.L. Inhibition of proteasome activities and subunit-specific amino-terminal threonine modification by lactacystin. *Science*. 268:726-731.
- Felgner P.L., Barenholz Y., Behr J.P., Cheng S.H., *et al.*, Nomenclature for synthetic gene delivery systems. *Human Gene Therapy*. 1997, 8:511-512.
- Feltkamp M.C., Smits H.L., Vierboom M.P., Minnaar R.P., de Jongh B.M., Drijfhout J.W., Ter Schegget J., Melief C.J., & Kast W.M. Vaccination with cytotoxic T lymphocyte epitope-containing peptide protects against a tumour induced by human papillomavirus type 16-transformed cells. *Eur. J. Immunol.* 1993, 23:2242-2249.
- Fernandez-Borja M., Verwoerd D., Sanderson F., Aerts H., Trowsdale J., Tulp A., & Neefjes J. HLA-DM and MHC class II molecules co-distribute with peptidase-containing lysosomal subcompartments. *Int. Immunol.* 1996, 8:625-640.
- Finlay C.A. Hinds P.W., & Levine A.J. The p53 proto-oncogene can act as a suppressor of transformation. *Cell*. 1989, 57: 1083-1093.
- Fisher B., Laboratory and clinical research in breast cancer: Contributions of the national surgical adjuvant breast and bowel project clinical trials. *Ca-A Cancer J. Clin.*, 1980a 41, 97-111.
- Fisher B., Laboratory and clinical research in breast cancer-a personal adventure, The David A. Karnofsky Memorial Lecture. *Cancer Res.* 1980b, 40:3863-3874.
- Fisher E.R., Gregorio R.M., & Fisher B. The pathology of invasive breast cancer. *Cancer*. 1974, 36:1-85.
- Flores-Romo L., Bjorck P., Duvert V., van Kooten C., Saeland S., & Banchereau J. CD40 ligation on human cord blood CD34⁺ hematopoietic progenitors induces their

- proliferation and differentiation into functional dendritic cells. *J.Exp.Med.* 1997, 185:341-349.
- Freisewinkel I.M., Schenck K., & Kocj N. The segment of invariant chain that is critical for association with major histocompatibility complex class II molecules contains the sequence of a peptide eluted from class II polypeptides. *Proc. Natl. Acad. Sci. USA.* 1993, 90:215-221.
- Fremont D.H., Crawford F., Marrack P., Hendrickson W.A., & Kappler J. Crystal structure of mouse H2-M. *Immunity.* 1998, 9:385-393.
- Gaugler B., Van Den Eynde B., Van der Bruggen P., *et al.* Human gene MAGE-3 codes for an antigen recognised on a melanoma by autologous cytolytic T lymphocytes. *J. Exp. Med.* 1994, 179:921-930.
- Gendler S., Taylor-Papadimitriou T J., Duhig T., Rothbard J., & Burchell J. A highly immunogenic region of a human polymorphic epithelial mucin expressed by carcinomas made up of tandem repeats. *J.Biol.Chem.* 1988, 263:1280-12823.
- Gendler S., Lancaster C., Taylor-Papadimitriou J., Duhig T., Peat N., Burchell J., Pemberton L., Lalani E.N., & Wilson D. Molecular cloning and expression of human tumour-associated polymorphic epithelial mucin. *J.Biol.Chem.* 1990, 265: 15286.
- Germain R.N., & Hendrix L.R. MHC class II structure, occupancy and surface expression determined by post-endoplasmic reticulum antigen binding. *Nature.* 1991, 353:134-139.
- Ghosh P., Amaya M., Mellins E., & Wiley D,C. The structure of an intermediate in class II MHC maturation:CLIP bound to HLA-DR3. *Nature.* 1995, 378:457-462.
- Gilboa E., Nair S.K., Lyerly H.K. Immunotherapy of cancer with dendritic-cell-based vaccines. *Cancer Immunol Immunother.* 1998, 46:82-87.
- Girolomoni G., & Ricciardi-Castagnoli P. Dendritic cells hold promise for immunotherapy. *Immunol. Today.* 1997, 18:102-104.
- Gnjatic S., Cai Z., Viguier M., *et al.*, Accumulation of the p53 protein allows recognition by human CTL of a wild-type p53 epitope presented by breast carcinomas and melanomas. *J. Immunol.* 1998, 160:328-333.
- Goedegebuure P.S., Douville C.C., Doherty J.M., Linehan D.C., Lee K-Y., Ganguly E.K., & Eberlein T.J. Simultaneous production of T Helper-1-like cytokines and cytolytic activity by tumour-specific T cells in ovarian and breast cancer. *Cellular Immunol.* 1997, 175: 150-156.
- Golumbek P.T., Lazenby A.J., Levitsky H.I., Jaffee L.M., Karasuyama H., Baker M., & Pardoll D.M. Treatment of established renal cancer by tumour cells engineered to secrete interleukin-4. *Science.* 1991, 254:713-716.
- Gong J., Chen D., Kashiwaba M., *et al.* Induction of antitumour activity immunisation with fusion of dendritic and carcinoma cells. *Nat. Med.* 1997, 3:558-561.

- Granelli-Piperno A., Pope M., Inaba K., & Steinman R.M. Coexpression of REL and SPI transcription factors in HIV-1 induced, dendritic cell-T cell syncytia. *Proc. Natl. Acad. Sci. USA.* 1995, 92:10940-10948
- Grewal I.S., Xu J., & Flavell R.A. Impairment of antigen-specific T-cell priming in mice lacking CD40 ligand. *Nature.* 1995, 378:617-620.
- Groettrup M., Soza A., Eggers M., Kuehn L., Dick T.P., Schild H., Rammensee H.-G., Koszinowski U.H., & Kloetzel P-M. A role for the protease regulator PA28a in antigen presentation. *Nature.* 1996, 381:166-168.
- Guagliardi L.E., Koppelman B., Blum J.S., Marks M.S., Cresswell P. & Brodsky F.M. Co-localisation of molecules involved in antigen processing and presentation in an early endocytic compartment. *Nature.* 1990, 343:133-139.
- Guarnieri F.G., Arterburn L.M., Penno M.B., Cha Y., & August J.T. The motif tyr-X-X-hydrophobic residue mediates lysosomal membrane targeting of lysosome-associated membrane protein-1. *J. Biol. Chem.* 1993, 268:1941-1946.
- Hadden J.W. T-cell adjuvancy. *Intl J. Immunopharmacol.* 1994, 16:703-710.
- Hadden J.W. The immunology of breast cancer, Prospects for immunotherapy. *Clin.Immunother.* 1995, 4:249-330.
- Hadden J.W. The immunology and immunotherapy of breast cancer: an update. *Int. J. Immunopharm.* 1999, 21:79-101.
- Hamada K., Zhang W-W., Alemany R., Wolf J., Roth J., & Mitchell M.F. Growth inhibition of human cervical cancer cells with the recombinant adenovirus p53 *in vitro*. *Gynecol. Oncol.* 1996, 60:373-379.
- Harding C.V., Collins D.S., Slot J.W., Geuze H.W., & Unanue E.R. Liposome-encapsulated antigens are processed in lysosomes, recycled and presented to T cells. *Cell.* 1991, 64:393-401.
- Harding C.V. & Geuze H.J. Class II MHC molecules are present in macrophages lysosomes and phagolysosomes that function in the phagocytic processing of *Listeria monocytogenes* for presentation to T cells. *J. Cell. Biol.* 1992, 119:531-542.
- Harding C.V. & Geuze H.J. Immunogenic peptides bind to class II MHC molecules in an early lysosomal compartment. *J. Immunol.* 1993, 151:3988-3998.
- Hareuveni M., Tsarfaty J., Zaretsky J., Kotkes P., Horev P., & Zrihner S. A transcribed gene, containing a variable number of tandem repeats, codes for a human epithelial tumour antigen: cDNA cloning, expression of the transfected gene and over-expression in breast cancer tissue. *Eur.J.Biochem.* 1990, 189:475.
- Heemels M-T., & Ploegh H. Generation, translocation and presentation of MHC class I-restricted peptides. *Annu. Rev. Biochem.* 1995, 64:463-491.
- Heim R., Cubitt A.B., & Tsien R.Y. Improved green fluorescence. *Nature*, 1995, 373:663-664.

- Hollstein M., Sidransky D., Vogelstein B., Harris C. p53 mutations in human cancers. *Science*. 1991, 253:49-53.
- Hollstein M., Shomer M., Greenblatt T., *et al.* Somatic point mutations in the p53 gene of human tumours and cell lines: updated compilation. *Nucleic Acid Res.* 1996, 24:141.
- Houbiers J.G.A., Nijman H.W., Van der Burg S.H., *et al.* In vitro induction of human cytotoxic T lymphocyte responses against peptides of mutant and wild type p53. *Eur. J. Immunol.* 1993, 23:2072-2077.
- Howard J.C. Supply and transport of peptides presented by class I MHC molecules. *Curr. Opin. Immunol.* 1995, 7:342-344.
- Hsu F.J., Benike C., Fagnoni F., *et al.* Vaccination of patients with B-cell lymphoma using autologous antigen-pulsed dendritic cells. *Nature Med.* 1996, 2:52-58.
- Huang A.Y., Golumbek P., Ahmadzadeh M., Jaffee E., Pardoll D., & Levitsky H. Role of bone marrow-derived cells in presenting MHC class I-restricted tumour antigens. *Science*. 1994, 264:961-965.
- Humbert M., Bertolino P., Forquet F., Raboutin Combe C., Gerlier D., Davoust J., & Salamero J. Major histocompatibility complex class II-restricted presentation of secreted and endoplasmic reticulum resident antigens requires the invariant chains and is sensitive to lysosomotropic agents. *Eur. J. Immunol.* 1993, 23:3167-3172.
- Humbert M., Raposo G., Cosson P., Reggio H., Davoust J., & Salamero J. The invariant chain induces compact forms of class II molecules localised in late endosomal compartments. *Eur. J. Immunol.* 1993b, 23:3158-3166.
- Hupp T.R., & Lane D.P. Allosteric activation of latent p53 tetramers. *Curr. Biol.* 1994, 4:865-875.
- Hurtley S.M., & Helenius A. Protein oligomerization in the endoplasmic reticulum. *Ann. Rev. Cell. Biol.* 1989, 5:277-307.
- Ignatowicz L., Winslow G., Bill J., Kappler J., & Marrack P. Cell surface expression of MHC class II proteins bound by a single peptide. *J. Immunol.* 1995, 154:3852-3862.
- Inaba K., Inaba M., Romani N., Aya H., *et al.* Generation of large numbers of dendritic cells from mouse bone cultures supplemented with granulocyte/macrophage colony-stimulating factor. *J. Exp. Med.* 1992, 176:1693-1702.
- Inaba K., Witmer-Pack M., Inaba M., *et al.* The tissue distribution of the B7-2 costimulator in mice: Abundant expression on dendritic cells *in situ* and during maturation *in vitro*. *J. Exp. Med.* 1994, 180:1849-1860.
- Ingulli E., Mondino A., Khortus A., & Jenkins M.K. *In vivo* detection of dendritic cell antigen presentation to CD4⁺ T cells. *J. Exp. Med.* 1997, 185:2133-2141.
- Ioannides C., Ioannides M., & O'Brian C. T cell recognition of oncogene products: a new strategy for immunotherapy. *Mol. Carcinog.* 1992, 6:77-82.

- Jackson M.R., Cohen-Doyle M.F., Peterson P.A. & Williams D.B. Regulation of MHC class I transport by the molecular chaperone calnexin (p88, IP90). *Science*. 1994, 263:384.
- Jacobson S., Sekaly R.P., Jacobson C.L., McFarland H.F., & Long E.O. HLA class II-restricted presentation of cytoplasmic measles virus antigens to cytotoxic T cells. *J. Virol.* 1989, 63:1756-1762.
- Jardetzky T.S., Lane W.S., Robinson R.A., Madden D.R., & Wiley D.C. Identification of self peptides bound to purified HLA-B27. *Nature*. 1991, 353:326-329.
- Jasanoff A., Park S.J., Wiley D.C. Direct observation of disordered regions in the major histocompatibility complex class II-associated invariant chain. *Proc. Natl. Acad. Sci. USA*. 1995, 92:9900-9904.
- Jensen P.E. Antigen processing: HLA-DO- a hitchhiking inhibitor of HLA-DM. *Curr. Biol.* 1998, 8:128-131.
- Jerome K.R., Domenech N., & Finn O.J. Tumour-specific cytotoxic T cell clones from patients with breast and pancreatic adenocarcinoma recognise EBV-immortalised B cells transfected with polymorphic epithelial mucin cDNA. *J. Immunol.* 1993, 151:1654-1662.
- Jiang W., Swiggard W.J., Heufler C., Peng M., Mirza A., Steinman R.M., & Nussenzweig M.C. The receptor DEC-205 expressed by dendritic cells and thymic epithelial cells is involved in antigen processing. *Nature*. 1995, 375:151-155.
- Jones E. MHC class I and class II structures. *Curr. Opin. Immunol.* 1997, 9:75-79.
- Kageshita T., Wang Z., Calorini L., Yoshii A., Kimura T., Ono T *et al.* Selective loss of human leukocyte class I allo-specificities and staining of melanoma cells by monoclonal antibodies recognizing monomorphic determinants of class I leukocyte antigens. *Cancer Res.* 1993, 53:3349-3354.
- Kantor J., Irvine K., Abrams S., Kaufman H., DiPietro J., & Schlom J. Antitumour activity and immune responses induced by a recombinant carcino embryonic antigen-vaccinia virus vaccine. *J.Natl. Cancer Inst.* 1992, 84:1084-1091.
- Karlsson L., & Peterson P.A. The α chain gene of H-2O has an unexpected location in the major histocompatibility complex. *J. Exp. Med.* 1992, 176:477-483.
- Karlsson L., Peleraux A., Lindstedt R., Liljedahl M., & Peterson P.A. Reconstitution of an operational MHC class II compartment in nonantigen-presenting cells. *Science*. 1994, 266:1569-1573.
- Karp S.E., Farber A., Salo J.C., Hwu P., Jaffe G., Asher A.L., Shiloni E., Restifo N.P., Mule J.J. & Rosenberg S.A. Cytokine secretion by genetically modified nonimmunogenic murine fibrosarcoma. Tumour inhibition by IL-2 but not tumour necrosis factor. *J Immunol.* 1993, 150:896-908.
- Kastan M.B., Zhan Q., El-Diery W.S., *et al.* A mammalian cell cycle checkpoint pathway utilising p53 and *GADD45* is defective in ataxia-telangiectasia. *Cell*. 1992, 71:587-597.

- Keene J.A., & Forman J. Helper activity is required for the in vivo generation of cytotoxic T lymphocytes. *J. Exp. Med.* 1982, 155:768-782.
- Kelly A.P., Monaco S., Cho S., & Trowsdale J. A new human HLA class II-related locus, DM. *Nature.* 1991, 353:571-573.
- Kleijmeer M.J., Oorschot V.M., & Geuze H.J. Human resident Langerhans cells display a lysosomal compartment enriched in MHC class II. *J. Invest. Dermatol.* 1994, 103:516-523.
- Kleijmeer M.J., Oorschot V.M., van Veen C.J.H, van Hellemond J.J. *et al.* MHC class II compartments and the kinetics of antigen presentation in activated mouse spleen dendritic cells. *J. Immunol.* 1995, 154:5715-5724.
- Klein C., Bueler H., & Mulligan R. Comparative analysis of genetically modified dendritic cells and tumour cells as therapeutic cancer vaccines. *J.Exp.Med.* 2000, 191:1699-1708.
- Koch N., Lauer W., Habicht J., Dobberstein B. Primary structure of the gene for the murine Ia antigen-associated invariant chains (Ii). An alternatively spliced exon encodes a cysteine-rich domain highly homologous to a repetitive sequence of the thyroglobulin. *EMBO. J.* 1987, 6:1677-1683.
- Koch F., *et al.* High level IL-12 production by murine dendritic cells: upregulation via MHC class II and CD40 molecules and downregulation by IL-4 and IL-10. *J. Exp. Med.* 1994, 180:1841-1847.
- Koopman J-O., Post M., Neeffjes J.J., Hammerling G.J., & Momburg F. Translocation of long peptides by transporters associated with antigen processing (TAP). *Eur. J. Immunol.* 1996, 26:1720-1728.
- Kovach J.S., Hartmann A., Blaszyk H., Cunningham J., Schaid D., & Sommer S.S. Mutation detection by highly sensitive methods indicates that p53 gene mutations in breast cancer can have important prognostic value. *Proc. Natl. Acad. Sci. USA.* 1996, 93:1093-1096.
- Kropshofer H., Vogt A.B., Moldenhauer G., *et al.*, Editing of the HLA-DR peptide repertoire by HLA-DM. *EMBO J.* 1996, 15:6144.
- Kropshofer H., Arndt S.O., Moldenhauer G., Hammerling G.J., & Vogt A.B. HLA-DM acts as a molecular chaperone and rescues empty HLA-DR molecules at lysosomal pH. *Immunity.* 1997, 6:293-302.
- Kudo S., Matsuno K., Ezaki T., & Ogawa M.A. A novel migration pathway for rat dendritic cells from the blood: Hepatic sinusoids-lymph translocation. *J. Exp. Med.* 1997, 185:777-784.
- Laemmli U.K. Cleavage of structural proteins during the assembly of the head of bacteriophage T4. *Nature.* 1970, 227:680-685.
- Lan M.S., Batra S.K., Qui W-N., Metzgar R.S., & Hollingsworth M.A. Cloning and sequencing of a human pancreatic tumour mucin cDNA. *J.Biol.Chem.* 1990, 265:15294.

- Lane D.P. & Benchimol S. p53: oncogene or anti-oncogene? *Genes Dev.* 1990, 4:1-8.
- Lechler R., Aichinger G., & Lightstone L. The endogenous pathway of MHC class II antigen presentation. *Immunol. Rev.* 1996, 151:51-79.
- Lehner P.J., & Cresswell P. Processing and delivery of peptides presented by MHC class I molecules. *Curr. Opin. Immunol.* 1996, 8:59-67.
- Levine A.J., Momand J., & Finlay C.A. The p53 tumour suppressor gene. *Nature.* 1991, 351: 453-456.
- Levine A.J. The tumour suppressor genes. *Annu Rev Biochem.* 1993, 62:636.
- Levine A.J. p53, the cellular gatekeeper for growth and division. *Cell.* 1997, 88:323-331.
- Liljedahl M., *et al.* HLA-DO is a lysosomal resident which requires associations with HLA-DM for efficient intracellular transport. *EMBO J.* 1996, 15:4817-4824.
- Lin K.Y., Guarnieri F.G., Staveley- O'Carroll K., Levitsky H.I., August J.T., Pardoll D.M., & Wu T.C. Treatment of established tumours with a novel vaccine that enhances major histocompatibility class II presentation of tumour antigen. *Cancer Res.* 1996, 56:21-26.
- Lindquist J.A., Jensen O.N., Mann M., & Hammerling G.J. ER-60, a chaperone with thiol-dependent reductase activity involved in MHC class I assembly. *EMBO J.* 1998, 17:2186-2195.
- Lindstedt R., Liljedahl M., Peleraux A., Peterson P.A., & Karlsson L. The MHC class II molecule H2-M is targeted to an Endosomal compartment by a tyrosine-based targeting motif. *Immunity.* 1995, 3:561.
- Liou W., Geuze H.J., Geelen M.J.H., & Slot J.W. The autophagic and endocytic pathways converge at the nascent autophagic vacuoles. *J. Cell. Biol.* 1997, 136:61-70.
- Liu S.H., Marks M.S., & Brodsky F.M. A dominant-negative clathrin mutant differentially affects trafficking of molecules with distinct sorting motifs in the class II major histocompatibility complex (MHC) pathway. *J. Cell. Biol.* 1998, 140:1023-1037.
- Lotteau V., Teyton L., Peleraux A., Nilsson T., Karlsson L., Schmid S.L., Quaranta V., & Peterson P.A. Intracellular transport of class II MHC molecules directed by invariant chain. *Nature.* 1990, 348:600-605.
- Luther S.A., Gulbranson-Judge A., Acha-Orbea H., & MacLennan I.C.M. Viral superantigen drives extrafollicular and follicular B differentiation leading to virus-specific antibody production. *J. Exp. Med.* 1997, 185:551-562.
- Lutze M.B., Rovere P., Kleijmeer M.J., Assmann C.U., Oorschot V.M., Rescigno M., Geuze H.J., Davoust J., & Ricciardi-Castagnoli P. A newly identified antigen retention compartment in the FSDC precursor dendritic cell line. *Adv. Exp. Med. Biol.* 1997, 417:167-169.

- Malnati M.S., Ceman S., Weston M., DeMars R., & Long E.O. Presentation of cytosolic antigen by HLA-DR requires a function encoded in the class II region of the MHC. *J. Immunol.* 1993, 151:6751-6756.
- Maltzman W., & Czyzyk L. UV irradiation stimulates levels of p53 cellular tumour antigen in nontransformed mouse cells. *Mol. Cell. Biol.* 1984, 4:1689-1694.
- Mandelboim O., Vadai E., Fridkin M., Katz-Hillel A., Feldman M., Berke G., & Eisenbach L. Regression of established murine carcinoma metastases following vaccination with tumour-associated antigen peptides. *Nat. Med.* 1995, 1:1179-1183.
- Marks M.S., Roche P.A., van Donselaar E., Woodruff L., & Peters P.J. A lysosomal targeting signal in the cytoplasmic tail of the b chain directs HLA-DM to the MHC class II compartments. *J. Cell. Biol.* 1995, 131:351-369.
- Matzinger P. Tolerance, danger and the extended family. *Annu. Rev. Immunol.* 1994, 12:991-1045.
- Mayordomo J.L., Zorina T., Storkus W.J., Zitvogel L., Celluzzi C., Falo L.D., Melief C.J., Ildstad S.T., Kast W.M., & DeLeo A.B. Bone marrow-derived dendritic cells pulsed with synthetic tumour peptides elicit protective and therapeutic antitumour immunity. *Nat. Med.* 1995, 1:1297-1302.
- McCarty T.M., Xiping L., Sun J-Y., Peralta E.A., Diamond D.J., & Ellenhorn J.D.I. Targeting p53 for adoptive T-cell immunotherapy. *Cancer Res.* 1998, 58:2601-2695.
- McKnight A.J., Mason D.W., & Barclay A.N. Sequence of a rat MHC class II-associated invariant chain cDNA clone containing a 64 amino acid thyroglobulin-like domain. *Nucleic Acids Res.* 1989, 17:3983-3984.
- McLure K.G., & Lee P.W. How p53 binds DNA as a tetramer. *EMBO J.* 1998, 17:3342-3350.
- Mellman I., Pierre P., & Amigorena S. Lonely MHC molecules seeking immunogenic peptides for meaningful relationships. *Curr. Opin. Cell. Biol.* 1995, 7:564-572.
- Melnick J., & Argon V. Molecular chaperones and the biosynthesis of antigen receptors. *Immunol. Today.* 1995, 16:243-250.
- Mercer W.E. *et al.* Negative growth regulation in a glioblastoma tumour cell line that conditionally expresses human wild type p53. *Proc. Natl. Acad. Sci. USA.* 1990, 87:6166-6170.
- Middeler G., Zerf K., Jenovai S., Thulig A., Tschodrich-Rotter M., et al. The tumour suppressor p53 is subject to both nuclear import and export, and both are fast, energy-dependent and lecin-inhibited. *Oncogene.* 1997, 14:1407-1417.
- Miyashita T., & Reed J.C. Tumour suppressor p53 is a direct transcriptional activator of the human *bax* gene. *Cell.* 1995, 80:293-299.
- Moll H., Fuchs., Blank C., & Rollinghoff M. Langerhans cells transport *Leishmania major* from infected skin to the draining lymph node for presentation to antigen-specific T cells. *Eur. J. Immunol.* 1993, 23:1595-1601.

- Moll U.M., Ostermeyer A.G., Haladay R., Winkfield B., Frazier M., & Zambetti G. Cytoplasmic sequestration of wild-type p53 protein impairs the G₁ checkpoint after DNA damage. *Mol. Cell. Biol.* 1996, 16:1126-1137.
- Moreno M.W., Vignali D.A., Nadimi F., Fuchs S., Adorini L., & Hammerling G.J. Processing of an endogenous protein can generate MHC class II-restricted T cell determinants distinct from those derived from exogenous antigen. *J. Immunol.* 147:3306-3316.
- Morrison L.A., Lukacher A.E., Braciale V.L., Fan D.P. & Braciale T.J. Differences in antigen presentation to MHC class I-and class-II restricted influenza virus-specific cytolytic T lymphocyte clones. *J. Exp. Med.* 1986, 163:903-921.
- Morse M., Lyerly H., Gilboa E., Thomas E., & Nair S. Optimisation of the sequence of antigen loading and CD40-ligand-induced maturation of dendritic cells. *Cancer Res.* 1998, 58:2965-2968.
- Mosyak L., Zaller D.M., & Wiley D.C. The structure of HLA-DM, the peptide exchange catalyst that loads antigen onto class II MHC molecules during antigen presentation. *Immunity.* 1998, 9:377-383.
- Mullis K.B. & Faloona F.A. Specific synthesis of DNA *in vitro* via a Polymerase catalysed chain reaction. *Meth. Enzymol.* 1987, 155:335-350.
- Nadeau K., Nadler S.G., Saulnier M., Tepper M.A. & Walsh C.T. Quantitation of the interaction of the immunosuppressant deoxyspergualin and analogs with Hsc70 and Hsp90. *Biochemistry.* 1994, 33:2561-2567.
- Nair S.K., Boczkowski D., Morse M., *et al.* Induction of primary carcinoembryonic antigen (CEA)-specific cytotoxic T lymphocytes *in vitro* using human dendritic cells transfected with RNA. *Nature Biotech.* 1998, 16:364-369.
- Nakano N., Rooke R., Benoist C., & Mathis D. Positive selection of T cells induced by viral delivery of neopeptides to the thymus. *Science.* 1997, 275:678-683.
- Neefjes J.J., Momburg F., & Hammerling G.J. Selective and ATP-dependent translocation of peptides by the MHC-encoded transporter. *Science.* 1993, 261:769-771.
- Neefjes J. CIIV, MIIC and other compartments for MHC class II loading. *Eur. J. Immunol.* 1999, 29:1421-1425.
- Nestle F.O., Alijagic S., Gilliet M., *et al.* Vaccination of melanoma patients with peptide- or tumour lysate-pulsed dendritic cells. *Nature Med.* 1998, 4:328-332.
- Nijenhuis M., Schmitt S., Armandola E.A., Obst R., Brunner J., & Hammerling G.J. Identification of a contact region for peptide on the TAP1 chain of the transporter associated with antigen processing. *J. Immunol.* 1996, 156:2186-2195.
- Nijman H.W., Kleijmeer M.J., Ossevoort M.A., Oorschot V.M.J., Vierboom M.P.M., van de Keur M., *et al.* Antigen capture and major histocompatibility class II compartments of freshly isolated and cultured human blood dendritic cells. *J. Exp. Med.* 1995, 182:163-174.

- Noessner E., & Parham P. Species-specific differences in chaperone interaction of human and mouse histocompatibility complex class I molecules. *J. Exp. Med.* 1995, 181:327-337.
- Norris P.S., & Haas M. A fluorescent p53GFP fusion protein facilitates its detection in mammalian cells while retaining the properties of wild-type p53. *Oncogene.* 1997, 15:2241-2247.
- Ohashi P.S., *et al.*, Ablation of tolerance and induction of diabetes by virus-infection in viral antigen transgenic mice. *Cell.* 1991, 65:305-317.
- Okamoto K., & Beach D. Cyclin G is a transcriptional target of the p53 tumour suppressor protein. *EMBO J.* 1994, 13:4816-4822.
- Oren M., Maltzman W., & Levine A.J. Posttranslational regulation of the 54K cellular tumour antigen in normal and transformed cells. *Mol. Cell. Biol.* 1981, 1:101-110.
- Ortmann B., Androlewicz M., & Cresswell P. MHC class I/ β_2 -microglobulin complexes associate with TAP transporters before peptide binding. *Nature.* 1994, 368:864-867.
- Ortmann B., Copeman J., Lehner P.J., Sadasivan B., Herbert J.A., Grandea A.G., Riddell S.R., Tampe R., Spies T., Trowsdale J., & Cresswell P. A critical role for tapasin in the assembly and function of multimeric MHC class I-TAP complexes. *Science.* 1997, 277:1306-1309.
- Osborne M.P. & Rosen P.P. Detection and management of bone marrow micrometastases in breast cancer. *Oncology.* 1994, 8:25-31.
- Ostrand-Rosenberg S. Tumour immunotherapy: the tumour cell as an antigen-presenting cell. *Curr. Opin. Immunol.* 1994, 6:722-727.
- Paciucci P.A., Holland J.F., Ryder J.S., Konefal., R.G., Bekesi G.J., Odchimer R., & Gorden R. Immunotherapy with interleukin 2 by constant infusion with and without adoptive cell transfer and with weekly doxorubicin. *Cancer Treat. Rep.* 1989, 16:67-81.
- Paglia P., Chiodoni C., Rodolfo M., *et al.* Murine dendritic cells loaded *in vitro* with soluble protein prime cytotoxic T lymphocytes against tumour antigen *in vivo*. *J. Exp. Med.* 1996, 183:317-322.
- Paik S., Hazan R., Fisher E., Sass R., Fisher B., Redmond C., Schlessinger J., Lippman M., & King C. Pathologic findings from the National Surgical Adjuvant breast and Bowel Project: prognostic significance of erbB-s protein overexpression in primary breast cancer. *J.Clin.Oncol.* 1990, 8:103-112.
- Pamer E., & Cresswell P. Mechanisms of the class I-restricted antigen processing. *Annu. Rev. Immunol.* 1998, 16:323-358.
- Pan Z.K., Ikonomidis G., Pardoll D., & Paterson Y. Regression of established tumours in mice mediated by the oral administration of a recombinant *Listeria monocytogenes* vaccine. *Cancer Res.* 1995, 55:4776-4779.
- Pardoll D.M. Cancer vaccines. *Nat. Med.* 1998, 4:525-531.

- Pardoll D.M., & Topalian S.L. The role of CD4⁺ T cell responses in antitumour immunity. *Curr. Opin. Immunol.* 1998, 10:588-594.
- Park S.J., Sadegh Nasser S., & Wiley D.C. Invariant chain made in *Escherichia coli* has an exposed N-terminal segment that blocks antigen binding to HLA-DR1 and a trimeric C-terminal segment that binds empty HLA-DR1. *Proc. Natl. Acad. Sci. USA.* 1995, 92:11289-11293.
- Peters P.J., Neeffjes J.J., Oorschot V., Ploegh H.L., & Geuze H.J. Segregation of MHC class II molecules from MHC class I molecules in the Golgi complex for transport to lysosomal compartments. *Nature.* 1991, 349:669-676.
- Peters P.J., Raposo G., Neeffjes J.J., Oorschot V., Leijendekker R.L., Geuze H.J., & Ploegh H.L. Major histocompatibility complex compartments in human B lymphoblastoid cells are distinct from early endosomes. *J. Exp. Med.* 1995, 182:325-334.
- Peterson M., & Miller J. Invariant chain influences the immunological recognition of MHC class II molecules. *Nature.* 1990, 345:172-174.
- Philip R., Brunette E., Ashton J., *et al.* Transgene expression in dendritic cells to induce antigen-specific cytotoxic T cells in healthy donors. *Cancer Gene Therapy.* 1998, 5:236-246.
- Pierce S.K. Molecular chaperones in the processing and presentation of antigen to helper T cells. *Experientia.* 1994, 50:1026-1030.
- Pierre P., *et al.* Developmental regulation of MHC class II transport in mouse dendritic cells. *Nature.* 1997, 388:787-792.
- Pieters J., Bakke O., & Dobberstein B., The MHC class II-associated invariant chain contains two endosomal sorting signals within its cytoplasmic tail. *J. Cell. Sci.* 1993, 106:831-846.
- Pieters J. MHC class II restricted antigen presentation. *Curr. Opin. Immunol.* 1997, 9:89-96.
- Pinet V.M., & Long E.O. Peptide loading onto recycling HLA-DR molecules occurs in early endosomes. *Eur. J. Immunol.* 1998, 28:799-804.
- Ploegh H.L., Orr H.T., & Strominger J.L. Major histocompatibility antigens: the human (HLA-A, -B, -C) and murine (H-2K, H-2D) class I molecules. *Cell.* 1981, 24:287-299.
- Pober J.S., Collins T., Gimbrone M.A. Jr, Cotran R.S., Gitlin J.D., Fiers W., Clayberger C., Krensky A.M., Burakoff S.J., & Reiss C.S. Lymphocytes recognise human vascular endothelial and dermal fibroblast I antigens induced by recombinant immune interferon. *Nature.* 1983, 305:726-729.
- Prasher D.C., Eckenrode V.K., Ward W.W., Prendergast F.C., & Cormier M.J. Primary structure of the *Aequorea victoria* green fluorescent protein. *Gene.* 1992, 111:229-233.
- Rammensee H.G. Chemistry of peptides associated with MHC class I and class II molecules. *Curr. Opin. Immunol.* 1995a, 7:85-96.

- Rammensee H-G., Friede T., & Stevanoic S. MHC ligands and peptide motifs: first listing. *Immunogenetics*. 1995b, 41:178-228.
- Ranges G.E., Figari I.S., Espevik T., & Palladino M.A. Inhibition of cytotoxic T cell development by transforming growth factor β and reversal by recombinant tumour necrosis factor α . *J. Exp. Med.* 1987, 166:991-998.
- Rapoport T.A., Jungnickel B., & Kutay U. Protein transport across the eukaryotic endoplasmic reticulum and bacterial inner membranes. *Annu. Rev. Biochem.* 1996, 65:271-303.
- Raposo G., *et al.* B-lymphocytes secrete antigen processing vesicles. *J. Exp. Med.* 1996, 183:1161-1172.
- Reeves M., Royal R., Lam J., *et al.* Retroviral transduction of human dendritic cells with tumour-associated antigen gene. *Cancer Res.* 1996, 56:5672-5677.
- Reimann J., & Schirmbeck R. Alternative pathways for processing exogenous and endogenous antigens that can generate peptides for MHC class I-restricted presentation. *Immunol. Rev.* 1999, 172:131-152.
- Reis e Sousa C., *et al.* *In vivo* microbial stimulation induces rapid CD40L-independent production of IL-12 by dendritic cells and their re-distribution to T cell areas. *J. Exp. Med.* 1997, 186:1819-1829.
- Reiser C., Bock G., Klocker H., Bartsch G., & Thurnher M. Prostaglandin E2 and tumour necrosis factor alpha cooperate to activate human dendritic cells: synergistic activation of interleukin 12 production. *J. Exp. Med.* 1997, 182:389-400.
- Restifo N.P., Marincola F.M., Kawakami Y., Taubenberger J., Yannelli J.R., & Rosenberg S.A. Loss of functional beta(2)-microglobulin in metastatic melanomas from five patients receiving immunotherapy. *J. Natl. Cancer. Inst.* 1996, 88:100-108.
- Riberdy J.M., Newcombe J.R., Surman M.J., Barbosa J.A., & Cresswell P. HLA-DR molecules from an antigen-processing mutant cell line are associated with invariant chain peptides. *Nature* 1992, 360:474-477.
- Riddell S.R., & Greenberg P.D. Principles for adoptive T cell therapy of human viral diseases. *Annu. Rev. Immunol.* 1995, 13:545-586.
- Ridge J., Di Rosa F., & Matzinger P. A conditioned dendritic cell can be a temporal bridge between a CD4+ T-helper and a T-killer cell. *Nature*. 1998, 392:474-478.
- Riese R.J., Wolf P.R., Bromme D., Natkin L.R., Villadangos J.A., Ploegh H.L., & Chapman H.A. Essential role for cathepsin S in MHC class II-associated invariant chain processing and peptide loading. *Immunity*. 1996, 4:357-366.
- Roche P.A., Marks M.S., & Cresswell P. Formation of a nine-subunit complex by HLA class II glycoproteins and the invariant chain. *Nature*. 1991, 354:392-394.
- Roche P.A. Intracellular protein in lymphocytes: "How do I get THERE from HERE?" *Immunity*. 1999, 11:391-398.

- Rock K.L., Gramm C., Rothstein L., Clark K., Stein R., Dick L., Hwang D., & Goldberg A.L. Inhibitors of the proteasome block the degradation of most cell proteins and the generation of peptides presented by MHC class I molecules. *Cell*. 1994, 78:761-771.
- Romani N., Gruner S., Brang D., *et al.* Proliferating dendritic cell progenitors in human blood. *J. Exp. Med.* 1994, 180:83-93.
- Ruppert J., Grey H.M., Sette A., Kubo R.T., Sidney J., & Celis E. Prominent role of secondary anchor residues in peptide binding to HLA-A2.1 molecules. *Cell*. 1993, 74:929-937.
- Russo V., Traversari C., Verrecchia A., Mottolese M., Natali P.G., & Bordignon C. Expression of the MAGE gene family in primary and metastatic human breast cancer: Implications for tumour antigen-specific immunotherapy. *Int.J.Cancer*. 1995, 64:216-221.
- Sadasivan B., Lehner P.J., Ortmann B., Spies T., & Cresswell P. Roles for calreticulin and a novel glycoprotein, tapasin, in the interaction of MHC class I molecules with TAP. *Immunity*. 1996, 5:105-114.
- Sahin U., Tureci O., Schmitt H., *et al.* Human neoplasms elicit multiple specific immune responses in the autologous host. *Proc. Natl. Acad. Sci. USA*. 1995, 92:11810-11813.
- Sallusto F., & Lanzavecchia A. Efficient presentation of soluble antigen by cultured human dendritic cells is maintained by granulocyte/macrophage colony-stimulating factor plus interleukin-4 and downregulated by tumour necrosis factor α . *J. Exp. Med.* 1994, 179:1109-1118.
- Sallusto F., Cella M., Danieli C., & Lanzavecchia A. Dendritic cells use macropinocytosis and the mannose receptor to concentrate macromolecules in the major histocompatibility complex class II compartment: downregulation by cytokines and bacterial products. *J.Exp.Med.* 1995, 182:389-400.
- Sambrook J., Fritsch E.F., & Maniatis T. *Molecular cloning: a laboratory manual* (2nd edition). Cold Spring Harbour Laboratory Press, New York, 1989.
- Sanderson F., Kleijmeer M.J., Kelly A., Verwood D., Tulp A., Neefjes J.J. Geuze H.J., & Trowsdale J. Accumulation of HLA-DM, a regulator of antigen presentation, in MHC class II compartments. *Science*. 1994, 266:1566-1569.
- Sanderson S., Frauwirth K., & Shastri N. Expression of endogenous peptide-major histocompatibility complex class II complexes derived from invariant chain-antigen fusion proteins. *Proc. Natl. Acad. Sci. USA*. 1995, 92:7217-7221.
- Scheffner M., Werness B.A., Huibregtse J.M., Levine A.J., & Howley P.M. The E6 oncoprotein encoded by human papillomavirus types 16 and 18 promotes the degradation of p53. *Cell*. 1990, 63:1129-1136.
- Schlom J., Kantor J., Abrams S., Tsang K.Y., Panicali D., & Hamilton M. Strategies for the development of recombinant vaccines for the immunotherapy of breast cancer. *Breast Cancer Res. Treatment*. 1996, 38:27-39.

- Schoenberger S., Toes R., van der Voort E., Offringa R., & Melief C. T-cell help for cytotoxic T lymphocytes is mediated by CD40-CD40L interactions. *Nature*. 1998, 393:480-483.
- Schutze M.P., Peterson P.A., & Jackson M.R. An N-terminal double-arginine motif maintains type II membrane proteins in the endoplasmic reticulum. *Int. Immunol.* 1994, 6:101-111.
- Schwartz R.H. A cell culture model for T lymphocyte clonal anergy. *Science* 1990, 248:1349-1356.
- Segrini M.S., Sabbioni S., Halder S., Possati L., Castagnoli A., Corallini A., Barbanti-Brodano G & Croce C. Tumour and growth suppression of breast cancer cells by chromosome 17-associated functions. *Cancer Res.* 1994, 54:1818-1824.
- Seo N., & Egaea K. Suppression of cytotoxic T lymphocyte activity by γ/δ T cells in tumour-bearing mice. *Cancer Immunol. Immunother.* 1995, 40:358-366.
- Serghini M.A., Ritzenthaler C., & Pinck I. A rapid and efficient 'miniprep' for isolation of plasmid DNA. *Nucleic Acids Res.* 1989, 17:3604.
- Shaulsky G., Goldfinger N., Ben-Ze'ev A., & Rotter V. Nuclear accumulation of p53 protein is mediated by several nuclear localisation signals and plays a role in tumorigenesis. *Mol. Cell. Biol.* 1990a, 10:6565-6577.
- Shaulsky G., Ben-Ze'ev A., & Rotter V. Subcellular distribution of the p53 protein during the cell cycle of Balb/c 3T3 cells. *Oncogene*. 1990b, 5:1707-1711.
- Shepherd J.C., Schumacher T.N.M., Ashton-Rickardt P.G., Imaeda S., Ploegh H.L., Janeway C.A.J. & Tonegawa S. TAP-1 dependent peptide translocation in vitro is ATP dependent and peptide selective. *Cell*. 1993, 74:577-584.
- Sherman M.A., Weber D.A., & Jensen P.E. DM enhances peptide binding to class II MHC by release of invariant chain-derived peptide. *Immunity*. 1995, 3:197-205.
- Shieh S.Y., Ikeda M., Taya Y., & Prives C. DNA damage-induced phosphorylation of p53 alleviates inhibition by MDM2. *Cell*. 1997, 91:325-334.
- Siena S., Di Nicola M., Bregni M., et al. Massive *ex vivo* generation of function dendritic cells from mobilized CD34+ blood progenitors for anticancer therapy. *Exp. Haematol.* 1995, 23:1463-1471.
- Sloan V.S., Cameron P., Porter G., Gammon M., Amaya M., Mellins E., & Zaller D.M. Mediation by HLA-DM of dissociation of peptides from HLA-DR. *Nature*. 1995, 375:802-806.
- Smith I. Breast cancer. *Medicine*. 1995, 464-468.
- Song W., Kong H., Carpenter H., *et al.* Dendritic cells genetically modified with an adenovirus vector encoding the cDNA for a model tumour antigen induce protective and therapeutic antitumour immunity. *J. Exp. Med.* 1997, 186: 1247-1256.

- Soong R., Robbins P.D., Dix B.R., *et al.* Concordance between p53 protein overexpression and gene mutation in a large series of common human carcinomas. *Hum. Pathol.* 1996, 27: 1050.
- Specht J.M., Wang G., Do M.T., *et al.* Dendritic cells retrovirally transduced with a model tumour antigen gene are therapeutically effective against pulmonary metastases. *J. Exp. Med.* 1997, 186:1213-1221.
- Speiser D.E., *et al.* Self antigens expressed by solid tumours do not efficiently stimulate naïve or activated T cells: Implications for immunotherapy. *J. Exp. Med.* 1997, 186:645-653.
- Srivastava P.K., Udono H., Blachere N.E., & Li Z. Hypothesis: heat shock proteins transfer peptides during antigen processing and CTL priming. *Immunogenetics.* 1994, 39:93-98.
- Staveley-O'Carroll K., Sotomayor E., Montgomery J., Borrello I., Hwang L., Fein S., Pardoll D., & Levitsky H. Induction of antigen-specific T cell anergy: An early event in the course of tumour progression. *Proc. Natl. Acad. Sci. USA.* 1998, 95:1178-1183.
- Steinman R.M. & Cohn Z.A. Identification of a novel cell type in peripheral lymphoid organs of mice: I. Morphology, quantitation, tissue distribution. *J. Exp. Med.* 1973, 137:1142-1162.
- Steinman R.M. The dendritic cell system and its role in immunogenicity. *Ann. Rev. Immunol.* 1991, 9:271-296.
- Stern L.J., Brown J.H., Jardetzky T.S., Gorga J.C., Urban R.G., Strominger J.L., & Wiley D.C. Crystal structure of the human class II MHC protein HLA-DR1 complexed with an influenza virus peptide. *Nature.* 1994, 368:215-221.
- Stommel J.M., Marchenko N.D., Jimenez G.S., Moll U.M., Hope T.J., & Wahl G.M. A leucine-rich nuclear export signal in the p53 tetramerization domain: regulation of subcellular localisation and p53 activity by NES masking. *EMBO J.* 1999, 18:1660-1672.
- Strand S., Hofmann W.J., Hug H., Muller M., Otto G., Strand D., *et al.* Lymphocyte apoptosis induced by CD95 (APO-1/Fas) ligand-expressing tumour cells – a mechanism of immune evasion? *Nat. Med.* 1996, 2:1361-1366.
- Strubin M., Long E.O., & Mach B. Two forms of the Ia antigen-associated invariant chain results from alternative initiations at two in-phase AUGs. *Cell.* 1986, 47:619-625.
- Sugie T., Bogenberger J., & Englemen E. Transfection of *in vitro* transcribed RNA using Effectene™ Transfection Reagent. *Qiagen News.* 1999, 5:10-11.
- Surh C.D., *et al.* Two subsets of epithelial cells in the thymic medulla. *J. Exp. Med.* 1992, 176:495-505.
- Svensson M., Stockinger B., & Wick M.J. Bone marrow-derived dendritic cells can process bacteria for MHC-I and MHC-II presentation to T cells. *J. Immunol.* 1997, 158:4229-4236.

- Tan M.C.A.A. *et al.*, Mannose-receptor mediated uptake of antigens strongly enhances HLA class II-restricted antigen presentation by cultured dendritic cells. *Eur. J. Immunol.* 1997, 27:2426-2435.
- Tanaka K., & Kasahara M. The MHC class-I ligand-generating system-roles of immunoproteasomes and the interferon-gamma-inducible proteasome activator PA28. *Immunol. Rev.* 1998, 163:161-176.
- Tang M.X., Redemann C.T., & Szoka, Jr F.C. In vitro gene delivery by degraded polyamidoamine dendrimers. *Bioconjugate Chem.* 1996, 7:703-714.
- Tarte K., Lu Z.Y., Fiol G., Legouffe E., Rossi J.F., Klein B. Generation of virtually pure and potentially proliferating dendritic cells from patients with multiple myeloma. *Blood.* 1997, 90:3482-3485.
- Taylor-Papadimitriou J. Report on the First International Workshop on Carcinoma-Associated Mucins. *Int.J.Cancer.* 1991, 49:1.
- Teyton L., O'Sullivan D., Dickson P.W., Lotteau V., Sette A., Fink P., & Peterson P.A. Invariant chain distinguishes between the exogenous and endogenous antigen presentation pathways. *Nature.* 1990, 348:39-44.
- Tilken A-F., Lubin R., Soussi T., *et al.* Primary proliferative T cell responses to wild-type p53 protein in patients with breast cancer. *Eur. J. Immunol.* 1995, 25:1765-1769.
- Toes R.E., Schoenberger S.P., van der Voort E.E., Offringa R., & Melief C.J. CD40-CD40 ligand interactions and their role in cytotoxic T lymphocyte priming and anti-tumour immunity. *Semin. Immunol.* 1998, 10:443-448.
- Toikkanen S., Helin H., Isola J., & Joensuu H. Prognostic significance of HER-2 oncoprotein expression in breast cancer: a 30-year follow-up. *J.Clin.Oncol.* 1992, 10:1044-1048.
- Topalian S.L., Solomon D., Avis F.P., Chang A.E., Freerksen D.L., Linehan W.M., Lotze M.T., Robertson C.N., Seipp C.A., Simon P., Simpson C.G., & Rosenberg S.A. Immunotherapy of patients with advanced cancer using tumour-infiltrating lymphocytes and recombinant interleukin-2: A pilot study. *J.Clin. Oncol.* 1992, 6:839-853.
- Torre-Amione G., Beauchamp R.D., Koeppen H., Park B.H., Schreiber H., Moses H.L., *et al.* A highly immunogenic tumour transfected with a murine TGF- β cDNA escapes immune surveillance. *Proc. Natl. Acad. Sci. USA.* 1990, 87:1486-1490.
- Townsend A.R.M., & Bodmer H. Antigen recognition by class I MHC-restricted T lymphocytes. *Annu. Rev. Immunol.* 1989, 7:601-624.
- Traversari C., Van der Bruggen P., Luescher I.F., *et al.* A nonapeptide encoded by human gene MAGE-1 is recognised on HLA-A1 by cytolytic T lymphocytes directed against tumour antigen MZ2-E. *J. Exp. Med.* 1992, 176:1453-1457.
- Tsang K., Zaremba S., Hamilton J.M., & Schlom J. Analysis of T-cell responses to carcinoembryonic antigen (CEA) in carcinoma patients following immunisation with a recombinant vaccinia CEA vaccine. *J. Natl. Cancer Inst.* 1995, 87:982-990.

- Urban J.L., Burton R.C., Holland J.M., Kripke M.L., & Schreiber H. Mechanisms of syngeneic tumour rejection susceptibility of host-selected progressor variants to various immunological effector cells. *J. Exp. Med.* 1982, 155:557-573.
- Uthayakumar S., & Granger B.L. Cell surface accumulation of over expressed hamster lysosomal membrane glycoproteins. *Cell. Mol. Biol. Res.* 1995, 41:405-420.
- Uyttenhove C., Maryanski J., & Boon T.J. Escape of mouse mastocytoma p815 after nearly complete rejection is due to antigen-loss variants rather than immunosuppression. *J. Exp. Med.* 1983, 157:1040-1052.
- van Bergen J., Schoenberger S.P., Verreck F., Amons R., Offringa R., & Koning F. Efficient loading of HLA-DR with a T helper epitope by genetic exchange of CLIP. *Proc. Natl. Acad. Sci. USA.* 1997, 94:7499-7502.
- van der Bruggen P., Traversari C., Chomez P., Lurquin C., de Plaene E., van der Eynde B., Knuth A., & Boon T. A gene encoding an antigen recognised by cytolytic T lymphocytes on a human melanoma. *Science* 1991, 254:1643-1647.
- van der Bruggen P., Szikora J.P., Boel P., Wildmann C., Somville M., Sensi M., & Boon T. Autologous cytolytic T lymphocytes recognise a MAGE-1 nonapeptide on melanomas expressing HLA-Cw1601. *Eur. J. Immunol.* 1994, 24:2134-2140.
- van Endert P.M., Tampe R., Meyer T.H., Tisch R., Bach J-F, & McDevitt H.O. A sequential mode for peptide binding and transport by the transporters associated with antigen processing. *Immunity.* 1994, 1:491-500.
- van Essen D., Kikutani H & Gray D. CD40 ligand-transduced co-stimulation of T cells in the development of helper function. *Nature.* 1995, 378:620-623.
- van Ham S.M. *et al.*, HLA-DO is a negative modulator of HLA-DM mediated MHC class II peptide loading. *Curr. Biol.* 1997, 7:950-957.
- van Tendeloo V.F.I., Snoeck H-W., Lardon F., *et al.* Nonviral transfection of distinct types of human dendritic cells: high-efficiency gene transfer by electroporation into haematopoietic progenitor-but not monocyte-derived dendritic cells. *Gene Therapy.* 1998: 5:700-707.
- Vassilakos A., Cohen-Doyle M.F., Peterson P.A., Jackson M.R., & Williams D.B. The molecular chaperone calnexin facilitates folding and assembly of class I histocompatibility molecules. *EMBO J.* 1996, 15:1495-1506.
- Vitolo D., Zerbe T., Kanbour A., Dahl C., Herberman R.B., & Whiteside T.L. Expression of mRNA for cytokines in tumour-infiltrating mononuclear cells in ovarian adenocarcinoma and invasive breast cancer. *Intl. J. Cancer.* 1992, 51:573-580.
- Vojtesek B., & Lane D.P. Regulation of p53 protein expression in human breast cancer cell lines. *J. Life. Sci.* 1993, 105:607-612.
- Vogelstein B., & Kinzler K.W. p53 function and dysfunction. *Cell.* 1992, 70: 523-526.

- Vogt A.B., Kropshofer H., Moldenhauer G., Hammerling G.J. Kinetic analysis of peptide loading onto HLA-DR molecules mediated by HLA-DM. *Proc. Natl. Acad. Sci. USA.* 1996, 93:9724-9729.
- Waldman T., Kinzler K., & Vogelstein B. p21 is necessary for p53-mediated G1 arrest in human cancer cells. *Cancer Res.* 1995, 55: 5187-5190.
- Wang K., Peterson P.A., & Karlsson L. Decreased Endosomal delivery of major histocompatibility complex class II-invariant chain complexes in dynamin-deficient cells. *J. Biol. Cell.* 1997, 272:17055-17060.
- Wang R-F., Wang X., Atwood A.C., Topalian S., & Rosenberg S.A. Cloning genes encoding MHC class II-restricted antigens: mutated CDC27 as a tumour antigen. *Science.* 1999a, 284: 1351-1354.
- Wang R-F., Wang X., & Rosenberg S.A. Identification of a novel major histocompatibility complex II-restricted tumour antigen resulting from a chromosomal rearrangement recognised by CD4⁺ T cells. *J. Exp. Med.* 1999b, 189: 1659-1668.
- Warren R.A., Green F.A. & Enns C.A. Saturation of the endocytic pathway for the transferrin receptor does not affect the endocytosis of the epidermal growth factor receptor. *J. Biol. Chem.* 1997, 272:2116-2121.
- Weber D.A., Evavold B.D., & Jensen P.E. Enhanced dissociation of HLA-DR bound peptides in the presence of HLA-DM. *Science.* 1996, 274:618.
- Werness B.A., Levine A.J., & Howley P.M. Association of human papillomavirus types 16 and 18 E6 proteins with p53. *Science.* 1990, 248:76-79.
- West M.A., Lucocq J.M., & Watts C. Antigen processing and class II MHC peptide-loading compartments in human B-lymphoblastoid cells. *Nature.* 1994, 369:147-151.
- Wick M., *et al.*, Antigenic cancer cells grow progressively in immune hosts without evidence for T cell evidence of T cell exhaustion or systemic anergy. *J. Exp. Med.* 1997, 186:229-238.
- Winzler C. *et al.*, Maturation stages of mouse dendritic cells in growth factor-dependent long-term cultures. *J. Exp. Med.* 1997, 185:317-328.
- Wortzel R.D., Philipps C., & Schreiber H. Multiple tumour-specific antigens expressed on a single tumour cell. *Nature.* 1983, 304:165-167.
- Wu X., Bayle J.H., Olsen D., & Levine A.J. The p53-mdm-2 autoregulatory feedback loop. *Genes. Dev.* 1993, 7:1126-1132.
- Wu L-C., Guarnier F.G., Staveley-O'Carroll K.F., Viscidi R.P. *et al.*, Engineering an intracellular pathway for major histocompatibility complex class II presentation of antigens. *Proc. Natl. Acad. USA.* 1995, 92:11671-11675.
- Wubbolts R.W., Fernandez -Borja M., Oomen L., *et al.* Direct vesicular transport of MHC class II molecules from lysosomal structures to the cell surface. *J. Cell. Biol.* 1996, 183:611-622.

- Wubbolts R. & Neefjes J. Intracellular transport and peptide loading of MHC class II molecules: regulation by chaperones and motors. *Immunol. Rev.* 1999, 172:189-208.
- Wyman T.B., Nicol F., Zelphati O., Scaria P.V., Plank C., & Szoka F.C. Design, synthesis and characterisation of a cationic peptide that binds to nucleic acids and permeabilises bilayers. *Biochem.* 1997, 36:3008-3017.
- Yarnold J. Breast cancer. In: *Treatment of Cancer*. 3rd Edition. Edited by Price and Sikora. Chapman & Hall, London 1995, pp 413-436.
- Yee C., Krishnan-Hewlett I., Baker C.C., Schlegel R., & Howley P.M. Presence and expression of human papillomavirus sequences in human cervical carcinoma cell lines. *Am. J. Pathol.* 1985, 119:361-366.
- Yewdell J.W., & Bennink J.R. The binary logic of antigen processing and presentation to T-cells. *Cell.* 1990, 62:203-206.
- Yoshimoto M., Sakamoto G., & Ohashi Y. Tumour infiltrating lymphocytes in breast cancer. *Igaku No Aymi (Tokyo)* 151:457-458.
- Young J.W., Kouлива L., Soergel S.A., Clark E.A., Steinman R.M. & Dupont B. The B7/BB1 antigen provides one of several costimulatory signals for the activation of CD4⁺ T lymphocytes by human blood dendritic cells *in vitro*. *J. Clin. Invest.* 1992, 90:229-237.
- Zhong L., Granelli-Piperno A., Choi Y., & Steinman R.M. Recombinant adenovirus is an efficient and non-perturbing genetic vector for human dendritic cells. *Eur. J. Immunol.* 1999, 29: 964-972.
- Zhou L-J., Tedder T.F. CD14⁺ blood monocytes can differentiate into functionally mature CD83⁺ dendritic cells. *Proc. Natl. Acad. Sci. U.S.A.* 1993, 93:2588.
- Zhou L-J., Tedder T.F. Human blood dendritic cells selectively express CD83, a member of the immunoglobulin superfamily. *J. Immunol.* 1995, 154:3821
- Zitvogel L., Mayordomo J.I., Tjandrawan T., *et al.* Therapy of murine tumours with tumour peptide-pulsed dendritic cells: Dependence on T cells, B7 costimulation and T helper cell 1-associated cytokines. *J. Exp. Med.* 1996, 183:87-97.